Tripartite Prodrugs of the Anthracycline Anticancer Drug Candidate Doxazolidine: New Methods and Mechanisms Relevant to Their Synthesis

Thomas Price Kirby

B.A. (Magna Cum Laude), Chemistry, University of Colorado – Boulder, 2008

B.A., Biochemistry, University of Colorado – Boulder, 2008

A thesis submitted to the

Faculty of the Graduate School of the

University of Colorado in partial fulfillment

of the requirement for the degree of

Doctor of Philosophy

Department of Chemistry

2019

This thesis entitled:

Tripartite Prodrugs of the Anthracycline Anticancer Drug Candidate Doxazolidine:

New Methods and Mechanisms Relevant to Their Synthesis

written by Thomas Price Kirby

has been approved for the Department of Chemistry

_____

Tad H. Koch

_____

Tarek Sammakia

Date_____

The final copy of this thesis has been examined by the signatories, and we find that both the content and the form meet acceptable presentation standards of scholarly work in the above mentioned discipline.

Kirby, Thomas Price (Ph.D., Chemistry)

Tripartite Prodrugs of the Anthracycline Anticancer Drug Candidate Doxazolidine: New Methods and Mechanisms Relevant to Their Synthesis

Thesis directed by Professor Tad H. Koch

This dissertation describes the development of a new method for the synthesis of tripartite prodrugs of the anticancer drug candidate doxazolidine, which utilizes, as the key transformation, the traceless Staudinger ligation (TSL) of an aryl azide. The rationale for developing a new synthetic methodology is presented in juxtaposition to the limitations of the preexisting route for preparation of prodrugs containing the Katzenellebogan-spacer and this discussion focuses on improving the efficiency with which the chemical space surrounding such target molecules may be explored. A critical limitation to the newly developed method, namely, the inability to stereoselectively esterify C-chiral peptides with 2-(diphenylphosphino)phenol, which ultimately affords a mixture of diastereomeric products and, thereby, complicates the structural characterization and biological evaluation of the prepared prodrugs, is also discussed along with possible solutions to the problem. Mechanistic studies provide evidence that the TSL of an aryl azide proceeds via acyl-transfer to a phosphazide intermediate, as opposed to the iminophosphorane intermediate invoked in the putative mechanism of the TSL of an alkyl azide, in a reaction that depends on the concentration of water present in the reaction medium at the outset of the reaction. A revised mechanism for the TSL of an aryl azide and phosphino phenyl ester is ultimately presented alongside kinetic analysis of the reaction run under consecutive pseudo-first-order conditions in the presence of an excess of azide and water.

Acknowledgements

Thank you to everyone who helped to make the CHEM department such a wonderful place to work over the years. My labmates in the Koch lab: Dr. Ben Barthel and Dr. Dan Rudnicki. My mates in the Sammakia lab: Dr. Ryan Michael, Dr. Jeff Gazaille, Dr. Will Hartwig, Dr. Cheng-Kang Mai and Ethan Miller. Working alongside you all has been a privilege and a pleasure. Thank you.

Many thanks must also go to the professors who have facilitated my learning of chemistry both in the classroom and in the laboratory:

First and foremost, I owe a great deal of gratitude to my research advisor, Professor Tad Koch. Tad, in 2007 you afforded me the opportunity to begin doing research in your laboratory when I was an undergraduate Chemistry/Biochemistry double−major. Over the years, you have offered me a wealth of knowledge and provided me with a platform to launch my research career. Without your support, none of this would have been possible. Thank you Tad.

I would also like to thank Professor Tarek Sammakia. Tarek, you too have taught me chemistry since I was an undergraduate. As a graduate student, your continued mentorship has been invaluable. Thank you Tarek.

I owe an additional heap of gratitude to Dr. Richard Shoemaker with whom I worked closely in the NMR facility. Rich, you provided me with an immeasurable amount of support and tutelage over the years for which I will forever remain grateful. Thank you Rich.

I would also like to thank Prof. David Brook of the San Jose State University Chemistry Department in San Jose, CA, for the kinetic fitting of the data in chapter 8 by numerical integration of the differential forms of the possible rate equations.

Finally, I wish to thank my parents, Jim and Jayne Kirby. I love you both and am eternally grateful for your unwavering support.

Contents

Tables

Figures

Schemes

Abbreviations

Å	=	Angstrom
a	=	D-Alanine
Ac	=	Acetyl
Ac_2O	=	Acetic anhydride
AcOH	=	Acetic acid
Alloc	=	Allyloxycarbonyl
Ar	=	Aryl
Bn	=	Benzyl
Cbz	=	Benzyloxycarbonyl
Cit	=	L-Citrulline
DCC	=	Dicyclohexylcarbodiimide
DCM	=	Dichloromethane
DCU	=	Dicyclohexylurea
DIEA	=	Diisopropylethylamine
DMAP	=	Dimethylaminopyridine
DMF	=	Dimethylformamide
DMSO	=	Dimethylsulfoxide
DOX	=	Doxorubicin
DOXAZ	=	Doxazolidine
DOXF	=	Doxoform
ESI	=	Electrospray ionization
EtOAc	=	Ethyl acetate

EtOH	=	Ethanol
F	=	L-Phenylalanine
FCC	=	Flash column chromatography
Fmoc	=	9-Fluorenylmethyloxycarbonyl
g	=	Glycine
HCl	=	Hydrochloric acid
HBTU	=	*N,N,N′,N′*-Tetramethyl-*O*-(1H-benzotriazol-1-yl)-uranium hexafluorophosphate
HOBt	=	*N*-Hydroxybenzotriazole
HRMS	=	High-resolution mass spectrometry
Hz	=	Hertz
IR	=	Infrared
K	=	L-Lysine
LCMS	=	Liquid chromatography mass spectrometry
MDR	=	Multi-drug resistant
MeCN	=	Acetonitrile
MeOH	=	Methanol
$MgSO_4$	=	Magnessium sulfate
$NaHCO_3$	=	Sodium bicarbonate
Na_2SO_4	=	Sodium sulfate
NMP	=	*N*-Methyl-2-pyrrolidone
NMR	=	Nuclear magnetic resonance
NaOH	=	Sodium hydroxide
PABA	=	*para*-Aminobenzyl alcohol

PABC	=	*para*-Aminobenzyloxycarbonyl
PBS	=	Phosphate-buffered saline
PEA	=	β-Phenethylamine
Pgp	=	P-170 glycoprotein
PhMe	=	Toluene
PNP	=	*para*-Nitrophenyl
^{i}PrOH	=	*iso*-Propyl alcohol
R_f	=	Retention factor
ROS	=	Reactive oxygen species
RP-HPLC	=	Reverse-phase high-performance liquid chromatography
R_T	=	Retention time
SPPS	=	Solid-phase peptide synthesis
TEA	=	Triethylamine
TFA	=	Trifluoroacetic acid
THF	=	Tetrahydrofuran
TLC	=	Thin-layer chromatography
TOF	=	Time of flight
TopoII	=	Toposiomerase II
TSL	=	Traceless Staudinger ligation
UV-vis	=	Ultraviolet-visible
V	=	L-Valine
v/v	=	Volume / Volume
VT	=	Variable temperature

Z	=	Benzyloxycarbonyl

Chapter 1

Anthracycline Antibiotics

1.1 Introduction

The identification and clinical application of chemical compounds possessing anti-tumor activity has long been a major focus of the pharmaceutical industry (Table 1.1).[1] While new and improved therapies are continually being developed, the anthracyclines have continued to find widespread application as anti-cancer chemotherapeutic agents more than fifty years after their initial discovery.[2,3] Anthracyclines comprise a class of ~500 naturally occurring aromatic polyketides belonging to the Rhodomycin-group of antibiotics.[3] The structures of four clinically approved anthracyclines: daunorubicin (Daunomycin) **1**, doxorubicin (Adriamycin) **2**, epidoxorubicin (Epirubicin) **3** and idarubicin (Idamycin) **4** are shown in Figure 1.1.

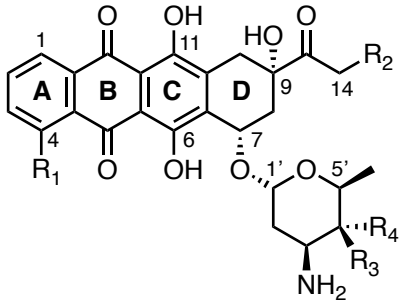

1 daunorubicin	R_1=OMe, R_2=R_4=H, R_3=OH
2 doxorubicin	R_1=OMe, R_2=R_3=OH, R_4=H
3 epidoxorubicin	R_1=OMe, R_2=R_4=OH, R_3=H
4 idarubicin	R_1=R_2=R_4=H, R_3=OH

Figure 1.1 Structures of the anthracyclines daunorubicin **1**, doxorubicin **2**, epidoxorubicin **3** and idarubicin **4**.

Table 1.1 Examples of FDA-approved anticancer chemotherapeutics developed over the last 60 years.[1]

Class of Chemotherapeutic	**Clinical Drugs**	**Date of FDA Approval** (mm / dd / yr)
Alkylating Agents	Chlorambucin	03 / 18 / 1957
	Cyclophosphamide	11 / 16 / 1959
	Melphalan	01 / 17 / 1964
	Cisplatin	12 / 19 / 1978
	Carboplatin	03 / 03 / 1989
Antimetabolites	Methotrexate	12 / 07 / 1953
	5-fluorouracil	04 / 25 / 1962
	Floxuridine	12 / 18 / 1970
	Gemcitabine	05 / 15 / 1996
Antimicrotubule Agents	Vincristine	07 / 10 / 1963
	Pacelitaxel	12 / 29 / 1992
	Vinorelbine	12 / 23 / 1994
	Docataxel	05 / 14 / 1996
Topoisomerase Inhibitors	Doxorubicin	08 / 07 / 1974
	Daunorubicin	12 / 19 / 1979
	Mitoxantrone	12 / 23 / 1987
	Topotecan	05 / 28 / 1996
	Irinotecan	06 / 14 / 1996
Antiandrogens	Flutamide	01 / 27 / 1989
	Bicalutamide	10 / 04 / 1995
	Enzalutamide	08 / 31 / 2012
	Apalutamide	02 / 14 / 2018

Key structural features common to the anthracyclines shown in Figure 1.1 include (1) the tetracyclic anthraquinone ring system, which constitutes the hydrophobic aglycone core of these molecules and is the chromophore responsible for their characteristic red color (λ_{max} = 480 nm);[3] and (2) the daunosamine aminosugar, which is attached to ring D of the anthraquinone at the 7-position and contains a vicinal amino alcohol in the 3'- and 4'-positions, respectively. Ring D is further functionalized with a geminal tertiary hydroxyl group and ketone side-chain at the 9-position, and the importance of these D-ring substituents is discussed below in the context of the biological activity of the anthracyclines.

To summarize, the structures of daunorubicin **1** and doxorubicin **2** differ only at the 14-position with **2** being the 14-hydroxy analogue of **1**. Epidoxorubicin **3**, as the name implies, is a diastereomer of **2** with the 4'-hydroxyl group of the daunosamine sugar epimerized, while idarubicin **4** is simply the 4-*des*-methoxy analogue of **1**. Thus, the close structural similarity between the anthracyclines is readily apparent. However, the seemingly minor alterations to molecular structure between analogues belies the substantial differences in biological activity such changes may impose, and the structure-activity relationships (SAR) observed with the anthracyclines underscores the value of this concept in medicinal chemistry (*vide infra*).

1.2 Discovery and Biological Activity of the Anthracyclines

Daunorubicin **1** was the first anthracycline to be reported following its isolation from a then-newly discovered soil microorganism, *Streptomyces peucetius*.[2] *S. peucetius* was found to produce a red alkaloid that could be isolated as its hydrochloride salt and was subsequently identified as possessing antibacterial, antifungal and anticancer activity.[3] Clinical trials of daunorubicin commenced in 1964 and these studies ultimately revealed that **1** was particularly

effective in the treatment of acute leukemia.[4] However, the drug's efficacy against a broader scope of cancer-types was quite limited.

Encouraged by the anti-leukemic properties of the newly discovered natural product, interest in the creation of analogues of **1** with improved activity against a wider range of tumor types swiftly developed. In 1969, an effort to obtain such derivatives undertaken by Arcamone *et al.*, working in Milan, Italy, led to the generation of a novel strain of the anthracycline-producing microbe using the known mutagen *N*-nitroso-*N*-methyl urethane (NMU).[5] Exposure of the wild-type anthracycline-producing strain *S. peucetius* to NMU produced the mutant strain *S. peucetius* var. *caesius*, which produced an analogue of **1** that differed only by the addition of a hydroxyl group at the 14-position of the exocyclic ketone. The new anthracycline was named doxorubicin (dox) **2** and the modest structural difference between **1** and **2** proved to have substantial biological implications of significant therapeutic import.

Dox **2** displayed improved efficacy in murine tumor models relative to **1**[6] and, importantly, had broad-spectrum activity against a panel of human cancers.[7,8] This improvement provided a driving force for the drug's rapid FDA approval in early-August of 1974, a mere 5 years after **2** had first been isolated.[9] While clinical application of **1**, which too ultimately won FDA approval in 1979, has remained limited to the treatment of acute myelocytic and lymphocytic leukemias,[10] the broad-spectrum activity of **2** has resulted in its application in the treatment of both Hodgkin's and non-Hodgkin lymphomas, multiple myeloma, myelogenous and lymphoid leukemias, sarcomas, as well as, solid breast, ovarian, thyroid, liver and lung carcinomas.[9,11] Similarly, epidoxorubicin **3** is a broad-spectrum drug that is widely used around the world; however, **3** has not yet been approved for use in the U.S.[12] The 4-demethoxydaunorubicin analogue **4** was first synthesized in 1976, by Arcamone, *et al.*, but only

received its initial FDA approval in 1990.[13] Nevertheless, **4** is an antileukemic agent with improved oral availability and reduced cardiotoxicity compared to that of the parent drug[14,15] and, as such, **4** continues to be used in combination therapies for the treatment of adult-onset acute myeloid leukemia.[16]

1.3 The Multiple Mechanisms of Action for the Anthracyclines

Despite their widespread clinical application, the mechanism of action (MoA) for the anthracyclines is not fully understood.[17,18] It is known that anthracyclines enter cells by passive diffusion through the cellular membrane and then migrate into the nucleus.[19,20] Once inside the nucleus, the anthracyclines efficiently target the chromosomes with >99% of the drug present associated with the nuclear DNA.[19] Anthracyclines strongly intercalate between base pairs, particularly in GC-rich sequences of the genome, such that the aglycone core sits in the double helix with the A-ring protruding into the major grove and the daunosamine sugar inserted deep into the minor groove of B-form dsDNA.[21] The 9-hydroxyl group on ring D is generally involved in two hydrogen (H)-bonding interactions with an adjacent base on one strand of dsDNA, which appears to be critical for the stability of the drug-DNA complex.

Once intercalated into cellular DNA, anthracyclines are known to produce topoisomerase II (TopoII)-induced double-stranded breaks or "lesions" in a process widely believed to be the primary MoA responsible for the observed cytotoxicity.[22,23] Topoisomerases are enzymes that catalyze the relaxation of supercoiled DNA by forming transient breaks in either one (type I enzymes) or both (type II enzymes) strands of duplex DNA.[24,25] TopoII functions in a variety of cellular processes, including transcription[26−28] and chromosomal manipulation during mitosis.[29,30] In each case, the enzyme catalyzes the relaxation of positively supercoiled DNA by (1) creating a double-stranded break in one DNA duplex; (2) passing a second duplex through

the break; and (3) re-ligating the broken DNA strand.[31,32] When intercalated into dsDNA, anthracyclines inhibit the re-ligation step of the mechanism, thereby stalling the process at a stage in which the DNA has been cleaved by the enzyme.[22] The increased half-life ($t_{1/2}$) of these ternary TopoII−DNA−drug 'cleavable complexes' results in various mutagenic events, such as chromosomal fragmentations, translocations, and ultimately, induction of the apoptotic pathway.[23] The conclusion that a TopoII-dependent MoA is responsible for the *in vivo* toxicity of the anthracyclines is supported by the observation that clinical dosages of **2** result in the accumulation of double-stranded breaks in the nuclear DNA, which is consistent with the damage that would result from TopoII-poisoning.[23,33] Additionally, altered or diminished TopoII activity is a common phenotype of dox-resistant cell lines.[34,35]

Prior to the 1984 discovery of TopoII-dependent formation of DNA lesions and evidence supporting this as the primary MoA of the anthracyclines, an alternative mechanism had been proposed to explain the activity of these compounds and focused on the redox potential of the anthraquinone ring system. "Bioreductive activation" of **2** via consecutive single electron reductions of the anthraquinone by a redox-active enzymatic system, such as cytochrome P450/NADPH, was believed to convert **2** into a high-energy, reactive intermediate capable of alkylating nuclear DNA and, thereby, triggering apoptosis.[36−40] The observation by Scottish researchers, Bartoszek and Wolf, that pre-incubation of **2** with cytochrome P450 reductase/NADPH prior to its use in the treatment of MCF-7 cells enhanced the drug's activity was also cited as strong evidence in support of the "bioreductive activation" mechanism.[41]

Koch *et al.* showed that, under anaerobic conditions, single electron transfer to the quinone of **2** afforded the semiquinone intermediate **5**, which was subsequently reduced again to afford the corresponding hydroquinone intermediate **6** (Scheme 1.1).[42−45] Spontaneous

Scheme 1.1 Mechanism of the consecutive single electron reductions of dox **2** and elimination of daunosamine **7** to afford quinone methide **8** and protonation of **8** to give the inactive 7-deoxyaglycon **9**.[31]

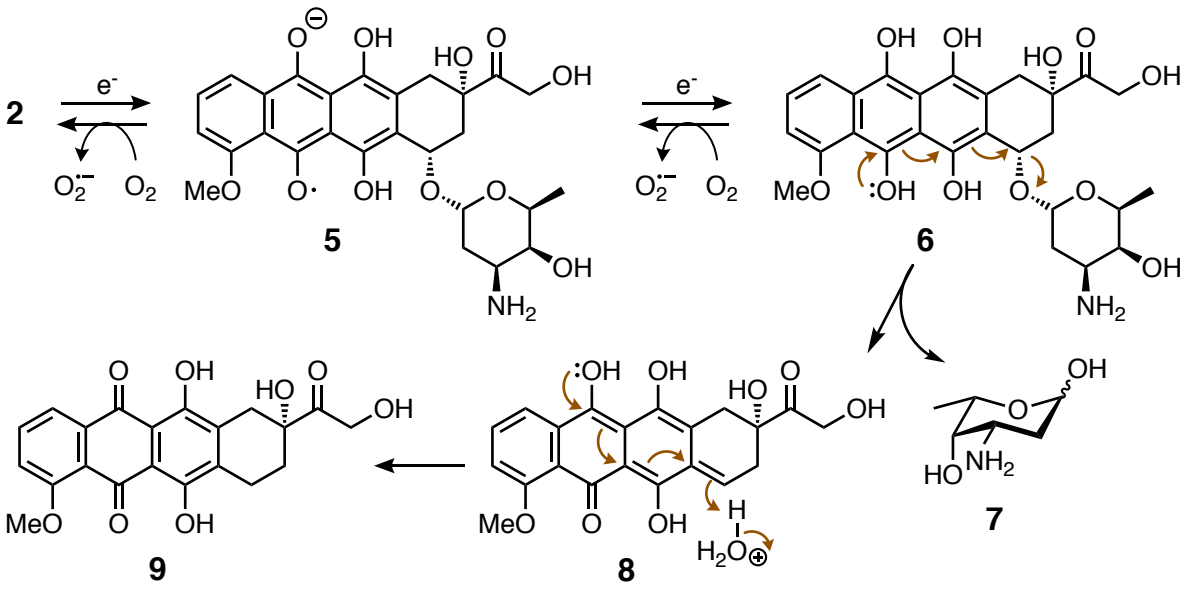

glycosidic bond cleavage of **6** resulted in elimination of the daunosamine aminosugar **7** with concomitant formation of intermediate **8**. The highly reactive quinone methide **8** was initially proposed to be the putative DNA alkylating agent responsible for the cytotoxicity of **2**. However, the experimentally determined $t_{1/2}$ of **8** with respect to protonation in a buffered MeOH solution at 25 °C was a mere 53 s and chemical intuition suggested **8** would have a similarly short $t_{1/2}$ *in vivo*.[42] As such, the notion that significant amounts of **8** could reach the target DNA more rapidly than the competitive protonation reaction would occur appeared highly implausible. A more reasonable axiom contends that the vast majority of **8** produced from "bioreductive activation" of **2** under anaerobic conditions is rapidly protonated at the 7-position on ring D to give the biologically inactive 7-deoxyaglycon **9**.

While the contribution to the therapeutic MoA from DNA alkylation by the quinone methide **8** is likely negligible, a portion of the overall toxicity of the anthracyclines is

nevertheless attributable to the redox activity of the anthraquinone ring system due to oxidative stress caused by the production of reactive oxygen species (ROS).[46] In general, the anthracyclines are excellent chealators of iron and copper ions. The dox−Fe(III) complex **10** forms readily and is reduced to the dox−Fe(II) complex **11** in the presence of single electron reducing agents, such as the flavoenzymes cytochrome P450 reductase/NADPH and xanthine oxidase/NADH (Scheme 1.2). When molecular oxygen is present, its reduction to superoxide may

Scheme 1.2 The putative biochemical mechanism of anthracycline-induced formation of ROS, which induces oxidative stress on cells and contributes both to cancer cell cytotoxicity and the dose-limiting cardiotoxicity associated with anthracycline chemotherapy.[46–51]

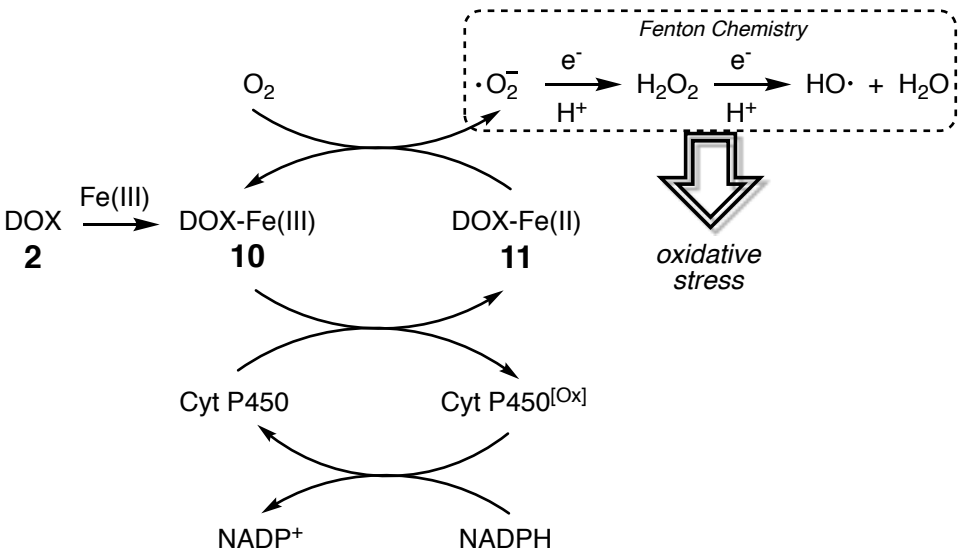

then be coupled to the anthracycline-iron redox chemistry in a cycle that regenerates the dox−Fe(III) complex **10** and allows for continual production of ROS. The superoxide formed from reduction of molecular oxygen may also react further in a series of single electron reductions, collectively referred to as Fenton chemistry, to generate additional ROS, such as hydrogen peroxide and the hydroxyl radical.[46–48] Production of ROS induces oxidative stress in

cells and, thus, accounts for some of the observed anti-cancer activity,[46−50] as well as, to the chronic cardiotoxicity associated with anthracycline chemotherapy.[51−54] The resulting cardiotoxicity has been linked to potentially fatal cardiomyopathy and congestive heart failure, which may manifest years after cessation of anthracycline chemotherapy.[55] This dose-limiting side effect is arguably the single greatest hindrance to anthracycline-containing chemotherapies used in the clinic for the treatment of cancer.

More recently, evidence has mounted that **2** functions by yet another mechanism: formation of formaldehyde-dependent covalent drug-DNA adducts. The earliest reports mentioning formation of covalent dox−DNA adducts appeared in the literature during the 1980s.[38−40] However, it was not until 1990 that Phillips *et al.*, working in Victoria, Australia, used a technique known as transcriptional footprinting to identify specific sites along DNA at which these covalent drug-DNA adducts were formed.[56] Subsequently, during the mid- to late-1990s, Koch and Taatjes, working in Boulder, CO, discovered that the combination of Fe(III), O_2, and a TRIS/DTT buffer system, conditions somewhat unwittingly used during the *in vitro* studies performed by Australians, would oxidize the amine of TRIS **12** to the corresponding nitroso or nitro compound **13**, which then decomposed via a retro-Henry reaction to release copious quantities of formaldehyde (Scheme 1.3).[57−59] Moreover, formaldehyde was shown to be essential for the formation of the covalent drug-DNA adducts reported by Phillips *et al*.[60]

The structure of the dox−DNA covalent adducts was determined empirically using a combination of mass spectrometry, X-ray crystallographic and 2D-NMR data (Figure 1.2).[57,61−63] Analogous to the putative MoA for the anthracyclines involving TopoII poisoning, it was postulated that the anthraquinone ring system intercalated between the C and N bases of a

Scheme 1.3 Mechanism of the retro-Henry reaction for the decomposition of 1 equiv of *tris*(hydroxymethyl)nitromethane **13** to give 3 equiv of formaldehyde; the buffer component TRIS **12**, is shown in the frame.[58]

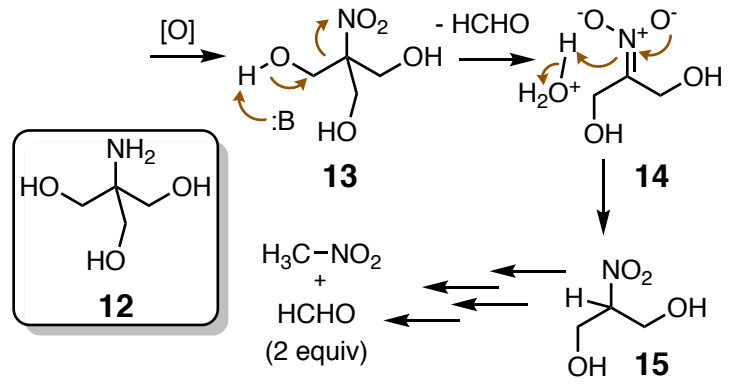

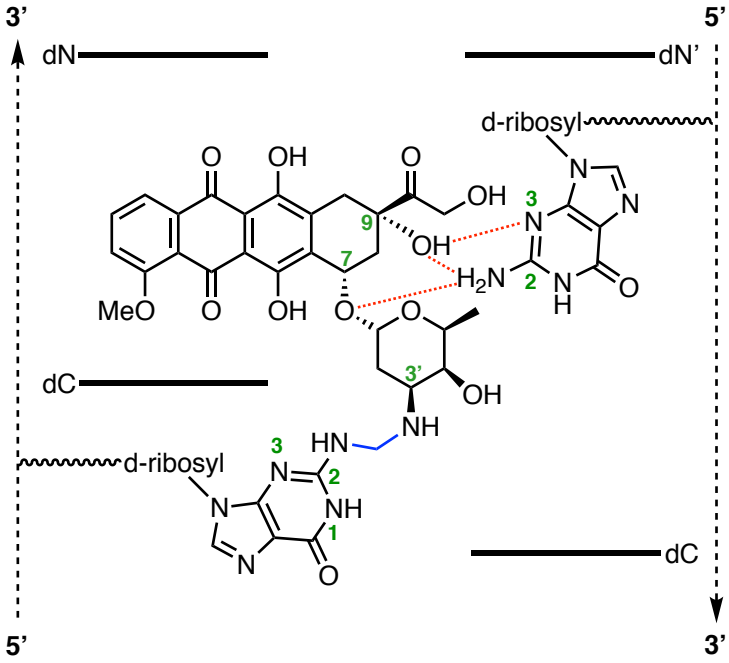

Figure 1.2 The structure of a dox−DNA covalent adduct, as determined empirically from a combination of MS, X-ray crystallographic and 2D-NMR data. For clarity, the bridging methylene is shown in blue, H-bonding interactions are shown as dotted lines in red and numbering of the anthracycline and guanine structures are provided in burgundy and green, respectively.[57–63]

5'-GCN-3' sequence of dsDNA with the daunosamine sugar projected into the minor groove.[64] Once in this position, however, the 3'-amino group of daunosamine then covalently bonds to the exocyclic 2-amino group of the guanine base on one strand of the dsDNA via an aminal bond. If the bridging methylene of the aminal was derived from formaldehyde, then the observed formaldehyde-dependency for formation of these adducts could be explained.[57−63]

Indirect evidence in support for this hypothesis was obtained during *in vitro* studies designed to assess the differences in cellular response to the parent anthracycline drugs **1**, **2** and **3** *vs*. the corresponding formaldehyde−drug conjugates.[60] Drug-sensitive MCF-7 breast cancer cells and drug-resistant MCF-7/ADR cells were used in these experiments and both cell lines showed substantially greater uptake of the formaldehyde-drug conjugates, as well as, a pronounced increase in the retention of the conjugates compared to that of the parent drugs. Fluorescent microscopy revealed that the formaldehyde-drug conjugates effectively targeted the nuclei of both cell lines and remained there long after the drug had been removed from the media. Finally, increased levels of tritium [^{3}H] were detected in DNA isolated from cells treated with isotopically-labeled drug-formaldehyde conjugates that had been prepared using [^{3}H]formaldehyde, thus, implicating the formation of formaldehyde-mediated drug−DNA adduct formation in the MoA responsible for the observed cytotoxicity.

Direct evidence in support of the dependency on formaldehyde in formation of covalent drug-DNA adducts was provided by a combination of X-ray crystallographic and ^{13}C NMR data. A report published in 1991 by Wang *et al.* used X-ray diffraction analysis of an adduct formed when **1** was co-crystallized with a 5'-CGCGC-3' DNA duplex to provide a crystal structure of the closely related covalent daunorubicin−DNA adduct (Figure 1.3).[61] In this case, it was found that trace formaldehyde present as an impurity in the crystallization solvent was responsible for

forming the aminal linkage.[62] The latter piece of evidence was published in 1998 by Crothers *et al.*, working in New Haven, Ct., and used isotopically labeled ^{13}C-formaldehyde to form drug−DNA adducts and confirmed that the labeled carbonyl carbon from ^{13}C-formaldehyde was incorporated into the aminal bond of the adducts to provide the methylene bridge that covalently linked the drug to the DNA.[63] Thus, any lingering doubt over the role of formaldehyde in adduct formation was unequivocally dismissed following publication of these experiments.

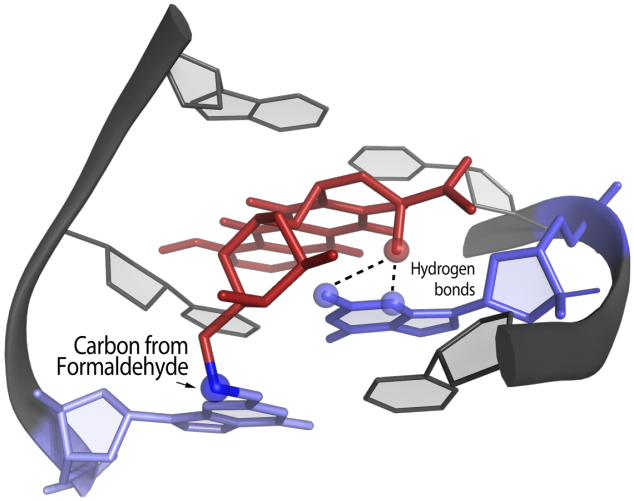

Figure 1.3 X-ray crystal structure of a *virtual* cross-linked 5'-GC-3' dsDNA sequence by the formaldehyde-daunorubicin drug adduct as elucidated by Wang *et al*.[61]

Substantial evidence now exists supporting a mechanism in which formaldehyde reacts *in vitro* and *in vivo* with the 3'-amino and 4'-hydroxyl groups of daunosamine to form an oxazolidine ring, which is then attacked by the 2-amino group of a guanine base on one strand of dsDNA to form the aminal bond and covalently link the drug to one strand of the dsDNA.[64,65] Additional contributions to the overall stability of these adducts is also provided from non-covalent, H-bonding interactions between the 9-hydroxyl group of the anthracycline to both the

3-amino and exocyclic 2-amino groups of a guanine base on the opposing strand of DNA. As such, these adducts were proposed to form a '*virtual* cross-links' to dsDNA,[64] which are sufficiently robust to permit their detection *in vitro* by denaturation-based crosslinking assays.[66−68] Initial studies suggested that the drug-DNA adducts had a $t_{1/2}$ of somewhere between 5−40 h under physiological conditions,[68,69] but more sensitive accelerator mass spectrometry (AMS) experiments using clinically relevant concentrations of **2** indicated that the adducts persist in cells with an average $t_{1/2}$ of 13 h at 37 °C.[70] Curiously, some adducts were observed to persist for as long as 12 days in breast cancer cells, only deepening the mystery of how cells deal with the accumulation of formaldehyde-dependent, covalent anthracycline−DNA adducts.

1.4 The New Semi-Synthetic Anthracyclines: Doxazolidine and Doxoform

Clinical application of the anthracyclines is subject to dose-limiting cardiotoxicity (*vide supra*), as well as, the development of resistance in tumor populations. As a result, sustained efforts have been made over the years towards developing new and improved anthracyclines capable of (1) minimizing the cardiotoxic side effects and (2) having efficacy against resistant tumors. While more than 2,000 anthracycline analogues have been developed in this pursuit, dox **2** still remains the most widely used anthracycline worldwide today.[16] A preformed dox-formaldehyde conjugate, however, was viewed as having the potential to address both of these needs and overcome the limitations inherent to the existing anthracyclines. Researchers in the Koch lab at the University of Colorado−Boulder aimed to capitalize on their discoveries related to formaldehyde-mediated dox-DNA adducts five years earlier and a summary of their efforts to develop and characterize a new semi-synthetic anthracycline-formaldehyde conjugate is given in this section.

When dox **2** was reacted with formaldehyde, the vicinal 3'-amino and 4'-hydroxyl groups were annulated, forming a 5-membered oxazolidine ring, to afford an isolable product that was named doxazolidine (doxaz) **16** (Scheme 1.4).[64] Further reaction *in situ* of 2 equiv of **16** with another equiv of formaldehyde then formed the dimeric compound, doxoform (doxf) **17**.

Scheme 1.4 Reaction of dox **2** with formaldehyde affords doxazolidine **16** and a reaction of 2 equiv of **16** with an additional equiv of formaldehyde gives doxoform **17**; their respective hydrolyses are also indicated.[64]

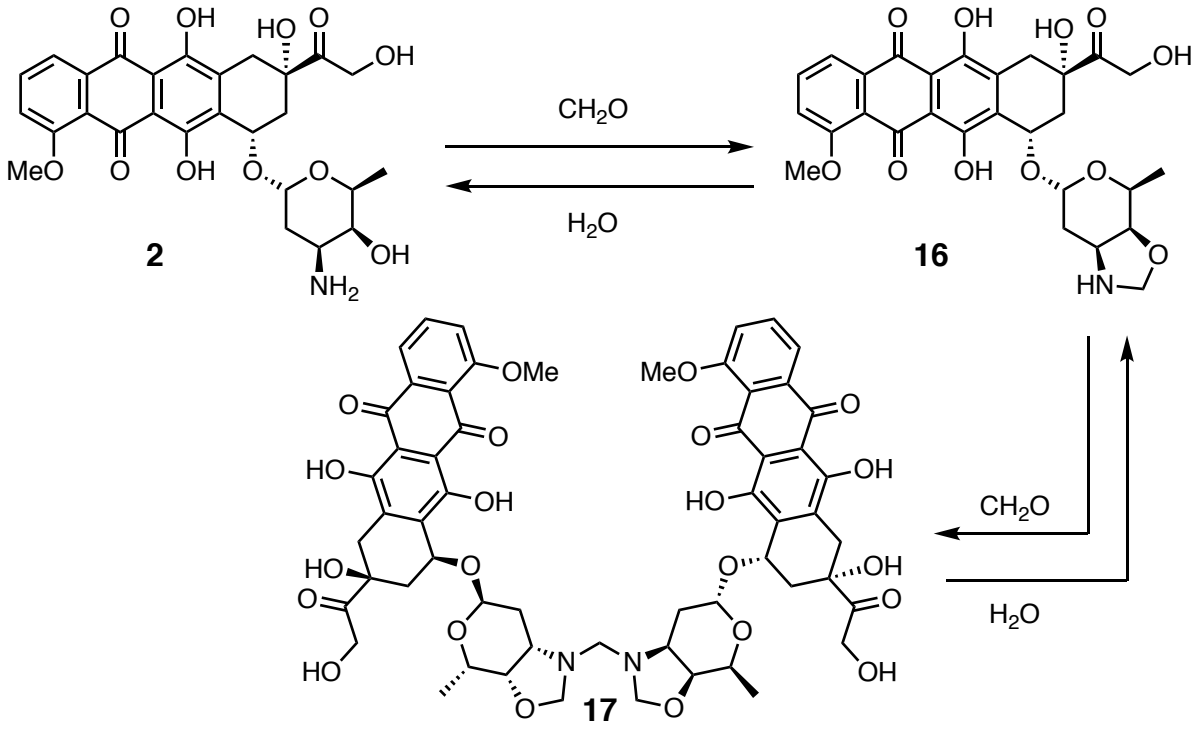

Gratifyingly, **16** and **17** were found to be exquisitely more cytotoxic than **2** in a variety of cancer cell lines, including some resistant cell lines, but not in cardiomyocytes, as a comparison of cell growth inhibition data shows (Table 1.2).[71,72]

Table 1.2 Comparison of cell growth inhibition data[a] for dox **2** and doxaz **16** in a variety of cancer cell lines.[71,72]

Cell Line	Cancer Type	2	16
H2122	Non Small-Cell Lung	-6.70	-8.40
SHP-77	Small-Cell Lung	> -6.00	-8.70
A375	Skin	-6.70	-9.00
PC-3	Prostate	-6.70	-9.00
DU-145	Prostate	-7.15	-8.52
MCF-7	Breast	-6.52	-8.70
ADR-RES	Ovarian	-5.00	-9.00
MDA-MB-435	Breast	-6.82	-7.96
Hep G2	Liver	-6.70	-7.96
SK-HEP-1	Liver	-7.00	-8.40
MiaPaCa-2	Pancreas	-6.52	-8.52
BxPC3	Pancreas	-6.52	-8.00
HeLaS3	Cervix	-7.46	-8.52
Mean	–	**> -6.60**	**-8.51**
H9c2(2-1)	Heart	-7.52	-7.52

[a] IC_{50} values are reported as log M.

Over the decades since doxaz **16** were first prepared, it has become evident that the **16** induces cell death through a mechanism distinct from that of **2**. First, **16** is >1.90 orders of magnitude more cytotoxic on average than **2** against a variety of cancer cell lines (Table 1.2).[72] Also, according to a National Cancer Institute (NCI) 67 human cancer cell line screen, the cytotoxicity of **16** correlates only modestly (0.68) with that of **2**, and instead correlates better with that of DNA crosslinking agents (Figure 1.4).[71,72] However, direct evidence that the MoA for **2** and that of **16** differ comes from a comparison of data showing the cell cycle distribution and induction of apoptosis in TopoII-positive *vs*. TopoII-deficient cells following treatment with **2**/**16**. Through a well-documented TopoII-dependent mechanism, dox **2** induces G2/M arrest in HCT-116 colon cancer cells and HL-60 leukimia cells; whereas, doxaz **16** does not induce G2/M arrest, despite inducing apoptosis 4-fold better than **2**, in the same cell lines.[72] Additionally,

growth inhibition from **16** is largely unchanged in TopoII-deficient cells (*e.g.* HL-60/MX2), while that of **2** is significantly diminished (Table 1.3).[72]

Figure 1.4 Best compare group for doxaz **16** using growth inhibition data in the National Cancer Institutes Developmental Therapeutics Program Database.* Correlation numbers are shown below each structure, NSC numbers are given in parentheses and generic names are provided when available.[72]

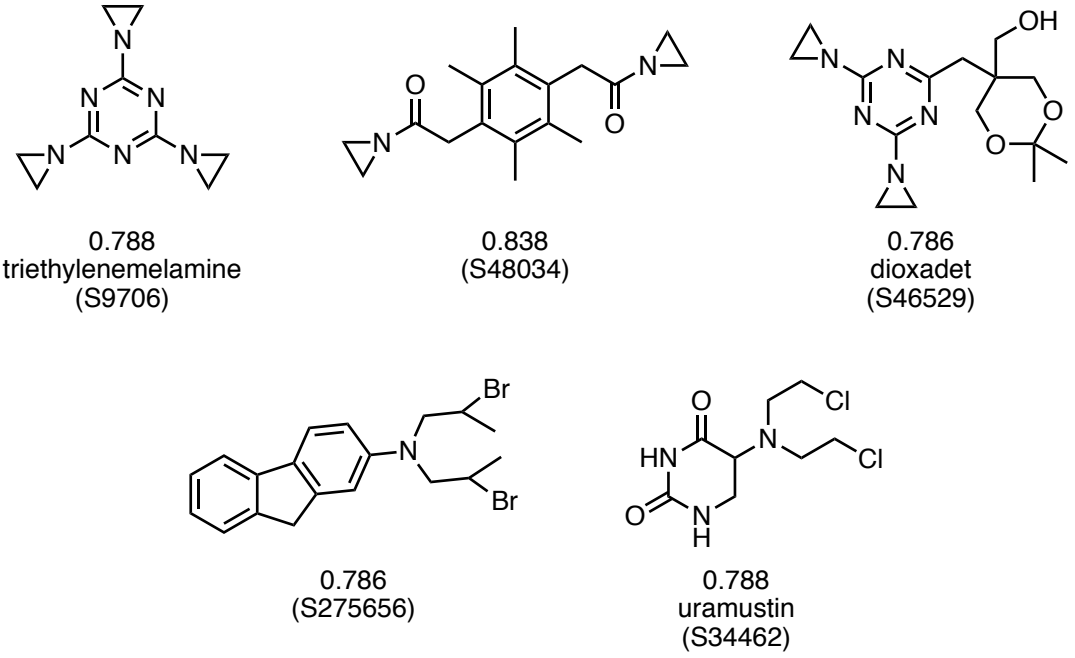

*Additional information on each compound can be found at the data search section of the NCIs DTP Web site, http://dtp.nci.nih.gov, using the NSC number.

Table 1.3 Comparison of cell growth inhibition data[a] for dox **2** and doxaz **16** in the HL-60 and HL-60/MX2 cell lines.[72]

Cell Line	Cancer Type	TopoII	2	16
HL-60	Leukimia	+	-6.96	-9.40
HL-60/MX2	Leukemia	-	-6.07	-9.22

[a] IC_{50} values are reported as log M.

The activity of **16** has additionally been shown to be independent of ROS-mediated cytotoxicity. As is evident from Table 1.4, growth inhibition of cells co-treated with either **2** or **16** and the clinically approved drug, dextrazoxane **19** (Scheme 1.5),[73] which is capable of removing iron from iron/anthracycline complexes thereby reducing free radical formation via Fenton chemistry, is largely unaffected for doxaz **16** but is significantly diminished for dox **2**.

Table 1.4 Comparison of cell growth inhibition data[a] for dox **2** and doxaz **16** with and without dextrazoxane **19** in a variety of cell lines.[72]

Cell Line	Tissue	2	2+19	16	16+19
MCF-7	Breast	-6.52	-5.52	-8.52	-8.52
SK-HEP-1	Liver	-7.00	-5.98	-8.40	-8.30
MiaPaCa-2	Pancreas	-6.52	-5.00	-8.52	-8.40
PC-3	Prostate	-6.40	-5.41	-7.96	-7.96
H9c2(2-1)	Heart	-7.52	-6.09	-7.52	-7.00

[a] IC_{50} values are reported as log M.

Scheme 1.5 Hydrolytic activation of dextrazoxane **19** (ICRF-187), a clinically approved drug for use in cancer patients to prevent anthracycline-mediated cardiotoxicity, to the iron-chelator **22** (ICRF-198).[73]

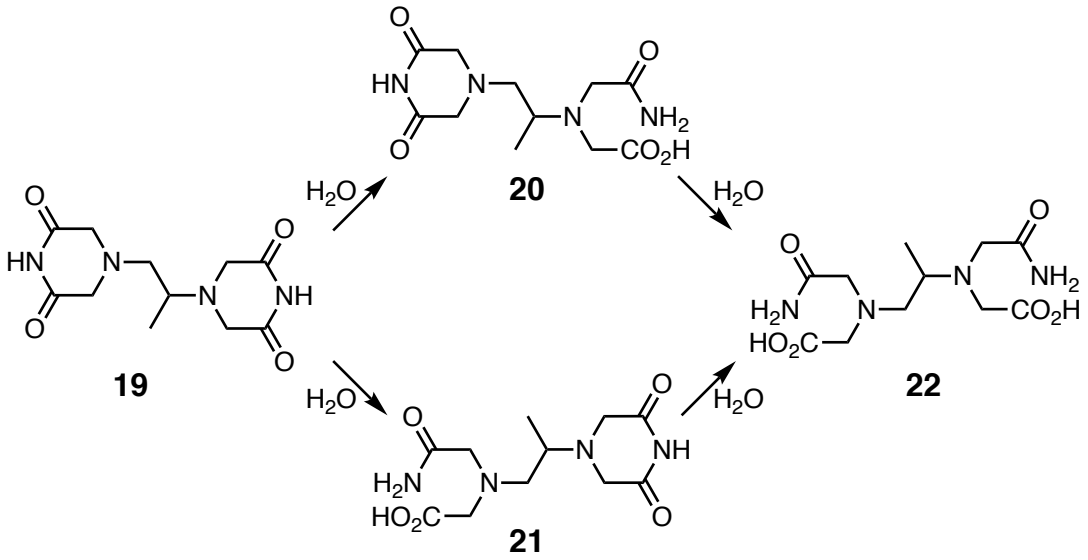

As mentioned above, chemotherapies using **2** are limited by (1) drug resistance and (2) chronic cardiotoxicity.[11] Doxaz **16** is believed to have the potential for overcoming these limitations by (1a) mediating cell death in a TopoII-independent fashion and (1b) by being neutrally charged at physiological pH and (2) by selectively increasing the drug's toxicity towards cancer cells over cardiomyocytes. First, the TopoII-independent MoA for doxaz **16** renders changes in TopoII expression or activity by cancer cells an ineffective resistance mechanism. Second, overexpression of the P-170 glycoprotein efflux pump protein is the primary mechanism by which resistant cell lines avoid the activity of drugs to which they are exposed. The P-170 efflux pump recognizes positively charged xenobiotics and selectively removes them from inside of the cell. Given that doxaz **16** is uncharged at physiological pH, **16** is not a substrate for the efflux pump. Finally, the equal toxicity of dox **2** and doxaz **16** towards cardiomyocytes (log IC_{50} = -7.52 in H9c2(2-1) heart cells), combined with the increased toxicity of **16** *vs.* **2** in tumor cells (Table 1.2), may therefore allow for a lower dose of **16** to be administered and, thus, provide a cardio-protective effect for patients.

However, systemic administration of unmodified **16** is not feasible. Due to the short half-life of the oxazolidine ring under physiological conditions ($t_{1/2}$ ~3−3.5 min), the super-potent drug-formaldehyde conjugate cannot reach the tumor environment *in vivo* and exert its effects as intended prior to hydrolysis. Additionally, despite encouraging *in vitro* data for **16**, a study conducted through the Developmental Therapeutics Program of the NCI determined that the LD_{50} of **16**/**17** formulated in DMSO and injected i.v. in mice is only ~0.2 mg/kg of body weight. A prodrug strategy would therefore be required to realize the potential of doxaz **16** as a chemotherapeutic.

1.5 References

1. Brighton, D.; Wood, M. *The Royal Marsden Hospital Handbook of Cancer Chemotherapy: A Guide for the Multidisciplinary Team*; Elsevier Churchill Livingstone: Edinburgh, NY, 2005.

2. Cassinelli, G.; Orezzi, P. "La Daunomicina: Un Nuovo Antibiotico ad Attivita Citostatica, Isolamento e Propriety" *G. Microbiol.* **1963**, *11*, 167−174.

3. Di Marco, A.; Gaetani, M.; Orezzi, P.; Scarpinato, B. M.; Silvestrini, R.; Soldati, M.; Dasdia, T.; Valentini, L. "Daunomycin: A New Antibiotic of the Rhodomycin Group" *Nature* **1964**, *201*, 706−707.

4. Tan, C.; Tasaka, H.; Yu, K. P.; Murphy, M. L.; Karnofsky, D. A. "Daunomycin, an Antitumor Antibiotic, In the Treatment of Neoplastic Disease: Clinical Evaluation with Special Reference to Childhood Leukemia" *Cancer* **1967**, *20*, 333−353

5. Arcamone, F.; Cassinelli, G.; Fantini, G.; Grein, A.; Orezzi, P.; Pol, C.; and Spalla, C. "Adriamycin, 14-Hydroxydaunomycin, a New Antitumor Antibiotic from *S. peucetius* var. *caesius*" *Biotechnol. Bioeng*. **1969**, *11*, 1101−1110.

6. Di Marco, A.; Gaetani, M; Scarpinato, B. "Adriamycin (NSC-123,127): A New Antibiotic with Antitumor Activity" *Cancer Chemother. Rep. (Part 1)* **1969**, *53*, 33−37.

7. Bonadonna, G.; Monfardini, S.; de Lena, M.; Fossati-Bellani, F.; Beretta, G. "Phase I and Preliminary Phase II Evaluation of Adriamycin (NSC 123127)" *Cancer Res*. **1970**, *30*, 2572−2582.

8. Tan, C.; Etcubanas, E.; Wollner, N.; Rosen, G.; Gilladoga, A.; Showel, J. "Adriamycin−An Antitumor Antibiotic in the Treatment of Neoplastic Diseases" *Cancer* **1973**, *32*, 9−17.

9. Arcamone, F. *Doxorubicin Anticancer Antibiotics*. Academic Press: New York, 1981.

10. DeVita, V. T.; Hellman, S.; Rosenberg, S. A. In *Cancer: Principles and Practice of Oncology*, 7th ed.; Lippincott-Raven: Philadelphia, PA, 2005.

11. Young, R. C.; Ozols, R. F.; Myers, C. E. "Medical Progress: The Anthracycline Antineoplastic Drugs" *New Engl. J. Med.* **1981**, *305*, 139−153.

12. Sweatman, T. W.; Isreal, M. Anthracyclines. In *Cancer Therapeutics, Experimental and Clinical Agents.* Teicher B. A., Ed.; Humana Press: Totowa, NJ, 1997; pp 113−135.

13. Arcamone, F.; Bernardi, L.; Giardino, P.; Patelli, B.; Di Marco, A.; Casazza, A. M.; Pratesi, G.; Reggiani, P. "Synthesis and Antitumor Activity of 4-

Demethoxydaunorubicin, 4-Demethoxy-7,9-diepidaunorubicin, and Their β-Anomers" *Cancer Treat. Rep*. **1976**, *60*, 829–834.

14. Casazza, A. M.; Di Marco, A.; Bonadonna, G.; Bonfante, V.; Bertazzoli, C.; Bellini, O.; Pratesi, G.; Sala, L.; Ballerini, L. Effects of Modifications in Position 4 of the Chromophore or in Position 4′ of the Aminosugar, on the Antitumor Activity and Toxicity of Daunorubicin and Doxorubicin. In *Anthracyclines: Current Status and New Developments*; Crooke, S. T., Reich, S. D., Eds.; Academic Press: New York, 1980; pp 403–430.

15. Casazza, A. M.; Pratesi, G.; Giuliani, F.; Di Marco, A. "Antileukemic Activity of 4-Demethoxydaunorubicin in Mice" *Tumori* **1980**, *66*, 549–564.

16. Weiss, R. B. "The Anthracyclines: Will We Ever Find a Better Doxorubicin?" *Semin. Oncol*. **1992**, *19*, 670−686.

17. Gewirtz, D. A. "A Critical Evaluation of the Mechanisms of Action Proposed for the Antitumor Effects of the Anthracycline Antibiotics Adriamycin and Daunorubicin" *Biochem. Pharmacol.* **1999**, *57*, 727−741.

18. Minotti, G., Menna, P., Salvatorelli, E., Cairo, G., and Gianni, L. "Anthracyclines: Molecular Advances and Pharmacologic Developments in Antitumor Activity and Cardiotoxicity" *Pharmacol. Rev*. **2004**, *56*, 185−229.

19. Gigli, M.; Doglia, S. M.; Millot, J. M.; Valentini, L.; Manfait, M. "Quantitative Study of Doxorubicin in Living Cell Nuclei by Microspectrofluorometry" *Biochim. Biophys. Acta* **1988**, *950*, 13−20.

20. Coley, H. M.; Amos, W. B.; Twentyman, P. R.; Workman, P. "Examination by Laser Scanning Confocal Fluorescence Imaging Microscopy of the Subcellular Localization of Anthracyclines in Parent and Multidrug Resistant Cell Lines" *Br. J. Cancer* **1993**, *67*, 1316−1323.

21. Manfait, M.; Alix, A. J.; Jeannesson, P.; Jardillier, J. C.; Theophanides, T. "Interaction of Adriamycin with DNA as Studied by Resonance Raman Spectroscopy" *Nucleic Acids Res*. **1982**, *10*, 3803−3816.

22. Tewey, K. M.; Rowe, T. C.; Yang, L.; Halligan, B. D.; Liu, L. F. "Adriamycin-Induced DNA Damge Mediated by Mammalian DNA Topoisomerase II" *Science* **1984**, *226*, 466−468.

23. Bellarosa, D.; Ciucci, A.; Bullo, A.; Nardelli, F.; Manzini, S.; Maggi, C. A." Apoptotic Events in a Human Ovarian Cancer Cell Line Exposed to Anthracyclines" *J. Pharmacol. Exp. Ther*. **2001**, *296*, 276−283.

24. Wang, J. C. "DNA Topoisomerases" *Annu. Rev. Biochem.* **1985**, *54*, 665−697.

25. Heck, M. M. S.; Earnshaw, W. C. "Topoisomerase II: A Specific Marker for Cell Proliferation" *J. Cell Biol.* **1986**, *103*, 2569−2581.

26. Harland, R. M.; Weintraub, H.; McKnight, S. L. "Transcription of DNA Injected Into *Xenopus* Oocytes is Influenced by Template Topology" *Nature* **1983**, *302*, 38−43.

27. Kaguni, J. M.; Kornberg, A. "Replication Initiated at the Origin (oriC) of E. coli Chromosome Reconstituted with Purified Enzymes" *Cell* **1984**, *38*, 183−190.

28. DiNardo, S.; Voelkel, K.; Sternglanz, R. "DNA Topoisomerase II Mutant of *Saccharomyces cerevisiae*: Topoisomerase II is Required for Segregation of Daughter Molecules at the Termination of DNA Replication" *Proc. Natl. Acad. Sci. U.S.A.* **1984**, *81*, 2616−2620.

29. Painter, R. B. "A Replication Model for Sister Chromatid Exchange" *Mutat. Res.* **1980**, *70*, 337−341.

30. Holm, C.; Goto, T.; Wang, J. C.; Botstein, D. "DNA Topoisomerase II is Required at the Time of Mitosis in Yeast" *Cell* **1985**, *41*, 553−563.

31. Liu, L. F.; Liu, C. C.; Alberts, B. M. "Type II DNA Topoisomerases: Enzymes that can Unknot a Topologically Knotted DNA Molecule via a Reversible Double-Strand Break" *Cell* **1980**, *19*, 697−707.

32. Liu, L. F.; Rowe, T. C.; Yang, L.; Tewey, K. M.; Chen, G. L. "Cleavage of DNA by Mammalian DNA Topoisomerase II" *J. Biol. Chem*. **1983**, *258*, 15365−15370.

33. Swift, L. P.; Rephaeli, A.; Nudelman, A.; Phillips, D. R.; Cutts, S. M. "Doxorubicin-DNA Adducts Induce a Non-Topoisomerase II–Mediated Form of Cell Death" *Cancer Res.* **2006**, *66*, 4863−4871.

34. Deffie, A. M.; Batra, J. K.; Goldenberg, G. J. "Direct Correlation Between DNA Topoisomerase II Activity and Cytotoxicity in Adriamycin−Sensitive and –Resistant P388 Leukimia Cell Lines" *Cancer Res*. **1989**, *49*, 58−62.

35. Webb, C. D.; Latham, M. D.; Lock, R. B.; Sullivan, D. M. "Attenuated Topoisomerase II Content Directly Correlates with a Low Level of Drug Resistance in a Chinese Hamster Ovary Cell Line" *Cancer Res*. **1991**, *51*, 6543−6549.

36. Moore, H. W. "Bioactivation as a Model for Drug Design Bioreductive Alkylation" *Science* **1977**, *197*, 527−532.

37. Moore, H. W.; Czerniak, R. "Naturally Occurring Quinones as Potential Bioreductive Alkylating Agents" *Med. Res. Rev.* **1981**, *1*, 249−280.

38. Sinha, B. K. "Binding Specificity of Chemically and Enzymatically Activated

Anthracycline Anticancer Agents to Nucleic Acids" *Chem. Biol. Interact.* **1980**, *30*, 67−77.

39. Sinha, B. K.; Gregory, J. L. "Role of One-Electron and Two-Electron Reduction Products of Adriamycin and Daunomycin in Deoxyribonucleic Acid Binding" *Biochem. Pharmacol*. **1981**, *30*, 2626−2629.

40. Sinha, B. K.; Trush, M. A.; Kennedy, K. A.; Mimnaugh, E. G. "Enzymatic Activation and Binding of Adriamycin to Nuclear DNA" *Cancer Res*. **1984**, *44*, 2892−2896.

41. Bartoszek, A.; Wolf, C. R. "Enhancement of Doxorubicin Toxicity Following Activation by NADPH Cytochrome P450 Reductase" *Biochem. Pharmacol.* **1992**, *43*, 1449−1457.

42. Kleyer, D. L.; Koch, T. H. "Electrophilic Trapping of the Tautomer of 7-Deoxy-daunomycinone. A Possible Mechanism for Covalent Binding of Daunomycin to DNA" *J. Am. Chem. Soc.* **1983**, *105*, 5154−5155.

43. Kleyer, D. L.; Koch, T. H. "Mechanistic Investigation of Reduction of Daunomycin and 7-Deoxydaunomycinone with Bi(3,5,5-trimethyl-2-oxomorpholin-3-yl)" *J. Am. Chem. Soc.* **1984**, *106*, 2380−2387.

44. Bolt, M.; Guadiano, G.; Koch, T. H. "Substituent Effects on the Redox Chemistry of Anthracycline Antitumor Drugs" *J. Org. Chem.* **1987**, *52*, 2146−2153.

45. Gaudiano, G.; Koch, T. H. "Redox Chemistry of Anthracycline Antitumor Drugs and Use of Captodative Radicals as Tools for its Elucidation and Control" *Chem. Res. Toxicol*. **1991**, *4*, 2−16.

46. Lown, W. J.; Chen, J. A.; Plambeck, J. A.; Acton, E. M. "Further Studies on the Generation of Reactive Oxygen Species from Activated Anthracyclines and the Relationship to Cytotoxic Action and Cardiotoxic Effects" *Biochem. Pharmacol.* **1982**, *31*, 575−581.

47. Imlay, J. A.; Chin, S. M.; Linn, S. "Toxic DNA Damage by Hydrogen Peroxide Through the Fenton Reaction *In Vivo* and *In Vitro*" *Science* **1988**, 2*40*, 640−642.

48. Minotti, G.; Menna, P.; Salvatorelli, E.; Cairo, G.; Gianni, L. "Anthracyclines: Molecular Advances and Pharmacologic Developments in Antitumor Activity and Cardiotoxicity" *Pharmacol Rev*. **2004**, *56*, 185−229.

49. Bagchi, D.; Bagchi, M.; Hassoun, E. A.; Kelly, J.; Stohs, S. J. "Adriamycin-Induced Hepatic and Myocardial Lipid Peroxidation and DNA Damage, and Enhanced Excretion of Urinary Lipid Metabolites in Rats" *Toxicology* **1995**, *95*, 1−9.

50. Myers, C. E.; Gianni, L.; Simone, C. B.; Klecker, R.; Greene, R. "Oxidative Destruction of Erythrocyte Ghost Membranes Catalyzed by the Doxorubicin-Iron Complex"

Biochemistry **1982**, *21*, 1707−1712.

51. Doroshow, J. H. Role of Reactive Oxygen Metabolism in Cardio Toxicity of Anthracycline Antibiotics. In *Anthracycline Antibiotics: New Analogues, Methods of Delivery and Mechanisms of Action* (Priebe, W., ed.); American Chemical Society: Washington, DC, 1995; pp 259−267.

52. Von Hoff, D. D.; Layard, M. W.; Basa, P.; Davis, H. L., Jr.; Von Hoff, A. L.; Rozencweig, M.; Muggia, F. M. "Risk Factors for Doxorubicin-induced Congestive Heart Failure" *Ann. Intern. Med*. **1979**, *91*, 710−717.

53. Ferreira, A. L.; Matsubara, L. S.; Matsubara, B. B. "Anthracycline-induced Cardiotoxicity" *Cardiovasc. Hematol. Agents Med. Chem*. **2008**, *6*, 278−281.

54. Simunek, T.; Sterba, M.; Popelova, O.; Adamcova, M.; Hrdina, R.; Gersl, V. "Anthracycline-induced Cardiotoxicity: Overview of Studies Examining the Roles of Oxidative Stress and Free Cellular Iron" *Pharmacol. Rep.* **2009**, *61*, 154−171.

55. Steinherz, L.; Steinherz, P. "Delayed Cardiac Toxicity from Anthracycline Therapy" *Pediatrician* **1991**, *18*, 49−52.

56. Cullinane, C.; Phillips, D. R. "Induction of Stable Transcriptional Blockage Sites By Adriamycin: GpC Specificity of Apparent Adriamycin-DNA Adducts and Dependence on Iron (III) Ions" *Biochemistry* **1990**, *29*, 5638−5646.

57. Taatjes, D. J.; Gaudiano, G.; Resing, K.; Koch, T. H. "Alkylation of DNA by the Anthracycline, Antitumor Drugs Adriamycin and Daunomycin" *J. Med. Chem.* **1996**, *39*, 4135−4138.

58. Taatjes, D. J.; Gaudiano, G.; Koch, T. H. "Production of Formaldehyde and DNA−Adriamycin or DNA−Daunomycin Adducts, Initiated through Redox Chemistry of Dithiothreitol/Iron, Xanthine Oxidase/NADH/Iron, or Glutathione/Iron" *Chem. Res. Toxicol*. **1997**, *10*, 953−961.

59. Taatjes, D. J.; Gaudiano, G.; Resing, K.; Koch, T. H. "Redox Pathway Leading to the Alkylation of DNA By the Anthracycline, Antitumor Drugs Adriamycin and Daunomycin" *J. Med. Chem.* **1997**, *40*, 1276−1286.

60. Taatjes, D. J.; Koch, T. H. "Growth Inhibition, Nuclear Uptake, and Retention of Anthracycline-Formaldehyde Conjugates in Prostate Cancer Cells Relative to Clinical Anthracyclines" *Anticancer Res*. **1999**, *19*, 1201−1208.

61. Wang, A. H. J.; Gao, Y. G.; Liaw, Y. C.; Li, Y. K. "Formaldehyde Crosslinks Daunorubicin and DNA Efficiently: HPLC and X-ray Diffraction Studies" *Biochemistry* **1991**, *30*, 3812−3815.

62. Gao, Y. G.; Liaw, Y. C.; Li, Y. K.; Van der Marel, G. A.; Van Boom, J. H.; Wang, A. H. J. "Facile Formation of a Crosslinked Adduct Between DNA and the Daunorubicin Derivative MAR70 Mediated by Formaldehyde: Molecular Structure of the MAR70-d(CGTnACG) Covalent Adduct" *Proc. Nat. Acad. Sci. U.S.A.* **1991**, *88*, 4845−4849.

63. Zeman, S. M.; Phillips, D. R.; Crothers, D. M. "Characterization of Covalent Adriamycin-DNA Adducts" *Proc. Natl. Acad. Sci. U.S.A.* **1998**, *95*, 11561−11565.

64. Post, G. C.; Barthel, B. L.; Burkhart, D. J.; Hagadorn, J. R.; Koch, T. H. "Doxazolidine, A Proposed Active Metabolite of Doxorubicin That Cross-Links DNA" *J. Med. Chem.* **2005**, *48*, 7648−7657.

65. Kato, S.; Burke, P. J.; Fenick, D. J.; Taatjes, D. J.; Bierbaum, V. M.; Koch, T. H. "Mass Spectrometric Measurement of Formaldehyde Generated in Breast Cancer Cells Upon Treatment with Anthracycline Antitumor Drugs" *Chem. Res. Toxicol*. **2000**, *13*, 509−516.

66. Cutts, S. M.; Phillips, D. R. "Use of Oligonucletides to Define the Site of Interstand Crosslinks Induced by Adriamycin" *Nucleic Acids Res*. **1995**, *23*, 2450−2456.

67. Cullinane, C.; Cutts, S. M.; Panousis, C.; Phillips, D. R. "Interstrand Cross-Linking by Adriamycin in Nuclear and Mitochondrial DNA of MCF-7 Cells" *Nucleic Acids Res.* **2000**, *28*, 1019−1025.

68. van Rosmalen, A.; Cullinane, C.; Cutts, S. M.; Phillips, D. R. "Stability of Adriamycin-induced DNA Adducts and Interstrand Crosslinks" *Nucleic Acids Res.* **1995**, *23*, 42−50.

69. Moufarij, M. A.; Cutts, S. M.; Neumann, G. M.; Kimura, K.; Phillips, D. R. "Barminomycin Functions as a Potent Pre-Activated Analogue of Adriamycin" *Chem. Biol. Interact*. **2001**, *138*, 137−153.

70. Coldwell, K. E.; Cutts, S. M.; Ognibene, T. J.; Henderson, P. T.; Phillips, D. R. "Detection of Adriamycin–DNA Adducts by Accelerator Mass Spectrometry at Clinically Relevant Adriamycin Concentrations" *Nucleic Acids Res*. **2008**, *36*, e100.

71. NCIS cancer cell line screen of doxazolidine.

72. Kalet, B. T.; McBryde, M. B.; Espinosa, J. M.; Koch, T. H. "Doxazolidine Induction of Apoptosis by a Topoisomerase II Independent Mechanism" *J. Med. Chem.* **2007**, *50*, 4493−4500.

73. Weiss, G.; Loyevsky, M.; Gordeuk, V. R. "Dextrazoxane (ICRF-187)" *Gen. Pharmacol. The Vascular Sys.* **1999**, *32*, 155−158.

CHAPTER 2

Prodrugs

2.1 Introduction

The term *prodrug* was first introduced into the lexicon by Albert in 1958 to describe a molecule that is biologically inert in its current form, but after administration is metabolized *in vivo* to produce a pharmacologically active drug.[1,2] Nature itself produces compounds that modern medicine has come to recognize as being prodrugs. For example, salicin **1** is a β-D-glucopyranoside of salicyl alcohol **2** that is traditionally obtained from hot water extractions of the ground bark from poplar (*Populus*) and willow (*Salix*) trees.[3] Salicin was used as a mild analgesic, anti-inflammatory and antipyretic agent in traditional herbal medicine long before its chemical structure and metabolism were understood. However, it is now recognized that salicin is a prodrug activated by hydrolysis of the glycosidic bond of **1** to give glucose and salicyl alcohol **2.** Subsequent oxidation of **2** gives salicylic acid **3**, which is the active drug responsible for the therapeutic effects (Scheme 2.1). Another prodrug of **3**, acetyl-salicylic acid was first prepared by the German chemists Hoffmann and Eichengrün at Bayer labs in 1897 and

Scheme 2.1 Salicin **1** is a naturally occurring prodrug of salicylic acid **3**.

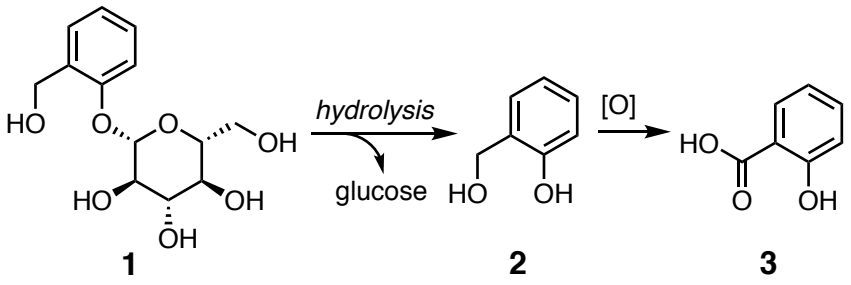

Aspirin™, as it is better known, is arguably the most widely used synthetic prodrug in the world today.[4,5]

Prodrugs, in general, are designed to mask undesirable properties of a compound and optimize the absorption, distribution, metabolism, and excretion (ADME) of the drug.[6] In principle, a prodrug strategy can be used to improve any aspect of a drug or drug candidate's pharmacokinetic profile: (1) improved absorption may be realized through a modification, such as acylation of an amine or alcohol, that allows a drug to become orally active[7-10] or to penetrate the blood-brain barrier;[11] (2) distribution of an administered drug may be influenced through the use of targeting carrier groups, such as peptides[12,13] and antibodies,[12] that bind to receptors overexpressed on the surface of the diseased cell, thereby increasing the localized concentration of the attached drug in that tissue while simultaneously minimizing its concentration in healthy tissues; (3) metabolism may, for example, be slowed to provide a time-release dosage of the drug, as was done in the case of Vyvanse,[14] a lysine dimesylate prodrug of *d*-amphetamine developed as a slow-release formulation for more efficacious treatment of pediatric ADHD; and (4) **e**xcretion may be modulated by increasing the size of the administered compound, by PEGylation for example, such that its removal from the body is delayed and a greater percentage of the drug circulates for a sufficiently long period of time to reach its intended target.[15-17] The tremendous scope of issues that can be addressed through prodrug strategies to improve the performance of existing drugs and develop promising drug candidates has resulted in significant interest in the field over the last several decades with an estimated 10% of all clinical drugs in use around the world today classified as prodrugs.[6] Numerous reviews on the various applications of prodrugs have been published and the reader is encouraged to explore the literature further for more exhaustive accounts on the subject.[18-20]

2.2 Prodrug Design in Anticancer Chemotherapy

The general principle of anticancer chemotherapy involves the killiong of rapidly dividing cells by agents which act upon cellular processes involved in cell proliferation, such as DNA, RNA and protein biosynthesis. However, as many types of normal cells also regenerate rapidly, such as the epithelia lining of the gut and hair folucles, they too are subject to the effects of drugs that disrupt these processes. As such, cancer therapy is often limited by undesirable side-effects accompanying chemotherapy which often restrict the tolerable dosages and duration of treatment a patient can receive. In order to improve upon the effectiveness of chemotherapeutics, prodrug strategies have been developed with the aim of selectively delivering drugs to neoplastic tissues so as to minimize the harmful side-effects encountered by systemic administration of the drugs, thereby affording patients a better quality of life.

However, designing highly selective, tumor-targeting prodrugs remains a difficult challenge for medicinal chemists today due, in general, to the narrow therapeutic window of the active drugs.[21] *A priori* prediction of the totality of effects a particular modification to a drug will have on the biological response to that molecule is simply not possible. Numerous factors contribute to the elicited response, including the three dimensional structure, molecular weight, solubility, permeability and immunogenicity of a molecule. Additionally, differences in enzyme expression, vascularization, and interstitial pressure may also affect the distribution of the prodrug *in vivo* and create variations in the amount of drug that is actually delivered. Therefore, optimizing the properties of a prodrug to meet the specific demands inherent to its application is a critical aspect of prodrug design.

Consider the generic dipartite prodrug shown in Figure 2.1, which is comprised of two domains: a drug **D** and a trigger **T**. The assembled **D-T** prodrug is biologically inert and can be

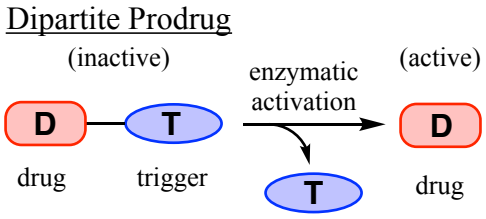

Figure 2.1 Activation of a generic dipartite prodrug.

administered systemically without exposing normal cells in healthy tissues to the cytotoxic effects of **D**. As **D-T** passes through the tumor environment, however, a tumor-associated enzyme (*e.g.* protease, glucuronidase or carboxylesterase) may cleave the **D-T** bond and release the active drug **D**. For this strategy to be successful, however, the coupling of **D** to **T** must produce a sufficiently robust **D-T** conjugate that does not release **D** in an uncontrolled fashion throughout the body following administration, but which also does not prevent the release of **D** when the prodrug comes into contact with the tumor-associated enzyme. For instance, sufficient serum stability is required for a prodrug administered i.v. to reach the tumor intact, but if the **D-T** bond is too robust and cannot be hydrolyzed in the tumor environment by the tumor-associated enzyme as intended, then the active drug will not be released and the prodrug will have no beneficial effect on the health of the recipient.

Such was the case with early attempts to create a carbamate prodrug of doxazolidine **4** by acylation of the 3'-nitrogen with alkyl chloroformates (Scheme 2.2).[22] The carbamate **5** effectively stabilized the oxazolidine ring towards hydrolysis and prevented the loss of formaldehyde. However, acylation also prevented formation of the covalent drug-DNA adduct responsible for the super-cytotoxicity of **4** and the carbamate bond of **5** was too hindered to be enzymatically hydrolyzed. So, despite what is known about carboxylesterases and their ability to

hydrolyze seemingly similar bonds,[23] the dipartite carbamate prodrugs **5** (R = alkyl) were devoid of activity and this approach had to be abandoned.

Scheme 2.2 Acylation of doxazolidine **4** afforded the stable but inactive dipartite prodrugs **5,** which could not be activated by carboxylesterases due to the stearic hindrance surrounding the carbamate.[22]

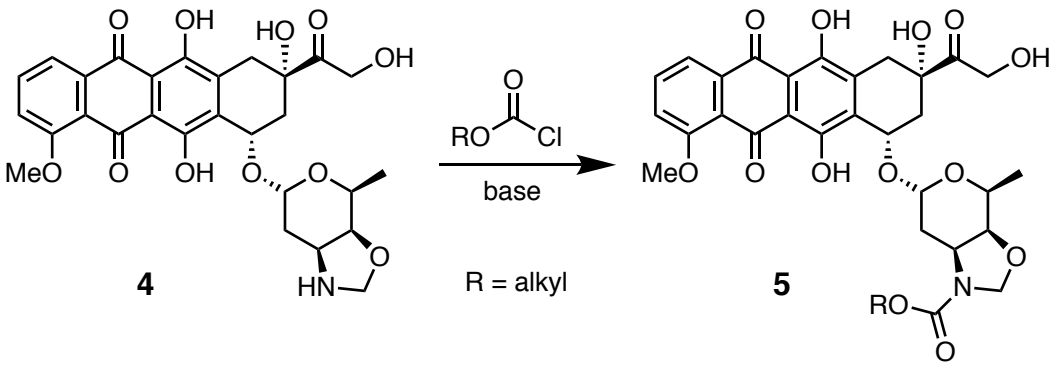

Now consider the generic tripartite prodrug shown in Figure 2.2, which is comprised of three domains: a drug **D** coupled indirectly to the trigger **T** via a spacer **S**. In this case, the ability of the prodrug to effectively localize at the tissue of interest is maintained through the action of **T**, but the release of the **D** from the prodrug at the targeted tissue may be greatly enhanced by the spatial separation between the bulky drug **D** and trigger **T** domains afforded by the spacer **S**. Of course, separation of the **D-S** fragment afforded after liberation of **T** would still be required to release the active drug. Thus, development of a self-immolative spacer that, upon enzymatic cleavage of the **S-T** bond of the intact **D-S-T** prodrug, would undergo a spontaneous elimination reaction to sever the remaining **D-S** linkage and release the active drug **D** was a critically important step in the evolution of prodrug design.

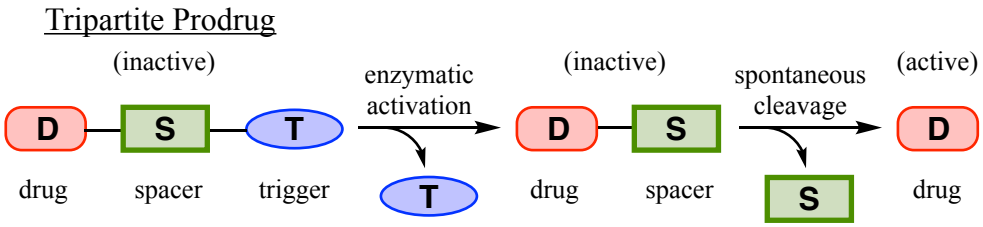

Figure 2.2 Activation of a generic tripartite prodrug.

The Katzenellenbogen-spacer, a *p*-amidobenzyloxy carbonyl-moiety (PABC), introduced in 1981 by Katzenellenbogen *et al.* is a self-immolative spacer used in tripartite prodrugs (Figure 2.3).[24]

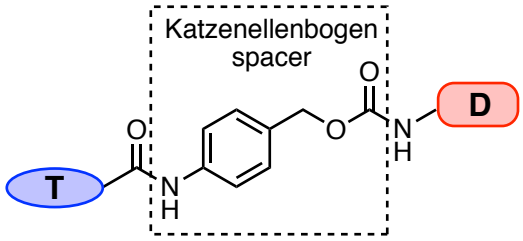

Figure 2.3 Generic tripartite prodrug containing the PABC Katzenellenbogen-spacer.[24]

After administration of the prodrug **6**, enzymatic cleavage of the anilide bond between the triggering group and PABC-spacer results in rapid 1,6-elimination of the iminoquinone methide **8** and, following spontaneous decarboxylation of the liberated carbamic acid, release of the active drug **9** (Scheme 2.3).[24]

Scheme 2.3 Activation mechanism of a prodrug **6** containing the Katzenellenbogen-spacer by 1,6-elimination of the iminoquinone methide **8** and, following spontaneous decarboxylation of the liberated carbamic acid, release of the active drug **9**.[24]

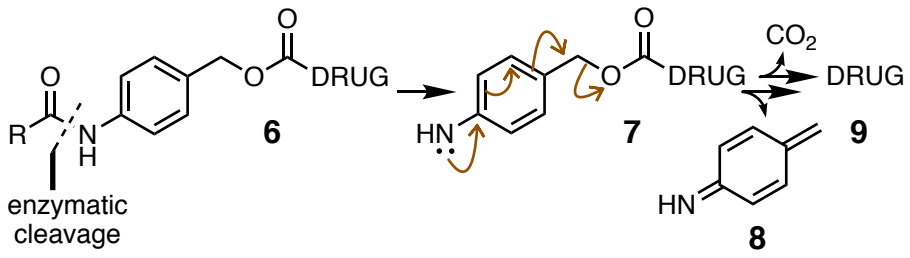

Tripartite prodrug designs incorporating the Katzenellenbogen-spacer have become quite common. Most notably, the mAb-targeted monomethylauristatin E antimitotic, Brentuximab Vedotin **10**, which began Phase-III clinical trials in 2010 and received accelerated FDA-approval in 2011 (Figure 2.4) for use in patients with Hodgkin's lymphoma that are at high risk of relapse or progression following autologous stem-cell transplantation, contains the PABC-spacer.[25] While other spacer designs have been developed over the years,[26-33] adoption of the PABC Katzenellenbogen-spacer into the design of our prodrugs was an early decision and the focus of this work will deal exclusively with aspects of this strategy.

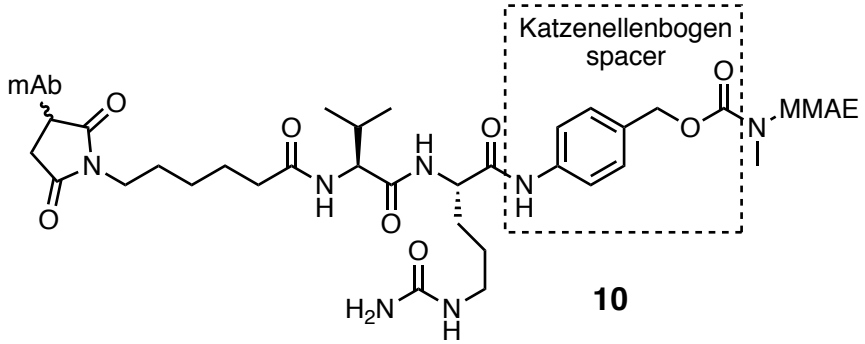

Figure 2.4 Structure of the mAb-targeted monomethylauristatin E antimitotic, Brentuximab Vedotin **6**, which contains the PABC Katzenellenbogen-spacer.[25]

2.3 Enzyme Targets for Anticancer Prodrug Therapy

The objective of anti-cancer prodrug therapy is the targeted delivery of an inert compound to cancer cells and the selective release of the active drug in or around the tumor environment. This avoids exposure of normal, healthy tissues to the cytotoxic drug whilst preserving an effective chemotherapy to combat the cancer. Due to the changes in gene expression that occur in cancer cells, elevated levels of certain enzymes have been linked to particular types of cancer and this can be exploited for targeted prodrug activation.[21] A summary of enzymes overexpressed in tumors and their substrate specificities is given in Table 2.1. In this section, two classes of enzymes (carboxylesterases and proteases) capable of activating tripartite prodrugs of doxazolidine and whose expression levels correlate with cancer progression and prognosis in difficult to treat cancer types are reviewed with an emphasis on their respective substrate specificities and how this influenced the design of our prodrugs.

Table 2.1 Summary of enzymes that are overexpressed in tumors.[21]

Enzyme	Function	Substrate Examples	Ref.
Carboxylesterases (CES1; CES2)	Hydrolysis or transesterification of xenobiotics	Esters, Carbamates & Thioesters	23, 34-38
Cathepsin B Cathepsin H Cathepsin L	Lysosomal degradation of proteins	Ala-Leu, Gly-Leu-Phe-Gly, Val-Cit Gly-Phe-Leu-Gly, Ala-Leu-Ala-Leu Arg-Arg-Leu	39-48
Cathepsin D	Degradation of ECM	Phe-Ala-Ala-Phe(NO_2)-Phe-Val-Leu-OM4P, Bz-Arg-Gly-Phe-Phe-Pro-4MβNA	49
Plasmin	Fibrinolysis, degradation of plasma proteins	D-Ala-Phe-Lys, D-Val-Leu-Lys, D-Ala-Trp-Lys	24, 50-58
uPA[a] tPA[b]	Activation of plasmin	Gly-Gly-Gly-Arg-Arg Arg-Val	59 60
PSA[c]	Liquefaction of semen	Mu[d]-His-Ser-Ser-Lys-Leu-Gln-Leu	61-69
M.Metalloproteases	Degradation of	Ac-Pro-Leu-Gly-Leu,	70-74

MMP-2 MMP-9	ECM and collagen	Ac-γE-Pro-Cit-Gly-Hof[e]-Tyr-Leu, Gly-Pro-Leu-Gly-Ile-Ala-Gly-Gln	
β-Glucuronidase	Hydrolysis of protein glucuronides	Glucuronosides	75-82

[a] Urokinase-type plasminogen activator.
[b] Tissue-type plasminogen activator.
[c] Prostate-specific antigen.
[d] Mu = morpholinocarbonyl.
[e] Hof = homophenylalanine.

Carboxylesterases

Carboxylesterases (CEs) are ubiquitous enzymes present in essentially all organisms, from *E. coli* to man, where they are believed to primarily play a protective role for the detoxification of xenobiotics.[23] Circumstantial evidence in support of this assertion is provided by the observation that CEs are highly expressed in the tissues most likely to encounter xenobiotics, such as the liver, kidney and the epithelial linings of the lung and gut and are promiscuous serine hydrolases capable of hydrolyzing esters, carbamates and thioesters present in wide range of structurally distinct and complex substrates.[34,35]

Five potential CE genes have been indentified in humans through genome sequencing analyses.[23] However, the biological activity of only three of these CEs (hCE1 [CES1], hiCE [CES2] and hBr3 [CES3]) has been evaluated to date and only hCE1 and hiCE have been exploited for prodrug activation.[34-38] Both hCE1 and hiCE are ~60 kDa cytoplasmic proteins that require processing in the endoplasmic reticulum (ER) to properly function, but have different substrate specificities and different expression levels in various tissues. Expression of hCE1 occurs primarily in the liver where it tends to hydrolyze esters consisting of small, planer alcohols and larger acid moieties, such as nitrophenylesters (NPEs), oseltamivir and heroin. Contrastingly, hiCE is primarily expressed in the gut and kidney and has variable expression in the liver. The substrate specificity for hiCE is roughly the inverse of that for hCE-1 with activity

against esters consisting of larger alcohols and smaller acid moieties. Despite their differences, both enzymes are capable of activating the anticancer prodrugs capecitabine **11** and irinotecan **12** (Figure 2.5) and considerable overlap exists between the substrates each enzyme is capable of hydrolysing.[23] A brief comparison of the two enzymes is summarized in Table 2.2 below.

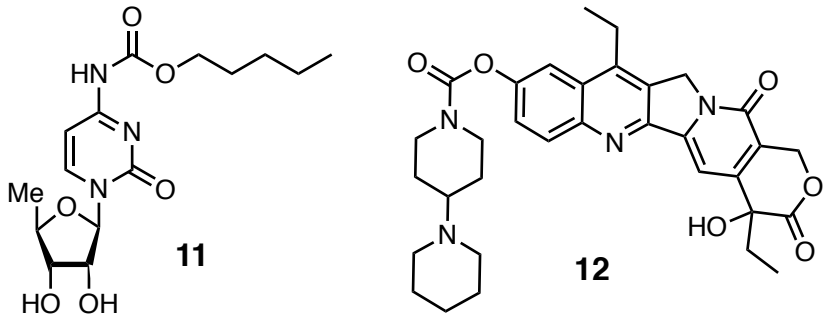

Figure 2.5 Structures of the clinically approved CE-activated anticancer prodrugs capecitabine **11** and irinotecan **12**.[23]

Table 2.2 Comparison of the properties of human carboxylesterases hCE-1 and hiCE.[23]

	Enzyme	
Property	**hCE-1**	**hiCE**
Gene Name	CES1	CES2
Size	60 kDa	60 kDa
Primary Sequence	567 a.a.	559 a.a.
Tissue of Expression	Liver, lung epithelia, monocytes	Intestinal epithelia, liver, kidneys
Cellular Location	Microsomes	Microsomes
Stability	Excellent[a]	Poor[b]
General Specificity	Smaller alcohols, Larger acids	Larger alcohols, Smaller acids
Prodrug Substrates[c]	Capecitabine	Irinotecan
Activity[d]	1	91

[a] hCE-1 is stable for months at r.t.
[b] hiCE rapidly loses activity under identical conditions.
[c] Primary CE implicated in the activation of either **11** or **12**.
[d] Relative rates for the hydrolysis of **12**.

A prodrug developed by Barthel *et al.,*[22,81] pentyl-PABC-doxazolidine (PPD) **13** (Figure 2.6), was modeled after the clinically approved drug capecitabine **11** for activation by hCE-1. *In vitro* studies using MCF-7 human breast cancer cells, however, implicated hiCE as the enzymatic activator of PPD, highlighting the difficulty in *de novo* predictions of enzyme substrate specificity.[81] Despite promising IC_{50} values for **13** in cells overexpressing hiCE,[82] the drug underperformed in murine animal models.[82] Serum esterase activity in rodents was identified as a likely cause for premature activation of the prodrug in the bloodstream and ultimately prompted the exploration of peptidase activated prodrugs of doxazolidine **4**.

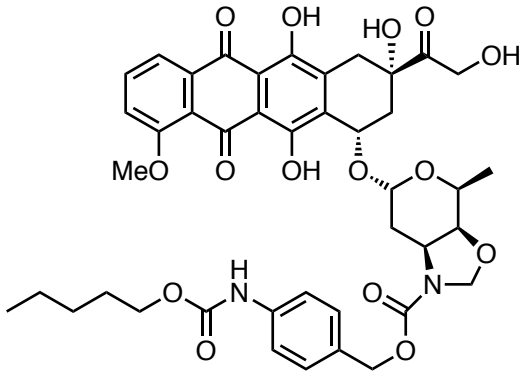

13

Figure 2.6 Structure of the hiCE-activated, pentyl-PABC-doxazolidine (PPD) **13**.[22, 81-2]

Proteases

Proteolytic activity is a common and widespread biomarker of neoplastic tissues. In addition to creating the physical space required for invasion and metastasis, tumor expressed proteases can assume a more active role in tumorigenic transformation and development. This is primarily manifested through protease liberation and activation of extracellular matrix (ECM) associated growth factors and cytokines, which in turn affect carcinogenesis, angiogenesis and

tumor growth.[83-87] Given the significance of proteolytic activity in tumor progression, metastasis and overall patient prognosis, combined with its tight regulation and essentially negligible functioning in healthy, static tissues, proteolytic activity makes an attractive target for tumor-selective prodrug activation. Furthermore, the substrate specificity of numerous proteases has been studied in detail and generally relies on the recognition of a small number of amino acids encompassing the scissile peptide bond.[88] Thus, short peptides with established sequences can be prepared synthetically and tested in a peptide-targeted prodrug model against cancer cell lines having phenotypes with high protease activities. The cathepsin and plasmin proteases, which have commonly been exploited in prodrug models, will briefly be reviewed here.

Protease specificity is determined by the recognition of particular amino acid sequences as they are brought into close proximity to the enzyme active site. The amino acid sequence surrounding a protease cleavage site is conventionally denoted:

$$H_2N\text{-}P_n\ldots P_3P_2\mathbf{P_1P_1'}P_2'P_3'\ldots P_n\text{-}CO_2H,$$

with the scissile peptide bond located at the $\mathbf{P_1P_1'}$ junction.[107] Substrate specificity is largely governed by the amino acids located at the $P_3\ldots P_3'$ positions, and we can further limit our considerations to the amino acids positioned at P_3, P_2 and P_1 because, in the context of prodrug design, the PABC-spacer and drug portions of the molecule occupy prime-sites of the sequence, which cannot be manipulated. Additionally, analysis of the amino acid preferences for each of these positions will be limited to those of Cathepsin B and plasmin (and uPA) as an exhaustive review of the other proteases is beyond the scope of this discussion and these proteases, which are overexpressed in several solid tumors,[39] were the focus of our efforts to develop protease-activated prodrugs of doxazolidine.

The Cathepsins

Cathepsins are a group of enzymes belonging to the papain family of cysteine proteases with eleven different members in man. Their primary role is considered to be their functioning in lysosomal protein degradation.[88] However, evidence supporting their role in extralysosomal activity, including functioning at the plasma membrane[89] and in the pericellular milieu[90] also exist and they have been implicated in numerous pathological processes, as well. Cathepsin B is a tumor promoter involved in carcinogenesis and metastasis.[91-93] It is not found extracellularly expect in pathological conditions, such as metastatic tumors[94] and in areas of tissue degradation in rheumatoid arthritis[95] Cathepsin L is involved in epidermal[96-98] and cardiac homeostasis[99,100], prohormone processing[101-102] and autophagy.[103] A putative tumor suppressor in the K14-HPV16 mouse model of epidermal carcinogenesis,[96] Cathepsin L nevertheless contributes to cell proliferation and tumor growth in a mouse model of pancreatic islet β-cell carcinogenesis.[93] Cathepsin S also plays an important role in the same pancreatic islet cell cancer model, where it is involved in antigen presentation, tumorigenesis and angiogenesis.[104-106]

The strongest substrate specificity determinant for Cathepsin B occurs at P_1 with high selectivity for substrates with a gly residue in this position having been observed. Cathepsin B endoproteolysis of substrates with a P_1 gly has been reported for several proteins, including aggrecan,[113] osteocalcin,[114] and thyroglobulin,[115] and this preference is also reflected in the sequences of fluorescent peptide substrates,[116] which were efficiently cleaved by Cathepsin B, as well as, in a series of irreversible inhibitors, all of which contained a P_1 gly residue.[117] In P_2, Ala and Val are the preferred residues for Cathepsin B, but as is true for most cathepsins, either aromatic or aliphatic amino acids are also well tolerated. In P_3, a slight preference for aromatic and aliphatic residues has been reported,[109-112] but these are minor specificity determinants and

substrates with all twenty naturally occurring amino acids in this position are known.[88]

Published reports on prodrugs designed to be activated by Cathepsin B have utilized the sequences Gly-Phe-Leu-Gly[118] and Ala-Leu-Ala-Leu,[119,120] which are lysosomally cleaved peptides. However, despite the analysis presented above, reports from researchers at Bristol-Myers Squibb on the use of a Val-Cit peptide motif, in which the unnatural amino acid citrulline is placed in the P_1 position, caught our attention.[120] In particular, incorporation of the Val-Cit dipeptide into the clinically used mAb-targeted antimitotic drug, Brentuximab Vedotin **6**[25] *(vide supra)*, prompted our exploration of some citrulline-containing sequences in potential Cathepsin B-activatable peptidyl prodrugs of doxazolidine, which are discussed in Chapter 5 of this thesis.

Plasmin

The plasmin system offers another attractive possibility for the tumor-selective activation of peptidyl prodrugs. In this system, the zymogen plasminogen is converted to the active serine protease plasmin at or near the cell surface by surface-bound urokinase-type plasminogen activator (uPA).[122] Active plasmin degrades the ECM and basement membrane components directly or indirectly through activation of a variety of other proteolytic proenzymes, including the matrix metalloproteases (MMPs).[123] Not surprisingly, high levels of plasmin pathway components often correlate with poor prognosis in a wide panel of tumor types,[122] including difficult to treat cancers such as lung,[124-126] liver,[127,128] and pancreas.[129-131]

The strongest substrate specificity determinant for plasmin occurs at the P_1 position with high selectivity for the basic residues Lys and Arg, with a slight preference for Lys over Arg, due to the presence of Asp189 at the base of the S_1 pocket of the enzyme active site.[132-134] In P_2, a strong preference for the aromatic amino acids Phe, Try and Tyr exists and this preference is believed to be conveyed by π-facial interactions between the amino group of Gln192 in the

enzyme active site and the aromatic ring of the substrate.[134] Structural models suggest that the P_3-side chain is directed away from the enzyme and into the bulk solvent and, thus, no significant interactions between the substrate and plasmin exists at this position. The plasminogen activator, uPA, shares the preference for basic residues at the P_1 position and prefers small amino acid residues in both the P_3 and P_2 positions (P_3 = Gly, Ser or Thr; P_2 = Gly, Ala, Ser or Thr).[135-136]

In 1980, Carl *et al.* reported the dipartite prodrug **14** in which activation was achieved through the plasmin-mediate hydrolysis of the anilide bond connecting the drug to the tripeptide D-Val-Leu-Lys and released the phenylenediamine mustard **15** (Scheme 2.4).[137] Compound **14** was tested against the parent drug **15** in an *in vitro* assay using wild-type chicken embryo fibroblasts, which express low levels of uPA, and transformed cells, which expressed high levels of uPA. The peptidyl prodrug **14** had a 7-fold increase in selective cytotoxicity for the transformed cells compared to **15** and, thus, served as a proof of concept for plasmin-activated peptidyl prodrugs.

Scheme 2.4 Plasmin-activation of the peptidyl prodrug **14** released the phenylenediamine mustard **15**.[137]

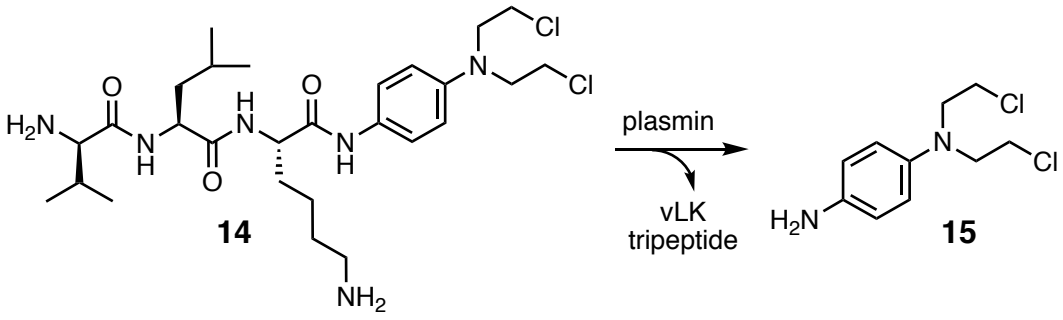

In 1999, de Groot *et al.* described a prodrug **16** in which activation was accomplished by plasmin cleavage of the tripeptide sequence D-Ala-Phe-Lys from the Katzenellenbogen-spacer

and released doxorubicin **17** (Scheme 2.5).[55] In animal models, **16** exhibited antitumor efficacy with a significantly better toxicity profile than **17**,[56] and served as the basis for the design of similar prodrugs prepared in our laboratory for the protease-activated, tumor-selective delivery of doxazolidine **4**, a significantly more active anthracycline than **17**.

Scheme 2.5 Plasmin-activation of the aFK-peptidyl prodrug **16** released doxorubicin **17**.[55]

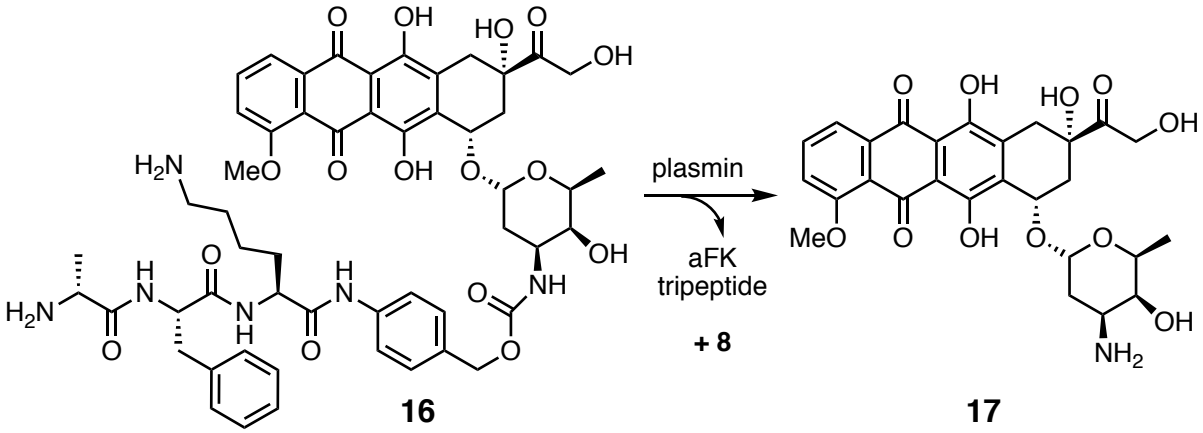

The tripartite prodrug aFK-PABC-DOXAZ **18** was of considerable interest to our research group (Figure 2.7).[83] However, difficulties in the synthesis of **18** significantly delayed its biological evaluation. The synthetic method being followed is shown in Scheme 2.6 and began

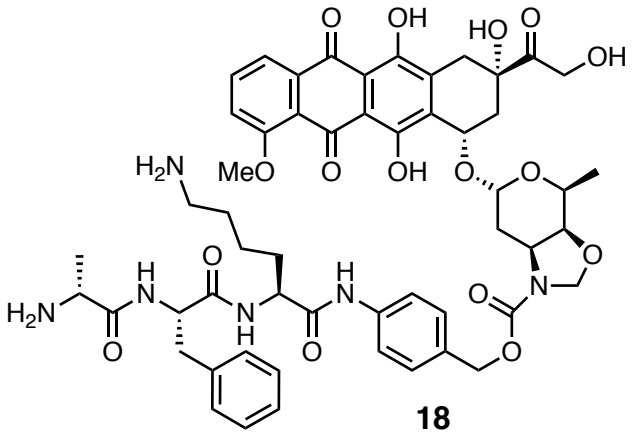

Figure 2.7 Structure of aFK-PABC-DOXAZ **18**, a tripeptidyl prodrug of doxazolidine **4**.

Scheme 2.6 Proposed synthesis of aFK-PABC-DOXAZ **18** (PSty = polystyrene bead).[83]

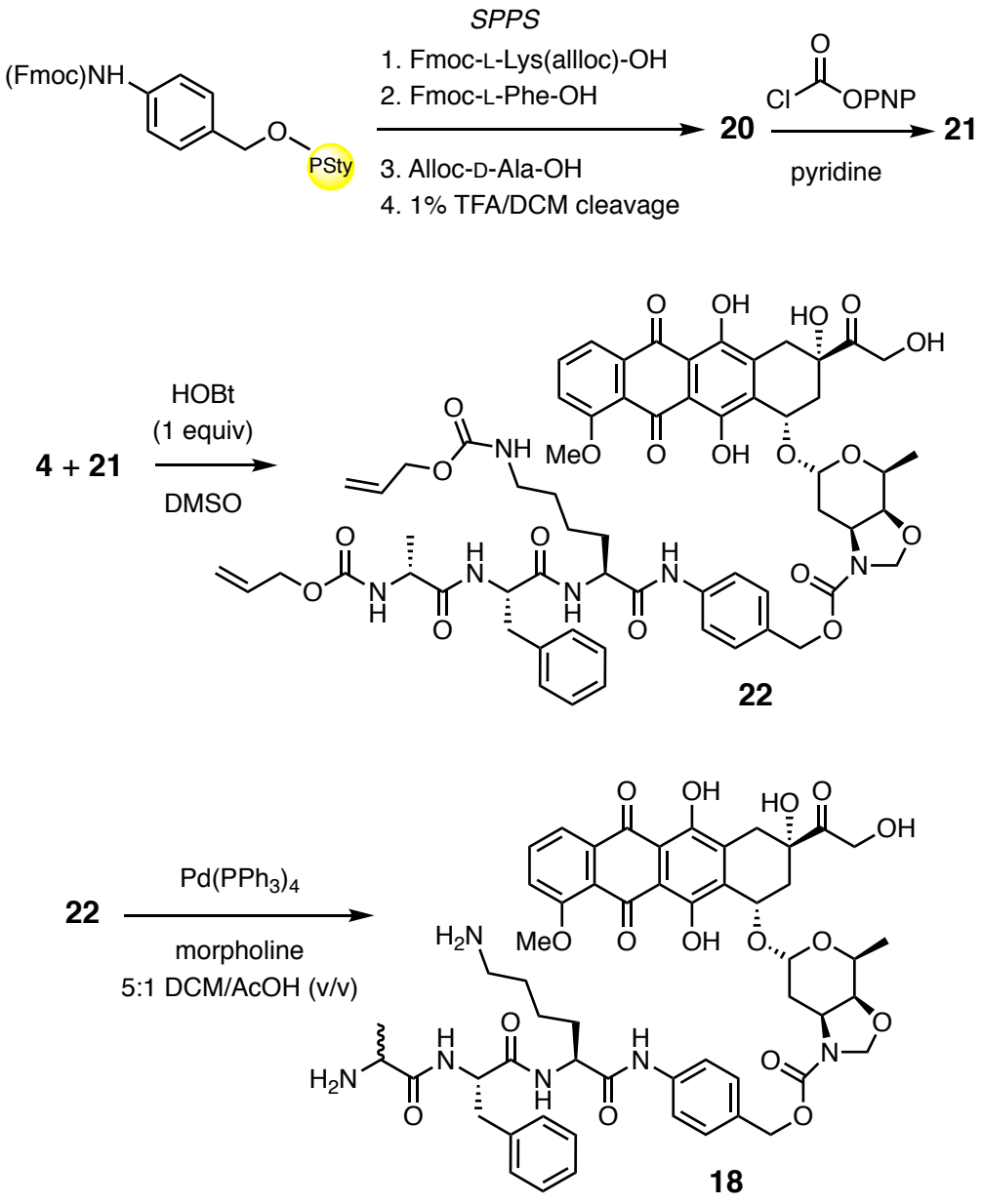

with SPPS of the bis(alloc)-protected peptidyl-PABA segment **20**, followed by conversion of the primary alcohol into the mixed PNP-carbonate **21** and subsequent coupling to the drug to afford the protected peptidyl prodrug, alloc-aFK(alloc)-PABC-DOXAZ **22**.[83]

Final deprotection of the alloc groups by palladium-catalyzed allyl transfer to morpholine

was accomplished with tetrakis(triphenylphosphine)Pd^0 with subsequent acidification (Scheme 2.6). However, ^1H NMR analysis of the crude reaction mixture obtained following the deprotection reaction indicated the presence of a side product representing approximately 15% of the total anthracycline composition. Based on chemical shift analysis, this impurity was tentatively assigned to be the diastereomer of aFK-PABC-DOXAZ arising from epimerization of the α-methyl group of the N-terminal D-Ala residue. All other peaks in the ^1H NMR spectrum appeared as expected, and integration of the duplicated alanine α-methyl signals summed to equaled the integration of the 5′-methyl peak on the daunosamine sugar, which was consistent with the anticipated 1:1 molar ratio of the respective methyl groups. A homonuclear gradient COSY experiment also confirmed coupling between the alanine α-proton and suspected L-alanine methyl signals, consistent with our assignment of the impurity as the diastereomer resulting from D-Ala epimerization. While RP-HPLC was able to distinguish the two diastereomers, poor chromatographic resolution prevented isolation of sufficient quantities of spectroscopically pure materials.

We hypothesized that the epimerization was occurring as a result of the acidification procedure following the final alloc-deprotection reaction. Additional attempts to salt-out the product by varying the temperature, time, and acidic reagent failed to yield satisfactory results. Moreover, no gains in purity were made during our exploration of various amino-protecting groups, including tBoc, Fmoc, and TFA. Modification of the proposed synthesis was therefore required to reduce the abundance of the diastereomer in order to simplify biological characterization of **18**.

2.4 Rationalization of New Methodology for Tripartite Prodrugs Synthesis

The need for an alternative method to prepare aFK-PABC-DOXAZ **18** emerged in order to overcome difficulties encountered in its synthesis using the existing methodologies. The primary issue that we faced involved epimerization of the D-Ala α-methyl group of (alloc)aFK(alloc)-PABC-DOXAZ **22** during the final deprotection step of the synthesis. However, upon further examination of the synthetic route being used, inefficiencies inherent to the reactivity of the functional groups being manipulated were identified at nearly every step of the synthesis.

The SPPS of **20** began with the loading of Fmoc-PABA-OH onto 2-ClTrtl chloride resin. This resin has two major advantages, in general, over other available resins used in peptide synthesis in that (1) loading of the first amino acid onto the resin proceeds via an S_N1 substitution reaction and, thus, no racemizationn of the first residue occurs as it may when an amino acid active ester is used in an S_N2 reaction with a nucleophilic resin and (2) following a completed synthesis, cleavage of protected peptides is possible due to the mild cleavage conditions (1% TFA in DCM) used to remove the peptide from the trityl resin and the availabilty of orthogonally protected amino acids. However, loading Fmoc-PABA-OH, in which no racemization is possible, does not benefit from the S_N1 mechanism and, in fact, the diminished reactivity of the alcohol relative to a carboxylate ion had in the past resulted in low loading efficiencies. Additionally, the first peptide coupling reaction in which Fmoc-Lys(alloc)-OH was condensed with the resin-bound PABA required significantly longer coupling times than normal (16 h vs. 1 h) owing to the poor nucleophilicity of the aniline. Next, when the mixed PNP carbonate **21** was being used to acylate doxazolidine, the poor nucleophilicity of the oxazolidine resulted in a sluggish reaction with a valuable advanced intermediate. As a result, low yields and

long reaction times plagued this reaction as well and reaction with a valuable intermediate precluded use of **21** in excess to help drive the reaction forward. Finally, the linear synthesis of every new prodrug we sought to explore posed more daunting of a task than perhaps necessary. If the peptide portion of the molecule, which is the only domain where we would like to introduce variations into the prodrug design, could be introduced in the penultimum step of the synthesis, then the efficiency with which we could explore the chemical space surrounding prodrugs of doxazolidine would be greatly enhanced.

How one could effect the acylation of the aniline in a late-stage reaction was not immediately obvious, however. The synthons **23** amd **24** requied for such a transformation are shown in Figure 2.8, but **24** has an unteneable relationship between the free amine and the *para*-substited carbamate, which would ordinarily undergo 1,6-elimination were it to be made. However, we hypothesized that the *p*-azidobenzyloxy carbamate **25** might allow for late-stage N→C amidative-installation of the Katzenellenbogen spacer via a traceless Staudinger ligation,[138] thereby offering a new synthetic route to these compounds capable of overcoming the inherent limitations within our system (Scheme 2.7).

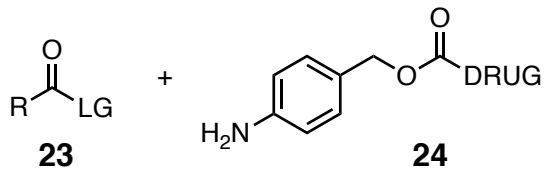

23 **24**

Figure 2.8 The synthons **23** and **24** required for late-stage N→C amidative-installation of the Katzenellenbogen spacer.

Scheme 2.7 Proposed traceless Staudinger ligation methodology for the synthesis of the tripartite prodrug **18**.

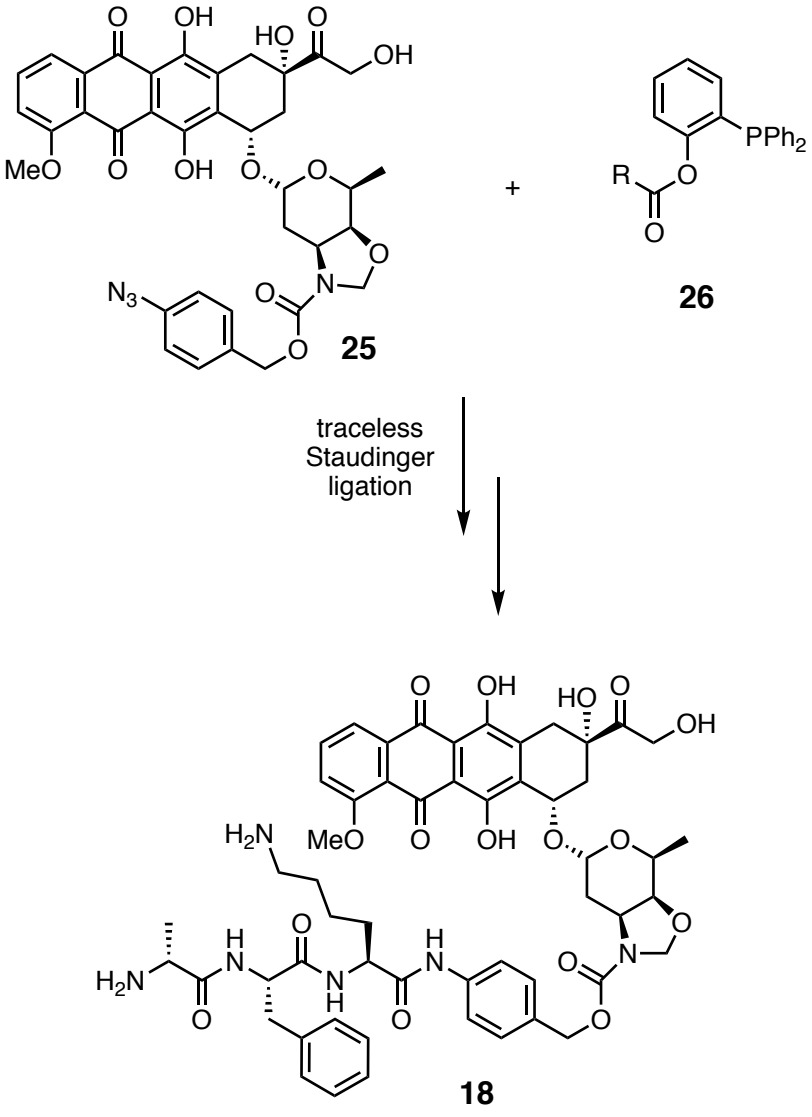

2.5 References

1. Albert, A. "Chemical Aspects of Selective Toxicity" *Nature*, **1958**, *182*, 421−423.

2. Albert, A. "Selective Toxicity" John Wiley and Sons Inc., New York, 1964; pp 57−63.

3. "Salicin" *Merck Index*, 11th Ed., Whitehouse Station, N.J. M9730.

4. Sneader, W. "The Discovery of Aspirin: A Reappraisal" *BMJ Clin. Res.* **2000**, *321*, 1591−1594.

5. van Cauwenberge, H. "Aspirin, An Always Current Drug" *Rev. Med. Liege* **1996**, *51*, 7−18.

6. Zawilska, J. B.; Wojciesza, J.; Olejniczak, A. B. "Prodrugs: A Challenge for the Drug Development" *Pharmacological Reports* **2013**, *65*, 1−14.

7. Maag, H. "Overcoming Poor Permeability: The Role of Prodrugs for Oral Drug Delivery" *Drug Discov. Today* **2012**, *9*, 121−130.

8. Liu, M.; Sun, Y.; Zhao, S.; Li, Y.; Piao, R.; Yang, Y.; Gu, J. "A Novel Prodrug Strategy to Improve the Oral Absorption of *O*-Desmethylvenlafaxine" *Exp. Ther. Med.* **2016**, *12*, 1611−1617.

9. Balant, L. P.; Doelker, E.; Burl, P. "Prodrugs for the Improvement of Drug Absorption via Different Routes of Administration" *Euro. J. Drug Metab. Pharmacokinet.* **1990**, *15*, 143−153.

10. Sun, J.; Dahan, A.; Amidon, G. L. "Enhancing the Intestinal Absorption of Molecules Containing the Polar Guanidine Functionality: A Double-Targeted Prodrug Approach" *J. Med. Chem.* **2010**, *53*, 624−632.

11. Muller, C. E. "Prodrug Approaches for Enhancing the Bioavailability of Drugs with Low Solubility" *Chem. Biodivers.* **2017**, *6*, 2071−2083.

12. Dubowchik, G. M.; Firestone, R. A; Padilla, L.; Willner, D.; Hofstead, S. J.; Mosure, K.; Knipe, J. O.; Lasch, S. J.; Trail, P. A. "Cathepsin B-Labile Dipeptide Linkers for Lysosomal Release of Doxorubicin from Internalizing Immunocon-jugates: Model Studies of Enzymatic Drug Release and Antigen-Specific in Vitro Anticancer Activity." *Bioconjugate Chem.* **2002**, *13*, 855–869.

13. Ryppa, C.; Mann-Steinberg, H.; Biniossek, M. L.; Satchi-Fainaro, R.; Kratz, F. "*In Vitro* and *In Vivo* Evaluation of a Paclitaxel Conjugate with the Divalent Peptide E-[c(RGDfK)$_2$] that Targets Integrin $\alpha_v\beta_3$" *Int. J. Pharm.* **2008**, *368*, 89−97.

14. Najib, J. “The Efficacy and Safety Profile of Lisdexamfetamine Dimesylate, a Prodrug of d-Amphetamine, for the Treatment of Attention-Deficit/Hyperactivity Disorder in Children” *Clin. Ther.* **2009**, *31*, 142−176.

15. Le, J. Drug Excretion. In *Merck Manual for Professionals*; Kenilworth, NJ, 2017.

16. Greenwald, R. B.; Conover, C. D.; Choe, Y. H. “Poly(ethylene glycol) Conjugated Drugs and Prodrugs: A Comprehensive Review” *Crit. Rev. Ther. Drug Carrier Syst.* **2000**, *17*, 101−161.

17. Greenwald, R. B.; “PEG Drugs: An Overview” *J. Control Release* **2001**, *74*, 159−171.

18. Stella, V. *Pro-drugs: An Overview and Definition*; ACS Symposium Series; American Chemical Society: Washington, DC, 1975.

19. Rautio, J.; Kumpulainen, H.; Heimbach, T.; Oliyai, R.; Oh, D.; Jaervinen, T.; Savolainen, J. "Prodrugs: Design and Clinical Applications" *Nature Rev. Drug Discovery* **2008**, *7*, 255−270.

20. Stella, V. J.; Burchardt, R. T.; Hageman, M. J.; Oliyai, R.; Maah, H.; Tilley, J. W. In *Prodrugs: Challenges and Rewards. Part 1*; Springer: New York, 2007.

21. Kratz, F.; Muller, I. A.; Ryppa, C.; Warnecke, A. “Prodrug Strategies in Anticancer Chemotherapy” *ChemMedChem* **2008**, *3*, 20−53.

22. Burkhart, D. J.; Barthel, B. L.; Post, G. C.; Kalet, B. T.; Nafie, J. W.; Shoemaker, R. K.; Koch, T. H. “Design, Synthesis, and Preliminary Evaluation of Doxazolidine Carbamates as Prodrugs Activated by Carboxylesterases” *J. Med. Chem.* **2006**, *49*, 7002−7012.

23. Hatfield, J. M.; Wierdl, M.; Wadknis, R. M.; Potter, P. M. “Modification of Human Carboxylesterase for Improved Prodrug Activation” *Expert Opin. Drug Metab. Toxical.* **2008**, *4*, 1153−1165.

24. Carl, P. L.; Chakravarty, P. K.; Katzenellenbogen, J. A. “A Novel Connector Linkage Applicable in Prodrug Design” *J. Med. Chem.* **1981**, *24*, 479−480.

25. Moskowitz, C. H.; Nademanee, A.; Masszi, T.; Agura, E.; Holowiecki, J.; Abidi, M. H.; Chen, A. I.; Stiff, P.; Gianni, A. M.; Carella, A.; Osmanov, D.; Bachanova, V.; Sweetenham, J.; Sureda, A.; Huebner, D.; Sievers, E. L.; Chi, A.; Larsen, E. K.; Hunder, N. N.; Walewsji, J. “Brentuximab vedotin as Consolidation Therapy After Autologous Stem-Cell Transplantation in Patients with Hodgkin's Lymphoma at Risk of Relapse or Progression (AETHERA): A Randomised, Double-Blind, Placebo-Controlled, Phase 3 Trial.” *Lancet* **2015**, *385*, 1853−1862.

26. Wakselman, M. “The 1,4 and 1,6 Eliminations from Hydroxy- and Amino-substituted Benzyl Systems: Chemical and Biochemical Applications” *Nouv. J. Chim***. 1983**, *7,* 439−447.

27. Greenwald, R. B.; Pendri, A.; Conover, C. D.; Zhao, H.; Choe, Y. H.; Martinez, A.;

Shum, K.; Guan, S. “Drus Delivery Systems Employing 1,4- or 1,6-Elimination: Poly(ethylene glycol) Prodrugs of Amine-Containing Compounds” *J. Med. Chem.* **1999**, *42*, 3657−3667.

28. Damen, E. W.; Nevalainen, T. J.; van den Bergh, T. J. M.; de Groot, F. M.; Scheeren, H. W. “Synthesis of Novel Paclitaxel Prodrugs Designed for Bio-reductive Activation in Hypoxic Tumour Tissue” *Bioorg. Med. Chem*. **2002**, *10,* 71−77.

29. Rivault, F.; Tranoy-Opalinski, I.; Gesson, J. P. “A New Linker for Glucuronylated Anticancer Prodrugs” *Bioorg. Med. Chem.* **2004**, *12*, 675−682.

30. Greenwald, R. B. ; Choe, Y. H.; Conover, C.; Shum, K.; Wu, D.; Royzen, M. “Drug Delivery Systems Based on Trimethyl Lock Lactonization: Poly(ethylene glycol) Prodrugs of Amino-Containing Compounds” *J. Med. Chem.* **2000**, *43*, 475−487.

31. Wang, B.; Zhang, H.; Zheng, A.; Wang, W. “Coumarin-based Prodrugs. Part 3: Structural Effects on the Release Kinetics of Esterase-Sensitive Prodrugs of Amines” *Bioorg. Med. Chem*. **1998**, *6*, 417−426.

32. Wang, B.; Zhang, H.; Wang, W. “Chemical Feasibility Studies of a Potential Coumarin-Based Prodrug System” *Bioorg. Med. Chem. Lett.* **1996**, *6*, 945−950.

33. de Groot, M.; van Berkom, L. W.; Scheeren, H. W. “Synthesis and Biological Evaluation of 2'-Carbamate-Linked and 2'-Carbonate-Linked Prodrugs of Paclitaxel: Selective Activation by the Tumor-Associated Protease Plasmin” *J. Med. Chem*. **2000**, *43*, 3093−3102.

34. Xu, G.; Zhang, W.; Ma, M. K.; McLeod, H. L. “Human Carboxylesterase 2 is Commonly Expressed in Tumor Tissue and is Correlated with Activation of Irinotecan” *Clin. Cancer Res*. **2002**, *8*, 2605−2611.

35. Tabata, T.; Katoh, M.; Tokudome, S.; Nakajima, M.; Yokoi, T. “Identification of the Cytosolic Carboxylesterase Catalyzing the 5’-Deoxy-5-fluorocytidine Formation from Capecitabine in Human Liver” *Drug. Metab. Dispos.* **2004**, *32*, 1103−1110

36. Miwa, M.; Ura, M.; Nishida, M.; Sawada, N.; Ishikawa, T.; Mori, K.; Shimma, N.; Umeda, I.; Ishitsuka, H. “Design of a Novel Oral Fluoropyrimidine Carbamate, Capecitabine, which Generates 5-Fluorouracil Selectively in Tumours by Enzymes Concentrated in Human Liver and Cancer Tissue” *Eur. J. Cancer* **1998**, *34*, 1274−1281.

37. Shimma, N.; Umeda, I.; Arasaki, M.; Murasaki, C.; Masubuchi, K.; Kohchi, Y.; Miwa, M.; Ura, M.; Sawada, N.; Tahara, H.; Kuruma, I.; Horii, I.; Ishitsuka, H. “The Design and Synthesis of a New Tumor-Selective Fluoropyrimidine Carbamate, Capecitabine” *Bioorg. Med. Chem***. 2000**, *8*, 1697−1706.

38. Sanghani, S. P.; Quinney, S. K.; Fredenburg, T. B.; Sun, Z.; Davis, W. I.; Murry, D. J.; Cummings, O. W.; Seitz, D. E.; Bosron, W. F. “Carboxylesterases Expressed in Human Colon Tumor Tissue and their Role in CPT-11 Hydrolysis” *Clin. Cancer Res*. **2003**, *9*, 4983−4991.

39. Kovar, M.; Strohalm, J.; Etrych, T.; Ulbrich, K.; Rihova, B. “Star Structure of Antibody-Targeted HPMA Copolymer-Bound Doxorubicin: A Novel Type of Polymeric Conjugate for Targeted Drug Delivery with Potent Antitumor Effect” *Bioconjugate Chem*. **2002**, *13*, 206−215.

40. Thomssen, C.; Schmitt, M.; Goretzki, L.; Oppelt, P.; Pache, L.; Dettmar, P.; Janicke, F.; Graeff, H. “Prognostic Value of the Cysteine Proteases Cathepsins B and Cathepsin L in Human Breast Cancer” *Clin. Cancer Res*. **1995**, *1*, 741−746.

41. Thanou, M.; Duncan, R. “Polymer-Protein and Polymer-Drug Conjugates in Cancer Therapy” *Curr. Opin. Invest. Drugs* **2003**, *4*, 701−709.

42. Demchik, L. L.; Sameni, M.; Nelson, K.; Mikkelsen, T.; Sloane, B. F. “Cathepsin B and Glioma Invasion” *Int. J. Dev. Neurosci.* **1999**, *17*, 483−494.

43. Mai, J.; Waisman, D. M.; Sloane, B. F. “Cell Surface Complex of Cathepsin B/Annexin II Tetramer in Malignant Progression” *Biochim. Biophys. Acta* **2000**, *1477*, 215−230.

44. Masquelier, M.; Baurain, R.; Trouet, A. “Amino Acid and Dipeptide Derivatives of Daunorubicin. 1. Synthesis, Physicochemical Properties, and Lysosomal Digestion” *J. Med. Chem*. **1980***, 23*, 1166−1170.

45. Duncan, R.; Cable, H. C.; Lloyd, J. B.; Rejmanov, P.; Kopecek, V. J. “Polymers Containing Enzymatically Degradable Bonds, 7. Design of Oligopeptide Side-Chains in Poly[*N*-(2-hydroxypropyl)methacrylamide] Copolymers to Promote Efficient Degradation by Lysosomal Enzymes” *Makromol. Chem*. **1983**, *184*, 1997−2008.

46. Versluis, A. J.; Rump, E. T.; Rensen, P. C.; van Berkel, T. J.; Bijsterbosch, M. K. “Synthesis of a Lipophilic Daunorubicin Derivative and Its Incorporation into Lipidic Carriers Developed for LDL Receptor-Mediated Tumor Therapy” *Pharm. Res.* **1998**, *15*, 531−537.

47. Studer, M.; Kroger, L. A.; DeNardo, S. J.; Kukis, D. L.; Meares, C. F. “Influence of a Peptide Linker on Biodistribution and Metabolism of Antibody-Conjugated Benzyl-EDTA. Comparison of Enzymatic Digestion In Vitro and In Vivo” *Bioconjugate Chem*. **1992**, *3*, 424−429.

48. Agarwal, N.; Rich, D. H. “An Improved Cathepsin-D Substrate and Assay Procedure” *Anal. Biochem*. **1983**, *130*, 158−165.

49. de Groot, F . M.; Loos, W. J.; Koekkoek, R.; van Berkom, L. W.; Busscher, G. F.; Seelen, A. E.; Albrecht, C.; de Bruijn, P.; Scheeren, H. W. “Elongated Multiple Electronic Cascade and Cyclization Spacer Systems in Activatable Anticancer Prodrugs for Enhanced Drug Release” *J. Org. Chem.* **2001**, *66*, 8815−8830.

50. Quax, P. H.; de Bart, A. C.; Schalken, J. A.; Verheijen, J. H. “Plasminogen Activator and Matrix Metalloproteinase Production and Extracellular Matrix Degradation by Rat Prostate

Cancer Cells In Vitro: Correlation with Metastatic Behavior In Vivo" *Prostate* **1997**, *32*, 196−204.

51. Groskopf, W. R.; Summaria, L.; Robbins, K. C. "Studies on the Active Center of Human Plasmin. Partial Amino Acid Sequence of a Peptide Containing the Active Center Serine Residue" *J. Biol. Chem*. **1969**, *244*, 3590−3597.

52. Andreasen, P. A.; Egelund, R.; Petersen, H. H. "The Plasminogen Activation System in Tumor Growth, Invasion, and Metastasis" *Cell. Mol. Life Sci*. **2000**, *57*, 25−40.

53. Vassalli, J. D.; Pepper, M. S. "Tumour Biology. Membrane Proteases In Focus" *Nature* **1994**, *370*, 14−15.

54. Hewitt, R.; Dano, K. "Stromal Cell Expression of Components of Matrix-Degrading Protease Systems in Human Cancer" *Enzyme Protein* **1996**, *49*, 163−173.

55. de Groot, F. M. H.; de Bart, A. C. W.; Verheijen, J. H.; Scheeren, H. W. "Synthesis and Biological Evaluation of Novel Prodrugs of Anthracyclines for Selective Activation by the Tumor-associated Protease Plasmin" *J. Med. Chem.* **1999**, *42*, 5277−5283.

56. Devy, L.; de Groot, F. H. M.; Blacher, S.; Hajitou, A.; Beusker, P.; Scheeren, W.; Foldart, J.-M.; Noel, A. "Plasmin-activated Doxorubicin Prodrugs Containing a Spacer Reduce Tumor Growth and Angiogenesis Without Systemic Toxicity" *FASEB J*. **2004**, *18*, 565−567.

57. Chung, D. E.; Kratz, F. "Development of a Novel Albumin-Binding Prodrug that is Cleaved by Urokinase-type-Plasminogen Activator (uPA)" *Bioorg. Med. Chem. Lett*. **2006**, *16*, 5157−5163.

58. Madison, E. L.; Coombs, G. S.; Corey, D. R. "Substrate Specificity of Tissue Type Plasminogen Activator. Characterization of the Fibrin Independent Specificity of t-PA for Plasminogen" *J. Biol. Chem*. **1995**, *270*, 7558−7562.

59. Lilja, H.; Abrahamsson, P. A.; Lundwall, A. "Semenogelin, the Predominant Protein in Human Semen. Primary Structure and Identification of Closely Related Proteins in the Male Accessory Sex Glands and on the Spermatozoa" *J. Biol. Chem*. **1989**, *264*, 1894−1900.

60. Denmeade, S. R.; Isaacs, J. T. "A History of Prostate Cancer Treatment" *Nat. Rev. Cancer* **2002**, *2*, 389−396.

61. Denmeade, S. R.; Sokoll, L. J.; Chan, D. W.; Khan, S. R.; Isaacs, J. T. "Concentration of Enzymatically Active Prostate-Specific Antigen (PSA) in the Extracellular Fluid of Primary Human Prostate Cancers and Human Prostate Cancer Xenograft Models" *Prostate* **2001**, *48*, 1−6.

62. Akiyama, K.; Nakamura, T.; Iwanaga, S.; Hara, M. "The Chymotrypsin-like Activity of Human Prostate-Specific Antigen, Gamma-Seminoprotein" *FEBS Lett*. **1987**, *225*, 168−172.

63. Lilja, H. “A Kallikrein-like Serine Protease in Prostatic Fluid Cleaves the Predominant Seminal Vesicle Protein” *J. Clin. Invest*. **1985**, *76*, 1899−1903.

64. Denmeade, S. R.; Nagy, A.; Gao, J.; Lilja, H.; Schally, A. V.; Isaacs, J. T. “Enzymatic Activation of a Doxorubicin-Peptide Prodrug by Prostate-Specific Antigen” *Cancer Res.* **1998**, *58*, 2537−2540.

65. Garsky, M.; Lumma, P. K.; Feng, D. M.; Wai, J.; Ramjit, H. G.; Sardana, M. K.; Oliff, A.; Jones, R. E.; DeFeo-Jones, D.; Freidinger, R. M. “The Synthesis of a Prodrug of Doxorubicin Designed to Provide Reduced Systemic Toxicity and Greater Target Efficacy” *J. Med. Chem*. **2001**, *44*, 4216−4224.

66. DeFeo-Jones, D.; Garsky, V. M.; Wong, B. K.; Feng, D. M.; Bolyar, T.; Haskell, K.; Kiefer, D. M.; Leander, K.; McAvoy, E.; Lumma, P.; Wai, J.; Senderak, E. T.; Motzel, S. L.; Keenan, K.; van Zwieten, M.; Lin, J. H.; Freidinger, R.; Huff, J.; Oliff, A.; Jones, R. E. “A Peptide-Doxorubicin 'Prodrug' Activated by Prostate-Specific Antigen Selectively Kills Prostate Tumor Cells Positive for Prostate-Specific Antigen In Vivo” *Nat. Med*. **2000**, *6*, 1248−1252.

67. Khan, S. R.; Denmeade, S. R. “In Vivo Activity of a PSA-activated Doxorubicin Prodrug Against PSA-producing Human Prostate Cancer Xenografts” *Prostate* **2000**, *45*, 80−83.

68. Mansour, A. M.; Drevs, J.; Esser, N.; Hamada, F. M.; Badary, O. A.; Unger, C.; Fichtner, I.; Kratz, F. “A New Approach for the Treatment of Malignant Melanoma: Enhanced Antitumor Efficacy of an Albumin-binding Doxorubicin Prodrug that is Cleaved by Matrix Metalloproteinase 2” *Cancer. Res.* **2003**, *63*, 4062−4066.

69. Albright, C. F.; Graciani, N.; Han, W.; Yue, E.; Stein, R.; Lai, Z.; Diamond, M.; Dowling, R.; Grimminger, L.; Zhang, S. Y.; Behrens, D.; Musselman, A.; Bruckner, R.; Zhang, M.; Jiang, X.; Hu, D.; Higley, A.; Dimeo, S.; Rafalski, M.; Mandlekar, S.; Car, B.; Yeleswaram, S.; Stern, A.; Copeland, R. A.; Combs, A.; Seitz, S. P.; Trainor, G. L.; Taub, R.; Huang, P.; Oliff, A. “Matrix Metalloproteinase-activated Doxorubicin Prodrugs Inhibit HT1080 Xenograft Growth Better than Doxorubicin with Less Toxicity” *Mol*. *Cancer Ther.* **2005**, *4*, 751−760.

70. Hofmann, U. B.; Westphal, J. R.; Waas, E. T.; Zendman, A. J.; Cornelissen, I. M.; Ruiter, D. J.; van Muijen, G. N. “Matrix Metalloproteinases in Human Melanoma Cell Lines and Xenografts: Increased Expression of Activated Matrix Metalloproteinase-2 (MMP-2) Correlates with Melanoma Progression” *Br. J. Cancer* **1999**, *81*, 774−782.

71. Kline, T .; Torgov, M. Y.; Mendelsohn, , B. A.; Cerveny, C. G.; Senter, P. D. “Novel Antitumor Prodrugs Designed for Activation by Matrix Metalloproteinases-2 and -9” *Mol. Pharm*. **2004**, *1*, 9−22.

72. Kratz, F.; Drevs, J.; Bing, G.; Stockmar, C.; Scheuermann, K.; Lazar, P.; Unger, C. “Development and In Vitro Efficacy of Novel MMP2 and MMP9 Specific Doxorubicin Albumin Conjugates” *Bioorg. Med. Chem. Lett.* **2001**, *11*, 2001−2006.

73. Bakina, E.; Wu, Z.; Rosenblum, M.; Farquhar, D. “Intensely Cytotoxic Anthracycline Prodrugs: Glucuronides” *J. Med. Chem*. **1997**, *40*, 4013−4018.

74. Sperker, B.; Werner, U.; Murdter, T. E.; Tekkaya, C.; Fritz, P.; Wacke, R.; Adam, U.; Gerken, M.; Drewelow, B.; Kroemer, H. K. “Expression and Function of β-Glucuronidase in Pancreatic Cancer: Potential Role in Drug Targeting” *Naunyn-Schmiedeberg’s Arch. Pharmacol*. **2000**, *362*, 110−115.

75. Murdter, T . E.; Sperker, B.; Kivisto, K. T.; McClellan, M.; Fritz, P.; Friedel, G.; Linder, A.; Bosslet, K.; Toomes, H.; Dierkesmann, R.; Kroemer, H. K. “Enhanced Uptake of Doxorubicin into Bronchial Carcinoma: β-Glucuronidase Mediates Release of Doxorubicin from a Glucuronide Prodrug (HMR 1826) at the Tumor Site” *Cancer Res.* **1997**, *57*, 2440−2445.

76. Bosslet, K.; Czech, J.; Hoffmann, D. “Tumor-selective Prodrug Activation by Fusion Protein-mediated Catalysis” *Cancer Res*. **1994**, *54*, 2151−2159.

77. Sperker, B.; Backman, J. T.; Kroemer, H. K. “The Role of β-Glucuronidase in Drug Disposition and Drug Targeting in Humans” *Clin. Pharmacokinet*. **1997**, *33*, 18−31.

78. Chen, X.; Wu, B.; Wang, G. W. “Glucuronides in Anti-Cancer Therapy” *Curr. Med. Chem. Anticancer Agents* **2003**, *3*, 139−150.

79. de Graaf, M.; Boven, E.; Scheeren, H. W.; Haisma, H. J.; Pinedo, H. M. “β-Glucuronidase-mediated Drug Release *Curr. Pharm. Des.* **2002**, *8*, 1391−1403.

80. Woessner, R.; An, Z.; Li, X.; Hoffman, R. M.; Dix, R.; Bitonti, A. “Comparison of Three Approaches to Doxorubicin Therapy: Free Doxorubicin, Liposomal Doxorubicin, and β-Glucuronidase-activated Prodrug” (HMR 1826) *Anticancer Res*. **2000**, *20*, 2289−2296.

81. Barthel, B. L.; Torres, R. C.; Hyatt, J. L.; Edwards, C. C.; Hatfield, J. M.; Potter, P. M.; Koch, T. H. “Identification of Human Intestinal Carboxylesterase as the Primary Enzyme for Activation of a Doxazolidine Carbamate Prodrug.” *J. Med. Chem.* **2008**, *51*, 298–304.

82. Barthel, B. L.; Zhang, Z.; Rudnicki, D. L.; Coldren, C. D.; Polinkovsky, M.; Sun, H.; Koch, G. G.; Chan, D. C. F. F.; Koch, T. H. “Preclinical Efficacy of a Carboxylesterase 2-Activated Prodrug of Doxazolidine“ *J. Med. Chem.* **2009**, *52*, 7678–7688.

83. Barthel, B. L.; Rudnicki, D. L.; Kirby, T. P.; Colvin, S. M.; Burkhart, D. J.; Koch, T. H. “Synthesis and Biological Characterization of Protease-Activated Prodrugs of Doxazolidine” *J. Med. Chem*. **2012**, *55*, 6595–6607.

84. Duffy, M. J.; O’Grady, P.; Devaney, D.; O’Siorain, L.; Fennelly, J. J.; Lijnen, H. R. “Tissue-type Plasminogen Activator, A New Prognostic Marker in Breast Cancer” *Cancer Res.* **1988**, *48*, 1348−1349.

85. Giannelli, G.; Falk-Marzillier, J.; Schiraldi, O.; Stetler-Stevenson, W. G.; Quaranta, V. "Induction of Cell Migration by Matrix Metalloprotease-2 Cleavage of Laminin-5" *Science* **1997**, *277*, 225−228.

86. Bemis, L. T.; Schedin, P. "Reproductive state of rat mammarygland stroma modulates human breast cancer cell migration and invasion" *Cancer Res.* **2000**, *60*, 3414−3418.

87. Choong, P. F.; Nadesapillai, A. P. "Urokinase plasminogen activator system: a multifunctional role in tumor progression and metastasis" *Clin. Orthop. Relat. Res.* **2003**, S46−58.

88. Biniossek, M. L.; Nagler, D. K.; Becker-Pauly, C.; Schilling, O. "Proteomic Identification of Protease Cleavage Sites Characterizes Prime and Non-Prime Specificity of Cysteine Cathepsins B, L, and S." *J. Proteome Res.* **2011**, *10*, 5363–5373.

89. Jane, D. T.; Morvay, L.; Dasilva, L.; Cavallo-Medved, D.; Sloane, B. F.; Dufresne, M. J. "Cathepsin B Localizes to Plasma Membrane Caveolae of Differentiating Myoblasts and is Secreted in an Active Form at Physiological pH" *Biol. Chem.* **2006**, *387*, 223–234.

90. Roshy, S.; Sloane, B. F.; Moin, K. "Pericellular Cathepsin B and Malignant Progression" *Cancer Metastasis Rev*. **2003**, *22*, 271–286.

91. Sevenich, L.; Schurigt, U.; Sachse, K.; Gajda, M.; Werner, F.; Muller, S.; Vasiljeva, O.; Schwinde, A.; Klemm, N.; Deussing, J.; Peters, C.; Reinheckel, T. "Synergistic Antitumor Effects of Combined Cathepsin B and Cathepsin Z Deficiencies on Breast Cancer Progression and Metastasis in Mice" *Proc. Natl. Acad. Sci. U.S.A.* **2010**, *107*, 2497–2502.

92. Vasiljeva, O.; Korovin, M.; Gajda, M.; Brodoefel, H.; Bojic, L.; Kruger, A.; Schurigt, U.; Sevenich, L.; Turk, B.; Peters, C.; Reinheckel, T. "Reduced Tumour Cell Proliferation and Delayed Development of High Grade Mammary Carcinomas in Cathepsin B-deficient Mice" *Oncogene* **2008**, *27*, 4191–4199.

93. Gocheva, V.; Zeng, W.; Ke, D.; Klimstra, D.; Reinheckel, T.; Peters, C.; Hanahan, D.; Joyce, J. A. "Distinct Roles for Cysteine Cathepsin Genes in Multistage Tumorigenesis" *Genes Dev.* **2006**, *20*, 543–556.

94. Sinha, A. A.; Jamuar, M. P.; Wilson, M. J.; Rozhin, J.; Sloane, B. F. "Plasma Membrane Association of Cathepsin B in Human Prostate Cancer: Biochemical and Immunogold Electron Microscopic Analysis*" Prostate* **2001**, *49*, 172−184.

95. Hashimoto, Y., Kakegawa, H., Narita, Y., Hachiya, Y., Hayakawa, T., Kos, J., Turk, V., and Katunuma, N. "Significance of Cathepsin B Accumulation in Synovial Fluid of Rheumatoid Arthritis" *Biochem. Biophys. Res. Commun*. **2001**, *283*, 334−339.

100. Spira, D.; Stypmann, J.; Tobin, D. J.; Petermann, I.; Mayer, C.; Hagemann, S.; Vasiljeva, O.; Gunther, T.; Schule, R.; Peters, C.; Reinheckel, T. "Cell Type-specific Functions of the

Lysosomal Protease Cathepsin L in the Heart" *J. Biol. Chem.* **2007**, *282*, 37045–37052.

101. Stypmann, J.; Glaser, K.; Roth, W.; Tobin, D. J.; Petermann, I.; Matthias, R.; Monnig, G.; Haverkamp, W.; Breithardt, G.; Schmahl, W.; Peters, C.; Reinheckel, T. "Dilated Cardiomyopathy in Mice Deficient for the Lysosomal Cysteine Peptidase Cathepsin L." *Proc. Natl. Acad. Sci. U.S.A.* **2002**, *99*, 6234–6239.

102. Friedrichs, B.; Tepel, C.; Reinheckel, T.; Deussing, J.; von Figura, K.; Herzog, V.; Peters, C.; Saftig, P.; Brix, K. "Thyroid Functions of Mouse Cathepsins B, K, and L" *J. Clin. Invest*. **2003**, *111*, 1733–1745.

103. Yasothornsrikul, S.; Greenbaum, D.; Medzihradszky, K. F.; Toneff, T.; Bundey, R.; Miller, R.; Schilling, B.; Petermann, I.; Dehnert, J.; Logvinova, A.; Goldsmith, P.; Neveu, J. M.; Lane, W. S.; Gibson, B.; Reinheckel, T.; Peters, C.; Bogyo, M.; Hook, V. "Cathepsin L in Secretory Vesicles Functions as a Prohormone-processing Enzyme for Production of the Enkephalin Peptide Neurotransmitter" *Proc. Natl. Acad. Sci. U.S.A.* **2003**, *100*, 9590–9595.

104. Dennemarker, J.; Lohmuller, T.; Muller, S.; Aguilar, S. V.; Tobin, D. J.; Peters, C.; Reinheckel, T. "Impaired Turnover of Autophagolysosomes in Cathepsin L Deficiency" *Biol. Chem.* **2010**, *391*, 913–22.

105. Shen, L.; Sigal, L. J.; Boes, M.; Rock, K. L. "Important Role of Cathepsin S in Generating Peptides for TAP-independent MHC Class I Crosspresentation In Vivo." *Immunity* **2004**, *21*, 155–165.

106. Pluger, E. B. E.; Boes, M.; Alfonso, C.; Schr€oter, C. J.; Kalbacher, H.; Ploegh, H. L.;Driessen, C. "Specific Role for Cathepsin S in the Generation of Antigenic Peptides In Vivo." *Eur. J. Immunol*. **2002**, *32*, 467–476.

107. Beck, H.; Schwarz, G.; Schroter, C. J.; Deeg, M.; Baier, D.; Stevanovic, S.; Weber, E.; Driessen, C.; Kalbacher, H. "Cathepsin S and an Asparagine-specific Endoprotease Dominate the Proteolytic Processing of Human Myelin Basic Protein In Vitro" *Eur. J. Immunol*. **2001**, *31*, 3726–3736.

108. Schlechter, I.; Berger, A. "On the Size of the Active Site in Proteases. I. Papain" *Biochem. Biophys. Res. Commun*. **1967**, *27*,157−162.

109. Taralp, A.; Kaplan, H.; Sytwu, I. I.; Vlattas, I.; Bohacek, R.; Knap, A. K.; Hirama, T.; Huber, C. P.; Hasnain, S. "Characterization of the S3 Subsite Specificity of Cathepsin B" *J. Biol. Chem.* **1995**, *270*, 18036−18043.

110. Choe, Y.; Leonetti, F.; Greenbaum, D. C.; Lecaille, F.; Bogyo, M.; Bromme, D.; Ellman, J. A.; Craik, C. S. "Substrate Profiling of Cysteine Proteases Using a Combinatorial Peptide Library Identifies Functionally Unique Specificities" *J. Biol. Chem.* **2006**, *281*, 12824–12832.

111. Greenbaum, D. C.; Arnold, W. D.; Lu, F.; Hayrapetian, L.; Baruch, A.; Krumrine, J.;

Toba, S.; Chehade, K.; Br€omme, D.; Kuntz, I. D.; Bogyo, M. "Small Molecule Affinity Fingerprinting. A Tool for Enzyme Family Subclassification, Target Identification, and Inhibitor Design." *Chem. Biol.* **2002**, *9*, 1085–1094.

112. Portaro, F. C.; Santos, A. B.; Cezari, M. H.; Juliano, M. A.; Juliano, L.; Carmona, E. "Probing the Specificity of Cysteine Proteinases at Subsites Remote from the Active Site: Analysis of P4, P3, P20 and P30 Variations in Extended Substrates" *Biochem. J.* **2000**, *347* (Pt 1), 123–129.

113. Fosang, A. J.; Neame, P. J.; Last, K.; Hardingham, T. E.; Murphy, G.; Hamilton, J. A. "The Interglobular Domain of Cartilage Aggrecan is Cleaved by PUMP, Gelatinases, and Cathepsin B" *J. Biol. Chem.* **1992**, *267*, 19470–19474.

114. Baumgrass, R.; Williamson, M. K.; Price, P. A. "Identification of Peptide Fragments Generated by Digestion of Bovine and Human Osteocalcin with the Lysosomal Proteinases Cathepsin B, D, L, H, and S" *J. Bone Miner. Res.* **1997**, *12*, 447–455.

115. Dunn, A. D.; Crutchfield, H. E.; Dunn, J. T. "Thyroglobulin Processing by Thyroidal Proteases. Major Sites of Cleavage by Cathepsins B, D, and L" *J. Biol. Chem.* **1991**, *266*, 20198–20204

116. Del Nery, E.; Alves, L. C.; Melo, R. L.; Cesari, M. H.; Juliano, L.; Juliano, M. A. "Specificity of Cathepsin B to Fluorescent Substrates Containing Benzyl Side-chain-substituted Amino Acids at P1 subsite." *J. Protein Chem.* **2000**, *19*, 33–38.

117. Bromme, D.; Kirschke, H. "*N*-peptidyl-*O*-carbamoyl Amino Acid Hydroxamates: Irreversible Inhibitors for the Study of the S2' Specificity of Cysteine Proteinases" *FEBS Lett.* **1993**, *322*, 211–214.

118. Kovar, M.; Strohalm, J.; Etrych, T.; Ulbrich, K.; Rihova, B. "Star Structure of Antibody-targeted HPMA Copolymer-bound Doxorubicin: A Novel Type of Polymeric Conjugate for Targeted Drug Delivery with Potent Antitumor Effect" *Bioconjugate Chem*. **2002**, *13*, 206-215.

119. Versluis, A. J.; Rump, E. T.; Rensen, P. C.; Van Berkel, T. J.; Bijsterbosch, M. K. "Synthesis of a Lipophilic Daunorubicin Derivative and its Incorporation into Lipidic Ccarriers Developed for LDL Receptor-mediated Tumor Therapy" *Pharm. Res.* **1998**, *15*, 531−537.

120. Studer, M.; Kroger, L. A.; DeNardo, S. J.; Kukis, D. L.; Meares, C. F. "Influence of a Peptide Linker on Biodistribution and Metabolism of Antibody-conjugated Benzyl EDTA. Comparison of Enzymatic Digestion In Vitro and In Vivo" *Bioconjugate Chem*. **1992**, *3*, 424−429.

121. Dubowchik, G. M.; Firestone, R. A.; Padilla, L.; Willner, D.; Hofstead, S. J.; Mosure, K.; Knipe, J. O.; Lasch, S. J.; Trail, P. A. "Cathepsin B-Labile Dipeptide Linkers for Lysosomal Release of Doxorubicin from Internalizing Immunoconjugates: Model Studies of Enzymatic Drug Release and Antigen-Specific In Vitro Anticancer Activity" *Bioconjugate Chem.* **2002**, *13*,

855–869.

122. Ulisse, S.; Baldini, E.; Sorrenti, S.; D'Armiento, M. "The Urokinase Plasminogen Activator System: A Target for Anti-Cancer Therapy" *Curr. Cancer Drug Targets* **2009**, *9*, 32−71.

123. Lijnen, H. R. "Plasmin and Matrix Metalloproteinases in Vascular Remodeling" *Thromb. Haemostasis* **2001**, *86*, 324−333.

124. Cobos, E.; Jumper, C.; Lox, C. "Pretreatment Determination of the Serum Urokinase Plasminogen Activator and its Soluble Receptor in Advanced Small-Cell Lung Cancer or Non-Small-Cell Lung Cancer" *Clin. Appl. Thromb./Hemostasis* **2003**, *9*, 241−246.

125. Werle, B.; Kotzsch, M.; Lah, T. T.; Kos, J.; Gabrijelcic-Geiger, D.; Spiess, E.; Schirren, J.; Ebert, W.; Fiehn, W.; Luther, T.; Magdolen, V.; Schmitt, M.; Harbeck, N. "Cathepsin B, Plasminogen Activator-Inhibitor (PAI-1) and Plasminogen Activator-Receptor (uPAR) are Prognostic Factors for Patients with Non-Small Cell Lung Cancer" *Anticancer Res.* **2004**, *24*, 4147−4161.

126. D'Amico, T. A.; Brooks, K. R.; Joshi, M. B.; Conlon, D.; Herndon, J.; Petersen, R. P.; Harpole, D. H. "Serum Protein Expression Predicts Recurrence in Patients with Early-stage Lung Cancer After Resection" *Ann. Thorac. Surg*. **2006**, *81*, 1982−1987; discussion on 1987.

127. de Petro, G.; Tavian, D.; Copeta, A.; Portolani, N.; Giulini, S. M.; Barlati, S. "Expression of Urokinase-type Plasminogen Activator (u-PA), u-PA Receptor, and Tissue-type PA Messenger RNAs in Human Hepatocellular Carcinoma" *Cancer Res.* **1998**, *58*, 2234−2239.

128. Zheng, Q.; Tang, Z. Y.; Xue, Q.; Shi, D. R.; Song, H. Y.; Tang, H. B. "Invasion and Metastasis of Hepatocellular Carcinoma in Relation to Urokinase-type Plasminogen Activator, its Receptor and Inhibitor" *J. Cancer Res. Clin. Oncol.* **2000**, *126*, 641−646.

129. Takeuchi, Y.; Nakao, A.; Harada, A.; Nonami, T.; Fukatsu, T.; Takagi, H. "Expression of Plasminogen Activators and Their Inhibitors in Human Pancreatic Carcinoma: Immunohisto-chemical Study" *Am. J. Gastroenterol*. **1993**, *88*, 1928−1933.

130. Cantero, D.; Friess, H.; Deflorin, J.; Zimmermann, A.; Brundler, M. A.; Riesle, E.; Korc, M.; Buchler, M. W. "Enhanced Expression of Urokinase Plasminogen Activator and its Receptor in Pancreatic Carcinoma" *Br. J. Cancer* **1997**, *75*, 388−395.

131. Shin, S. J.; Kim, K. O.; Kim, M. K.; Lee, K. H.; Hyun, M. S.; Kim, K. J.; Choi, J. H.; Song, H. S. "Expression of E-cadherin and uPA and Their Association with the Prognosis of Pancreatic Cancer" *Jpn. J. Clin. Oncol.* **2005**, *35*, 342−348.

132. Harris, J. L.; Backes, B. J.; Leonetti, F.; Mahrus, S.; Ellman, J. A.; Craik, C. S. "Rapid and General Profiling of Protease Specificity by Using Combinatorial Fluorogenic Substrate Libraries" *Proc. Natl. Acad. Sci. U.S.A.* **2000**, *97*, 7754−7759.

133. Harris, J. L.; Niles, A.; Burdick, K.; Maffitt, M.; Backes, B. J.; Ellman, J. A.; Kunts, I.; Haak-Frendscho, M.; Craik, C. S. "Difinition of the Extended Substrate Specificity Determinants of β-Tryptases I and II" *J. Biol. Chem.* **2001**, *276*, 34941−34947.

134. Backes, B. J.; Harris, J. L.; Leonetti, F.; Craik, C. S.; Ellman, J. A. "Synthesis of Positional-Scanning Libraries of Fluorogenic Peptide Substrates to Define the Extended Substrate Specificity of Plasmin and Thrombin" *Nature Biotechnology* **2000**, *18*, 187−193.

135. Gosalia, D. N.; Salisbury, C. M.; Maly, D. J.; Ellman, J. A.; Diamond, S. L. "Profiling Serine Protease Substrate Specificity with Solution Phase Fluorogenic Peptide Microarrays" *Proteomics* **2005**, *5*, 1292−1298.

136. Takeuchi, T.; Harris, J. L.; Huang, W.; Yan, K. W.; Coughlin, S. R.; Craik, C. S. "Cellular Localization of Membrane-type Serine Protease 1 and Identification of Protease-activated Receptor-2 and Single-chain Urokinase-type Plasminogen Activator as Substrates" *J. Biol. Chem*. **2000**, *275*, 26333–26342.

137. Carl, P. L.; Chakravarty, P. K.; Katzenellenbogen, J. A.; Weber, M. J. "Protease activated prodrugs for cancer chemotherapy" *Proc. Natl. Acad. Sci. U.S.A*. **1980**, *77*, 2224−2228.

138. Saxon, E.; Armstrong, J. I.; Bertozzi, C. R. " A Traceless Staudinger Ligation for the Chemoseldective Synthesis of Amide Bonds" *Org. Lett.* **2000**, *2*, 2141−2143.

Chapter 3

Staudinger Chemistry

3.1 The Staudinger Reaction

The classical Staudinger reaction was first reported by Staudinger and Meyer[1] in 1919 and has since been the focus of detailed examinations to establish the mechanism of the reaction. Based on Leffler's seminal studies,[2,3] the Staudinger reaction can be described as a two-electron reduction of an azide **1** by a phosphine **2** (Figure 3.1). Initial attack from the phosphorus lone pair on the terminal nitrogen of the azide reversibly produces a mixture of resonance-stabilized *cis*- and *trans*-phosphazide intermediates **3a** and **3b**, respectively. The *cis*-phosphazide **3a** is then proposed to eliminate dinitrogen gas via a four-membered transition state to form iminophosphorane **4**. Hydrolysis of **4** affords the familiar products of the Staudinger reaction, amine **5** and phosphine oxide **6**. However, the reaction of **4** with various electrophiles, most commonly carbonyl compounds, provides a means for their conversion into a

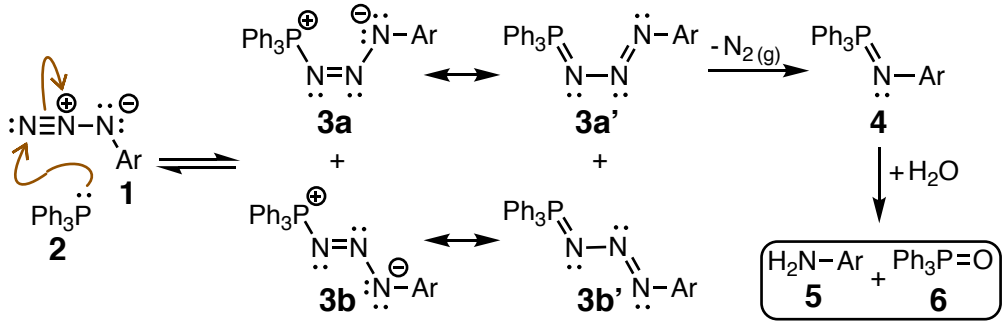

Figure 3.1 Putative mechanism of the classical Staudinger reaction.[2,3]

variety of additional products, such as amides,[4,5] amines,[6] nitro alkanes,[7] imines,[5,8] isocyanates and isothiocyantes,[9] carbamates,[6] ketenimines,[10] aziridines[11,12] and carbodiimides,[8,13] for example, thereby increasing the utility of iminophosphoranes as synthetic intermediates (Figure 3.2).

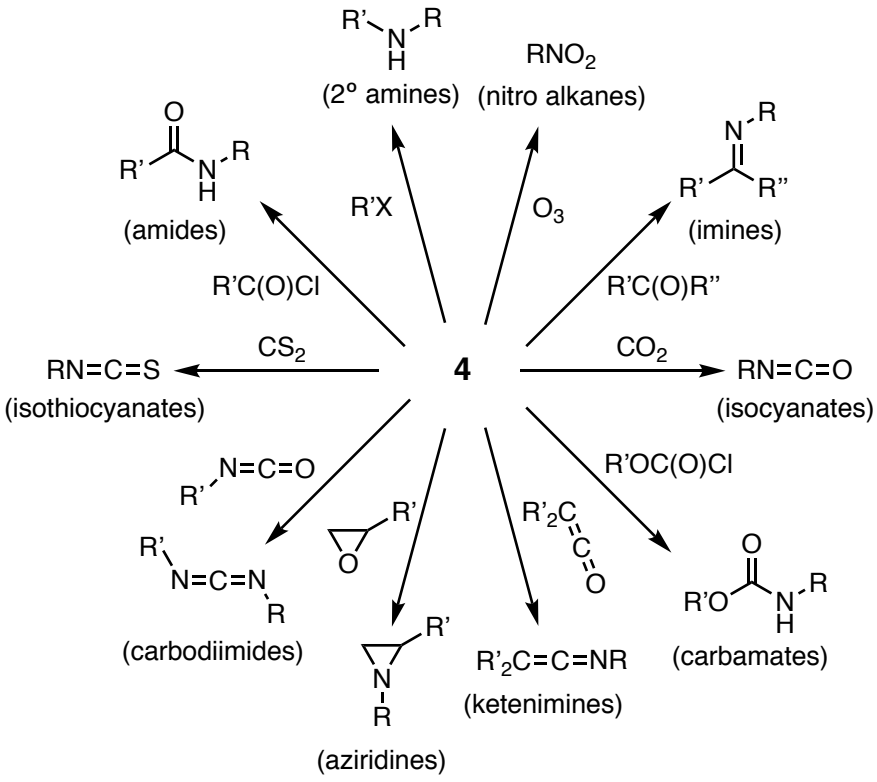

Figure 3.2 Various reactions of iminophosphorane **4** provides access to a variety of synthetically useful products.[4–13]

3.2 The Staudinger Ligation

While acylation of iminophosphoranes was known well in advance of the advent of the Staudinger ligation (Figure 3.2), the Staudinger ligation eloquently joined the acylating and reducing moieties into a single reagent **7a** (Scheme 3.1) to afford an amide product.[14] This concept was then further refined by positioning the phosphine in the leaving group position of

Scheme 3.1 Illustrations of (a) Bertozzi's Staudinger ligation[14] (b) Bertozzi's traceless Staudinger ligation[15] & (c) Raines' traceless Staudinger ligation[16] of phosphines **7a-c** and an alkyl azide; iminophosphoranes **8a-c** were proposed as intermediates in all cases.[16,17]

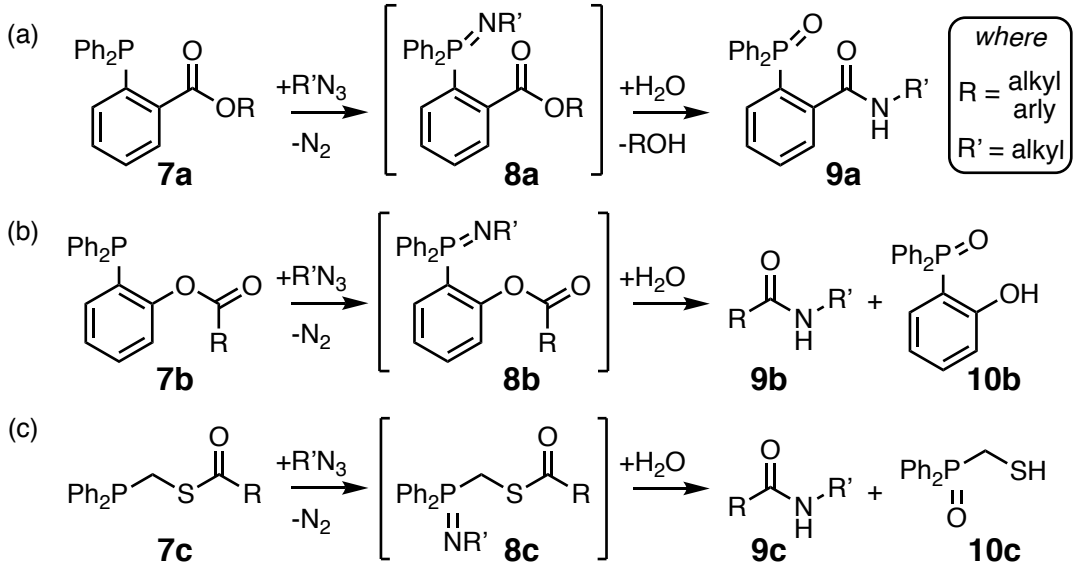

the acylating moiety, thereby providing reagents such as **7b** and **7c** that react with azides to afford amides **9b** and **9c** as products free from the phosphine oxide co-products **10b** and **10c** also formed during the reaction.[15,16] The latter two examples shown in Schemes 3.1b and 3.1c have been termed the "traceless" Staudinger ligation (TSL) to reflect the fact that the desired products are formed without a trace of the phosphine oxide co-product being retained in the newly formed amides.

Development of bioorthogonal amide bond-forming transformations, such as the Staudinger ligation, native chemical ligation and other acyl transfer methodologies, has heralded the opportunity for significant advances in the chemical and biological sciences.[19-22] The Staudinger ligation of organic azides and trivalent phosphines[15-17] is a relatively new reaction on the synthetic organic chemisty timescale, introduced by Bertozzi in 2000, that was immediately

hailed for its bioorthogonality. The azide and phosphine functional groups are essentially absent in nature allowing for highly selective reactions to be effected in extremely complex environments. For example, the Staudinger ligation has found applications in the investigation of cellular metabolism,[23,24] *in vitro*[25] and *in vivo*[26] imaging, protein engineering,[27,28] proteomics,[29,30] and as a bioconjugation technique.[31,32] Application of the Staudinger ligation in whole animals further underscores the high selectivity and remarkably mild nature of the reaction.[19,25,26] Finally, reported application[27] of the TSL in the presence of amines, such as Lys-containing proteins and peptides, suggested to us the potential of using the reaction to introduce a fully-deprotected peptide in the final step of prodrug synthesis. Such a transformation would greatly facilitate construction of our prodrugs by obviating the need for a final deprotection reaction to be carried out in the presence of the delicate anthracycline.

3.3 Aryl Azides in the Staudinger Ligation

At the outset of our investigation, use of aryl azides in the Staudinger ligation to prepare anilides was not well documented in the literature.[33,34] Although both Schultz and Bertozzi had proposed their use, neither provided sufficient evidence to refute a 2003 report in which Restituyo *et al.* claimed that the Staudinger ligation between various aryl azides and 2-(diphenylphosphino)benzoates **11** resulted in their conversion to isolable *O*-alkyl imidates **12** (Scheme 3.2).[36] Additional independent reports[37,38] of both aryl- and allyl-azides giving rise to *O*-alkyl imidates via the Staudinger ligation were found to corroborated the claim. Nevertheless, it was reasoned that in the case of the TSL of 2-(diphenylphosphino)phenyl esters, the phenol's enhanced leaving group ability would provide additional driving force for amide formation. Still, successful implementation of a new tripartite prodrug synthetic methodology based on the

TSL remained predicated on the ability of a triarylphosphine to properly shuttle the *p*-azidobenzyloxy carbamate along the desired ligation route and away from an unfruitful elimination pathway. A model system was therefore needed to assess the TSL of a *p*-azidobenzyloxy carbamate.

Scheme 3.2 Literature precedent for *O*-alkyl imidate **12** formation from a Staudinger ligation of an aryl (and allyl) azides.[36–38]

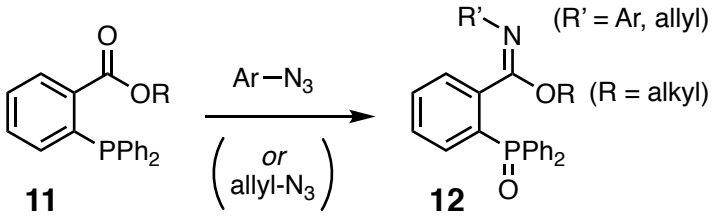

3.4 References

1. Staudinger, H.; Meyer, J. "Über Neue Organische Phosphorverbindungen III. Phosphinmethylenderivate und Phosphinimine" *Helv. Chim. Acta* **1919**, *2*, 635−646.

2. Leffler, J. E.; Temple, R. D. "The Staudinger Reaction Between Triarylphosphines and Azides. A Study of the Mechanism." *J. Am. Chem. Soc.* **1967**, *89*, 5235−5246.

3. Leffler, J. E.; Tsuno, Y. "Some Decomposition Reactions of Acid Azides" *J. Org. Chem.* **1963**, *28*, 902−906.

4. Fuchs, J. R.; Funk, R. L. "Total Synthesis of (±) Perophoramidine" *J. Am. Chem. Soc.* **2004**, *126*, 5068−5069.

5. Brase, S.; Gil, C.; Knepper, K.; Zimmermann, V. "Organic Azides: An Exploding Diversity of a Unique Class of Compounds" *Angew. Chem., Int. Ed.* **2005**, *44*, 5188−5240.

6. Johnson, A. W. In *Ylides and Imines of Phosphorus*, Wiley: New York, 1993.

7. Corey, E. J.; Samuelsson, B.; Luzzio, F. A. "A New Method for the Synthesis of Nitro Compounds" *J. Am. Chem. Soc.* **1984**, *106*, 3682−3683.

8. Johnson, A. W.; Wong, S. C. K. "The Chemistry of Ylides: Mechanism of the Reaction of Iminophosphoranes with Carbonyl Compounds" *Can*. *J. Chem.* **1966**, *44*, 2793−2803.

9. Lorenzo, A.; Aller, E.; Molina, P. "Iminophosphorane-based Synthesis of Multinuclear Ferrocenyl Urea, Thiourea and Guanidine Derivatives and Exploration of Their Anion Sensing Properties" *Tetrahedron* **2009**, *65*, 1397−1401.

10. Tsuge, O.; Kanemasa, S.; Matsuda, K. "One-pot Synthesis of *N*-[(Trimethylsilyl) Methyl] Imines and (Trimethylsilyl) Methyl-substituted Heterocumulenes from (Trimethylsilyl) Methyl Azide" *J. Org. Chem.* **1984**, *49*, 2688−2691.

11. Legters, J.; Thijs, L.; Zwanenburg, B. "A Convenient Synthesis of Optically Active 1H-Aziridine-2-Carboxylic Acids (Esters)" *Tetrahedron Lett*. **1989**, *30*, 4881−4884.

12. Pöchlauer, P.; Müller, E. P.; Peringer, P. "On the Mechanism of Aziridine Synthesis from 2-Azido-Alcohols and Triphenylphosphine" *Helv. Chim. Acta* **1984**, *67*, 1238−1247.

13. Fernandez, J. M. G.; Mellet, C. O.; Diaz, V. M.; Fuentes, P. J.; Kovacs, J.; Pinter, I. "Aza-Wittig Reaction of Sugar Isothiocyanates and Sugar Iminophosphoranes: An Easy Entry to Unsymmetrical Sugar Carbodiimides" *Tetrahedron Lett.* **1997**, *38*, 4161−4164.

14. Saxon, E.; Bertozzi, C. R. "Cell Surface Engineering by a Modified Staudinger Reaction" *Science* **2000**, *287*, 2007−2010.

15. Saxon, E.; Armstrong, J. I.; Bertozzi, C. R. "A “Traceless” Staudinger Ligation for the Chemoselective Synthesis of Amide Bonds" *Org. Lett.* **2000**, *2*, 2141−2143.

16. Nilsson, B. L.; Kiessling, L. L.; Raines, R. T. "Staudinger Ligation: A Peptide from a Thioester and Azide" *Org. Lett.* **2000**, *2*, 1939−1941.

17. Lin, F. L.; Hoyt, H. M.; Halbeek, H. Van; Bergman, R. G.; Bertozzi, C. R.; Berkeley, L. “Mechanistic Investigation of the Staudinger Ligation” *J. Am. Chem. Soc.* **2005**, *127*, 2686−2695.

18. Soellner, M. B.; Nilsson, B. L.; Raines, R. T. “Reaction Mechanism and Kinetics of the Traceless Staudinger Ligation” *J. Am. Chem. Soc.* **2006**, *128*, 8820−8828.

19. Hang, H. C.; Bertozzi, C. R. "From Mechanism to Mouse: A Tale of Two Bioorthogonal Reactions" *Acc. Chem. Res.* **2001**, *34*, 727−736.

20. Kohn, M.; Breinbauer, R. "The Staudinger Ligation - A Gift to Chemical Biology" *Angew. Chem. Int. Ed.* **2004**, *43*, 3106−3116.

21. Dawson, P. E.; Kent, S. B. H. "Synthesis of Native Proteins by Chemical Ligation" *Ann. Rev. Biochem.* **2000**, *69*, 923−960.

22. McGrath, N. A.; Raines, R. T. "Chemoselectivity in Chemical Biology: Acyl Transfer Reactions with Sulfur and Selenium" *Acc. Chem. Res.* **2011**, *44*, 752−761.

23. Saxon, E.; Luchansky, S. J.; Hang, H. C.; Yu, C.; Lee, S. C.; Bertozzi, C. R. "Investigating Cellular Metabolism of Synthetic Azidosugars with the Staudinger Ligation" *J. Am. Chem. Soc.* **2002**, *124*, 14893−14902.

24. Luchansky, S. J.; Argade, S.; Hayes, B. K.; Bertozzi, C. R. “Metabolic Functionalization of Recombinant Glycoproteins” *Biochem*istry **2004***, 43,* 12358−12366.

25. Cohen, A. S.; Dubikovskaya, E. A.; Rush, J. S.; Bertozzi, C. R. “Real-Time Bio-luminescent Imaging of Glycans on Live Cells and in Living Animals” *J. Am. Chem. Soc.* **2010**, *132*, 8563−8565.

26. Shah, L.; Laughlin, S. T.; Carrico, I. S. “Light-Activated Staudinger-Bertozzi Ligation within Living Animals” *J. Am. Chem. Soc.* **2016**, *138*, 5186−5189.

27. Tsao, M.-L.; Tian, F.; Schultz, P. G. “Selective Staudinger Modification of Proteins Containing p-Azidophenylalanine” *ChemBioChem* **2005**, *6*, 2147−2149.

28. Nilsson, B. L.; Hondal, R. J.; Soellner, M. B.; Raines, R. T. "Site-Specific Protein Immobilization by Staudinger Ligation" *J. Am. Chem. Soc.* **2003**, *125*, 5268−5269.

29. Kiick, K. L.; Saxon, E.; Tirrell, D. A.; Bertozzi, C. R. “Incorporation of Azides into Recombinant Proteins for Chemoselective Modification by the Staudinger Ligation” *Proc. Natl. Acad. Sci. U.S.A.* **2002**, *99*, 19−24.

30. Hang, H. C.; Yu, C.; Kato, D. L.; Bertozzi, C. R. “A Metabolic Labeling Approach Toward Proteomic Analysis of Mucin-type *O*-linked Glycosylation” *Proc. Natl. Acad. Sci. U.S.A.* **2003**, *100*, 14846−14851.

31. Vocadlo, D. J.; Hang, H. C.; Kim, E. J.; Hanover, J. A.; Bertozzi, C. R. “A Chemical Approach for Identifying *O*-Glc*N*Ac-modified Proteins in Cells” *Proc. Natl. Acad. Sci. U.S.A.* **2003**, *100*, 9116−9121.

32. Kohn, M.; Wacker, R.; Peters, C.; Schroder, H.; Soulere, L.; Breinbauer, R.; Niemeyer, C. M.; Waldmann, H. “Staudinger Ligation: A New Immobilization Strategy for the Preparation of Small-Molecule Arrays” *Angew. Chem., Int. Ed.* **2003**, *42*, 5830−5834.

33. Nilsson, B. L.; Soellner, M. B.; Hondal, R. J.; Raines, R. T. “Protein Assembly by Orthogonal Chemical Ligation Methods” *J. Am. Chem. Soc.* **2003**, *125*, 5268−5269.

34. Park, C-M.; Niu, W.; Liu, C.; Biggs, T. D.; Guo, J.; Xian, M. “A Proline-based Phosphine Template for Staudinger Ligation” *Org. Lett.* **2012**, *14*, 4694−4697.

35. Kosal, A. D.; Wilson, E. E.; Ashfeld, B. L. “Phosphine-based Redox Catalysis in the Direct Traceless Staudinger Ligation of Carboxylic Acids and Azides” *Angew. Chem., Int. Ed. Engl.* **2012**, *51*, 12036−12040.

36. Restituyo, J. A.; Comstock, L. R.; Petersen, S. G.; Stringfellow, T.; Rajski, S. R. “Conversion of Aryl Azides to *O*-Alkyl Imidates via Modified Staudinger Ligation” *Org. Lett.* **2003**, *5*, 4357−4360.

37. Xu, J.; DeGraw, A. J.; Duckworth, B. P.; Lenevich, S.; Tann, C.-M.; Jenson, E. C.; Gruber, S. J.; Barany, G.; Distefano, M. D. “Synthesis and Reactivity of 6,7-Dihydrogeranylazides: Reagents for Primary Azide Incorporation into Peptides and Subsequent Staudinger Ligation” *Chem. Biol. Drug Des.* **2006**, *68*, 85−96.

38. Shalimov, A. A.; Malenko, D. M.; Repina, L. A.; Sinitsa, A. D. “*N*-Substituted *N*-Phosphinotrifluoroacetamides in the Staudinger Reaction” *Russ. J. Gen. Chem.* **2005**, *75*, 1376−1378.

CHAPTER 4

Model Prodrug Synthesis via the Traceless Staudinger Ligation

4.1 Synthesis of a Model Aryl Azide

Conversion of *p*-aminobenzyl alcohol **1** to the corresponding azide **2** was accomplished in a two-step procedure of diazotization followed by displacement with azide (Scheme 4.1).[1] After conversion of **2** to the mixed *p*-nitrophenyl carbonate **3**, a reaction with β-phenethylamine provided the model aryl azide **4** in 94% yield. Note, the aryl azides **2**-**4** described here present little hazard at ambient temperature and appear stable indefinitely when protected from light and stored at -20 °C, allowing for large-scale laboratory syntheses (≥10 grams) of these compounds. Furthermore, recrystallization of intermediates **2** and **3** provided a straightforward and readily scalable means of purification.

Scheme 4.1 Synthesis of the model azide, *p*-azidobenzyloxy β-phenethylcarbamate **4**; isolated %-yields are shown in parenthesis beneath the compound numbers.[1]

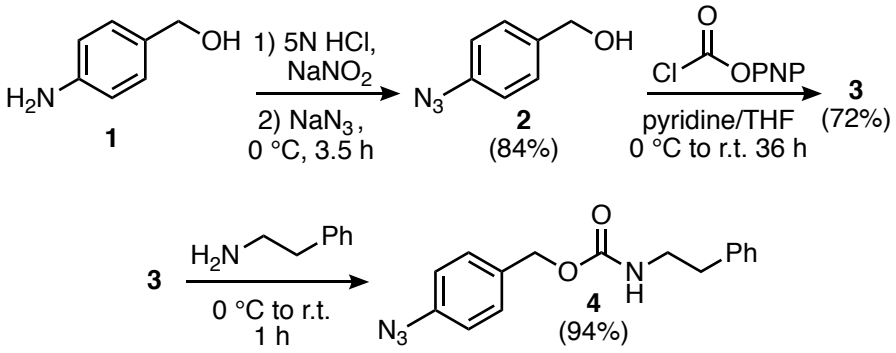

4.2 Syntheses of the Model Phosphino Phenyl Esters and Carbonates

Acylation of commercially available 2-(diphenylphosphino)phenol **5** afforded phosphino phenyl esters **6a-h** in good to near quantitative yields (Scheme 4.2 & Table 4.1). The majority of these compounds were prepared using the corresponding acid chloride or chloroformate with triethylamine in cold DCM (*method A*). This is a most convenient method that affords high yields in short reaction times. The limited solublity of protected amio acids and peptides in halogenated solvents and the need to use other coupling reagents prompted us to also explore a modified Steglich esterification, in which DCC and DMAP were combined with the carboxylic acid before adding **5** (*method B)*.[2]

Scheme 4.2 Synthesis of 2-(diphenylphosphino)phenyl esters **6a-h**.

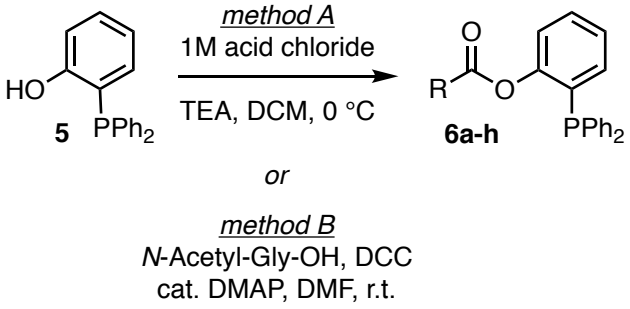

Using either method, the isolated compounds obtained following flash column chromatography (FCC) were found to be stable towards air oxidation over a period of several weeks when stored neat under argon or in a thoroghly degassed solution. However, the phosphines are not stable in the presence of either dissolved oxygen or (hydro)peroxides. The former gave ~ 50% phosphine oxide after 24 h in undegassed *d3*-acetonitrile, while dissolution of a phosphino phenyl ester in THF capped after distillation under N_2 and left to stand on the

bench for 1 h before use resulted in near quantitative oxidation to the corresponding phosphine oxide. As a result, all solvents coming into contact with the prepared phosphino phenyl esters should be thoroughly degassed and ethereal solvents freshly distilled immediately prior to use.

4.3 Results of the Model TSL for the Synthesis of Simple Anilides

The traceless Staudinger ligation between the model *p*-azidobenzyloxy carbamate **4** and phosphines **6a-h** in wet THF at ambient temperature gave the desired anilides **7a-h** in all cases (Table 4.1). Linear acyl groups transferred readily, affording excellent yields of the ligated products (entries 1, 2 and 8). Entry 8 is particularly noteworthy as the Staudinger ligation here affords the carbamate **7h** in high yield. With increasing α-substitution, the yields were diminished (entries 3-7) and an isolable iminophosphorane **9** was obtained as the major product when pivalate **6d** was examined (entry 4). Evidently, in the latter case, ester hydrolysis was a more facile reaction than hydrolysis of the P=N bond of the iminophosphorane **8** as only the phenolic iminophosphorane **9** was obtained after silica gel chromatography (Scheme 4.3, Figure 4.1). Finally, ^{1}H and ^{31}P NMR indicated that the isolated products were uncontaminated with the putative *O*-aryl imidate product previously reported to be the product obtained from the TSL of an aryl azide.[3]

Table 4.1 The traceless Staudinger ligation between aryl azide **4** and phosphines **6a–h** afforded anilides **7a–g** and the aryl carbamate **7h** in all cases.

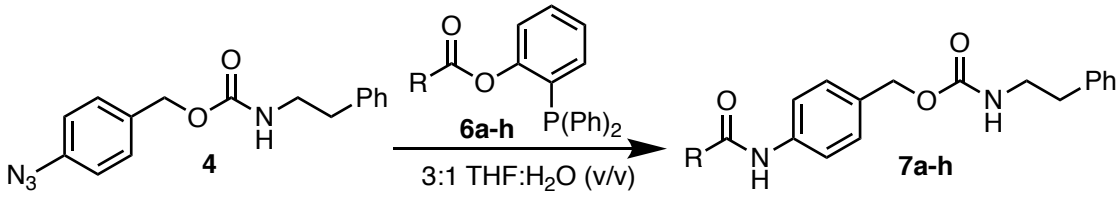

Entry	R-group	Phosphine (yield)[a]	Anilide (yield)[a,b]
1		**6a** (97%)	**7a** (93%)
2	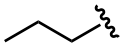	**6b** (97%)	**7b** (98%)
3		**6c** (97%)	**7c** (83%)
4		**6d** (84%)	**7d** (10%)[c]
5	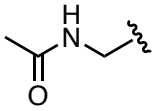	**6e** (86%)	**7e** (81%)
6	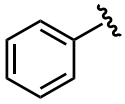	**6f** (94%)	**7f** (62%)
7	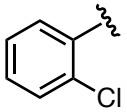	**6g** (87%)	**7g** (50%)
8	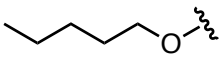	**6h** (93%)	**7h** (94%)

[a] Isolated yields after FCC purification.
[b] Average yields of at least two experiments.
[c] Iminophosphorane was the major product of reaction.

Scheme 4.3 TSL of azide **4** and pivalate **6d** afforded the iminophosphorane **8** as the major product following aqueous work-up of the reaction. However, the phenolic iminophosphorane **9** was the isolated product after FCC over silica gel.

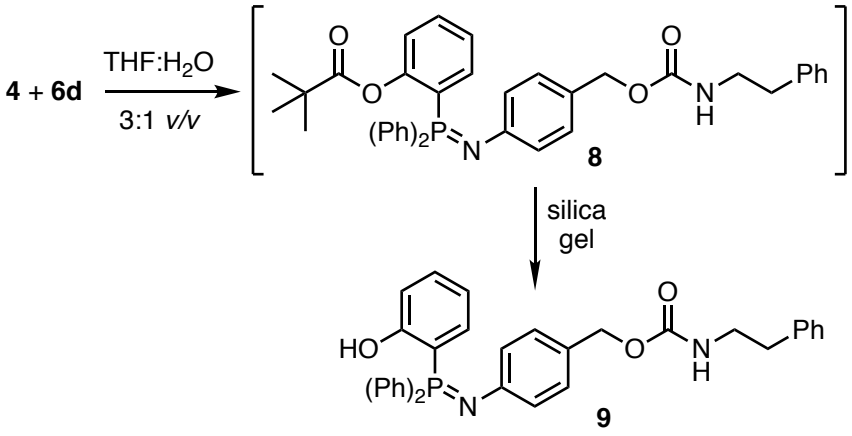

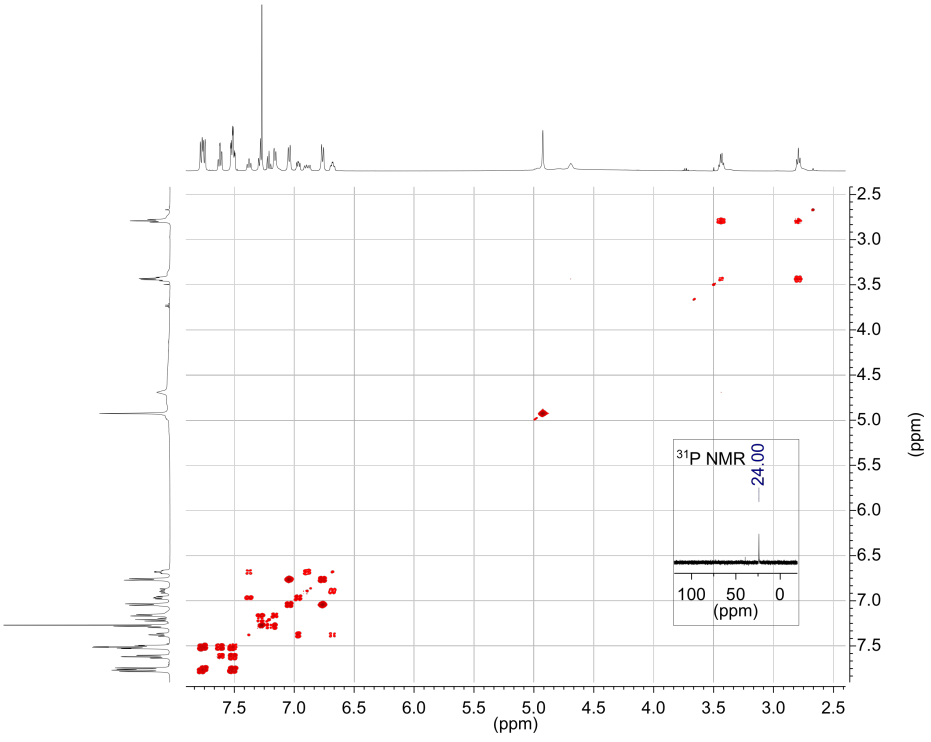

Figure 4.1 gCOSY and ^{31}P NMR spectra of the isolated iminophosphorane **9**.

4.4 Synthesis of a Model Double-PABC Spacer Containing Prodrug

Encouraged by the successful ligation of azide **4** and carbonate **6h** in preparation of carbamate **7h** (Table 4.1, entry 8), we next sought to further exploit this transformation in order to overcome the deminished yield obtained in the preparation of pivalamide **7d** (Table 4.1, entry 4). A one-pot, two-step sequential acylation of *p*-aminobenzyl alcohol (PABA) **1** was performed by initial treatment of **1** with pivaloyl chloride followed by a reaction with *p*-nitrophenyl chloroformate to afford 4-pivalamidobenzyl *p*-nitrophenyl carbonate **10** in 70% overall yield (Scheme 4.4). Subsequent displacement of *p*-nitrophenol by 2-(diphenylphosphino)phenol **5** in the presence of a two-fold excess of TEA in DCM afforded the mixed carbonate **11**, 2-(diphenylphosphino)phenyl 4-pivalamidobenzyl carbonate, in 88% yield after FCC.

Scheme 4.4 Synthesis of the mixed carbonate **11**, for installation of an elongated PABC-PABC double spacer in a subsequent TSL.

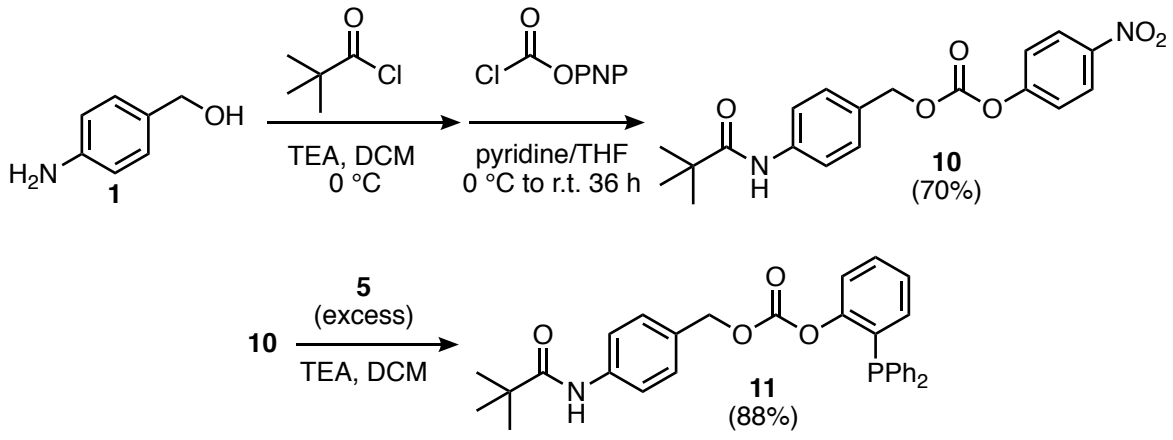

Scheme 4.5 Synthesis of an elongated PABC-PABC double spacer-containing model prodrug **12** via the TSL of azide **4** and phosphine **11**.

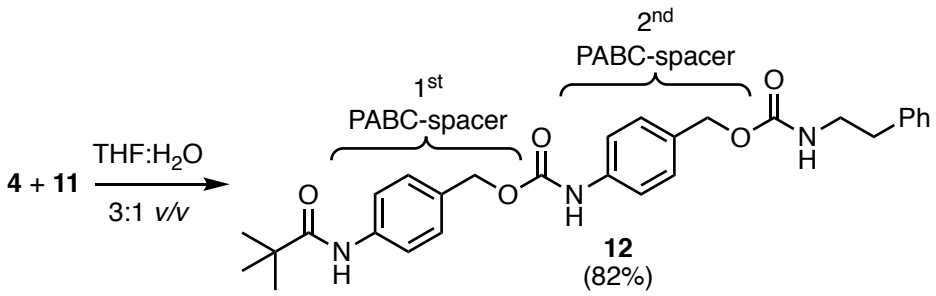

A traceless Staudinger ligation between azide **4** and phosphino phenyl carbonate **11** in wet THF afforded the elongated PABC-PABC double spacer-containing model prodrug **12**, 4-pivalamidobenzyl-PABC β-phenethylcarbamate**,** in 82% isolated yield (Scheme 4.5). In this example, the TSL was used to synthesize a model prodrug containing the sterically demanding pivalanilide group with a 72% improvement in yield for the final step of the synthesis and >40%-improved overall yield for the unoptimized 4-step sequence compared to the synthesis of **7d** (10% yield for the TSL; 8.4% yield from **5**), which relied on direct installation of the pivalanilide bond (Table 4.1, entry 4).

4.5 Conclusion

The above model studies demonstrated that a *p*-azidobenzyloxy carbamate will successfully undergo the TSL with either a phosphino phenyl ester or carbonate to afford the desired anilide or aryl carbamate in synthetically useful yields. Decomposition of the reaction intermediates from 1,6-elimination of the iminoquinone methide was not a significant side reaction. Additionally, the TSL of PABC carbonates such as **11**, offers (1) a method for the

installation of the Katzenellenbogen spacer[4] that is independent of the steric nature of the target anilide and (2) facile access to elongated prodrugs containing two Katzenellenbogen spacers.

Elongated PABC-PABC double spacer-containing prodrugs are of interest because they have been shown to exhibit improved enzymatic activation kinetics (k_{act} = 2− to 10−fold higher) compared to the analogous single-PABC spacer-containing prodrugs.[5] Correspondingly, enhanced tumor-growth inhibition and decreased systemic toxicity were observed *in vivo* for a double-PABC spacer-containing prodrug of dox relative to the single-spacer containing analogue. Presumably, the improved efficacy resulted from a more pronounced localization of drug-realease at the site of enzyme over-expression in and around the tumor.[6]

4.6 Experimental

General Methods. Unless otherwise specified, all reactions were performed in oven- or flame-dried glassware, cooled to ambient temperature inside of a desiccator prior to use, under an inert atmosphere of nitrogen or argon. Molecular sieves (3Å & 4Å) were activated in a vacuum drying oven at 180 °C and 10^{-2} Torr for 72 h and stored in a drying oven at 160 °C prior to use. Anhydrous THF was distilled from Na benzophenone ketyl under nitrogen and used immediately. MeCN was degassed by vacuum filtering through a 0.4 μm filter prior to use. Wet solvent systems were prepared using either D_2O or purified water obtained from a Milli-Q Direct water purification system from EMD Millipore (Burlington, MA). Unless specifically indicated, all reagents were acquired from reputable commercial suppliers and used as received. The *p*-aminobenzyl alcohol (PABA) used was purchased from Atomax Chemical Company (Shanghai, China) and dried under high-vacuum ($\leq$ 5 x 10^{-2} Torr) at ambient temperature for 48 h, purified by flash column chromatography (hexanes−EtOAc) and subsequently recrystallized from EtOAc

and petroleum ether (40−60 °C). Flash column chromatography (FCC)[7] was performed using 60 Å silica gel (37−75 μm, 230−400 mesh) with hexanes−EtOAc or $CHCl_3$−MeOH solvent systems as eluent. EMD glass thin-layer chromatography (TLC) plates (silica gel 60 F_{254}) were used for analytical TLC and the results visualized under 254 nm light or following exposure of the developed plate to an I_2/silica gel slurry. Retention factors (R_f) are reported along with other compound characterization data below. ^{1}H NMR spectra were recorded at 400 or 500 MHz on Varian Unity INOVA spectrometers (Palo Alto, CA) or at 300 MHz on a Bruker-Avance III spectrometer (Billerica, MA). Ambient temperature $^{13}C\{^1H\}$ and $^{31}P\{^1H\}$ NMR spectra were recorded at 75 MHz and 122 MHz, respectively, on a Bruker-Avance III spectrometer. Chemical shifts are reported in δ values of ppm with internal referencing to the residual solvent peak, whose frequencies are given by Gottlieb *et al*.[8] Coupling constants are reported as *J*-values in Hertz (Hz) with resonance multiplicities abbreviated as follows: s = singlet, d = doublet, t = triplet, q = quartet, p = pentet, sept = septet, m = multiplet, br = broad. NMR data processing and plotting, including x-referencing of $^{31}P\{^1H\}$ and ^{15}N NMR spectra, was performed using MestReNova NMR software v12.0.1 (Mestrelab Research, Santiago de Compostela, Spain). UV−vis spectroscopy was performed on a Hewlett-Packard/Agilent 8452A diode array instrument. Infrared (IR) spectra were recorded on a Thermo-Nicolet FT-IR spectrometer as thin films on NaCl plates. High-resolution mass spectra (HRMS) were obtained with a Perkin-Elmer Sciex API III+ (Waltham, MA) or ABI Pulsar QqT high-resolution instrument (Foster City, CA), equipped with an ion-spray source at atmospheric pressure. The purity of all characterized compounds was verified to be at least 95% from a combination of ^{1}H and ^{13}C NMR data.

Synthesis of compounds 2, 3 and 4. The synthesis of compounds **2** and **3** followed a scaled procedure of Griffin *et al.*[1] Assignments of the azide IR bands were taken from the published work of Lieber *et al*.[9]

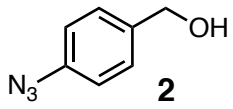

2

4-Azidobenzyl alcohol (2). A 1.8 M aqueous solution of sodium nitrite (21.0 g in 170 mL, 304 mmol) was added via dropping funnel over 90 min to a well-stirred, ice-water bath cooled solution of *p*-aminobenzyl alcohol **1** (25.0 g, 203 mmol) in 5N HCl (380 mL). Sodium azide (52.0 g, 800 mmol) was then added in small portions over 1 h maintaining vigorous N_2 evolution. The reaction was stirred at 0 °C for an additional 1 h, combined with ice water (450 mL) and basified to pH 8 with the cautious addition of solid $NaHCO_3$. Following extraction with EtOAc (5 x 50 mL), the combined organic layers were dried over anh. $MgSO_4$, filtered and concentrated under reduced pressure. The yellow oil obtained was triturated with petroleum ether (40−60 °C) and recrystallization of the resulting solid from warm EtOAc and petroleum ether (40−60 °C) afforded azide **2** (25.4 g, 84%) as cream colored crystals: mp 32–34 °C (dec.); lit. 31–33 °C.[1] R_f = 0.37 (95:5 $CHCl_3$−MeOH). IR (cm^{-1}): 3400 (O-H), 3151 (aromatic, C-H stretch), 2107 (azide, N_3 asymmetric stretch).[9] ^{1}H NMR (500 MHz, $CDCl_3$) δ 7.36 (d, 2H, *J* = 8.3 Hz, PABA-2,6), 7.02 (d, 2H, *J* = 8.3 Hz, PABA-3,5), 4.67 (d, 2H, *J* = 5.2 Hz, Bn), 1.82 ppm (t, 1H, *J* = 5.2 Hz, OH). ^{13}C NMR (75 MHz, $CDCl_3$) δ 139.6 (C-4), 137.8 (C-1), 128.7 (C-2,6), 119.3 (C-3,5), 64.9 ppm (Bn).

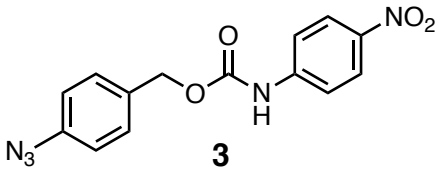

3

4-Azidobenzyl 4'-nitrophenylcarbonate (3). A solution of azido alcohol **2** (15.0 g, 100 mmol) in THF (100 mL) was added over 1 h via dropping funnel to an ice-water bath cooled suspension of 4-nitrophenyl chloroformate (20.5 g, 100 mmol) and pyridine (17.5 mL, 210 mmol) in THF (100 mL). The reaction was allowed to reach ambient temperature overnight and stirring continued until TLC indicated that the starting alcohol had been consumed (36 h). The reaction was filtered and the filtrate concentrated under reduced pressure at ambient temperature. The residual solid was dissolved in DCM (200 mL), washed with water (3 x 50 mL), brine (1 x 50 mL), then dried over anh. Na_2SO_4 and concentrated under reduced pressure. Recrystallization of the crude product from warm EtOAc and petroleum ether (40−60 °C) afforded the mixed carbonate **3** (22.5 g, 72% yield) as long white needles: mp 90−91 °C (dec.); lit. 101−102 °C.[1] R_f = 0.79 (95:5 $CHCl_3$−MeOH). IR (cm^{-1}): 2123 (azide, N_3 asymmetric stretch), 1754 (carbonyl, C=O stretch), 1519 (nitro, N-O asymmetric stretch).[9] ^{1}H NMR (300 MHz, $CDCl_3$) δ 8.41 – 8.17 (m, 2H, PNP), 7.51 – 7.42 (m, 2H, PABC-2,6), 7.42 – 7.34 (m, 2H, PNP), 7.14 – 7.02 (m, 2H, PABC-3,5), 5.27 ppm (s, 2H, Bn). ^{13}C NMR (75 MHz, $CDCl_3$) δ 155.7, 152.6, 147.4, 141.2, 131.0, 130.7, 125.5, 122.0, 119.6, 70.6 ppm. HRMS (ESI-TOF) *m/z*: $[2M+Li]^+$ calcd for $C_{28}H_{20}LiN_8O_{10}$ 635.1463; found 635.1467.

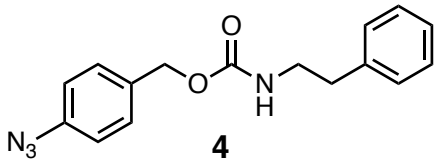

4

4-Azidobenzyl β-phenethylcarbamate (4). To a stirred solution of the mixed carbonate **3** (3.1 g, 10 mmol, 1 equiv) in THF (50 mL) at 0 °C was added β-phenethylamine (1.9 mL, 15 mmol, 1.5 mmol) as a neat liquid. The ice bath was removed and the solution was stirred at ambient temperature for 1 h. Following rotary evaporation, the residue was dissolved in EtOAc (50 mL) and washed with 0.1 M HCl (3 x 10 mL), 0.1 M NaOH (3 x 10 mL), water (1 x 10 mL) and brine (1 x 50 mL). The organic phase was dried over anh. Na_2SO_4, and concentrated under reduced pressure. Purification by FCC eluting with $CHCl_3$−MeOH (98:2 v/v) afforded the desired carbamate **4** (2.80 g, 94%) as a white solid: mp 94−96 °C. R_f = 0.67 (95:5 $CHCl_3$−MeOH). IR (cm^{-1}): 3315 (carbamate, N-H stretch), 2117 (azide, N_3 asymmetric stretch), 1682 (carbonyl, C=O stretch).[9] ^{1}H NMR (500 MHz, $CDCl_3$) δ 7.34 (d, 2H, *J* = 8.4 Hz, PABC-2,6), 7.31 (t, 2H *J* = 7.4 Hz, PEA-3,5), 7.26 – 7.22 (m, 1H, PEA-4), 7.19 (d, 2H, *J* = 7.4 Hz, PEA-2,6), 7.02 (d, 2H, *J* = 8.4 Hz, PABC-3,5), 5.06 (s, 2H, Bn), 4.78 (br. t, 1H, NH), 3.48 (apparent q, 2H, *J* = 6.7 Hz, PEA-β-CH_2), 2.83 ppm (t, 2H, *J* = 6.7 Hz, PEA-α-CH_2). ^{13}C NMR (75 MHz, $CDCl_3$) δ 156.4 (carbamate C=O), 140.1, 138.8, 133.6, 130.0, 129.0, 128.9, 126.8, 119.3, 66.2 (Bn), 42.4 (PEA-β), 36.3 ppm (PEA-α). ^{15}N NMR (40 MHz, $CDCl_3$) δ 242.6 (azide-Nβ), 233.4 (azide-Nγ), 91.9 (azide-Nα), 81.6 ppm (carbamate-NH); assignments made using ^{15}N-^{1}H HSQC and HMBC, and are in excellent agreement with the reported shifts for ^{15}N-enriched phenyl azide.[1] HRMS (ESI-TOF) *m/z*: $[2M+Na]^+$ calcd for $C_{32}H_{32}N_8NaO_4$, 615.2439; found 615.2441.

General procedure for the acylation of 2-(diphenylphosphino)phenol (5). Preparation of phosphino phenyl esters 6a-h. *Method A.* To a stirred 0.12 M solution of 2-(diphenylphosphino)phenol **5** (1 equiv) and TEA (1.4 equiv) in DCM at 0 °C was added a 1 M solution of the acid chloride or chloroformate (1.4 equiv) by syringe. The reaction was stirred in the cold until complete consumption of **5** was observed by TLC. Silica gel was added and the reaction mixture was concentrated to dryness under reduced pressure. Purification by FCC eluting with a gradient of hexane−EtOAc (1:0 to 4:1 v/v) afforded the desired alkanoic and aryloic acid esters or carbonates **6a-d** and **6f-h**. *Method B.*[2] To a stirred 0.25 M solution of *N*-acetyl glycine (1.0 equiv) and DMAP (0.1 equiv) in DMF at 0 °C was added a solution of DCC (1.0 equiv). After precipitated DCU was observed, the ice-water bath was removed and a 1 M solution of 2-(diphenylphosphino) phenol **5** (1.2 equiv) was added. The reaction was stirred under argon for 4 h, filtered and concentrated to dryness under reduced pressure. The residual solid was dissolved in $CHCl_3$ containing a small volume of MeOH and concentrated under reduced pressure onto silica gel. Purification by FCC eluting with a gradient of $CHCl_3$−MeOH (1:0 to 9:1 v/v) afforded the desired *N*-acetyl-glycinyl ester **6e**. Compounds **6a-h** were obtained in > 95% purity with the corresponding phosphine oxides as the major impurity.

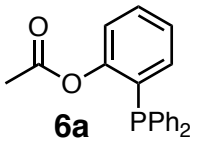

6a

2-(Diphenylphosphino)phenyl acetate (6a). 323 mg (97%) as a white solid: mp 86−88 °C. R_f = 0.27 (9:1 hexanes−EtOAc). ^{1}H NMR (500 MHz, $CDCl_3$) δ 7.44 – 7.29 (m, 11H), 7.19 – 7.11 (m, 2H), 6.87 – 6.84 (m, 1H), 1.99 ppm (s, 3H). ^{31}P NMR (122 MHz, $CDCl_3$) δ -15.9 ppm. (Note: This material was analytically identical to that obtained from the reaction of **5** with Ac_2O and cat. DMAP.)

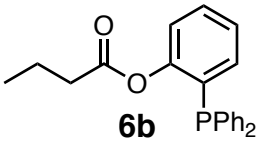

6b

2-(Diphenylphosphino)phenyl butyrate (6b). 258 mg (96%) as a white solid: mp 76−78 °C. R_f = 0.38 (9:1 hexanes−EtOAc). ^{1}H NMR (300 MHz, $CDCl_3$) δ 7.43 – 7.29 (m, 11H), 7.21 – 7.10 (m, 2H), 6.85 (dddd, 1H, *J* = 7.6, 4.3, 1.7, and 0.4 Hz), 2.23 (t, 2H, *J* = 7.3 Hz), 1.56 (sextet, 2H, *J* = 7.3 Hz), 0.90 ppm (t, 3H, *J* = 7.3 Hz). ^{13}C NMR (75 MHz, $CDCl_3$) δ 171.6, 153.0 (d, *J* = 17 Hz), 135.8 (d, *J* = 10 Hz), 134.2 (d, *J* = 20.5 Hz), 133.9 (d, *J* = 1.5 Hz), 130.4 (d, *J* = 14.5 Hz), 130.0, 129.2, 128.8 (d, *J* = 7 Hz), 126.2, 122.8, 36.0, 18.2, 13.8 ppm. ^{31}P NMR (122 MHz, $CDCl_3$) δ -16.1 ppm. HRMS (ESI-TOF) *m/z*: $[M+H]^+$ calcd for $C_{22}H_{22}O_2P$ 349.1357; found 349.1357.

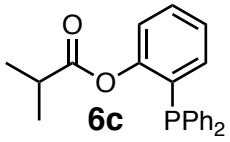

6c

2-(Diphenylphosphino)phenyl isobutyrate (6c). 118 mg (97%) as a clear oil: R_f = 0.44 (9:1 hexanes−EtOAc). ^{1}H NMR (300 MHz, $CDCl_3$) δ 7.47 – 7.28 (m, 11H), 7.22 – 7.10 (m, 2H), 6.87 – 6.77 (m, 1H), 2.57 (hept, 1H, *J* = 7.0 Hz), 1.12 ppm (d, 6H, *J* = 7.0 Hz). ^{13}C NMR (75 MHz, $CDCl_3$) δ 174.9, 153.1 (d, *J* = 17 Hz), 135.8 (d, *J* = 10 Hz), 134.1 (d, *J* = 20 Hz), 133.8 (d, *J* = 1 Hz), 130.3 (d, *J* = 15 Hz), 130.0, 129.1, 128.7 (d, *J* = 7 Hz), 126.1 (d, *J* = 0.5 Hz), 122.6 (d, *J* = 2 Hz), 34.3, 18.8 ppm. ^{31}P NMR (122 MHz, $CDCl_3$) δ -16.3 ppm. HRMS (ESI-TOF) *m/z*: $[M+H]^+$ calcd for $C_{22}H_{22}O_2P$ 349.1357; found 349.1357.

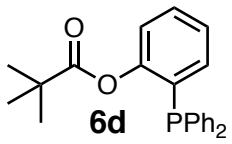

2-(Diphenylphosphino)phenyl pivalate (6d). 92 mg (84%) as a clear oil: R_f = 0.62 (4:1 hexanes−EtOAc). ^{1}H NMR (300 MHz, $CDCl_3$) δ 7.42 − 7.28 (m, 11H), 7.17 − 7.10 (m, 2H), 6.79 − 6.74 (m, 1H), 1.16 ppm (s, 9H). ^{13}C NMR (75 MHz, $CDCl_3$) δ 176.31, 153.27 (d, *J* = 17.5 Hz), 135.85 (d, *J* = 10.5 Hz), 134.09 (d, *J* = 20.5 Hz), 133.68, 130.15 (d, *J* = 15 Hz), 129.90, 129.00 (d, *J* = 0.5 Hz), 128.63 (d, *J* = 7 Hz), 125.98, 122.34 (d, *J* = 1.5 Hz), 39.25, 27.02 ppm. ^{31}P NMR (122 MHz, $CDCl_3$) δ -16.2 ppm. HRMS (ESI-TOF) *m/z*: $[M+H]^+$ calcd for $C_{23}H_{24}O_2P$ 363.1514; found 363.1517.

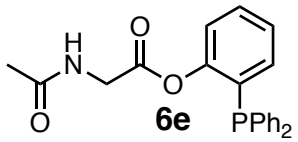

2-(Diphenylphosphino)phenyl 2-acetamidoacetate (6e). 140 mg (86%) as a clear oil: R_f = 0.36 (95:5 $CHCl_3$−MeOH). ^{1}H NMR (300 MHz, $CDCl_3$) δ 7.43 − 7.29 (m, 11H), 7.21 − 7.15 (m, 2H), 6.88 − 6.84 (m, 1H), 5.77 (br. s, 1H), 3.99 (d, 2H, *J* = 5.2 Hz), 1.96 ppm (s, 3H). ^{13}C NMR (75 MHz, $CDCl_3$) δ 170.3, 168.2, 152.4 (d, *J* = 17 Hz), 135.4 (d, *J* = 10 Hz), 134.1 (d, *J* = 20 Hz), 134.0 (d, *J* = 2 Hz), 132.2 (d, *J* = 10 Hz), 130.3 (d, *J* = 15 Hz), 130.3, 129.3, 128.9 (d, *J* = 7 Hz), 126.8 (d, *J* = 1 Hz), 122.6 (d, *J* = 1.5 Hz), 41.4, 23.0 ppm. ^{31}P NMR (122 MHz, $CDCl_3$) δ -15.9 ppm. HRMS (ESI-TOF) *m/z*: $[M+Na]^+$ calcd for $C_{22}H_{20}NNaO_3P$ 400.1078; found 400.1071.

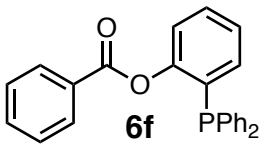

6f

2-(Diphenylphosphino)phenyl benzoate (6f). 97 mg (94%) as an opaque oil: R_f = 0.51 (4:1 hexanes−EtOAc). ^{1}H NMR (300 MHz, $CDCl_3$) δ 7.91 − 7.88 (m, 2H), 7.60 – 7.52 (m, 1H), 7.50 – 7.42 (m, 1H), 7.42 – 7.29 (m, 13H), 7.25 – 7.16 (m, 1H), 6.90 ppm (ddd, 1H, *J* = 7.6, 4.3, 1.6 Hz). ^{13}C NMR (75 MHz, $CDCl_3$) δ 164.4, 153.0 (d, *J* = 17 Hz), 135.6 (d, *J* = 10 Hz), 134.3 (d, *J* = 20.5 Hz), 133.7 (d, *J* = 1.5 Hz), 133.5, 130.9 (d, *J* = 15 Hz), 130.3, 130.1, 129.3, 129.2, 128.7 (d, *J* = 7.5 Hz), 128.4, 126.3, 122.8 ppm (d, *J* = 1.5 Hz). ^{31}P NMR (122 MHz, $CDCl_3$) δ -15.5 ppm. HRMS (ESI-TOF) *m/z*: $[M+H]^+$ calcd for $C_{25}H_{20}O_2P$ 383.1201; found 383.1199.

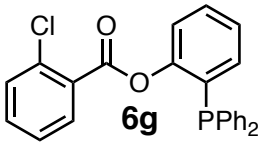

6g

2-(Diphenylphosphino)phenyl 2-chlorobenzoate (6g). 130 mg (82%) as a yellow oil: R_f = 0.32 (9:1 hexanes−EtOAc). ^{1}H NMR (300 MHz, $CDCl_3$) δ 7.72 − 7.67 (m, 1H), 7.52 − 7.30 (m, 14H), 7.26 − 7.17 (m, 2H), 6.92 ppm (ddd, 1H, *J* = 7.6, 4.3, 1.6 Hz). ^{13}C NMR (75 MHz, $CDCl_3$) δ 162.9, 152.9 (d, *J* = 17.5 Hz), 135.6 (d, *J* = 10 Hz), 134.8, 134.2 (d, *J* = 20.5 Hz), 133.2, 132.2 (d, *J* = 2 Hz), 131.3, 130.6 (d, *J* = 15 Hz), 130.2, 129.2, 128.8 (d, *J* = 7 Hz), 128.6, 126.6 (d, *J* = 2 Hz), 122.8 ppm. ^{31}P NMR (122 MHz, $CDCl_3$) δ -16.3 ppm. HRMS (ESI-TOF) *m/z*: $[M+H]^+$ calcd for $C_{25}H_{19}ClO_2P$ 417.0811; found 417.0812.

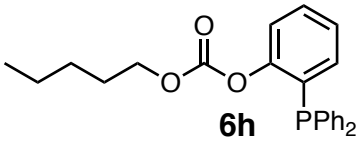

6h

2-(Diphenylphosphino)phenyl *n*-pentyl carbonate (6h). 147 mg (93%) as a clear oil: R_f = 0.28 (9:1 hexanes−EtOAc). ^{1}H NMR (500 MHz, $CDCl_3$) δ 7.43 − 7.35 (m, 11H), 7.24 (ddd, 1H, *J* = 8.1, 4.2, 1.1 Hz), 7.18 (td, 1H, *J* = 7.5, 1.1 Hz), 6.91 (ddd, 1H, *J* = 7.7, 4.2, 1.6 Hz), 4.05 (t, 2H, *J* = 6.7 Hz), 1.67 − 1.57 (m, 2H), 1.42 − 1.27 (m, 4H), 0.95 ppm (t, 3H, *J* = 7.0 Hz). ^{13}C NMR (75 MHz, $CDCl_3$) δ 153.5, 153.3, 135.8 (d, *J* = 10.5 Hz), 134.2 (d, *J* = 20.5 Hz), 132.1 (d, *J* = 10 Hz), 130.9 (d, *J* = 16 Hz), 130.4, 129.2, 128.7 (d, *J* = 7 Hz), 126.6, 122.4 (d, *J* = 1.5 Hz), 69.1, 28.3, 27.9, 22.5, 14.2 ppm. ^{31}P NMR (122 MHz, $CDCl_3$) δ -17.4 ppm. HRMS (ESI-TOF) *m/z*: $[M+Na]^+$ calcd for $C_{24}H_{25}NaO_3P$ 415.1439; found 415.1437.

General procedure for the TSL. Preparation of anilides 7a-h. To a 0.36 M solution of phosphine **6** (1.0 equiv) was added an equal volume of azide **4** (1.0 equiv) in 3:1 THF−H_2O (v/v). The reaction was stirred at ambient temperature and monitored by TLC. The precipitated phosphine oxide was removed by filtration, the filtrate diluted with DCM and washed with sat. $NaHCO_3$ and brine. The organic phase was dried over anh. Na_2SO_4 and concentrated under reduced pressure onto silica gel. Purification by FCC eluting with a gradient of $CHCl_3$−MeOH (1:0 to 9:1 v/v) provided the desired anilide **7** as a white solid in > 95% purity. Recrystallization from EtOAc and petroleum ether (40−60 °C) afforded the analytically pure compound.

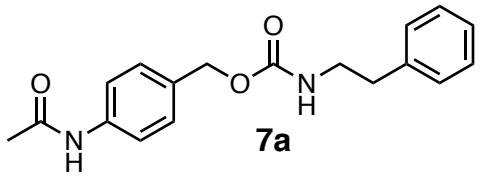

7a

4-Acetamidobenzyl phenethylcarbamate (7a). 50 mg (93%) as a white solid: mp 145−146 °C. R_f = 0.18 (98:2:1 $CHCl_3$−MeOH−AcOH). ^{1}H NMR (500 MHz, $CDCl_3$) δ 7.49 (d, 2H, *J* = 8.5 Hz), 7.44 (s, 1H), 7.35 − 7.27 (m, 4H), 7.26 − 7.20 (m, 1H), 7.18 (d, 2H, *J* = 7.3 Hz), 5.04 (s, 2H), 4.81 (s, 1H), 3.46 (t, 2H, *J* = 6.9 Hz), 2.82 (t, 2H, *J* = 6.9 Hz), 2.17 ppm (s, 3H). ^{13}C NMR (75 MHz, $CDCl_3$) δ 168.6, 156.5, 138.9, 138.0, 132.6, 129.2, 129.0, 128.8, 126.7, 120.0, 66.4, 42.4, 36.3, 24.8 ppm. HRMS (ESI-TOF) *m/z*: $[M+Na]^+$ calcd for $C_{18}H_{20}N_2NaO_3$ 335.1372; found 335.1373.

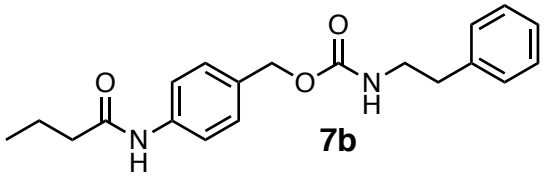

7b

4-Butyramidobenzyl phenethylcarbamate (7b). 59 mg (98%) as a white solid: mp 146−147 °C. R_f = 0.25 (98:2:1 $CHCl_3$−MeOH−AcOH). ^{1}H NMR (500 MHz, $CDCl_3$) δ 7.60 (s, 1H, PABC-NH), 7.51 (d, 2H, *J* = 8.4 Hz, PABC-3,5), 7.32 – 7.25 (m, 4H, PABC-2,6 and PEA-2,6), 7.25 – 7.20 (m, 1H, PEA-6), 7.18 (d, 2H, *J* = 7.3 Hz, PEA-3,5), 5.03 (s, 2H, Bn), 4.88 (br. s, 1H, NH), 3.45 (apparent q, 2H, *J* = 6.8 Hz, PEA-β-CH_2), 2.81 (t, 2H, *J* = 6.8 Hz, PEA-α-CH_2), 2.33 (t, 2H, *J* = 7.5 Hz, Bu-α-CH_2), 1.75 (sext, 2H, *J* = 7.4 Hz, Bu-β-CH_2), 1.00 ppm (t, 3H, *J* = 7.4 Hz, Bu-γ-CH_3). ^{13}C NMR (75 MHz, $CDCl_3$) δ 171.6, 156.5, 138.9, 138.1, 132.4, 129.2, 129.0, 128.8, 126.7, 120.0, 66.4, 42.4, 39.8, 36.3, 19.2, 14.0 ppm. HRMS (ESI-TOF) *m/z*: $[M+Na]^+$ $C_{20}H_{24}N_2NaO_3$ 363.1685; found 363.1683.

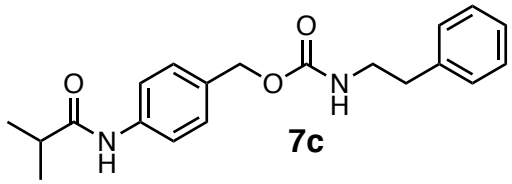

7c

4-Isobutyramidobenzyl phenethylcarbamate (7c). 53 mg (83%) as a white solid: mp 154−155 °C. R_f = 0.23 (98:2:1 $CHCl_3$−MeOH−AcOH). ^{1}H NMR (300 MHz, $CDCl_3$) δ 7.52 (d, 2H, *J* = 8.4 Hz), 7.47 (s, 1H), 7.38 − 7.28 (m, 3H), 7.26 − 7.19 (m, 2H), 7.17 (d, 2H, *J* = 7.0 Hz), 5.04 (s, 2H), 4.85 (s, 1H), 3.45 (q, 2H, *J* = 6.8 Hz), 2.81 (t, 2H, *J* = 6.8 Hz), 2.52 (hept, 1H, *J* = 6.9 Hz), 1.25 ppm (d, 6H, *J* = 6.9 Hz). ^{13}C NMR (75 MHz, $CDCl_3$) δ 175.6, 156.5, 138.8, 138.2, 132.4, 129.2, 129.0, 128.8, 126.7, 120.0, 66.4, 42.4, 36.8, 36.3, 19.8 ppm. HRMS (ESI-TOF) *m/z*: $[M+Na]^+$ $C_{20}H_{24}N_2NaO_3$ 363.1685; found 363.1685.

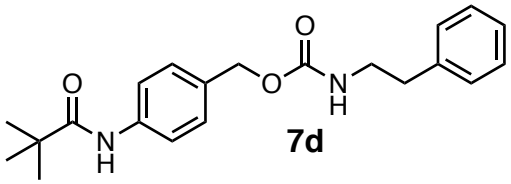

7d

4-Pivalamidobenzyl phenethylcarbamate (7d). 10 mg (10%) as a white solid: mp 128−130 °C. R_f = 0.11 (4:1 hexanes−EtOAc). ^{1}H NMR (300 MHz, $CDCl_3$) δ 7.53 (d, 2H, *J* = 8.5 Hz), 7.48 (s, 1H), 7.34 – 7.21 (m, 5H), 7.17 (d, 2H, *J* = 8.5 Hz), 5.04 (s, 2H), 4.90 (br. s, 1H), 3.45 (apparent q, 2H, *J* = 6.7 Hz), 2.81 (t, 2H, *J* = 6.9 Hz), 1.32 ppm (s, 9H). ^{13}C NMR (75 MHz, $CDCl_3$) δ 176.75, 156.47, 138.16, 136.86, 132.54, 129.27, 128.99, 128.85, 126.74, 120.05, 66.45, 42.42, 39.86, 36.31, 27.85 ppm. HRMS (ESI-TOF) *m/z*: $[M+Na]^+$ calcd for $C_{21}H_{26}N_2NaO_3$ 377.1841; found 377.1842.

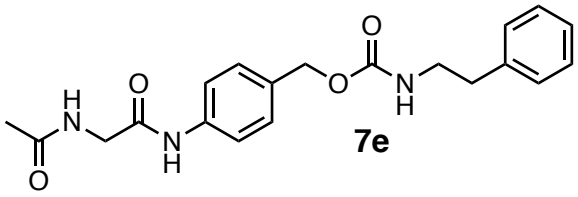

7e

4-(2-Acetamidoacetamido)benzyl phenethylcarbamate (7e). 46 mg (81%) as a white solid: mp 202−204 °C. R_f = 0.40 (9:1 $CHCl_3$−MeOH). ^{1}H NMR (500 MHz, DMSO) δ 10.06 (s, 1H), 8.25 (t, 1H, *J* = 5.5 Hz), 7.57 (d, 2H, *J* = 8.2 Hz), 7.32 (t, 1H, *J* = 5.3 Hz), 7.30 − 7.27 (m, 4H), 7.26 − 7.18 (m, 3H), 4.93 (s, 2H), 3.86 (d, 2H, *J* = 5.5 Hz), 3.21 (dd, 2H, *J* = 7.3, 5.3 Hz), 2.71 (t, 2H, *J* = 7.3 Hz), 1.88 ppm (s, 3H). ^{13}C NMR (75 MHz, DMSO) δ 169.7, 167.9, 156.1, 139.3, 138.5, 131.8, 128.6, 128.5, 128.3, 126.1, 118.9, 64.9, 42.7, 41.9, 35.4, 22.4 ppm. HRMS (ESI-TOF) *m/z*: $[M+Na]^+$ calcd for $C_{20}H_{23}N_3NaO_4$ 392.1586; found 392.1584.

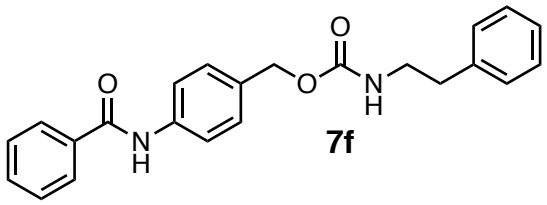

7f

4-Benzamidobenzyl phenethylcarbamate (7f). 49 mg (62%) as a white solid: mp 156−158 °C. R_f = 0.10 (80:20:1 hexanes−EtOAc−AcOH). ^{1}H NMR (300 MHz, $CDCl_3$) δ 7.99 (s, 1H), 7.93 – 7.83 (m, 2H), 7.65 (d, 2H, *J* = 8.5 Hz), 7.60 – 7.43 (m, 3H), 7.40 – 7.28 (m, 4H), 7.24 (dt, 1H, *J* = 5.5, 2.3 Hz), 7.21 – 7.09 (m, 2H), 5.07 (s, 2H), 4.82 (br. t, 1H, *J* = 6.3 Hz), 3.46 (dd, 2H, *J* = 6.8, 6.3 Hz), 2.82 ppm (t, 2H, *J* = 6.8 Hz). ^{13}C NMR (75 MHz, $CDCl_3$) δ 166.0, 156.5, 138.9, 138.1, 135.1, 132.9, 132.1, 129.3, 129.0, 128.8, 127.3, 126.7, 120.4, 66.4, 42.4, 36.3 ppm. HRMS (ESI-TOF) *m/z*: $[M+Na]^+$ calcd for $C_{23}H_{22}N_2NaO_3$ 397.1528; found 397.1536.

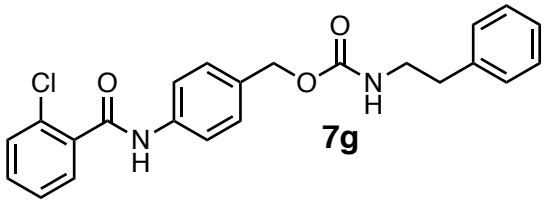

7g

4-(2-Chlorobenzamido)benzyl phenethylcarbamate (7g). 42 mg (50%) as a white solid: mp 133−134 °C. R_f = 0.64 (9:1:0.1 $CHCl_3$−MeOH−AcOH). ^{1}H NMR (300 MHz, $CDCl_3$) δ 7.94 (s, 1H), 7.81 − 7.72 (m, 1H), 7.65 (d, 2H, *J* = 8.5 Hz), 7.50 − 7.28 (m, 7H), 7.26 − 7.21 (m, 1H), 7.19 (d, 2H, *J* = 7.0 Hz), 5.08 (s, 2H), 4.77 (br. t, 1H), 3.47 (apparent q, 2H, *J* = 6.8 Hz), 2.83 ppm (t, 2H, *J* = 6.8 Hz). ^{13}C NMR (75 MHz, $CDCl_3$) δ 164.6, 156.4, 138.9, 137.6, 135.3, 133.3, 132.0, 130.8, 130.6, 130.6, 129.4, 129.0, 128.8, 127.5, 126.7, 120.3, 66.4, 42.4, 36.3 ppm. HRMS (ESI-TOF) *m/z*: $[M+Na]^+$ calcd for $C_{23}H_{21}ClN_2NaO_3$ 431.1138; found 431.1139.

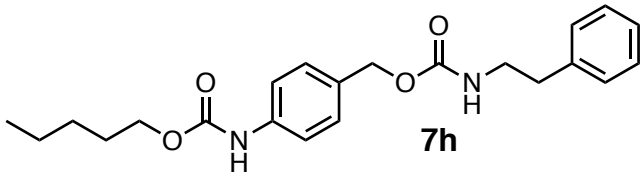

7h

***n*-Pentyl (4-(((phenethylcarbamoyl)oxy)methyl)phenyl)carbamate (7h).** 53 mg (94%) as a white solid: mp 90−92 °C. R_f = 0.16 (80:20:1 hexanes−EtOAc−AcOH). ^{1}H NMR (300 MHz, $CDCl_3$) δ 7.39 (d, 2H, *J* = 8.4 Hz), 7.35 − 7.28 (m, 4H), 7.26 − 7.21 (m, 1H), 7.19 (d, 2H, *J* = Hz), 6.85 (s, 1H), 5.05 (s, 2H), 4.83 (br. t, 1H), 4.17 (t, 2H, *J* = 6.7 Hz), 3.47 (apparent q, 2H, *J* = 6.7 Hz), 2.82 (t, 2H, *J* = 7.0 Hz), 1.75 − 1.61 (m, 2H), 1.43 − 1.31 (m, 4H), 0.98 − 0.89 ppm (m, 3H). ^{13}C NMR (75 MHz, $CDCl_3$) δ 156.5, 153.9, 138.9, 138.2, 131.5, 129.4, 128.9, 128.8, 126.7, 118.7, 66.5, 65.6, 42.4, 36.2, 28.8, 28.2, 22.5, 14.2 ppm. HRMS (ESI-TOF) *m/z*: $[M+Na]^+$ calcd for $C_{22}H_{28}N_2NaO_4$ 407.1947; found 407.1947.

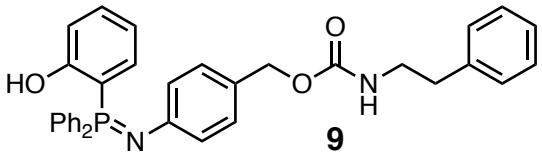

9

Iminophosphorane (9). Isolation of iminophosphorane **9** occurred during the attempted purification of iminophosphorane **8**, which was obtained as the major product from the TSL of azide **4** and phosphine **6d**. Purification of crude **8** by FCC eluting with a gradient of $CHCl_3$−MeOH (1:0 to 9:1 v/v) resulted in ester hydrolysis while the material was on the column and instead afforded iminophosphorane **9** (30.6 mg, 56%) as a clear oil: ^{1}H NMR (500 MHz, $CDCl_3$) δ 7.78 (dd, 4H, *J* = 12.3, 7.5 Hz), 7.65 – 7.60 (m, 2H), 7.51 (td, 4H, *J* = 7.7, 2.9 Hz), 7.38 (t, 1H, *J* = 7.8 Hz), 7.29 (t, 2H, *J* = 7.3 Hz), 7.21 (dd, 1H, *J* = 8.3, 6.4 Hz), 7.16 (d, 2H, *J* = 7.3 Hz), 7.04 (d, 2H, *J* = 8.1 Hz), 6.97 (dd, 1H, 6.2, 5.4 Hz), 6.89 (dd, 1H, *J* = 15.4, 7.8 Hz), 6.76 (d, 2H, *J* = 8.2 Hz), 6.68 (td, 1H, *J* = 7.4, 3.17 Hz), 4.93 (s, 2H), 4.69 (br. s, 1H), 3.44 (q, 2H, *J* = 6.7 Hz), 2.79 ppm (t, 2H, *J* = 6.9 Hz). ^{13}C NMR (75 MHz, $CDCl_3$) δ 156.77, 156.56, 134.93, 133.32, 133.19, 133.09, 132.19, 132.02, 131.73, 129.71, 129.43, 129.26, 128.98, 128.82, 126.69, 121.121.83, 121.69, 117.33, 66.97, 42.35. 36.28, 29.93 ppm. ^{31}P NMR (122 MHz, $CDCl_3$) δ 24.0 ppm.

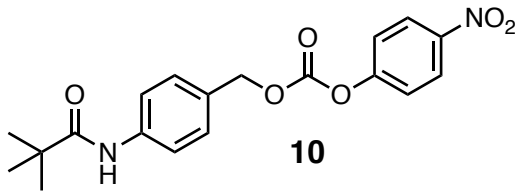

10

4-Nitrophenyl 4'-pivalamidobenzyl carbonate (10). To a stirred solution of *p*-aminobenzyl alcohol **1** (1.23 g, 10 mmol) and DIEA (1.75 mL, 10 mmol) in DCM (30 mL) at 0 ^{0}C was added a 1 M solution of pivaloyl chloride (1.23 mL, 10 mmol) in DCM. The reaction was stirred under argon until complete consumption of **1** was observed by TLC. Pyridine (805 μL, 10 mmol) was

then added to the reaction flask followed by a 1 M solution of *p*-nitrophenyl chloroformate (2.02 g, 10 mmol) in DCM. The ice-water bath was removed and the reaction was stirred at ambient temperature until complete consumption of the benzyl alcohol was observed (72 h). The reaction was filtered, the filtrate diluted with DCM (150 mL) and washed with sat. $NaHCO_3$ (3 x 50 mL), water (3 x 50 mL), brine (1 x 50 mL) and dried over anh. Na_2SO_4. The organic phase was concentrated under reduced pressure and purified by FCC over silica gel eluting with hexanes−EtOAc (4:1 v/v) to afford the desired mixed carbonate **11** (2.61 g, 70% from **1**) as a white solid: mp 124−126 °C. R_f = 0.10 (4:1 hexanes−EtOAc). ^{1}H NMR (300 MHz, $CDCl_3$) δ 8.30 – 8.23 (m, 2H), 7.63 – 7.55 (m, 2H), 7.44 – 7.39 (m, 2H), 7.38 (s, 1H), 7.40 – 7.34 (m, 2H), 5.25 (s, 2H), 1.33 ppm (s, 9H). HRMS (ESI-TOF) *m/z*: $[M+Na]^+$ calcd for $C_{19}H_{20}N_2NaO_6$ 395.1219; found 395.1217.

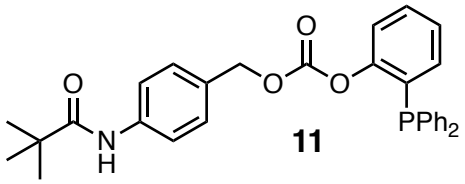

11

2-(Diphenylphosphino)phenyl 4-pivalamidobenzyl carbonate (11). To a stirred 0.18 M solution of the mixed carbonate **10** (93 mg, 250 μmol, 1.0 equiv) and phenol **5** (70 mg, 250 μmol, 1.0 equiv) in DCM (1.43 mL) was added neat TEA (70 μL, 500 μmol, 2.0 equiv) in one portion by syringe. Addition of the base immediately caused the solution to turn slightly yellow and the intensity of the color steadily increased as the reaction progressed indicating *p*-nitrophenol was being formed. The reaction was stirred at ambient temperature, under argon, until complete consumption of **10** was observed by TLC and ^{31}P NMR indicated that complete consumption of **5** had also occurred. Silica gel was added to the flask and the reaction mixture was concentrated to dryness under reduced pressure. Purification by FCC eluting with a gradient

of hexane−EtOAc (1:0 to 4:1 v/v) afforded the desired phosphino phenyl carbonate **11** (116.4 mg, 91%) as a yellow oil: R_f = 0.16 (4:1 hexanes−EtOAc). ^{1}H NMR (300 MHz, $CDCl_3$) δ 7.56 – 7.52 (m, 2H), 7.42 – 7.30 (m, 12H), 7.29 – 7.23 (m, 2H), 7.22 – 7.13 (m, 2H), 6.91 – 6.83 (m, 1H), 4.98 (s, 2H), 1.33 ppm (s, 9H). ^{13}C NMR (75 MHz, $CDCl_3$) δ 176.81, 153.46, 153.23, 153.18, 138.51, 135.73, 135.60, 134.31, 134.07, 134.04, 132.10, 131.96, 130.98, 130.76, 130.67, 130.39, 129.53, 129.45, 129.18, 128.78, 128.69, 128.59, 126.67, 122.33, 122.31, 120.06, 119.98, 70.02, 39.87, 27.84 ppm. ^{31}P NMR (122 MHz, $CDCl_3$) δ -17.5 ppm. HRMS (ESI-TOF) *m/z*: $[M+H]^+$ calcd for $C_{31}H_{32}NO_4P$ 512.1986; found 512.1990.

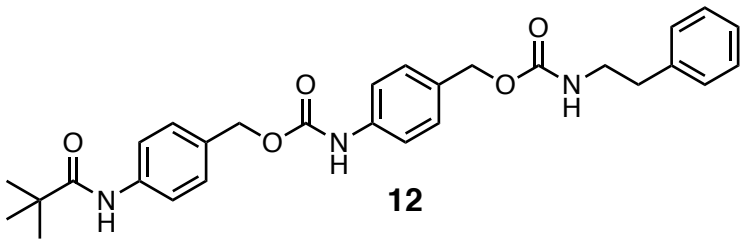

12

4-Pivalamido-PABC-PABC β-phenethylcarbamate (12). Carbamate **12** (42 mg, 82%) was prepared according to the general procedure for the traceless Staudinger ligation described above and was isolated as a white solid: mp 162−163 °C. R_f = 0.16 (80:20:1 hexanes−EtOAc−AcOH). ^{1}H NMR (500 MHz, $CDCl_3$) δ 7.59 – 7.52 (m, 2H, $PABC_1$-3,5), 7.47 – 7.36 (m, 4H, $PABC_1$-2,6 & $PABC_2$-3,5), 7.35 (s, 1H, $PABC_1$-NH), 7.33 – 7.28 (m, 4H, $PABC_2$-2,6 & PEA-3,5), 7.25 – 7.21 (m, 1H, PEA-4), 7.18 (d, 2H, *J* = 7.3 Hz, PEA-2,6), 6.69 (s, 1H, $PABC_2$-NH), 5.16 (s, 2H, $PABC_1$-Bn), 5.04 (s, 2H, $PABC_2$-Bn), 4.73 (br. t, 1H, *J* ~ 5.5 Hz, PEA-β-NH), 3.46 (apparent q, 2H, *J* = 6.7 Hz, PEA-β), 2.82 (t, 2H, *J* = 7.0 Hz, PEA-α), 1.33 ppm (s, 9H, Piv-methyls). HRMS (ESI-TOF) *m/z*: $[M+Na]^+$ calcd for $C_{29}H_{33}N_3NaO_5$ 526.2318; found 526.2319.

4.7 References

1. Griffin, R. J.; Evers, E.; Davison, R.; Gibson, A. E.; Layton, D.; Irwin, W. J. "The 4-Azidobenzyloxycarbonyl Function: Application as a Novel Protecting Group and Potential Prodrug Modification for Amines" *J. Chem. Soc., Perkin Trans. 1* **1996**, 1205−1211.

2. Neises, B.; Steglich, W. "A Simple Method for the Esterification of Carboxylic Acids" *Angew. Chem., Int. Ed.* **1978**, *17*, 522−524.

3. Restituyo, J. A.; Comstock, L. R.; Petersen, S. G.; Stringfellow, T.; Rajski, S. R. "Conversion of Aryl Azides to *O*-Alkyl Imidates via Modified Staudinger Ligation" *Org. Lett.* **2003**, *5*, 4357−4360.

4. Carl, P. L.; Chakravarty, P. K.; Katzenellenbogen, J. A. "A Novel Connector Linkage Applicable in Prodrug Design" *J. Med. Chem.* **1981**, *24*, 479−480.

5. de Groot, F. H.; Loos, W. J.; Koekkoek, R.; van Berkom, L. W. A.; Busscher, G. F.; Seelen, A. E.; Albrecht, C.; de Bruijn, P.; Scheeren, H. W. "Elongated Multiple Electronic Cascade and Cyclization Spacer Systems in Activatible Anticancer Prodrugs for Enhanced Drug Release" *J. Org. Chem.* **2001**, *66*, 8815−8830.

6. Devy, L.; de Groot, F. H. M.; Blacher, S.; Hajitou, A.; Beusker, P.; Scheeren, W.; Foldart, J.-M.; Noel, A. "Plasmin-activated Doxorubicin Prodrugs Containing a Spacer Reduce Tumor Growth and Angiogenesis Without Systemic Toxicity" *FASEB J.* **2004**, *18*, 565−567.

7. Still, C. W.; Kahn, M.; Mitra, A. "Rapid Chromatographic Technique for Preparative Separations with Moderate Resolution" *J. Org. Chem.* **1978**, *43*, 2923−2925.

8. Fulmer, G. R.; Miller, A. J. M.; Sherden, N. H.; Gottlieb, H. E.; Nudelman, A.; Stoltz, B. M.; Bercaw, J. E.; Goldberg, K. I. "Chemical Shifts of Trace Impurities: Common Laboratories Solvents, Organics, and Gases in Deuterated Solvents Relevant to the Organometallic Chemist" *Organometallics* **2010**, *29*, 2176−2179.

9. Lieber, E.; Rao, C. N. R.; Chao, T. S.; Hoffman, C. W. W. "Infrared Spectra of Organic Azides" *Anal. Chem.* **1957**, *29*, 916−918.

Chapter 5

Peptide-Specifiers and Phosphinyl Phenyl Esters Thereof

5.1 Introduction

Our first design of a proteolytically-activated tripartite prodrug of doxazolidine was based upon previously published work on dox,[1] but was limited in its development potential by persistent epimerization of the terminal, non-natural D-alanine residue during the final deprotection step of synthesis.[2] The loss of the non-natural isomer at the N-terminus would be expected to increase the susceptibility of the prodrug to degradation by nonspecific aminopeptidase activity and, in turn, this may result in diminished plasma stability of the intact prodrug. Perhaps more importantly, a mixture of peptidyl substrates could result in unknown catalytic hydrolysis rates from the targeted enzymes, which may change the profile of activating proteases and potentially introduce a host of side effects that may otherwise not be present in therapy which used a single diastereomer. From the small amounts of optically pure aFK-PABC-Doxaz that could be isolated, we were able to demonstrate that additional efforts to improve the design and synthesis of a protease-activated doxaz prodrug were warranted. Encouraged by the results of our model study, application of the traceless Staudinger ligation[3] for the late-stage installation of the Katzenellenbogen-spacer in the synthesis of peptidyl prodrugs of doxaz appeared poised to allow for rapid exploration of the surrounding chemical space. As proposed, this methodology required that peptidyl esters of Bertozzi's 2-(diphenylphosphino)phenol be prepared. This chapter deals with the synthesis of the selected peptide-specifiers and their subsequent conversion to phosphinyl phenyl esters.

5.2 Syntheses of Protected Peptides

Five peptide sequences were selected based on the enzyme substrate specificities discussed in Ch. 2.3 of this thesis: *N*-Acetyl-Gly-D-Ala-L-Phe-L-Lys-OH (*N*-Ac-GaFK) **1**,[1,2] *N*-Acetyl-Gly-L-Val-L-Cit-OH **2**,[4,5] *N*-Acetyl-L-Val-L-Cit-OH **3**,[4,5] *N*-Acetyl-Gly-L-Ala-OH **4**,[6] and *N*-Acetyl-L-Val-L-Ala-OH **5**.[6] The tetrapeptide *N*-Ac-GaFK **1** was designed to avoid the potential loss of defined stereogenicity of the D-alanine residue by incorporating an achiral, *N*-acetylated glycine residue at the *N*-terminus of the peptide. Hence, only the lysine ε-amino group of **1** required orthogonal protection during synthesis and two different protecting group strategies were selected for this purpose: Cbz[7,8] (**1a**) and alloc[8,9] (**1b**). Based on the reported bioorthogonality of the TSL, we proposed using a deprotected peptidyl ester in the final synthetic step to obtain *N*-Ac-GaFK-PABC-Doxaz. Catalytic hydrogenation of a Cbz-protecting group was proposed to be a sufficiently mild deprotection reaction compatible with a phenyl ester substrate based on precedent from Williams, *et al*.[10] However, given the general lability of phenyl esters, the success of the proposed Cbz-deprotection strategy was not certain. As we wished to move forward quickly with preparation of the target prodrug and begin its biological characterization, a contingency plan was also proposed. In the event that the Cbz strategy proved to be problematic, the TSL of a protected peptidyl ester would instead be used in the penultimate step of synthesis and the alloc-protecting group subsequently removed using η^3-allylpalladium chemistry.[9,11] Thus, a total of six peptides were selected and their respective syntheses by solid-phase peptide synthesis (SPPS) using an N^{α}-Fmoc strategy[12,13] are shown in Scheme 5.1.

Loading of the first amino acid onto 2-chlorotrityl chloride [Trt(2-Cl)-Cl] resin[14] was performed by combining the desired C-terminal N^{α}-Fmoc amino acid and resin with DIEA and DCM in a pear-shaped flask equipped with a glass frit side-arm and PTFE stop cock, which was

Scheme 5.1 SPPS[a] of peptides **1a** *N*-Ac-Gly-D-Ala-L-Phe-L-Lys(Cbz)-OH,[1,2] **1b** *N*-Ac-Gly-D-Ala-L-Phe-L-Lys(alloc)-OH,[1,2] **2** *N*-Ac-Gly-L-Val-L-Cit-OH,[4,5] **3** *N*-Ac-L-Val-L-Cit-OH,[4,5] **4** *N*-Ac-Gly-L-Ala-OH,[6] and **5** *N*-Ac-L-Val-L-Ala-OH;[6] (where Ac = acetyl).

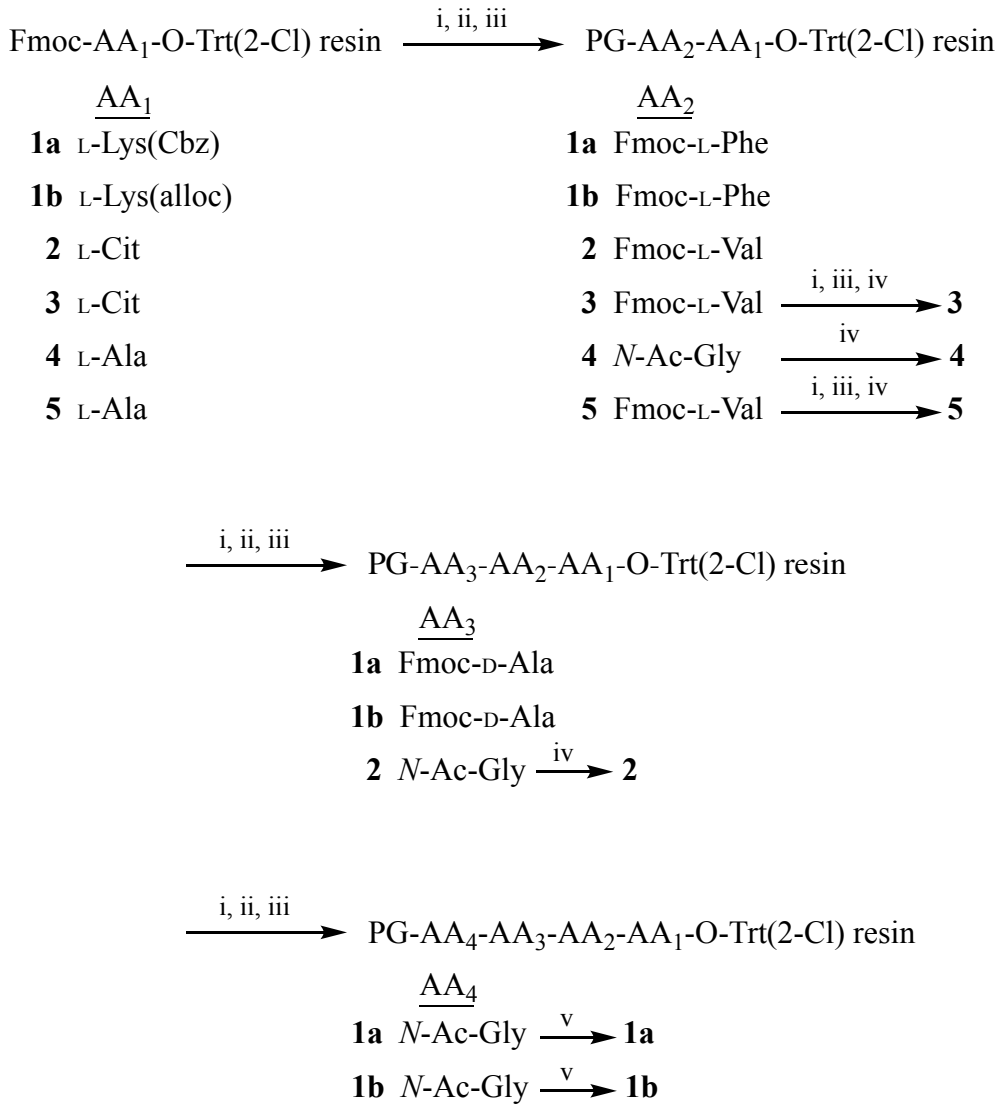

[a] Conditions: (i) 20% piperidine/DMF (v/v);[15,16] (ii) AA_n (4 equiv), 0.5 M DIEA/DMF, 0.45 M HBTU/HOBt/NMP;[15,16] (iii) Ac_2O/HOBt/DIEA/NMP;[15,16] (iv) 1% TFA/DCM (v/v).[14]

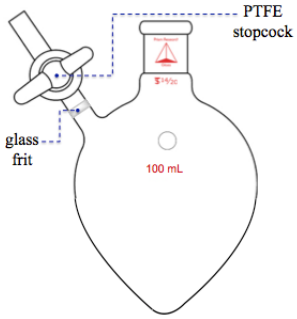

Figure 5.1 Custom-made 100 mL pear-shaped flask with glass frit side-arm and PTFE stopcock used in SPPS for resin loading and cleavage procedures.

custom-made in the glass shop (Figure 5.1). The mixture was periodically agitated by hand over 2 h, filtered through the side-arm using positive N_2-pressure and unreacted sites on the resin quenched with MeOH. Following thorough washing of the resin and drying under reduced pressure, the resin loading was determined spectrophotometrically at 294 nm ($\varepsilon = 8794\ M^{-1}\ cm^{-1}$) using DBU **6** (Scheme 5.2b) according to the method of Gude *et al*.[17] Calculated resin loading values typically ranged from 0.5−1.0 mmol of Fmoc amino acid per gram of resin, which is considered to be ideal as higher loadings may diminish the efficiency of reactions occurring near the surface of the bead and degrade the purity of the isolated peptide.[18]

During SPPS, standard Fmoc-deprotection conditions of 20% piperidine **7** in DMF (v/v) were used. Liberation of dibenzofulvene (DBF) **12** via an $E1_cB$ mechanism involving intermediate **10** has been proposed (Scheme 5.2).[17,19] After decarboxylation of the liberated carbamic acid, DBF **12** is trapped by **7**, which is present in large excess during deprotection cycles. *In situ* activation of the incoming N^{α}-protected amino acid was accomplished by deprotonation with 2 M DIEA/NMP **t**o generate carboxylate **14**, followed by the addition of 0.45 M HBTU/HOBt (**15/16**) in DMF to generate the active ester **20** (Scheme 5.3).[20-22] A 4-fold excess of **20** was then added to the resin-bound free base **11** to effect peptide bond

Scheme 5.2 E1cB mechanism of Fmoc-deprotection showing (a) the reversible formation of the piperidine-dibenzofulvene adduct **13** from piperidine **7** and (b) the structure of DBU **6**, the base used for Fmoc-deprotection in resin loading determinations.[17,19]

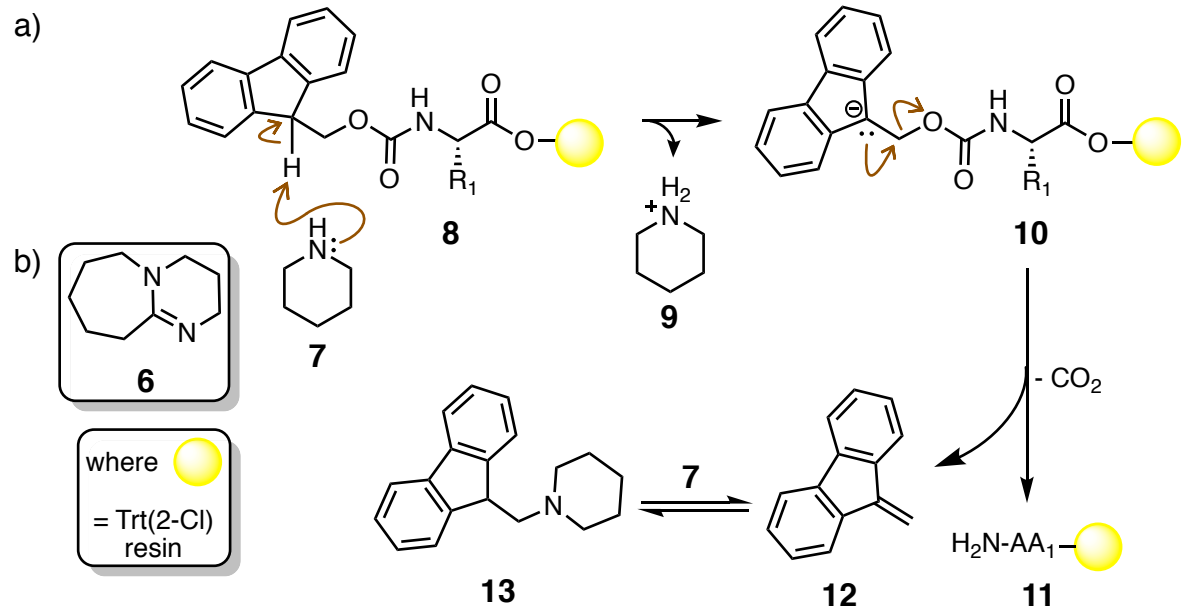

Scheme 5.3 *In situ* activation of carboxylate **14** with HBTU/HOBt **15/16** generated the active ester **20**, which was then added to the resin **11** to effect peptide bond formation.[20-22]

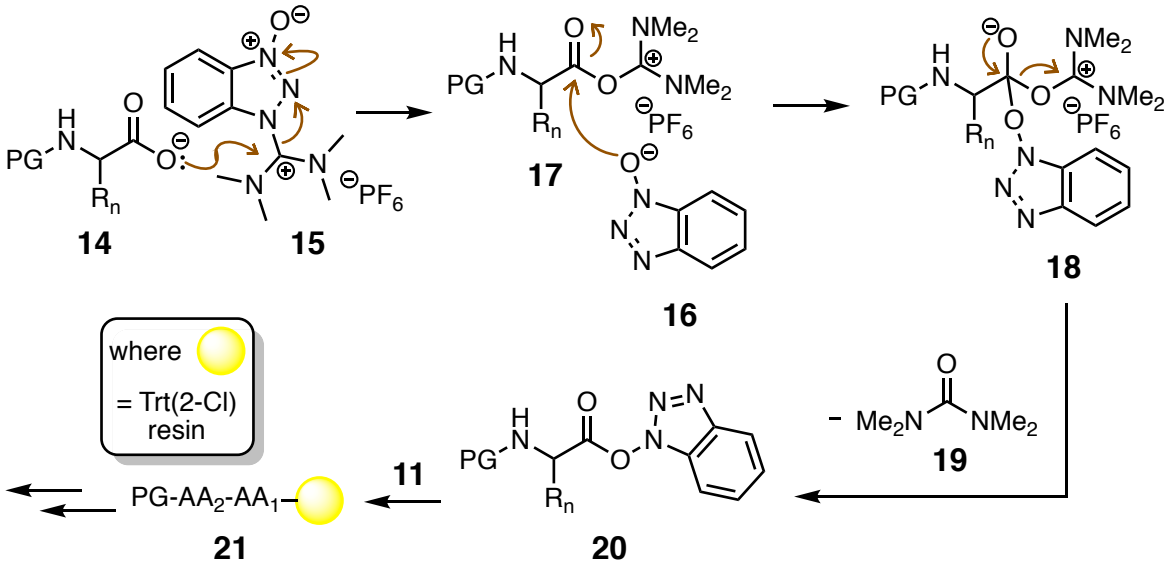

formation, and afforded **21**. Coupling reactions were followed by treatment of the peptide resin with Ac_2O/HOBt/DMF to cap unreacted amines that remained following the coupling reaction. Successive iterations of deprotection, coupling and capping reactions were used in this way until the synthesis of each peptide was complete.

Following a completed synthesis, the peptidyl resin was thoroughly washed with DMF, DCM and MeOH, and then dried under reduced pressure. The dried resin was transferred back to the side-arm flask shown in Figure 5.1 and suspended in 1% TFA in DCM (10 mL/g) to cleave the peptide from the solid support. Formation of the trityl cation upon addition of the acid to the resin was apparent from the color change, in which the resin turned from yellow to dark red.[23] The solution of protected peptide was filtered into a flask containing PhMe and the cleavage procedure repeated (2x). The resin was then thoroughly washed with DCM and MeOH, which instantly turned the color of the resin back to yellow, and the combined filtrates concentrated to ~25% volume under reduced pressure. Additional PhMe was added to the flask and the azeotropic removal of TFA−PhMe continued until again ~25% of the initial volume remained. Additional PhMe was added and the process repeated (3x) before the solution was finally concentrated to dryness. Trace residual TFA was nonetheless observed by ^{19}F NMR, but its presence posed no problem to the stability of the peptides in our experience. Following a final solvent exchange with $CHCl_3$ to remove residual PhMe and drying under high vacuum (10^{-2} Torr), the desired peptides were obtained as white solids in near quantitative yields and used without further purification. The ^1H NMR spectra of the six peptides (**1a**, **1b**, **2**, **3**, **4**, and **5**) are shown in Figures 5.2−5.7, respectively, as an indication of their purity.

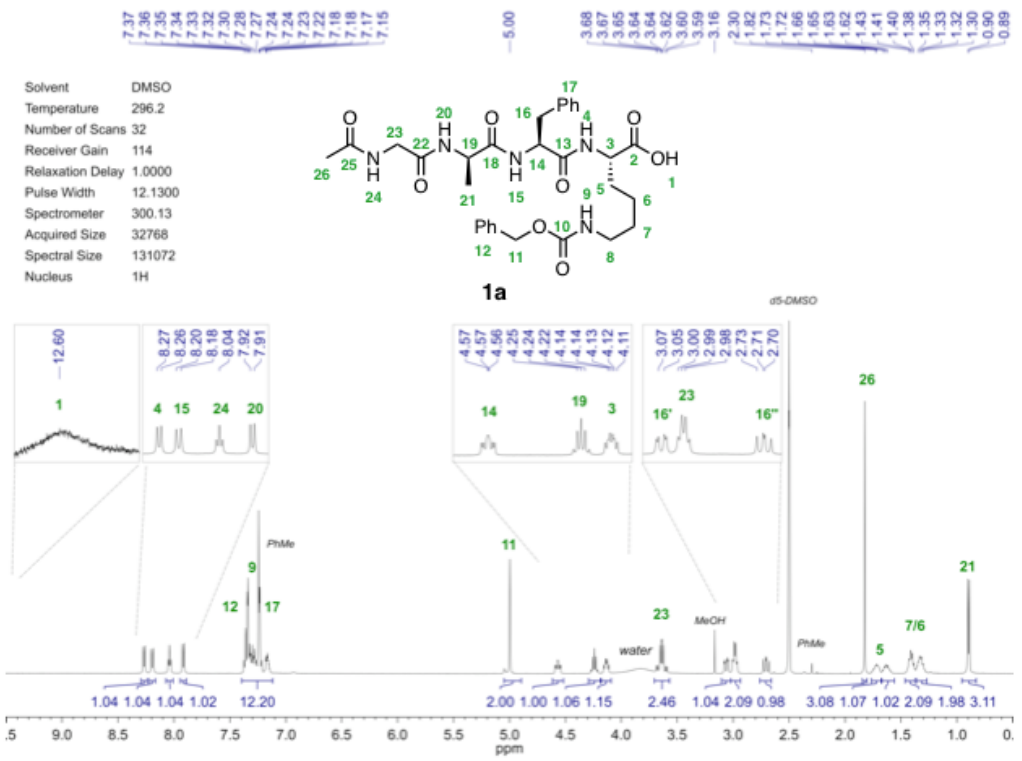

Figure 5.2 ^{1}H NMR spectrum of peptide **1a** in *d6*-DMSO at 300 MHz.

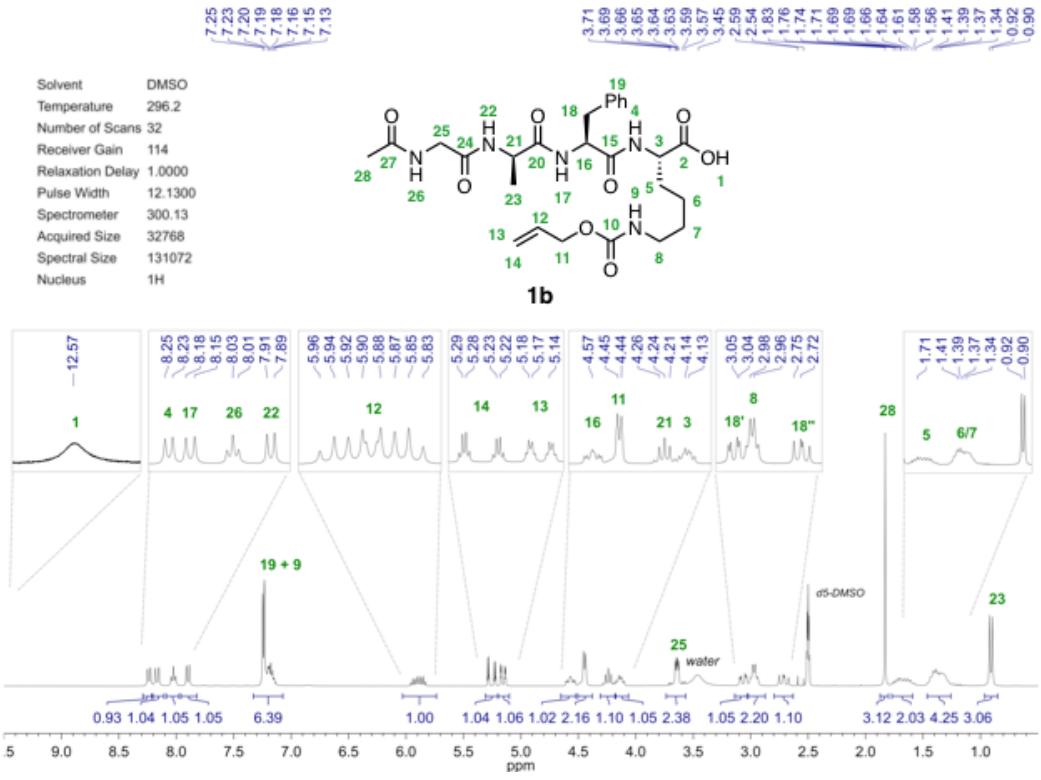

Figure 5.3 ^{1}H NMR spectrum of peptide **1b** in *d6*-DMSO at 300 MHz.

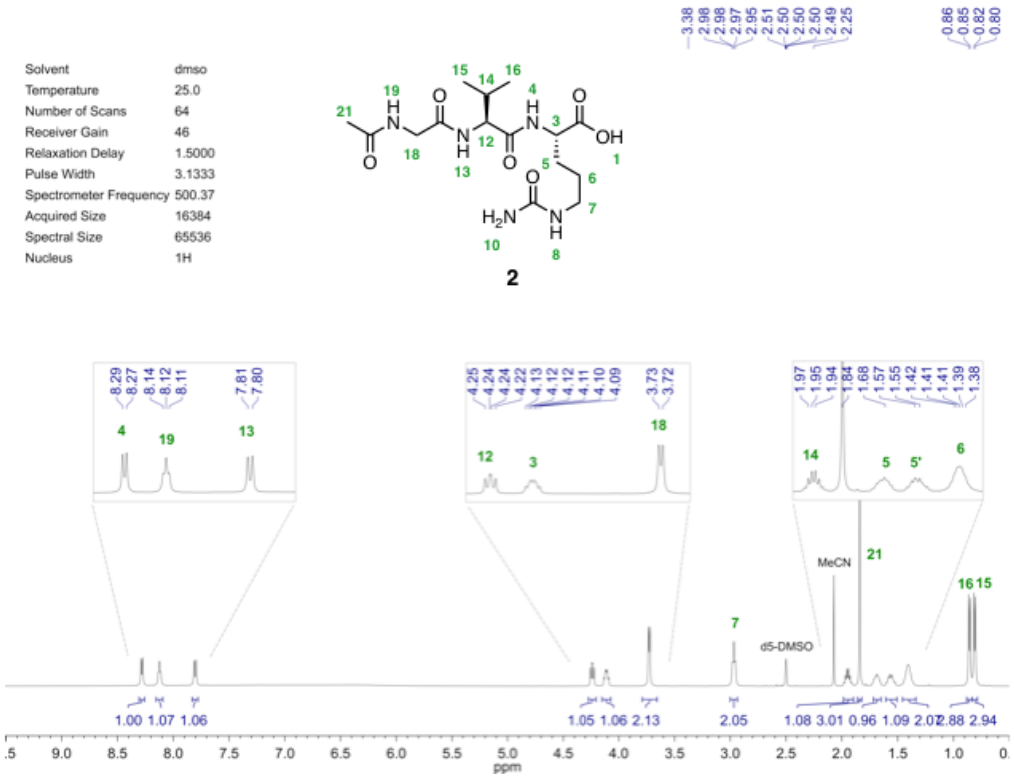

Figure 5.4 [1]H spectrum of peptide **2** in *d6*-DMSO at 500 MHz.

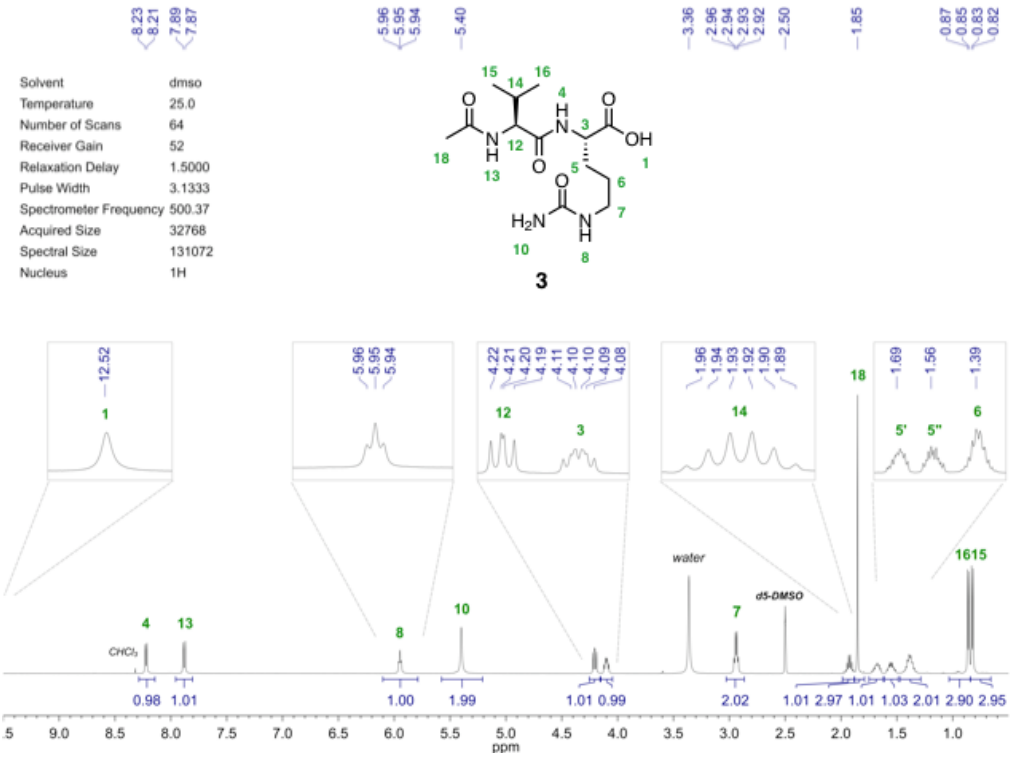

Figure 5.5 [1]H spectrum of peptide **3** in *d6*-DMSO at 500 MHz.

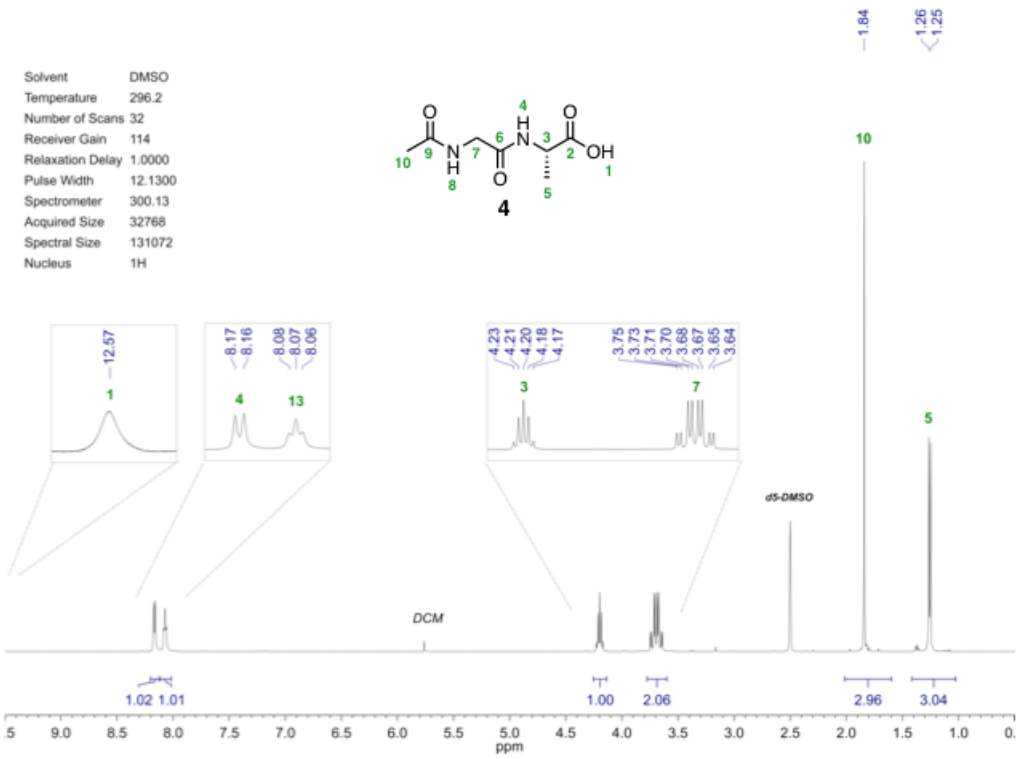

Figure 5.6 ^{1}H NMR spectrum of peptide **4** in *d6*-DMSO at 300 MHz.

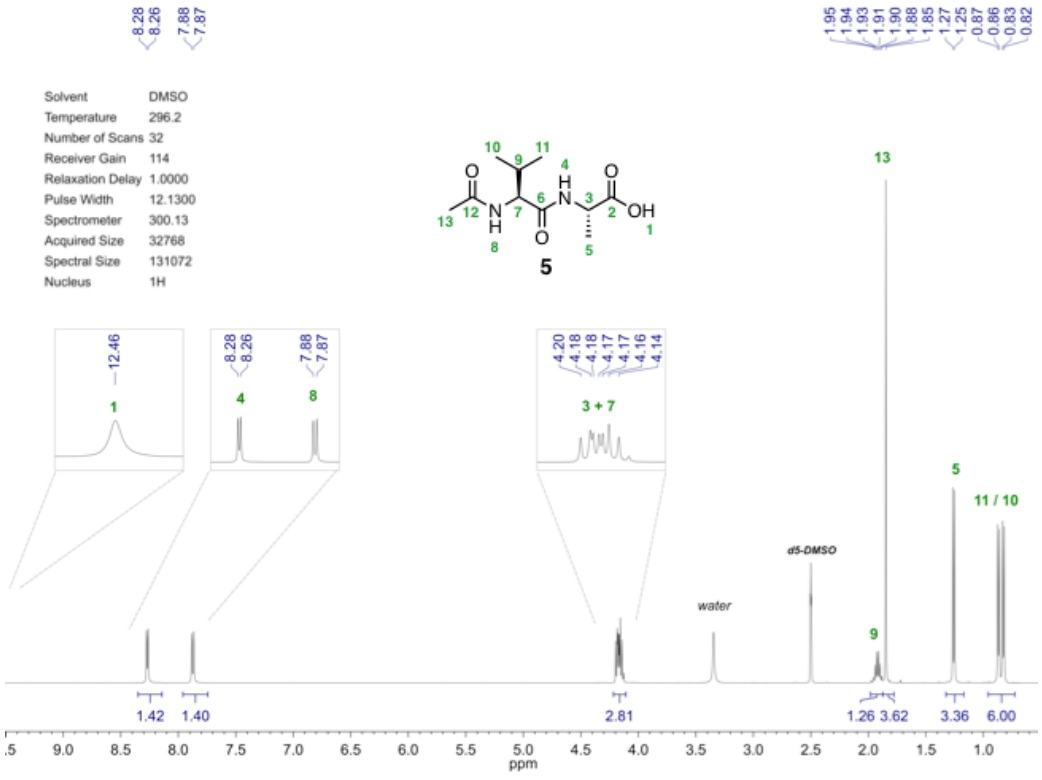

Figure 5.7 ^{1}H NMR spectrum of peptide **5** in *d6*-DMSO at 300 MHz.

5.3 Synthesis of Peptidyl Phosphinyl Phenyl Esters

The Cbz-protected tetrapeptide **1a** was the first selected to carry forward into the esterification reaction with 2-(diphenylphosphino)phenol **22**. (Scheme 5.4). However, unlike the vast majority of the previous esterification reactions conducted in the model studies, which used acid chlorides in DCM to acylate the phenol, the *N*-acetyl peptides were found to be poorly soluble in halogenated solvents, which placed restrictions on the methods available for their estification. For instance, although acid chlorides are excellent acylating agents, they cannot be used in DMF– or DMSO–solutions, solvents in which the peptides would dissolve, due to their tendency to react violently with the solvent molecules; nor could a mixed anhydride be prepared from ethyl chloroformate. Given the prior success in reacting *N*-acetyl-glycine with 2-(diphenylphospino)phenol **22** using a modified Steglich-esterificaton,[24] this was the method selected for the inaugural esterification of peptide **1a**.

Scheme 5.4 Proposed reaction of the protected tetrapeptide *N*-Ac-Gly-D-Ala-L-Phe-L-Lys(Cbz)-OH **1a** with 2-(diphenylphosphino)phenol **22** by a modified Steglich esterification to give the phosphino phenyl ester **23**.[24]

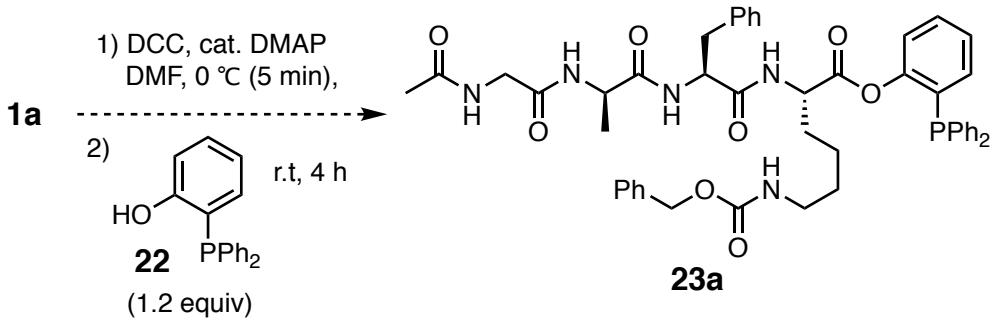

The modified Steiglich esterification of peptide **1a** with phenol **22** appeared to proceed as expected by TLC and, after 4 h of stirring at ambient temperature, the reaction was concentrated

and the product isolated by FCC. ^{1}H & ^{31}P NMR spectra of the isolate were then recored in *d6*-DMSO. Immediately, however, it was recognized that there was doubling of the signals present in the ^{1}H NMR spectrum (Figure 5.8). Two sharpe signals of roughyl equal intensity were also observed in the ^{31}P NMR spectrum (δ -18.2 & -18.3 ppm) upfield of the starting phosphine **22** (δ -17.4 ppm), as the model phopshino phenyl esters had been. RP-HPLC analysis similarly revealed the presence of two signals, albeit only partially resolved, with retention times of R_{T1} ~ 16.1 min & R_{T2} ~ 16.3 min (Figure 5.9). So, while the reaction had resulted in esterificiation of peptide **1a** with phenol **22**, a mixture of diasteromeric products had been obtained.

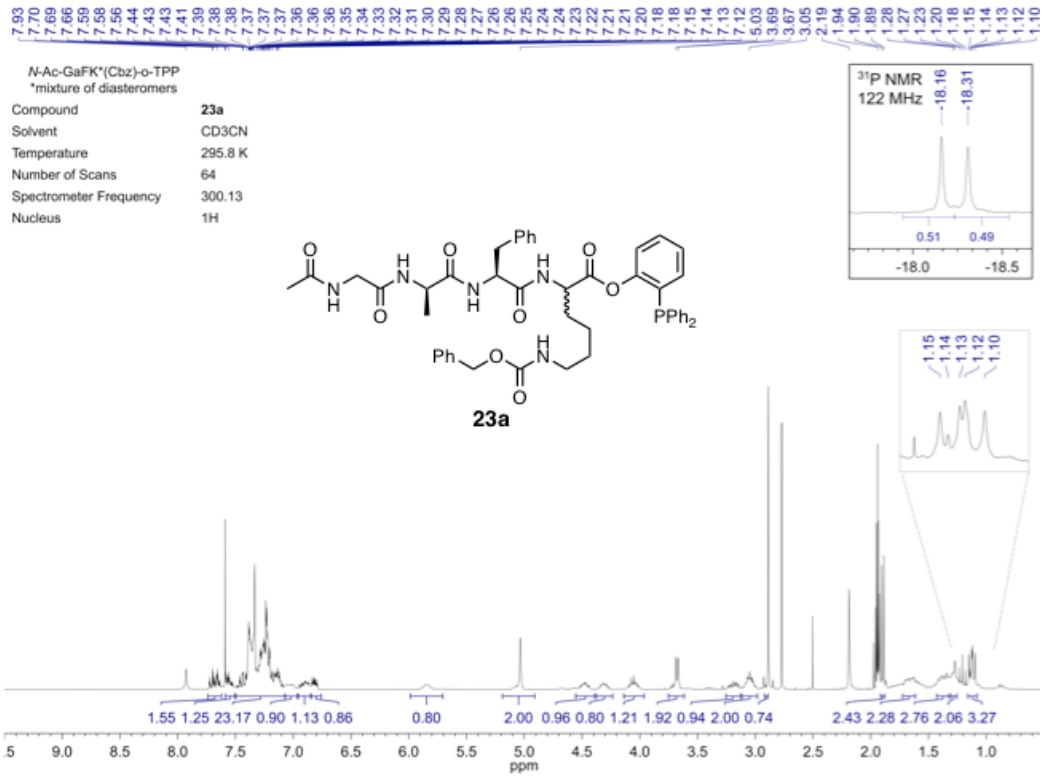

Figure 5.8 ^{1}H & ^{31}P NMR spectra of compound **23a** in CD_3CN at 300 MHz and 122 MHz, respectively.

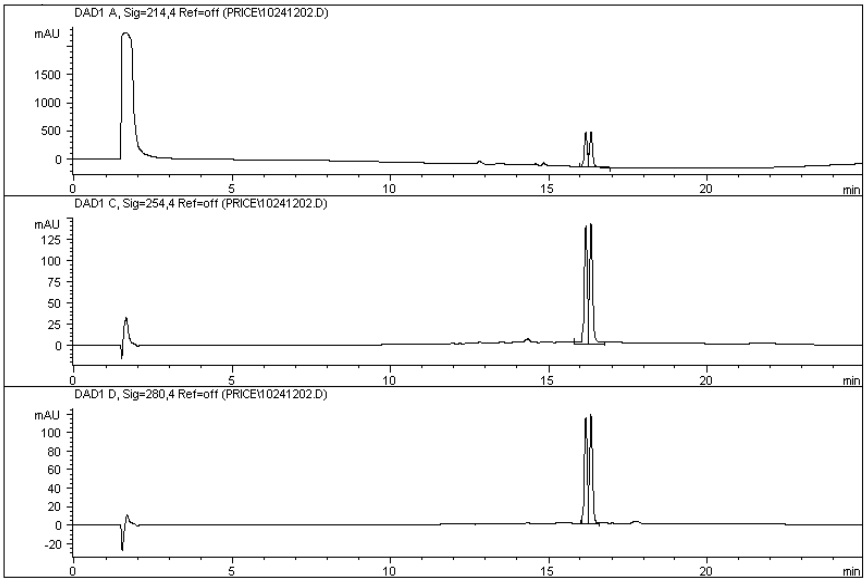

Figure 5.9 Analytical RP-HPLC chromatogram of compound **23a** (220, 254 and 280 nm) showing two partially resolved peaks with R_{T_1} ~16.1 min & R_{T_2} ~16.3 min, respectively using HPLC method 1; see Section 5.7 under *General Methods* for a description of the method.

Analagous results were also obtained in the esterification of peptide **1b** (Figure 5.10); whereas, compound **24,** the phosphinyl phenyl ester of dipeptide **4**, which contained a single stereogenic residue, prodruced a ^{1}H NMR spectrum indistinguishable from that of an optically pure compound (Figure 5.11). Given these results, plans to prepare the corresponding phosphinyl esters of the remaining peptides **2**, **3**, and **5** were placed on hold until the issue over isolation of a diasteromeric mixture of products could be resolved.

As **23a** was the first chiral phosphinyl ester prepared in our lab, the question arose as to whether epimerization of the lysine residue had occurred during the esterification reaction or if, perhaps, a mixture of atropisomers had been obtained due to inhibition of the ring flipping mechanism of triarylphosphines. Triaryl phosphines are known to adopt a propeller-like helical

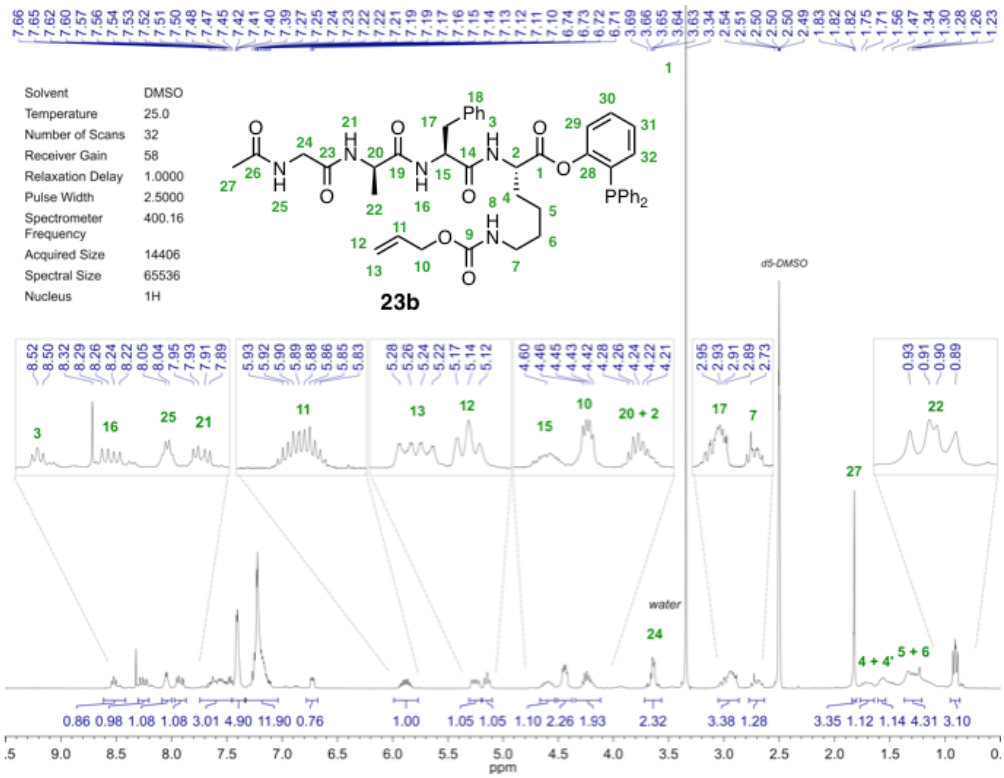

Figure 5.10 ^{1}H NMR spectrum of compound **23b** in *d6*-DMSO at 400 MHz.

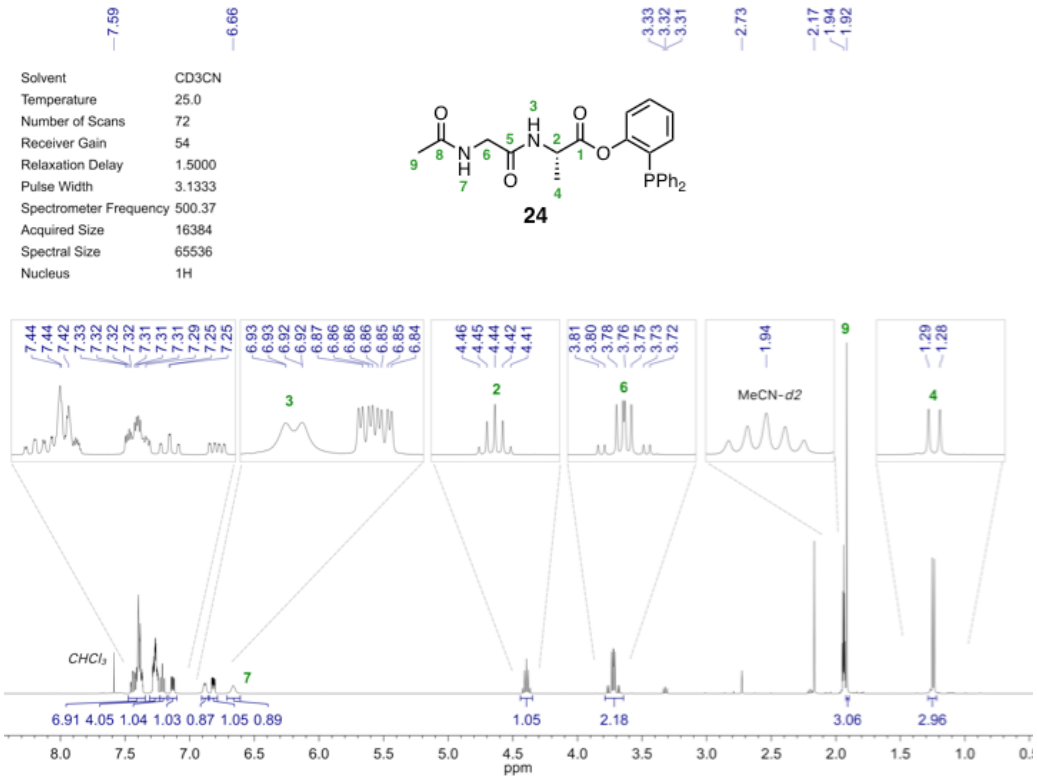

Figure 5.11 ^{1}H NMR spectrum of compound **24** in CD_3CN at 500 MHz.

conformation, resulting in a stereogenic center at the phosphorus atom. Molecules with a single *ortho*-substituted phenyl ring may also differ in the orientation of this substituent with respect to a plane defined by the three *ipso*-carbon atoms.[25] Four helical structures are therefore possible through the combination of conformers with the ester moiety pointed either up (*exo*) or down (*endo*) and the phenyl rings twisted in either a left- (*sinister*) or right-handed (*dexter*) orientation (Figure 5.12). With a large chiral tetrapeptidyl ester inhibiting rotation of the rings, denoted χ_C, these conformers become diastereotopic in the absence of helix inversion, which may be slow on the NMR timescale. Unlike nitrogen, which readily inverts at room temperature thereby interconverting the position of substituents bound to nitrogen and rendering the bonds achirotopic, the barrier to inversion for phosphines is substantially higher and does not occur readily at ambient temperature, as a comparison of the calculated energy barries for trimethylamine (~8 kcal·mol^{-1}) and trimethylphosphine (~45 kcal·mol^{-1}) at 25 °C indicates.[26] With such a high energy barrier to inversion, phosphines retain chirality at ambient temperature and, in the absence of ring flipping, the observation of a diasteromeric mixture of atropisomers would be expected.

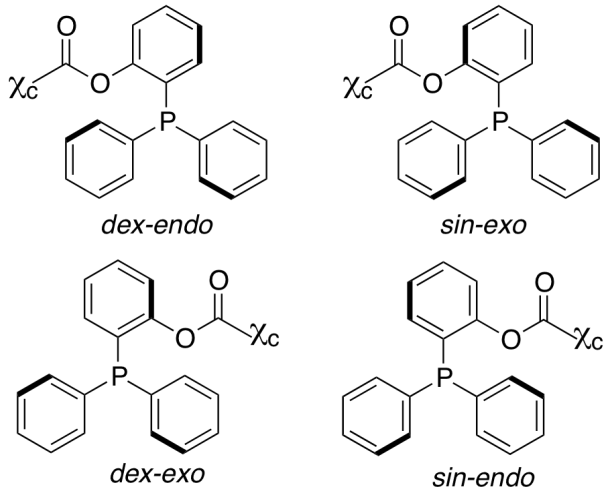

Figure 5.12 Structures of hypothetical atropisomeric *o*-(diphenylphosphino)phenyl esters bearing a large chiral ester substituent, χ_C.

Initial efforts to test the atropisomer hypothesis used VT-NMR in an attempt to determine if the two sets of peaks observed in the ^{1}H and ^{31}P NMR spectra of compound **23a** would coalesce at elevated temperature. If coalescence could be observed, this would support the hypothesis that atropisomerism was responsible for the isolation of a diastereomeric mixture of products. Both ^{1}H and ^{31}P NMR spectra of compound **23a** were acquired at elevated temperatures up to 70 °C, but only partial coalescence was observed (data not shown). As this could not be distinguished from a coincidental temperature-dependent change in chemical shift, we next sought to address the question through a series of ^{31}P NMR 2D-exchange experiments. The T_1 relaxation time for the two phosphorus signals was estimated to be > 3.5 s and, thus, experiments with a range of mixing times (t_{mix} = 100 ms to 2.5 s) and over a temperature range of 20 to 70 °C were conducted. After exhaustive efforts, no evidence of phosphorus nuclear exchange could be detected (Figure 5.13) and we concluded that the esterification reaction had indeed racemized the stereogenic center at the C-terminus of the peptidyl esters.

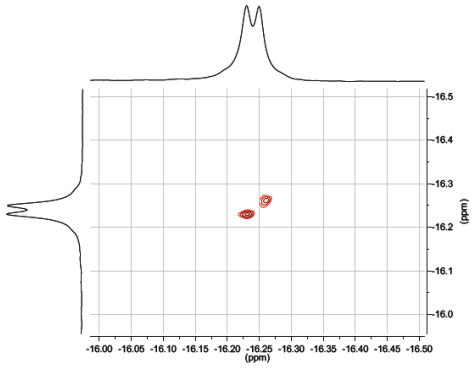

Figure 5.13 ^{31}P NMR NOESY spectrum of **23a** at 70 °C and 122 MHz in *d6*-DMSO showing no nuclear exchange (off-diagonal signals) between the two diastereomers.

Poor stereoselectivity in the esterification of chiral C-terminal peptides is a well-known and long standing problem in organic synthesis.[27-30] Thus, epimerization of the our peptides during the esterification reaction with phosphino phenol **22** could easily be rationalized. Activation of the carboxylic acid of the peptide gives the active ester intermediate **25** (Scheme 5.5). Attack from the oxygen of the carbonyl of the adjacent peptide bond on the carbonyl of the ester, followed by elimination of the leaving group from the tetrahedral intermediate **26**, gives oxazolone **27**. Formation of **27** renders the α-stereogenic center vulnerable to racemization via the base-catalyzed mechanism shown.[27] Substantial driving force exists for the deprotonation of **28** due to the formation of an aromatic ring in compound **29**. Subsequent protonation of **29** is equally facile from either face of the planar ring system and racemization of the α-stereogenic center readily results. The oxazolonium ion intermediate **30** may then react with the phenol **22**

Scheme 5.5 Mechanism of racemization of active esters via oxazolone formation.[27]

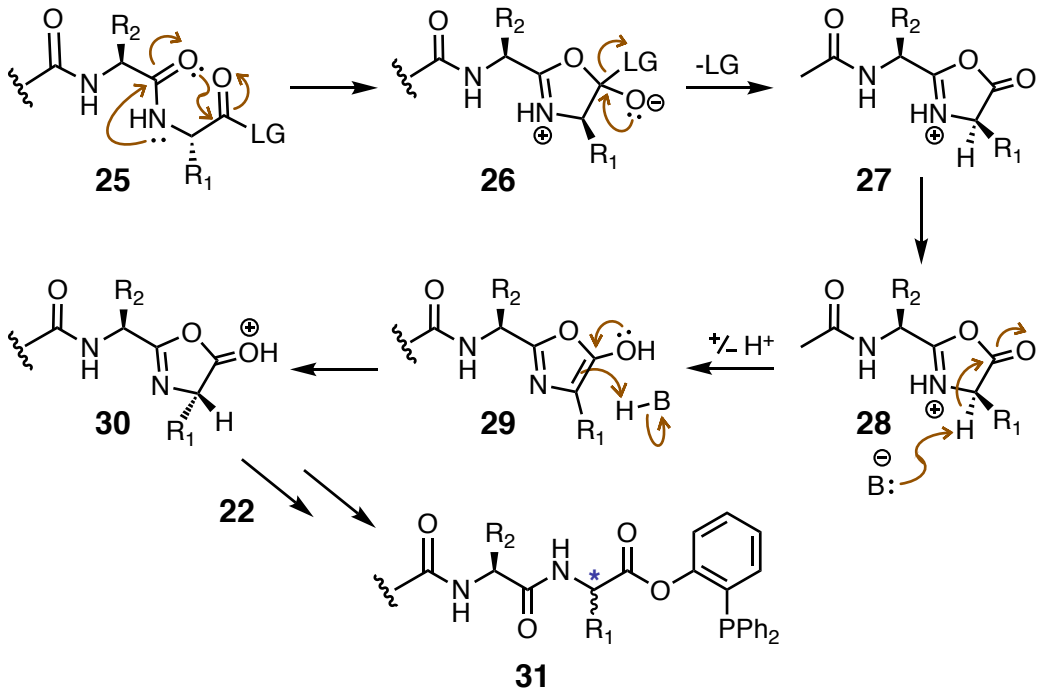

or, alternatively, an additive such as DMAP present in solution. In either case, esterification ultimately proceeds to afford the peptidyl ester **31** as a mixture of diasteromers.

If the rate of oxazolidone formation is substantially greater than that of attack on the active ester by the intended coupling partner, then epimerization will occur to a proportionatly substantial degree before the ester is formed and isolation of a mixture of diasteromers would be expected.[27] Furthermore, the rate of esterification with a large, poorly nucleophilic phenol, such as **22**, is inherently slow and little can be done to overcome this issue, which highlights a fundamental limitation to the use of 2-(diphenylphosphino)phenol **22** in the *traceless* Staudinger ligation for the synthesis of chiral C-terminal peptide-derivatives and calls into question the literature precedent for its use in such applications.[31] Nevertheless, a screen of coupling reagents and reaction conditions was undertaken in order to determine heuristically if greater stereoselectivity could be achieved during the esterification of our peptides with **22** and the results of those experiments are summarized in Table 5.1.

Despite considerable efforts to minimize the epimerization of the C-terminal residues by lowering the temperature, changing the coupling reagent and varying the nature and amount of additive used in the reaction, only modest improvements to the stereoselectivity could be achieved. The best result was obtained using the oxonium coupling reagents HATU/HOAt[32] at 0 °C with 5 equiv of **22** (Table 5.1, entry 10). The superior effectiveness of HATU over the related HBTU coupling reagent has been proposed to result from a neighboring group effect from the pyridine and the formation of a hydrogen-bonded 7-membered ring with the approaching nucleophile, which is thought to stabilize the developing positive charge on the attacking atom thereby lowering the energy of the associated transition state (Figure 5.14).[33] However, the improvement in stereoselectivity obtain here was unremarkable and, as such, a revision to the proposed synthetic targets was made.

Table 5.1 Comparison of the results obtained with various reaction conditions for the esterification of peptides **1a** or **1b** with 2-(diphenylphino)phenol **22**.

Entry	Peptide[a]	22 (equiv)	Coupling Reagent	Additive	Solvent	Temp. (°C)[b]	Time (h)	d.r.[c]
1	**1b**	1.2	DCC	DMAP (10 mol-%)	DMF	r.t	4	1.1:1
2	**1b**	1.5	DCC	DMAP (10 mol-%)	DMF	0	8	1.2:1
3	**1b**	1.5	DCC	DMAP (1 equiv)	DCM–DMA 95:5 (v/v)[d]	0	6	1:1
4	**1a**	2	DCC	HOBt[e] (1 equiv)	DMF	0	4	1.3:1
5	**1a**	2	EEDQ[f]	n/a	DMF	0	12	n.r.
6	**1a**	2	EEDQ[f]	-	DMF	40	12	1:1
7	**1b**	1.4	Oxalyl Chloride[g]	cat. DMF	$CDCl_3$[d]	r.t	4	1.2:1
8	**1a**	2	T3P[h]	DIEA	DMF	0	2	1.5:1
9	**1b**	2	HBTU[i]	HOBt	NMP	r.t.	5	2:1
10	**1a**	5	HATU[j]	HOAt	NMP	0	2	2.3:1
11	**1a**	2	3Pfp·DCC[k]	-	DMF	r.t	8	n.r.

[a] Reactions used ~10 mg of the indicated peptide (1 equiv)
[b] Indicates the bath temperature maintained over the course of the reaction.
[c] Determined from the ratio of signals in the ^{31}P NMR spectrum.
[d] Peptide was only partially soluble in the solvent.
[e] See ref. 22
[f] See ref. 34 and 35
[g] Peptides were only partially soluble in the indicated solvent system.
[h] 50% Propylphosphonic anhydride in EtOAc solution (wt/v); see slo ref. 36
[i] See ref. 20 and 21
[j] See ref. 32 and 33
[k] See ref. 38

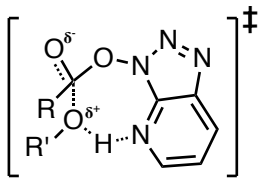

Figure 5.14 Proposed transition state of HATU-mediated acylation showing the neighboring group effect of pyridine.[33]

5.4 Solution-Phase Synthesis of an Achiral C-Terminal Peptide & Phosphinyl Phenyl Ester

Preparation of a peptide containing an achiral glycine residue at the C-terminus was ultimately determined to be the most reasonable way of moving forward with the project. Based on the Cathepsin B substrate specificity requirements reported in the literature,[6] the N$^{\alpha}$-protected dipeptide Cbz-L-valylglycine **33** was prepared by solution-phase chemistry according to the sequence of reactions outlined in Scheme 5.6. Commercially available Cbz-L-Val-OH was first converted into the mixed anhydride using ethyl chloroformate and then coupled *in situ* to ethyl 2-

Scheme 5.6 Solution-phase peptide synthesis of Cbz-L-Val-Gly-OH **33**.

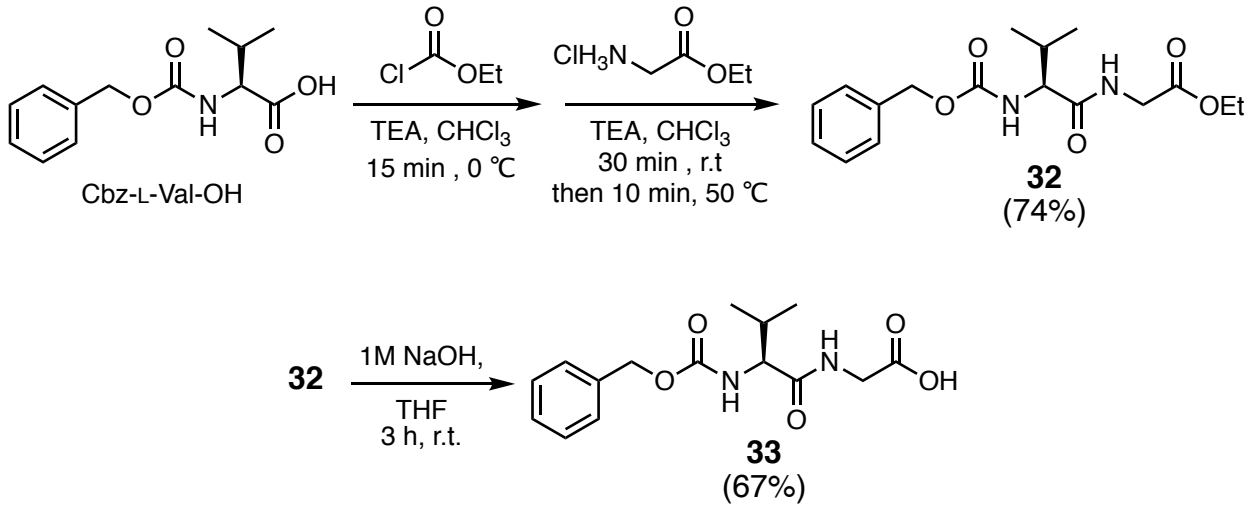

aminoacetate. The 2-step, one-pot procedure afforded Cbz-L-Val-Gly-OEt **32** in a 90% crude yield following aqueous work-up, and recrystallization of that material from boiling EtOAc/ether gave cylindrical needles of pure **32** in 74% overall yield. An analytical RP-HPLC chromatogram of **32** monitoring absorbance at 214, 220 and 254 nm is shown in Figure 5.14 and the ^{1}H and ^{13}C NMR spectra are shown in Figures 5.15 and 5.16, respectively, as an indication of purity. Saponification of the ethyl ester of **32** with 1M aq. NaOH was monitored by RP-HPLC and complete after 3 h (Figure 5.16). Following extractive work-up, recrystallization of the crude product afforded the dipeptide acid **33** in 67% yield and high optical purity: $[\alpha]^{23}_{D}$ −5.5° (*c* 1.0, EtOAc); lit. -6.0°.[39]

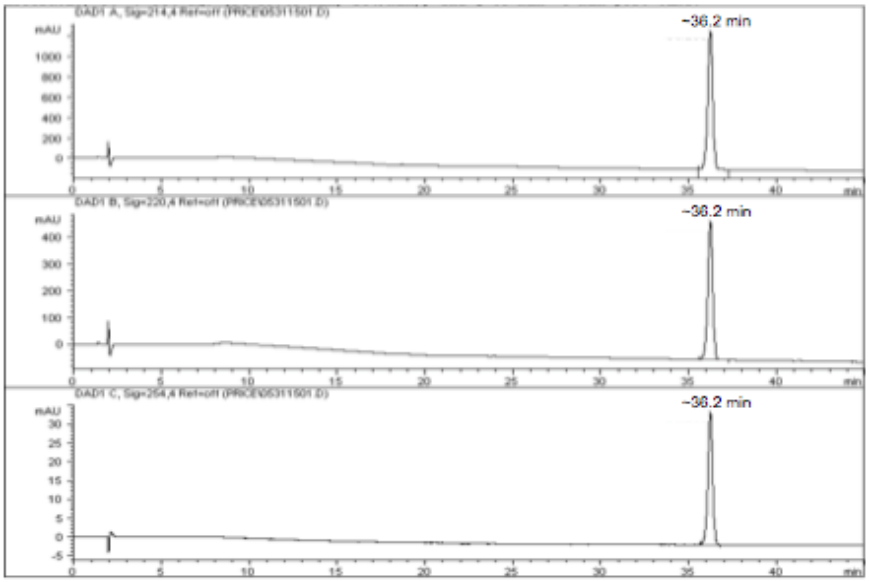

Figure 5.15 Analytical RP-HPLC chromatogram of **32** (RT ~36.2 min) monitoring absorbance at 214, 220 and 254 nm (top-to-bottom) using method 2; a description of HPLC method is provided in Section 5.7 Experimental under *General Methods*.

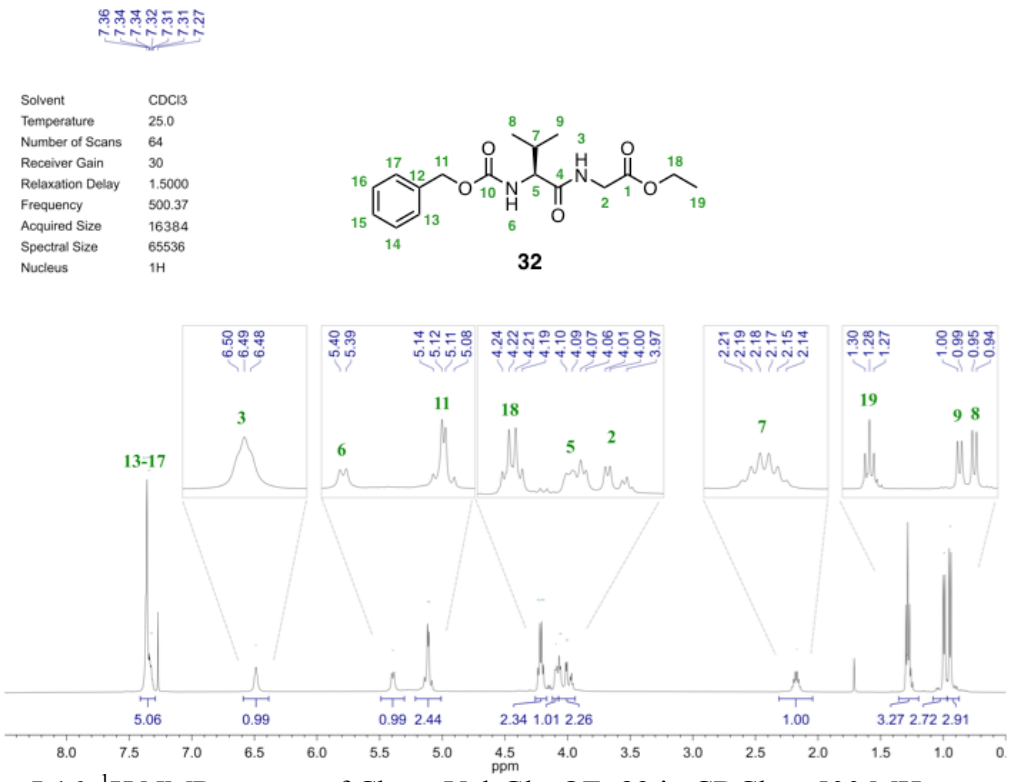

Figure 5.16 ^{1}H NMR spectra of Cbz-L-Val-Gly-OEt **32** in $CDCl_3$ at 500 MHz**.**

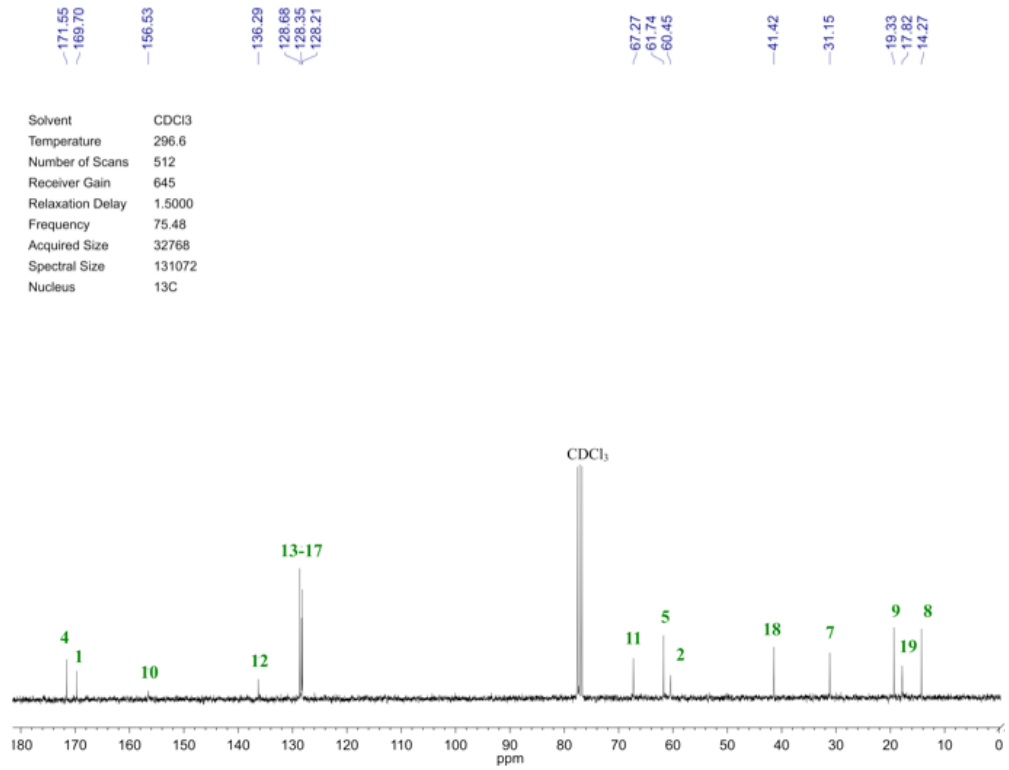

Figure 5.17 ^{13}C NMR spectra of Cbz-L-Val-Gly-OEt **32** in $CDCl_3$ at 75 MHz**.**

(a)

(b)

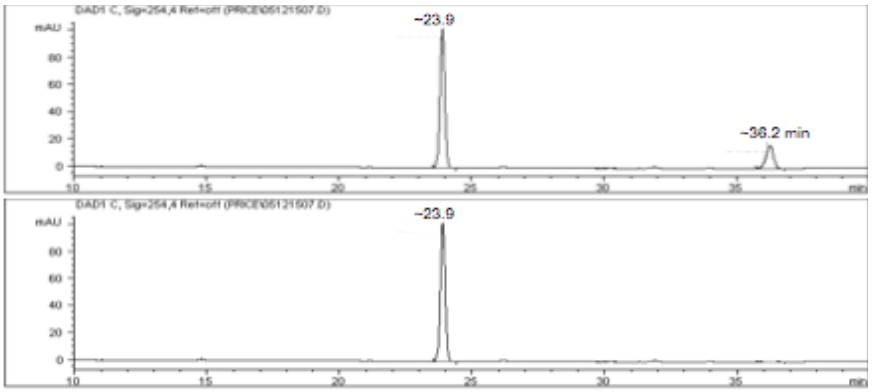

Figure 5.18 Analytical RP-HPLC chromatograms (254 nm) monitoring the hydrolysis of **32** (RT ~36.2 min) **t**o **33** (RT ~23.9 min) at (a) t = 1 h and (b) t = 3 h; HPLC method 2.

Esterification of **33** was accomplished using the mixed anhydride method previously applied to its own preparation in solution-phase peptide synthesis (Scheme 5.7). The solubility properties of the Cbz-protected dipeptide were significantly improved relative to the *N*-acetyl derivatives previously under investigation and allowed for ready dissolution of **33** in chloroform. The mixed anhydride formed *in situ* from activation of **33** with ethyl chloroformate was reacted with phenol **22**. Carbon dioxide evolution was observed during the addition of **22** and

Scheme 5.7 Esterification of dipeptide **33** with phosphino phenol **22** via mixed anhydride afforded the phosphinyl ester of Cbz-L-valylglycine **34**.

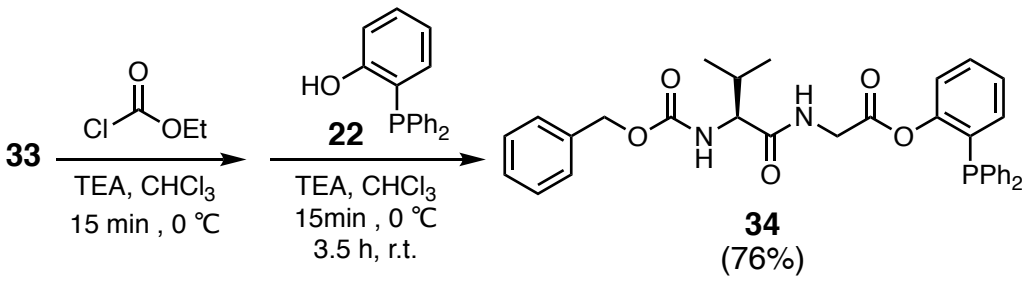

the reaction was complete after 3.5 h at ambient temperature. Following extractive workup, FCC over silica gel afforded the desired phosphinyl phenyl ester of Cbz-L-valylglycine **34** as a clear

oil in 76% yield. Compound **34** was fully characterized by ^{1}H, ^{13}C and ^{31}P NMR spectroscopy with unambiguous assignment of the observed non-aromatic resonances made using a combination of homonuclear and heteronuclear 2D-NMR. The 1D-spectra are provided in Figures 5.19 and 5.20 as a measure of purity. Note that seven doublets are observed in the ^{13}C NMR spectrum of **34** due to carbon-phosphorus heteronuclear coupling and that the ^{31}P NMR spectrum shown has a spectral window ranging from -50 to +150 ppm with a single observable resonance present.

5.5 Conclusions

Preparation of the requisite phosphinyl phenyl esters of peptide-specifiers proposed as synthetic intermediates in tripartite prodrug synthesis via the *traceless* Staudinger ligation was accomplished. However, for sequences containing a stereogenic C-terminal residue, the esterification with 2-(diphenylphosphino)phenol **22** resulted in epimerization of the α-stereo-center in all cases. Efforts to find conditions affording a stereoselective esterification reaction were unsuccessful. Nonetheless, we were able to obtain a phosphinyl ester of Cbz-L-valylglycine, compound **34**, which contains the achiral glycine residue at the C-terminus, for the preparation of an optically pure peptidyl prodrug of doxaz via the *traceless* Staudinger ligation. The results obtained from application of this methodology for tripartite prodrug synthesis are discussed in the following chapter of this thesis.

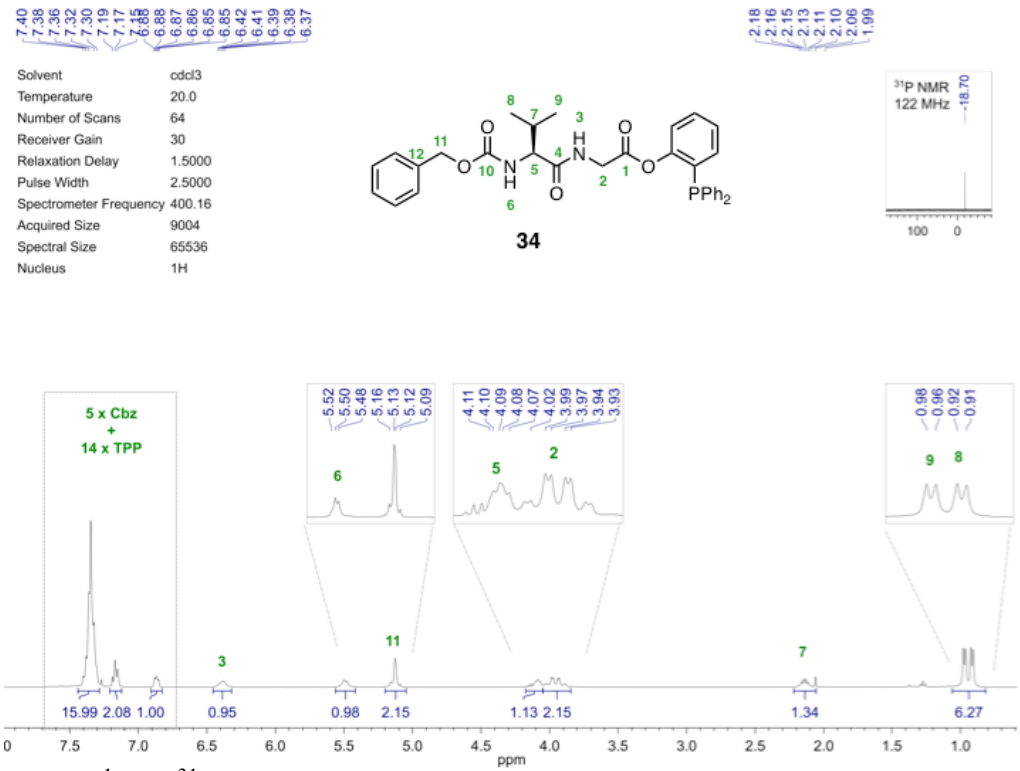

Figure 5.19 ^{1}H & ^{31}P NMR spectrum of phosphanyl-phenyl ester **34** in $CDCl_3$.

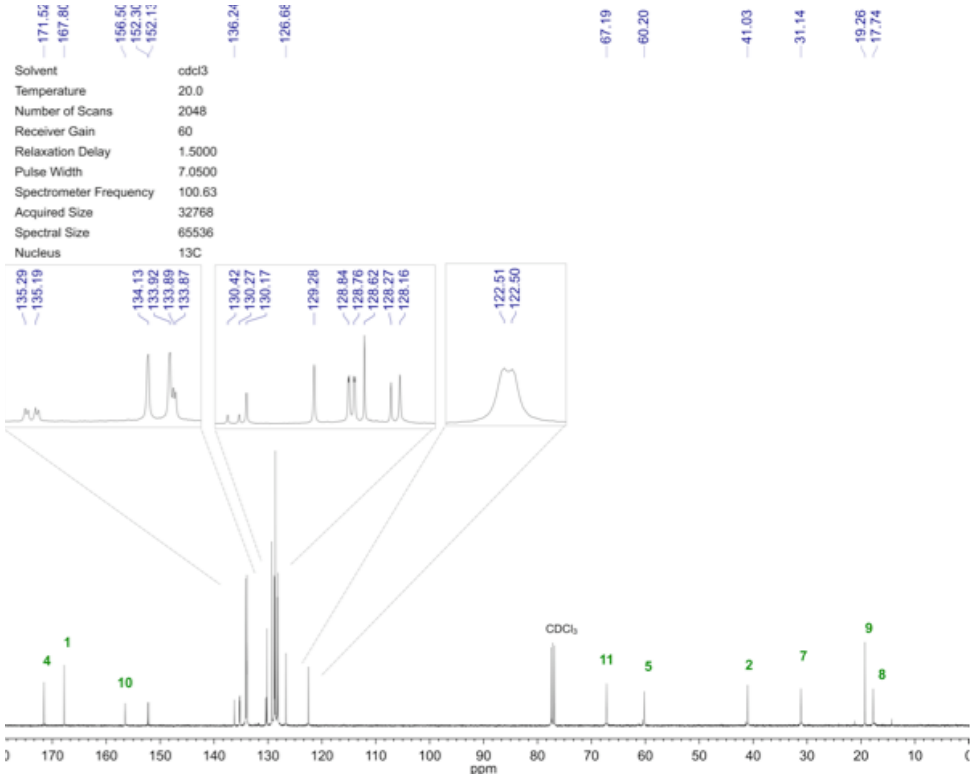

Figure 5.20 ^{13}C NMR spectrum of phosphinyl-phenyl ester **34** in $CDCl_3$.

5.6 Experimental

General Methods. Unless otherwise specified, all reactions were performed in oven- or flame-dried glassware, cooled to ambient temperature inside of a desiccator prior to use, under an inert atmosphere of nitrogen or argon. Molecular sieves (3Å & 4Å) were activated in a vacuum drying oven at 180 °C and 10^{-2} Torr for 72 h and stored in a drying oven at 160 °C prior to use. Anhydrous THF was distilled from Na benzophenone ketyl under nitrogen and used immediately. MeCN was degassed by vacuum filtering through a 0.4 μm filter prior to use. Wet solvent systems were prepared using either D_2O or purified water obtained from a Milli-Q Direct water purification system from EMD Millipore (Burlington, MA). Unless specifically indicated, all reagents were acquired from reputable commercial suppliers and used as received. The *p*-aminobenzyl alcohol (PABA) used was purchased from Atomax Chemical Company (Shanghai, China) and dried under high-vacuum ($\leq$ 5 x 10^{-2} Torr) at ambient temperature for 48 h, purified by flash column chromatography (hexanes−EtOAc) and subsequently recrystallized from EtOAc and petroleum ether (40−60 °C). Flash column chromatography (FCC)[40] was performed using 60 Å silica gel (37−75 μm, 230−400 mesh) with hexanes−EtOAc or $CHCl_3$−MeOH solvent systems as eluent. EMD glass thin-layer chromatography (TLC) plates (silica gel 60 F_{254}) were used for analytical TLC and the results visualized under 254 nm light or following exposure of the developed plate to an I_2/silica gel slurry. Retention factors (R_f) are reported along with other compound characterization data below. Analytical RP-HPLC was performed on Agilent 1050/1100 hybrid instruments equipped with a 1050 series pump and autoinjector and a 1100 series UV/visible diode array detector (Santa Clara, CA). Sample solutions (5 μL) were injected onto an Agilent Zorbax octadecylsilyl (C18) reverse phase column (4.6 mm i.d. × 150 mm, 5 μm) at ambient temperature and eluted with an 15 mM PO_4 (pH 4.5)−MeCN solvent system

(1 mL/min). The gradient elution method was programmed in terms of %-aq. buffer as follows Method 1: 0 min (75%), 2.5 min (50%), 5 min (40%), 25 min (20%), 30 min (75%); Method 2: 0−5 min (95%), 15 min (75%), 45 min (60%), 51 min (10%), 54 min (0%), 60 min (95%). All RP-HPLC analyses monitored absorbance at 220, 254 and 280 nm. Retention times (R_T) are reported along with other compound characterization data below. ^{1}H NMR spectra were recorded at 400 or 500 MHz on Varian Unity INOVA spectrometers (Palo Alto, CA) or at 300 MHz on a Bruker-Avance III spectrometer (Billerica, MA). Ambient temperature $^{13}C\{^{1}H\}$ and $^{31}P\{^{1}H\}$ NMR spectra were recorded at 75 MHz and 122 MHz, respectively, on a Bruker-Avance III spectrometer. $^{31}P\{^{1}H\}$ VT-NMR spectra were acquired at 164 MHz on a Varian Unity INOVA spectrometer. Chemical shifts are reported in δ values of ppm with internal referencing to the residual solvent peak, whose frequencies are given by Gottlieb *et al*.[41] Coupling constants are reported as *J*-values in Hertz (Hz) with resonance multiplicities abbreviated as follows: s = singlet, d = doublet, t = triplet, q = quartet, p = pentet, sext = sextet, sept = septet,, h = heptet, m = multiplet, br = broadened. NMR data processing and plotting, including x-referencing of $^{31}P\{^{1}H\}$ spectra, was performed using MestReNova NMR software v12.0.1 (Mestrelab Research, Santiago de Compostela, Spain). UV−vis spectroscopy was performed on a Hewlett-Packard/Agilent 8452A diode array instrument. Infrared (IR) spectra were recorded on a Thermo-Nicolet FT-IR spectrometer as thin films on NaCl plates. High-resolution mass spectra (HRMS) were obtained with a Perkin-Elmer Sciex API III+ (Waltham, MA) or ABI Pulsar QqT high-resolution instrument (Foster City, CA), equipped with an ion-spray source at atmospheric pressure. The purity of all characterized compounds was verified to be at least 95% from a combination of RP-HPLC and NMR data.

Solid-Phase Peptide Synthesis (SPPS). Peptides **1a**, **1b**, **2**, **3**, **4** and **5** were prepared by SPPS using a standard Fmoc-strategy[12,13] and the N$^{\alpha}$-protected amino acids: Fmoc-L-Ala-OH, Fmoc-D-Ala-OH, Fmoc-L-Cit-OH, *N*-Acetyl-Gly-OH, Fmoc-L-Lys(PG)-OH (where PG = (a) Cbz and (b) alloc), Fmoc-L-Phe-OH and Fmoc-L-Val-OH. The C-terminal Fmoc-amino acids were manually loaded onto 2-chlorotrityl chloride resin[14] and the loading determined spectrophotometrically.[17] The peptides were prepared on a 0.25 mmol scale by automated synthesis on an Applied Biosystems 433A peptide synthesizer using single amino acid couplings with a 4-fold excess of Fmoc-amino acid per coupling. Fmoc groups were removed by sequential treatment with 20% piperidine in DMF (*v*/*v*) and the incoming amino acids were activated with a 0.45 M solution of HBTU/HOBt in NMP and 2 M DIEA in DMF. Following a completed synthesis, the peptidyl resin was washed thoroughly with DMF, DCM and MeOH before being dried under reduced pressure. Peptides were cleaved from the solid support by repeated exposure to 1% TFA in DCM *v*/*v* (5 x 10 mL/g of resin for 3 min intervals). The filtrates were combined in a flask containing 100 mL of toluene and concentrated to approximately one-quarter volume. Additional toluene (50 mL) was added to the flask and the process repeated (3x) before the suspension was concentrated to dryness under reduced pressure with gentle heating. Peptides **1a**, **1b**, **2**, **3**, **4** and **5** were obtained in nearly quantitative yields and used without further purification.

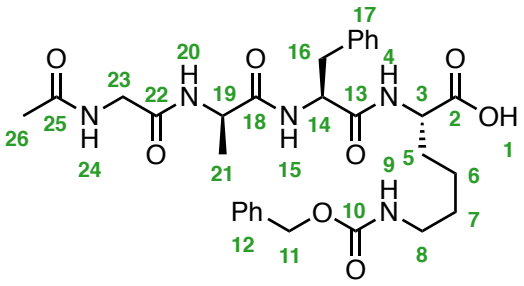

1a

***N*-Ac-Gly-D-Ala-L-Phe-L-Lys(Cbz)-OH (1a)**. 148 mg (99%) as a white solid: R_f = 0.10 (9:1 $CHCl_3$–MeOH); mp 187−190 °C (dec); ^{1}H NMR (300 MHz, *d6*-DMSO) δ 12.62 (br. s, 1H, **1**), 8.24 (d, 1H, *J* = 7.6 Hz, **4**), 8.17 (d, 1H, *J* = 8.8 Hz, **15**), 8.03 (t, 1H, *J* = 5.8 Hz, **24**), 7.90 (d, 1H, *J* = 7.5 Hz, **20**), 7.47 – 7.04 (m, 11H, **12**, **17** and **9**), 5.02 (s, 2H, **11**), 4.62 – 4.52 (m, 1H, **16**), 4.24 (p, 1H, *J* = 7.0 Hz, **19**), 4.18 – 4.09 (m, 1H, **3**), 3.74 – 3.54 (m, 2H, **23**), 3.07 (dd, 1H, *J* = 13.6, 3.6 Hz, **16**), 2.99 (dd, 2H, *J* = 12.9, 6.4 Hz, **8**), 2.71 (dd, 1H, *J* = 13.6, 10.8 Hz, **16'**), 1.83 (s, 3H, **26**), 1.78 – 1.51 (m, 2H, **5**), 1.49 – 1.37 (m, 2H, **7**), 1.36 – 1.24 (m, 2H, **6**), 0.91 ppm (d, 3H, *J* = 7.0 Hz, **21**) assignments made using homonuclear (^{1}H, ^{1}H) gCOSY spectrum; ^{13}C NMR (75 MHz, *d6*-DMSO) δ 173.45 (**2**), 171.77 (**18**), 171.26 (**13**), 169.55, **25**), 168.46 (**22**), 156.09 (**10**), 137.27, 129.30, 128.90, 128.34, 128.20, 127.89, 127.72, 126.19, 65.12 (**11**), 53.35 (**14**), 52.07 (**3**), 47.99 (**19**), 41.94 (**22**), 39.59 (**8**), 37.68 (**16**), 30.60 (**5**), 29.10 (**7**), 22.85 (**6**), 22.42 (**26**), 18.45 ppm (**21**) assignments made using a combination of heteronuclear (^{1}H, ^{13}C) gHSQC and gHMBC spectra; HRMS (ESI-TOF) *m/z*: $[M+Na]^+$ calcd for $C_{30}H_{39}N_5NaO_8$ 620.2697; found 620.2711.

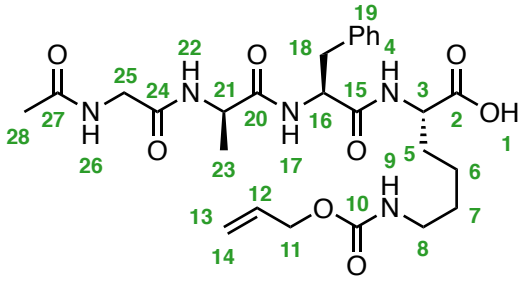

1b

***N*-Ac-Gly-D-Ala-L-Phe-L-Lys(alloc)-OH (1b).** 134 mg (98%) as a white solid: R_f = 0.10 (95:5 $CHCl_3$–MeOH); RT = 8.1 min (HPLC method 3); mp 168–172 °C (dec); ^{1}H NMR (300 MHz, *d6*-DMSO) δ 12.57 (br. s, 1H, **1**), 8.24 (d, 1H, *J* = 7.6 Hz, **4**), 8.17 (d, 1H, *J* = 8.8 Hz, **17**), 8.03 (t, 1H, *J* = 5.7 Hz, **26**), 7.90 (d, 1H, *J* = 7.5 Hz, **22**), 7.33 – 7.07 (m, 6H, **19** & **9**), 6.03 – 5.74 (m, 1H, **12**), 5.26 (dq, 1H, *J* = 17.2, 1.6 Hz, **14**), 5.16 (dq, 1H, *J* = 10.5, 1.6 Hz, **13**), 4.65 – 4.52 (m, 1H, **16**), 4.45 (d, 2H, *J* = 5.3 Hz, **11**), 4.24 (apparent p, 1H, *J* = 6.7 Hz, **21**), 4.14 (m, 1H, **3**), 3.73 – 3.56 (m, 2H, **25**), 3.07 (dd, 1H, *J* = 13.7, 3.6 Hz, **18**), 2.97 (apparent q, 2H, *J* = 6.3 Hz, **8**), 2.71 (dd, 1H, *J* = 13.7, 10.8 Hz, **18'**), 1.83 (s, 3H, **28**), 1.69 (m, 2H, **5**), 1.50 – 1.38 (m, 4H, **6** & **7**), 0.91 ppm (d, 3H, *J* = 7.0 Hz, **23**). HRMS (ESI-TOF) *m/z*: $[M+Na]^+$ calcd for $C_{26}H_{37}N_5NaO_8$ 570.2642; found 570.2646

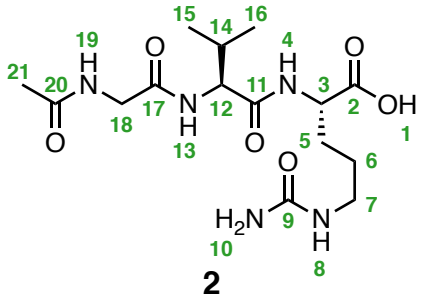

2

***N*-Ac-Gly-L-Val-L-Cit-OH (2).** 92 mg (99%) as a white solid: R_f = 0.16 (9:1 $CHCl_3$–MeOH); mp 190–195 °C; ^{1}H NMR (300 MHz, *d6*-DMSO) δ 8.28 (d, 1H, *J* = 7.3 Hz, **4**), 8.12 (t, 1H, *J* = 6.0 Hz, **11**), 7.80 (d, 1H, *J* = 9.0 Hz, **13**), 4.24 (dd, 1H, *J* = 7.0, 6.6 Hz, **12**), 4.11

(td, 1H, J = 8.2, 5.1 Hz, **3**), 3.73 (d, 2H, J = 5.7 Hz, **18**), 2.97 (t, 2H, J = 6.9 Hz, **7**), 1.95 (hept, 1H, J = 6.8 Hz, **14**), 1.84 (s, 3H, **21**), 1.68 (p, 1H, J = 6.8, 5.5 Hz, **5**), 1.56 (dtd, 1H, J = 14.0, 9.3, 5.6 Hz, **5'**), 1.40 (tq, 2H, J = 13.5, 6.6 Hz, **6**), 0.86 (d, 3H, J = 6.7 Hz, **16**), 0.81 ppm (d, 3H, J = 6.8 Hz, **15**); ^{13}C NMR (75 MHz, CD_3OD) δ 175.10 (**2**), 174.11 (**20**), 173.80 (**11**), 171.79 (**17**), 162.40 (**9**), 60.19 (**12**), 53.47 (**3**), 43.64 (**18**), 40.68 (**7**), 32.18 (**14**), 29.94 (**5**), 27.62 (**6**), 22.58 (**21**), 19.82 (**16**), 18.81 ppm (**15**) *Relative assignments of the Val-methyl signals (**15** & **16**) were based on the ACD-lab predicted spectrum; HRMS (ESI-TOF) *m/z*: $[M+H]^+$ calcd for $C_{15}H_{28}N_5O_6$ 374.2040; found 374.2038.

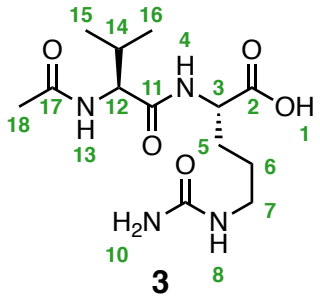

3

***N*-Ac-L-Val-L-Cit-OH (3).** 78 mg (99%) as a white solid: R_f = 0.18 (9:1 $CHCl_3$–MeOH); ^{1}H NMR (500 MHz, *d6*-DMSO) δ 8.21 (d, 1H, J = 7.3 Hz, **4**), 7.87 (d, 1H, J = 9.0 Hz, **13**), 5.99 (s, 1H, **8**), 5.8 – 4.8 (br. s, 2H, **10**), 4.24 – 4.17 (m, 1H, **12**), 4.14 – 4.07 (m, 1H, **3**), 2.94 (t, 2H, J = 6.2 Hz, **7**), 1.93 (dq, 1H, J = 8.0, 6.9 Hz, **14**), 1.85 (s, 3H, **18**), 1.74 –1.62 (m, 1H, **5a**), 1.59 –1.47 (m, 1H, **5b**), 1.49 –1.28 (m, 2H, **6**), 0.86 (d, 3H, J = 6.7 Hz, **16**), 0.83 ppm (d, 3H, J = 6.7 Hz, **15**) *Relative assignments of the Val-methyl signals (**15** & **16**) were based on the ACD-lab predicted spectrum; ^{13}C NMR (75 MHz, *d6*-DMSO) δ 173.55 (**2**), 171.42 (**11**), 169.39 (**17**), 159.18 (**9**), 57.44 (**12**), 51.93 (**3**), 39.06 (**7**), 30.73 (**14**), 28.32 (**5**), 26.63 (**6**), 22.55 (**18**), 19.24 (**16**), 18.28 ppm (**15**) *Relative assignments of the Val-methyl signals (**15** & **16**) were based on the ACD-lab predicted spectrum; HRMS (ESI-TOF) *m/z*: $[M+H]^+$ calcd for $C_{13}H_{24}N_4NaO_5$ 317.1825; found 317.1822.

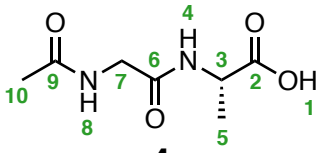

4

***N*-Ac-Gly-L-Ala-OH (4).** 46 mg (99%) as a white solid: R_f = 0.21 (9:1:0.1 $CHCl_3$−MeOH −AcOH); mp 132−134 °C; ^{1}H NMR (500 MHz, *d6*-DMSO) δ 12.58 (br. s, 1H, **1**), 8.17 (d, 1H, *J* = 7.3 Hz, **4**), 8.07 (X of ABX, 1H, $J_{AX} = J_{BX}$ = 5.7 Hz, **8**), 4.20 (p, 1H, *J* = 7.3 Hz, **3**), 3.75 − 3.64 (m, 2H, **7**), 1.84 (s, 3H, **10**), 1.26 ppm (d, 3H, *J* = 7.3 Hz, **5**); ^{13}C NMR (75 MHz, *d6*-DMSO) δ 174.02 (**2**), 169.46 (**6**), 168.72 (**9**), 47.42 (**7**), 41.63 (**3**), 22.49 (**10**), 17.26 ppm (**5**); HRMS (ESI-TOF) *m/z*: $[M+H]^+$ calcd for $C_7H_{13}N_2O_4$ 189.0875; found 189.0874

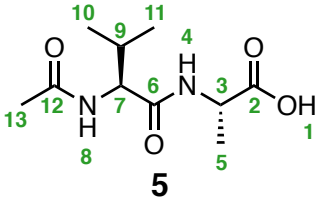

5

***N*-Ac-L-Val-L-Ala-OH (5).** 57 mg (99%) as a white solid: R_f = 0.16 (95:5 $CHCl_3$−MeOH); mp 134−135 °C; ^{1}H NMR (500 MHz, *d6*-DMSO) δ 12.46 (br. s, 1H, **1**), 8.27 (d, 1H, *J* = 8.3 Hz, **4**), 7.87 (d, 1H, *J* = 9.1 Hz, **9**), 4.21 − 4.12 (m, 2H, **3**+**7**), 1.92 (h, 1H, *J* = 8.3 Hz, **9**), 1.85 (s, 3H, **13**), 1.26 (d, 3H, *J* = 8.3 Hz, **5**), 0.87 (d, 3H, *J* = 6.8 Hz, **11**), 0.83 ppm (d, 3H, *J* = 6.9 Hz, **10**); ^{13}C NMR (75 MHz, *d6*-DMSO) δ 174.00 (**2**), 170.96 (**6**), 169.11 (**12**), 57.18 (**7**), 47.42 (**3**), 30.69 (**9**), 22.48 (**13**), 19.12 (**10**), 18.19 (**11**), 16.98 ppm (**5**) *Relative assignments of the Val-methyl signals (**10** & **11**) were based on the ACD-lab predicted spectrum; HRMS (ESI-TOF) *m/z*: $[M+H]^+$ calcd for $C_{10}H_{19}N_2O_4$ 231.1345; found 231.1341

General Procedure for the Preparation of Peptide Phosphinyl Esters (23a, 23b and 24). C-terminal esterification of peptides **1a**, **1b** and **4** was carried out according to a modified Steglich procedure.[24] To a stirred 0.25 M solution of the N^{α}-acetylated peptide (200 μmol, 1.0 equiv) and DMAP (20 μmol, 0.1 equiv) in dry DMF (750 μL) at 0°C was added a 0.25 M solution of DCC (200 μmol, 1.0 equiv) in DMF (750 μL). After precipitated DCU was observed, a 1M solution of 2-(diphenylphosphino)phenol **22** (240 μmol, 1.2 equiv) in DMF (240 μL) was added via syringe. The ice-water bath was removed and the mixture stirred under an Ar-atmosphere for 4 h, after which time AcOH (1 mL) was added to quench unreacted DCC. The slurry was filtered through a 0.2 μm PFTE syringe filter and concentrated by high-vacuum rotary evaporation (10^{-2} Torr). The residual solid was dissolved in DCM containing a small volume of methanol, filtered, and concentrated under reduced pressure onto silica gel. Purification by FCC eluting with a gradient of $CHCl_3$–MeOH (1:0 to 9:1 *v/v*) under N_2-pressure afforded the desired peptide phosphinyl esters **23a**, **23b**, and **24**; **23a** and **23b** were obtained as an inseparable mixture of diastereomers and **24** as a racemic mixture.

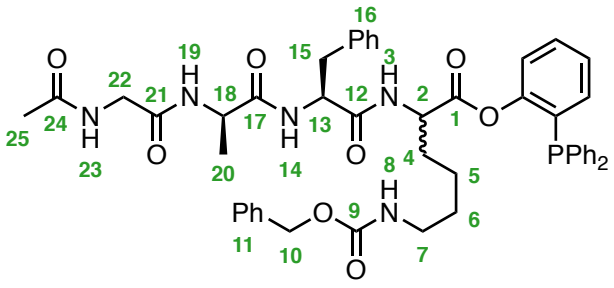

23a

***o*-(Diphenylphosphinyl)phenyl *N*-Ac-GaFK(Cbz) ester (23a).** 117 mg (68%) as a clear oil: R_f = 0.24 (9:1 $CHCl_3$–MeOH). ^{1}H NMR at 70 °C (400 MHz, CD_3CN) δ 7.8 – 7.6 (m, 1H, **3**), 7.6 – 7.5 (m, 1H, **14**), 7.5 – 7.4 (m, 1H, **23**), 7.4 – 7.0 (m, 21H), 6.9 – 6.8 (m, 2H), 6.7 (br. s, 1H),

5.64 (br. s, 1H, **8**), 5.0 − 4.9 (m, 2H, **10**), 4.7 – 4.5 (m, 1H, **13**), 4.4 – 4.3 (m, 1H, **2**), 4.2 – 4.0 (m, 1H, **18**), 3.80 − 3.60 (m, 2H, **22**), 3.25 – 3.15 (m, 1H, **15**), 3.15 – 3.02 (m, 1H, **7**), 3.0 – 2.9 (m, 1H, **15'**), 1.91 (s, 3H, **25**), 1.87 – 1.67 (m, 2H, **5**), 1.71 – 1.39 (m, 2H, **4**), 1.42 – 1.18 (m, 2H, **6**), 1.1 − 1.0 ppm (d, 3H, **20**). ^{13}C NMR (75 MHz, CD_3CN) δ 173.23, 173.21, 172.3, 172.2, 172.1, 172.0, 171.3, 171.27, 170.8, 170.76, 157.5, 154.23, 154.2, 154.0, 153.9, 138.9, 138.8, 136.6, 136.5, 135.6, 135.57, 134.9, 134.8, 134.7, 134.6, 134.5, 133.8, 133.7, 133.3, 133.2, 132.7, 132.6, 131.4, 131.38, 131.2, 131.0, 130.3, 130.2, 130.0, 129.9, 129.8, 129.7, 129.4, 129.3, 129.2, 128.8, 128.79, 128.7, 128.6, 127.5, 127.4, 123.52, 123.5, 120.4, 120.3, 119.0, 118.9, 118.7, 118.69, 118.63, 118.6, 118.3, 118.0, 117.99, 117.97, 79.1, 66.7, 55.8, 55.5, 53.7, 50.5, 44.1, 44.0, 41.2, 38.1, 37.7, 36.5, 34.5, 31.3, 31.2, 31.1, 31.0, 30.04, 30.0, 26.4, 25.8, 23.5, 23.0, 17.5, 17.4 ppm; ^{31}P NMR (122 MHz, CD_3CN) δ -18.2, -18.4 ppm (diastereomers); HRMS (ESI-TOF) *m/z*: $[M+Na]^+$ calcd for $C_{48}H_{52}N_5NaO_8P$ 880.3553; found 880.3561.

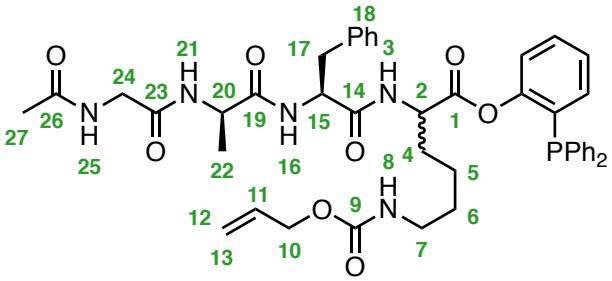

23b

***o*-(Diphenylphosphino)phenyl *N*-Ac-GaFK(alloc) ester (23b).** 123 mg (76%) as a clear oil: R_f = 0.27 (9:1 $CHCl_3$−MeOH); ^{1}H NMR (400 MHz, *d6*-DMSO) δ 8.6 – 8.5 (m, 1H, **3**), 8.4 – 8.2 (m, 1H, **16**), 8.1 – 8.0 (m, 1H, **25**), 7.95 – 7.8 (m, 1H, **21**), 7.7 – 7.1 (m, 20H), 6.8 − 6.7 (m, 1H), 6.0 − 5.8 (m, 1H, **11**), 5.3 − 5.2 (m, 1H, **13**), 5.18 – 5.1 (m, 1H, **12**), 4.7 – 4.5 (m, 1H, **15**), 4.46 – 4.4 (m, 2H, **10**), 4.3 − 4.2 (m, 2H, **2** and **20**), 3.8 – 3.6 (m, 2H, **24**), 3.1 – 2.9 (m, 3H, **7** and **17**),

2.8 – 2.6 (m, 1H, **17'**), 1.83 (s, 3H, **27**), 1.82 – 1.6 (m, 1H, **4**), 1.55 – 1.4 (m, 1H, **4'**), 1.35 – 1.2 (m, 4H, **5** and **6**), 1.0 − 0.8 ppm (m, 3H, **22**). ^{31}P NMR (122 MHz, CD_3CN) δ -18.9, -18.8 ppm (diastereomers); HRMS (ESI-TOF) *m/z*: $[M+Na]^+$ calcd for $C_{44}H_{50}N_5NaO_8P$ 830.3295; found 830.3302.

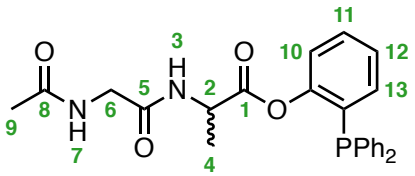

24

***o*-(Diphenylphosphino)phenyl *N*-Ac-Gly-DL-Ala ester (24).** 48 mg (53%) as a clear oil: R_f = 0.30 (9:1:0.1 $CHCl_3$−MeOH−AcOH); ^{1}H NMR (400 MHz, *d6*-DMSO) δ 7.44 (td, 1H, *J* = 7.8, 1.5 Hz, **10** *or* **13**), 7.42 − 7.38 (m, 5H), 7.38 − 7.35 (m, 1H), 7.30 − 7.23 (m, 4H), 7.21 (td, 1H, *J* = 7.6, 0.9 Hz, **10** *or* **13**), 7.13 (ddd, 1H, *J* = 8.1, 4.3, 0.9 Hz, **11** *or* **12**), 6.88 (br. d, 1H, *J* = 6.6 Hz, **3**), 6.82 (ddd, 1H, *J* = 7.7, 4.1, 1.6 Hz, **11** *or* **12**), 6.66 (br. s, 1H, **7**), 4.39, (p, 1H, *J* = 7.2 Hz, **2**), 3.81 − 3.72 (m, 2H, **6**), 1.92 (s, 3H, **9**), 1.24 (d, 3H, *J* = 7.3 Hz, **4**) HRMS (ESI-TOF) *m/z*: $[M+H]^+$ calcd for $C_{25}H_{26}N_2O_4P$ 449.1630; found 449.1624.

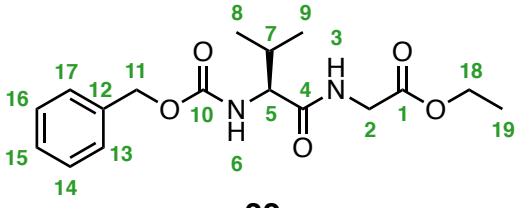

32

***N*-Cbz-L-Val-Gly-OEt (32).** Cbz-L-Valine-OH (1.26 g, 5 mmol, 1 equiv) was dissolved in dry chloroform (9.3 mL) containing TEA (700 μL, 5 mmol, 1 equiv) and the mixture cooled to 0 °C with an external ice-water bath. Ethyl chloroformate (476 μL, 5 mmol, 1 equiv) was added neat dropwise via syringe and the mixture stirred at 0 °C for 15 min during which time a

precipitate formed. To the heterogeneous mixture was added a suspension of glycine ethyl ester hydrochloride (698 mg, 5 mmol, 1 equiv) in dry chloroform (9.3 mL) containing TEA (700 μL, 5 mmol, 1 equiv). Carbon dioxide was observed to evolve as the solids went into solution. After the reaction mixture became homogeneous, the ice-water bath was removed and the solution stirred at ambient temperature for 30 min, then warmed to 50 °C for 10 min, diluted with additional chloroform (70 mL) and transferred to a separatory funnel. The organic phase was washed successively with water (30 mL), 1 M aq. HCl (30 mL), 0.5 M sodium bicarbonate (2 x 20 mL) and again with water (30 mL). The organic phase was dried over anh. Na_2SO_4 and concentrated under reduced pressure to afford crude Cbz-L-valylglycine ethyl ester (1.514 g, 90%) as a white solid. Recrystallization of the crude material from boiling EtOAc−ether gave analytically pure **32** (1.245 g, 74%) as cylindrical white needles: R_f = 0.23 (98:2 $CHCl_3$−MeOH); RP-HPLC, RT = 6.4 min (method 1) and 36.2 min (method 2); mp 134−135 °C; ^{1}H NMR (500 MHz, $CDCl_3$) δ 7.36 – 7.31 (m, 5H, **13**−**17**), 6.49 (br. t, 1H, *J* = 4.6 Hz, **3**), 5.38 (apparent d, 1H, *J* = 8.4 Hz, **6**), 5.13 and 5.10 (AB-pattern, 2H, *J* = 12.2 Hz, **11**), 4.22 (q, 2H, *J* = 7.2 Hz, **18**), 4.16 − 3.95 (m, 3H, **2** and **5**), 2.18 (sext, 1H, *J* = 6.6 Hz, **7**), 1.28 (t, 3H, *J* = 6.9 Hz, **19**), 1.00 (d, 3H, *J* = 6.7 Hz, **9**), 0.95 ppm (d, 3H, *J* = 6.7 Hz, **8**) *Relative assignments of the Val-methyl signals (**8** & **9**) were based on the ACD-lab predicted spectrum; ^{13}C NMR (75 MHz, *d6*-DMSO) δ 171.55 (**4**), 169.70 (**1**), 156.53 (**10**), 136.29 (**12**), 128.68 (**3**), 128.35 (**15**), 128.21 (**13**), 67.27 (**11**), 61.74 (**5**), 60.45 (**18**), 41.42 (**2**), 31.15 (**18**), 19.33 (**9**), 17.82 (**8**), 14.27 ppm (**19**) *Relative assignments of the Val-methyl signals (**8** & **9**) were based on the ACD-lab predicted spectrum; HRMS (ESI-TOF) *m/z*: $[M+H]^+$ calcd for $C_{17}H_{25}N_2O_5$ 337.1763; found 337.1769.

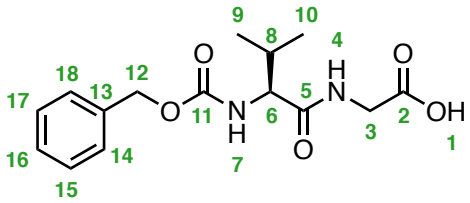

33

***N*-Cbz-L-Val-Gly-OH (33)**. To a stirred 0.17 M solution of Cbz-L-Valylglycine-OEt **32** (337 mg, 1.0 mmol, 1.0 equiv) in THF (6.0 mL) cooled to 0 °C with an external ice-water bath was added ice-cold 1 M aq. NaOH (1 mL, 1.0 mmol, 1.0 equiv). The reaction mixture was stirred at 0 °C until complete consumption of the starting ester was observed by RP-HPLC. The solution was concentrated to ~20% of the initial volume under reduced pressure and then acidified by the addition of cold 1 M aq. HCl (5 mL). The white precipitate that formed was isolated by vacuum filtration, washed with cold water, air-dried for 30 min and further dried under high-vacuum (10^{-2} Torr) overnight. Recrystallization of the crude material from hot EtOAc and Et_2O afforded the desired dipeptide acid, *N*-Cbz-L-valylglycine, **33** (206 mg, 67%) as a white solid: RP-HPLC, R_T = 4.8 min (method 1) and 23.9 min (method 2); ^{1}H NMR (300 MHz, *d6*-DMSO) δ 12.53 (br. s, 1H, **1**), 8.25 (br. t, 1H, *J* = 5.2 Hz, **4**), 7.5 − 7.1 (m, 6H, **7** and **14**−**18**), 5.04 and 5.02 (AB-pattern, 2H, *J* = 13.0 Hz, **11**), 3.89 (t, 1H, *J* = 7.5 Hz, **6**), 3.84 − 3.62 (m, 2H, **3**), 1.97 (sext, 1H, *J* = 6.8 Hz, **8**), 0.88 (d, 3H, *J* = 6.9 Hz, **9**), 0.86 ppm (d, 3H, *J* = 6.8 Hz, **10**) *Relative assignments of the Val-methyl signals (**9** & **10**) were based on the ACD-lab predicted spectrum.

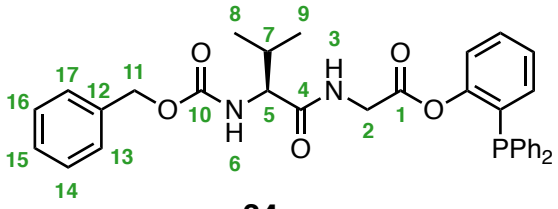

34

***o*-(Diphenylphosphino)phenyl *N*-Cbz-L-Val-Gly ester (34).** Cbz-L-Valylglycine-OH **33** (100 mg, 324 μmol, 1 equiv) was dissolved in THF (2.0 mL) containing TEA (45.3 μL, 325 μmol, 1 equiv) and the mixture cooled to 0 °C with an ice-water bath. Neat ethyl chloroformate (30 μL, 315 μmol, 0.97 equiv) was added in 3 equal portions in via syringe. The reaction was stirred at 0 °C for 15 min and then to the mixture was added a 0.25 M solution of *o*-(diphenylphosphino)phenol **22** (112 mg, 400 μmol, 1.2 equiv) and TEA (86 μL, 618 μmol, 1.9 equiv) in THF (1.2 mL). The reaction mixture was stirred at 0 °C for 15 min, the ice-water bath removed and the reaction stirred at ambient temperature for an additional 3.5 h. The solution was then concentrated to dryness, DCM (35 mL) added to dissolve the solids, the solution transferred to a separatory funnel, and further diluted with hexanes (25 mL). The DCM−hexanes solution was washed successively with water (10 mL), 0.1 M aq. HCl (10 mL), 0.1 M $NaHCO_3$ (10 mL) and again with water (10 mL). The organic phase was dried over anh. Na_2SO_4 and concentrated under reduced pressure to afford the crude ester, which was purified by FCC over silica gel eluting with a gradient of $CHCl_3$−MeOH (1:0 to 9:1 *v/v*), to give compound **34** (140 mg, 76%) as a colorless oil: R_f = 0.28 (98:2 $CHCl_3$−MeOH); ^{1}H NMR (300 MHz, $CDCl_3$) δ 7.44 – 7.28 (m, 15H), 7.22 – 7.08 (m, 2H), 6.87 (ddd, 1H, *J* = 7.6, 4.7, 1.5 Hz), 6.34 (t, 2H, *J* = 5.0 Hz, **3**), 5.47 (d, 1H, *J* = 8.7 Hz, **6**), 5.13 (s, 2H, **11**), 4.12 – 4.02 (m, 1H, **5**), 4.02 – 3.75 (m, 2H, **2**), 2.14 (dq, 1H, *J* = 13.3, 6.7 Hz, **7**), 0.97 (d, 3H, *J* = 6.7 Hz, **9**), 0.92 ppm (d, 3H, *J* = 6.7 Hz, **8**) *Relative assignments of the Val-methyl signals (**8** & **9**) were made using the ACD-lab

predicted spectrum; ^{13}C NMR (75 MHz, $CDCl_3$) δ 171.56 (**4**), 167.86 (**1**), 156.56 (**10**), 152.31 (d, *J* = 16.9 Hz), 136.33, 135.40 (d, *J* = 2.2 Hz), 135.27 (d, *J* = 2.2 Hz), 134.24 (d, *J* = 0.8 Hz), 133.97 (d, *J* = 0.8 Hz), 130.43 (d, *J* = 15.3 Hz), 130.25, 129.36, 128.92 (d, *J* = 1.1 Hz), 128.82 (d, *J* = 1.0 Hz), 128.70, 128.35, 128.23, 126.76 (d, *J* = 0.8 Hz), 122.59 (d, *J* = 1.5 Hz), 67.28 (**11**), 60.31 (**5**), 41.12 (**2**), 31.21 (**7**), 19.34 (**9**), 17.81 ppm (**8**) *Relative assignments of the Val-methyl signals (**8** & **9**) were made using the ACD-lab predicted spectrum; ^{31}P NMR (122 MHz, $CDCl_3$) δ -16.11; +28.05 ppm (oxide); HRMS (ESI-TOF) *m/z*: $[M+H]^+$ calcd for $C_{33}H_{33}N_2NaO_5P$ 591.2025; found 591.2020.

5.7 References

1. de Groot, F. M. H.; de Bart, A. C. W.; Verheijen, J. H.; Scheeren, H. W. "Synthesis and Biological Evaluation of Novel Prodrugs of Anthracyclines for Selective Activation by the Tumor-associated Protease Plasmin" *J. Med. Chem*. **1999**, *42*, 5277−5283.

2. Barthel, B. L.; Rudnicki, D. L.; Kirby, T. P.; Colvin, S. M.; Burkhart, D. J.; Koch, T. H. "Synthesis and Biological Characterization of Protease-Activated Prodrugs of Doxazolidine" *J. Med. Chem*. **2012**, *55*, 6595–6607.

3. Saxon, E.; Armstrong, J. I.; Bertozzi, C. R. " A Traceless Staudinger Ligation for the Chemoselective Synthesis of Amide Bonds" *Org. Lett.* **2000**, *2*, 2141−2143.

4. Dubowchik, G. M.; Firestone, R. A; Padilla, L.; Willner, D.; Hofstead, S. J.; Mosure, K.; Knipe, J. O.; Lasch, S. J.; Trail, P. A. "Cathepsin B-Labile Dipeptide Linkers for Lysosomal Release of Doxorubicin from Internalizing Immunoconjugates: Model Studies of Enzymatic Drug Release and Antigen-Specific in Vitro Anticancer Activity." *Bioconjugate Chem.* **2002**, *13*, 855–869.

5. Senter, P. D.; Sievers, E. L. "The Discovery and Development of Brentuximab Vedotin for Use in Relapsed Hodgkin Lymphoma and Systemic Anaplastic Large Cell Lymphoma" *Nat. Biotechnol.* **2012**, *30*, 631−637.

6. Biniossek, M. L.; Nagler, D. K.; Becker-Pauly, C.; Schilling, O. "Proteomic Identification of Protease Cleavage Sites Characterizes Prime and Non-Prime Specificity of Cysteine Cathepsins B, L, and S." *J. Proteome Res.* **2011**, *10*, 5363–5373.

7. Boissonnas, R. A.; Preitner, G. "Comparisons of Cleavage of Various α-Amino Function-Blocking Groups of α-Amino Acids" *Helv. Chim. Acta*. **1953**, *36*, 875−886.

8. Greene, T. W.; Wuts, P. G. M. In *Protective Groups in Organic Synthesis*, 2nd ed.; John Wiley, New York, 1991.

9. Trost, B. M.; Verhoeven, T. R. In *Comprehensive Organometallic Chemistry*; Wilkenson, G., Stone, F. G. A., Abel, E. W., Eds.; Pergamon Press: Oxford, 1982; Vol. 8, pp 799−854.

10. Williams, R. M.; Liu, J. "Asymmetric Synthesis of Differentially Protected 2,7-Diaminosuberic Acid, a Ring-Closure Metathesis Approach" *J. Org. Chem.* **1998**, *63*, 2130−2132.

11. Guibé, F. "Allylic Protecting Groups and Their Use in a Complex Environment Part II: Allylic Protecting Groups and Their Removal Through Catalytic Palladium π-Allyl Methodology" *Tetrahedron* **1998**, *54*, 2967−3042.

12. Carpino, L. A.; Han, G. Y. "9-Fluorenylmethoxycarbonyl Amino-Protecting Group" *J. Org. Chem.* **1972**, *37*, 3404−3409.

13. Atherton, E.; Logan, C. J.; Sheppard, R. C. "Peptide Synthesis. Part 2. Procedures for Solid-Phase Synthesis Using N^{α}-Fluorenylmethoxycarbonyl Amino Acids on Polyamide Supports. Synthesis of Substance P and of Acyl Carrier Protein 65–74 Decapeptide" *J. Chem. Soc. Perkin Trans. I* **1981**, 538−546.

14. Barlos, K.; Chatzi, O.; Gatos, D.; Stavropoulos, G. "2-Chlorotrityl Chloride Resin. Studies on Anchoring of Fmoc-Amino Acids and Peptide Cleavage" *Int. J. Pept. Protein Res.* **1991**, *37*, 513−520.

15. Atherton, E.; Sheppard, R. C. in *Solid Phase Synthesis: A Practical Approach*; IRL Press: Oxford, U.K., 1989.

16. Chan, W. C., White, P. D., Eds.; *Fmoc Solid Phase Peptide Synthesis: A Practical Approach*; Oxford University Press: New York, 2000.

17. Gude, M.; Ryf, J.; White, P. D. "An Accurate Method for the Quantitation of Fmoc-derivatized Solid Phase Supports" *Lett. Pept. Sci.* **2002**, *9*, 203−206.

18. Goodman, M., Felix, A., Moroder, L., Toniolo, C., Eds.; Synthesis of Peptides and Peptidomimetics. In *Methods of Organic Synthesis*; Thieme Stuttgart: New York, 2004; Vol. E22a, pp 716.

19. Fields, G. B.; Tian, Z.; Barany, G. In *Synthetic Peptides: A User's Guide*; Grant, G. A. Ed.; W. H. Freeman: New York, 1992; pp 77−183.

20. Knorr, R.; Trzeciak, A.; Bannwarth, W.; Gillessen, D. "New Coupling Reagents in Peptide Chemistry" *Tetrahedron Lett.* **1989**, *30*, 1927−1930.

21. Alberichio, F.; Bofill, J. M.; El-Faham, A.; Kates, S. A. "Use of Onium Salt-Based Coupling Reagents in Peptide Synthesis" *J. Org. Chem.* **1998**, *63*, 9678−9683.

22. Avan, I.; Tala, S. R.; Steel, P. J.; Katritsky, A. R. "Benzotriazole-Mediated Syntheses of Depsipeptides and Oligoesters" *J. Org. Chem.* **2011**, *76*, 4884−4893.

23. Bolihaggen, R.; Schmiedberger, M.; Barlos, K.; Grell, E. "A New Reagent for the Cleavage of Fully Protectede Peptides Synthesised on 2-Chlorotrityl Chloride Resin" *J. Chem. Soc., Chem Commun.* **1994**, 2559−2560.

24. Neises, B.; Steglich, W. "A Simple Method for the Esterification of Carboxylic Acids" *Angew. Chem., Int. Ed.* **1978**, *17*, 522−524.

25. Fey, N.; Howell, J. A.; Lovatt, J. D.; Yates, P. C.; Cunningham, D.; McArdle, P.; Gottlieb, H. E. Coles, S. J. "A Molecular Mechanics Approach to Mapping the Conformational Space of Diaryl and Triarylphosphines" *Dalton Trans.* **2006**, 5464−5475.

26. Kölmel, C.; Ochsenfeld, C. Ahlrichs, R. “An *Ab Initio* Investigation of Structure and Inversion Barrier of Triisopropylamine and Related Amines and Phosphines” *Theor. Chim. Acta* **1991**, *82*, 271−284.

27. Goodman, M.; Stueben, K. C. “Amino Acid Active Esters. III. Base-Catalyzed Racemization of Peptide Active Esters” *J. Org. Chem.* **1962**, *27*, 3409−3416.

28. Williams, M. W.; Young, G. T. “Amino-acids and Peptides. Part XIXJ The Mechanism of Racemization During Peptide Synthesis. The Chloride Effect" *J. Chem. Soc.* **1964**, 3701−3708.

29. Goodman, M.; Levine, L. “Peptide Synthesis via Active Esters. IV. Racemization and Ring-Opening Reactions of Optically Active Oxazolones” *J. Am. Chem. Soc.* **1964**, *86*, 2918−2922.

30. Goodman, M.; McGahren, W. J. “Optically Active Peptide Oxazolones. Preliminary Racemization Studies Under Peptide Coupling Conditions” *J. Am. Chem. Soc.* **1965**, *87*, 3028−3029.

31. Merkx, R.; Rijkers, D. T. S.; Kemmink, J. Liskamp, R. M. J. “Chemoselective Coupling of Peptide Fragments Using the Staudinger Ligation” *Tetrahedron Lett.* **2003**, *44*, 4515−4518.

32. Carpino, L. A. "1-Hydroxy-7-azabenzotriazole. An Efficient Peptide Coupling Additive” *J. Am. Chem. Soc*. **1993**, *115*, 4397−4398.

33. Carpino, L. A; Imazumi, H.; Foxman, B. M.; Vela, M. J; Henklein, P.; El-Faham, A.; Klose, J.; Bienert, M. "Comparison of the Effects of 5- and 6-HOAt on Model Peptide Coupling Reactions Relative to the Cases for the 4- and 7-Isomers" *Org. Lett.* **2000**, *2*, 2253− 2256.

34. Belleau, B.; Malek, G. “A New Convenient Reagent for Peptide Syntheses” *J. Am. Chem. Soc.* **1968**, *90*, 1651−1652.

35. Cremin, D. J.; Hergarty, A. F.; Begley, M. J. “Mechanism of Reaction of 2-Ethoxy-1 -ethoxycarbonyl-I ,2-dihydroquinoline (EEDQ) with Nucleophiles and its Crystal Structure” *J. Chem. Soc. Perkin II* **1980**, 412−420.

36. Hiebel, J.; Baumgartner, H.; Bernwieser, I.; Blanka, M.; Bodenteich, M.; Leitner K.; Rio , A.; Rovenszky, F.; Alberts, D. P.; Bhatnagar, P. K.; Banyard , A. F.; Baresch , K.; Esch, P. M.; Kollmann , H.; Mayrhofer, G.; Weihtrager, H.; Welz, W.; Winkler, K.; Chen, T.; Patel, R.; Lantos, I.; Stevenson, D.; Tubman, K. D.; Undheim, K. “Large-scale Synthesis of Hemato-regulatory Nonapeptide SK&F 107647 by Fragment Condensation” *J. Pept. Res.* **1999**, *54*, 54−65.

38. Kovacs, J.; Kisfaludy, L.; Ceprini, M. Q. “On the Optical Purity of Peptide Active Esters Prepared by N,N'-Dicydohexylcarbodiimide and Complexes of N,N'-Dicyclohexylcarbodiimide-

Pentachlorophenol and N,N'-Dicyclohexylcarbodiimide Pentafluorophenol" *J. Am. Chem. Soc.* **1967**, *89*, 183−184.

39. Bergel, F.; Stock, J. A. "Cyto-active Amino Acids and Peptides. Part VIII. N^{α}-Acyl, Amide, Ester and Peptide Derivatives of Melphalan" *J. Chem. Soc.* **1960**, 3658−3669.

40. Still, C. W.; Kahn, M.; Mitra, A. "Rapid Chromatographic Technique for Preparative Separations with Moderate Resolution" *J. Org. Chem.* **1978**, *43*, 2923−2925.

41. Gottlieb, H. E.; Kotlyar, V.; Nudelman, A "NMR Chemical Shifts of Common Laboratory Solvents as Trace Impurities" *J. Org. Chem.* **1997**, *62*, 7512−7515.

Chapter 6

p-Azidobenzyl Anthracycline Carbamates and Derivatives Thereof

6.1 Introduction

With the synthesis of the "peptide-specifying" phosphinyl phenyl esters complete, issues with stereoselectivity notwithstanding, implementation of the *traceless* Staudinger ligation (TSL)[1] in the synthesis of tripartite prodrugs of doxazolidine (doxaz)[2] now depended on the preparation of the key "spacer-drug" intermediate, *p*-azidobenzyl doxazolidyl carbamate **1** (Figure 6.1). With the azido precursors required for the preparation of **1** having been synthesized during the exploratory studies on aryl azides in the TSL (Chapter 4), the proposed route to **1** was a short three-step synthesis from the available starting materials**.** The anticipated benefits from a head−to−head comparison of the corresponding peptidyl prodrugs of dox and doxaz during biological studies also prompted us to prepare the analogous dox "spacer-drug" intermediate, *p*-azidobenzyl doxorubicyl carbamate **2** (Figure 6.1). Chapter 6 describes the synthesis of compounds **1** and **2** and their subsequent derivatization into peptidyl prodrugs via the TSL.

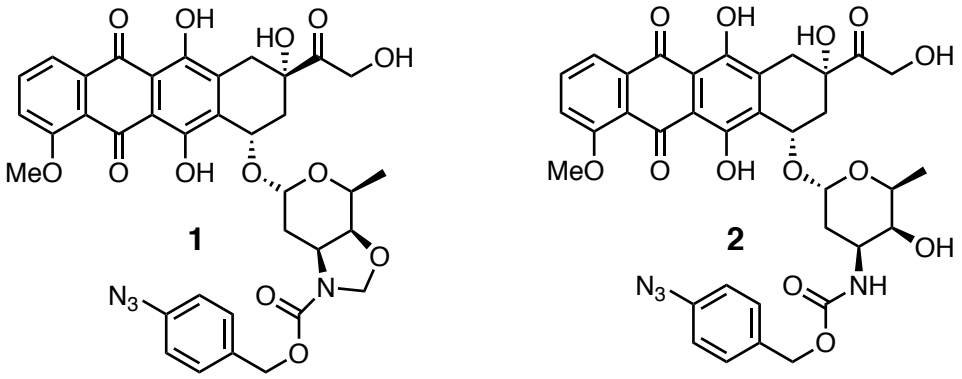

Figure 6.1 Structures of the key aryl azide "spacer-drug" intermediates *p*-azidobenzyl doxazolidyl carbamate **1** and *p*-azidobenzyl doxorubicyl carbamate **2**.

6.2 Synthesis of *p*-Azidobenzyl Anthracyline Carbamates

Clinical samples of doxorubicin hydrochloride **3** were dissolved in MeOH, neutralized with 100 mM phosphate buffer (pH 8.5) and the free-base extracted into DCM (Scheme 6.1). **Prilled* paraformaldehyde was then used to annulate the vicinal amino alcohol of daunosamine to give doxaz **4**.[3,4] In the presence of excess formaldehyde, 2 equiv of **4** reacted to form the dimer, doxofom (doxf) **5**, with an additional methylene derived from formaldehyde forming a bridging aminal bond between the two doxaz molecules.[3]

Scheme 6.1 Synthesis of doxazolidine **4** from clinical samples of doxorubicin•HCl **3** and prilled paraformaldehyde, as well as, the condensation of 2 equiv of **4** with an additional equiv of CH_2O to give doxoform **5**.[3,4]

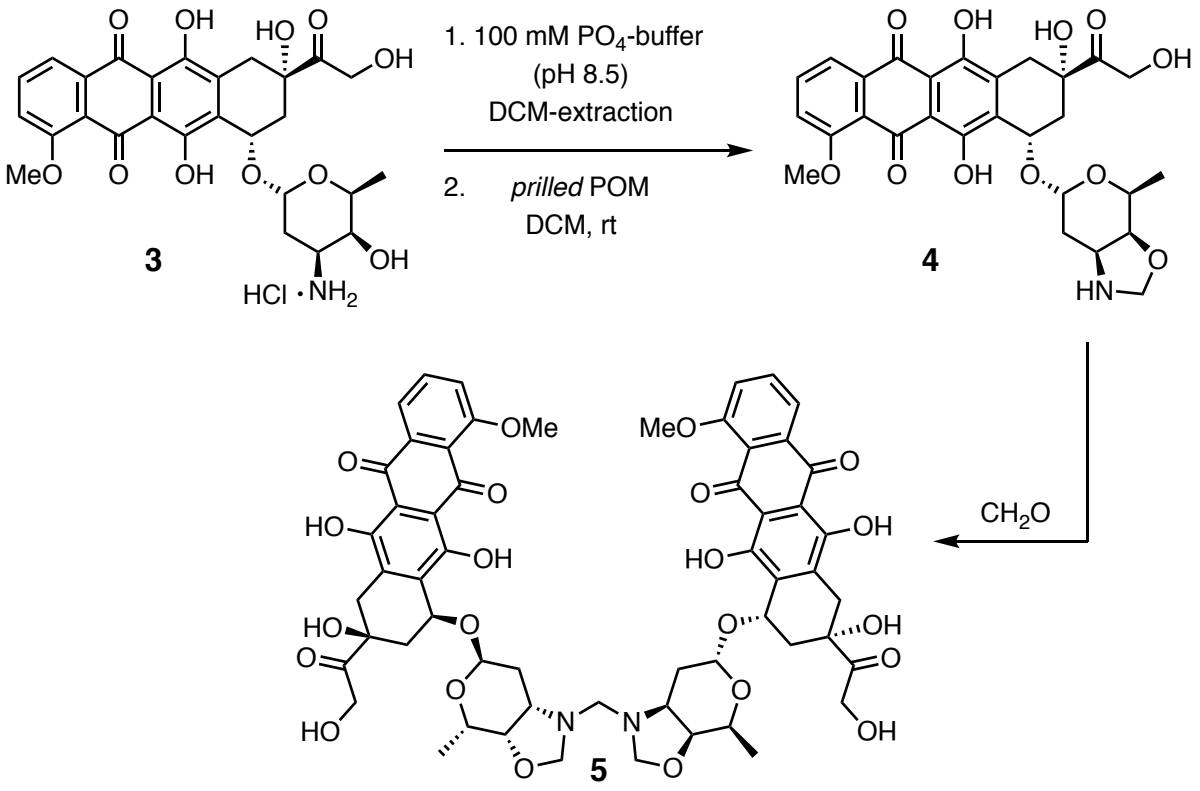

*The term "*prilled*" is used in mining and manufacturing to describe a material that has been pelletized. While the origin of its usage to denote a particular type of paraformaldehyde - a fine powder - is unclear, the importance of the term as applied to this reagent is in its indication of the bis-hemiacetal functional groups terminating the polyformaldehyde oligomers [a.k.a. poly(oxy-methylene) or POM], a reagent having the chemical formula $HO{-}(CH_2O)_n{-}H$. Other varieties of POM are end-capped with alkoxy groups and these reagents require "cracking" by either acid or heat in order to liberate monomeric formaldehyde. The use of *prilled* POM in the synthesis of doxaz **4** offered a marked improvement over previous methods and this innovation coincided with the start of the author's work in the Koch lab. The ^{1}H NMR spectrum of prilled POM in d6-DMSO (Figure 6.2) shows coupling of the hydroxyl proton to the adjacent methylene, thereby demonstrating the hemiacetal structure and was the second NMR spectrum ever acquired by the author; the first being POM in $CDCl_3$.

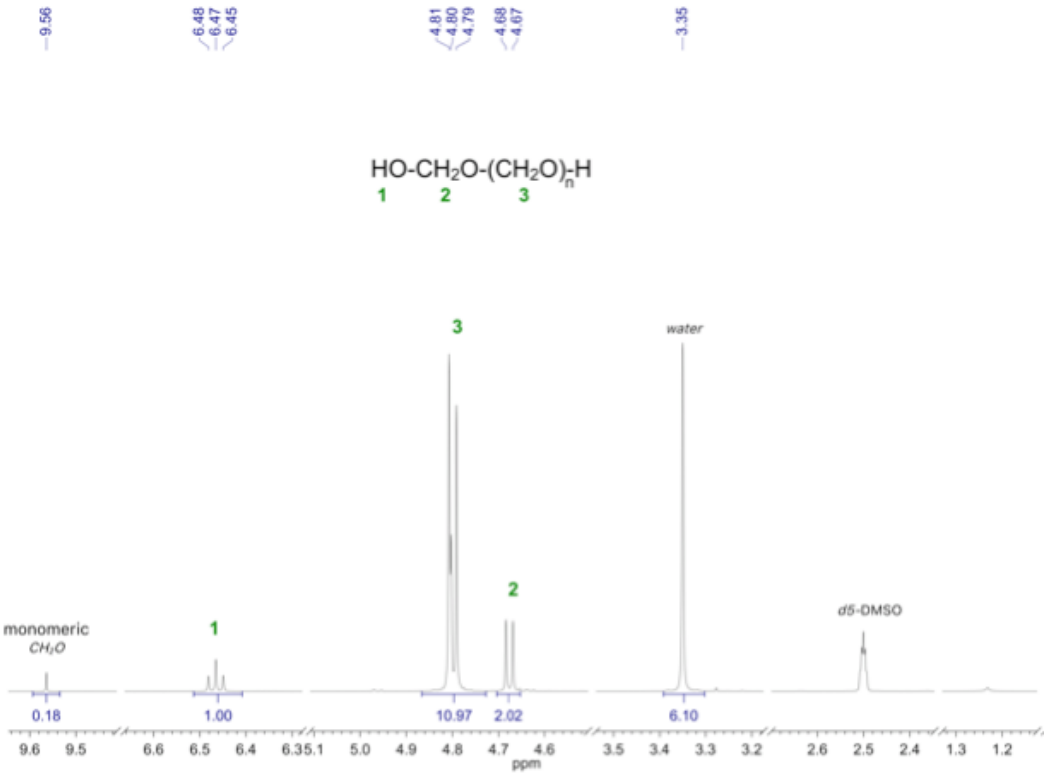

Figure 6.2 ^{1}H NMR spectrum of *prilled* POM in *d6*-DMSO at 500 MHz.

A mixture of doxaz **4** and doxf **5** was dissolved in wet NMP, which rapidly hydrolyzed **5** to 2 equiv of **4**, and an excess of the mixed *p*-nitrophenyl carbonate **6**[5,6] was added (Scheme 6.2).

Scheme 6.2 Synthesis of the key "spacer-drug" intermediate, *p*-azidobenzyl doxazolidyl carbamate **1**, from a mixture of doxaz **4** and doxf **5** combined with mixed carbonate **6**.[5,6]

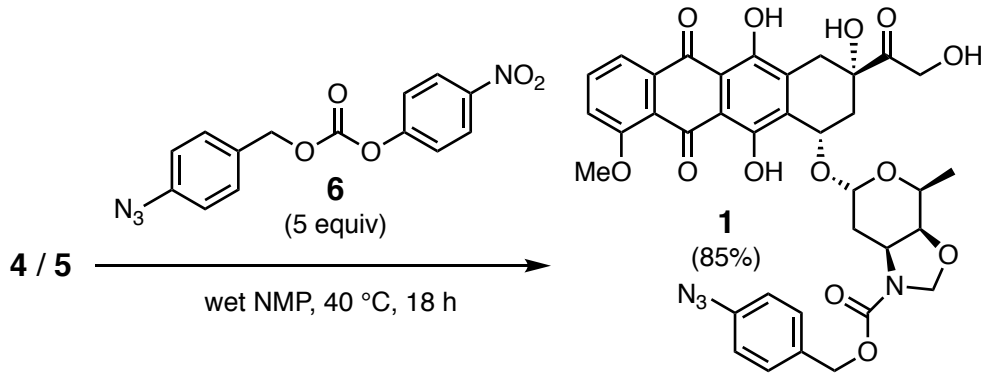

The reaction was stirred in the dark at 40 °C until complete consumption of **4** was observed by TLC (~18 h). Following aqueous work-up of the reaction mixture, the crude product was passed over a short plug of silica gel, eluting with 95:5 $CHCl_3$–MeOH (v/v), to afford the desired *p*-azidobenzyl doxazolidyl carbamate **1** as an oil in 85% overall yield from the clinical starting material. Crystallization of the isolated material from MeCN at 4 °C then afforded carbamate **1** as a red solid in 68% yield and excellent purity. The ^{1}H and gCOSY NMR spectra of **1** acquired at 400 MHz and 40 °C in $CDCl_3$, as well as, an analytical RP-HPLC chromatogram of **1** are shown in Figures 6.3–6.5, respectively, as an indication of purity. The elevated temperature at which the NMR spectra were acquired was used to overcome inhibition of the daunosamine ring flipping mechanism that occurs upon acylation of the oxazolidine, which at ambient temperature occurs at an intermediate rate on the NMR-timescale and may otherwise complicate interpretation of the data.

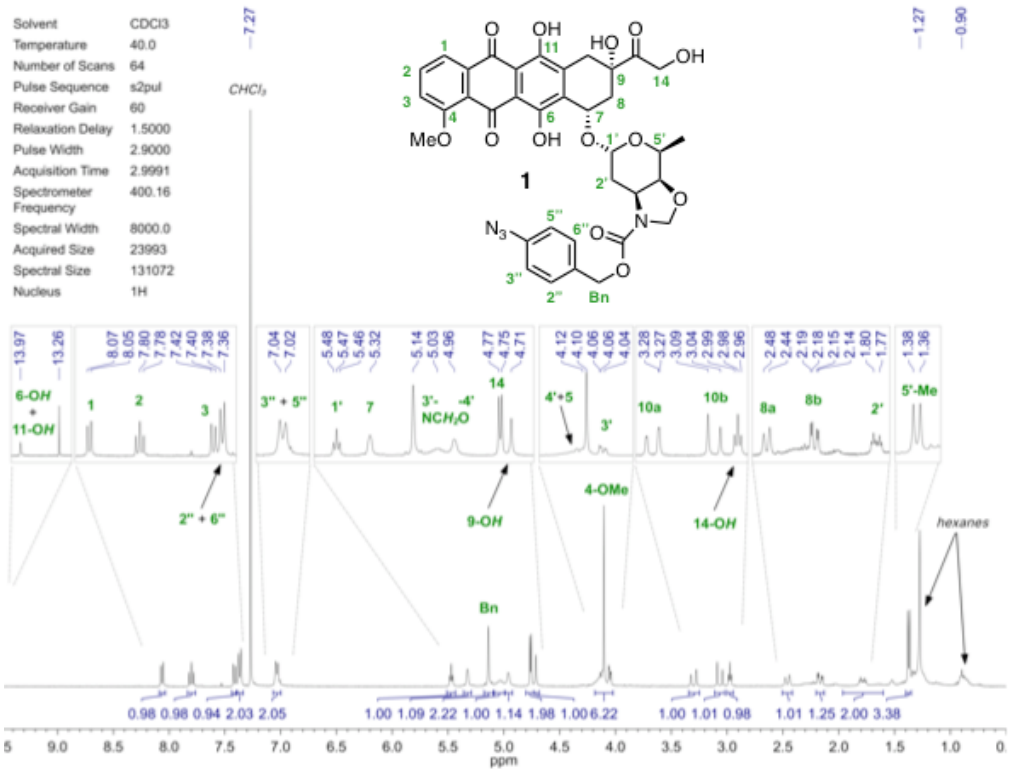

Figure 6.3 ^{1}H NMR spectrum of **1** in $CDCl_3$ at 40 °C and 400 MHz.

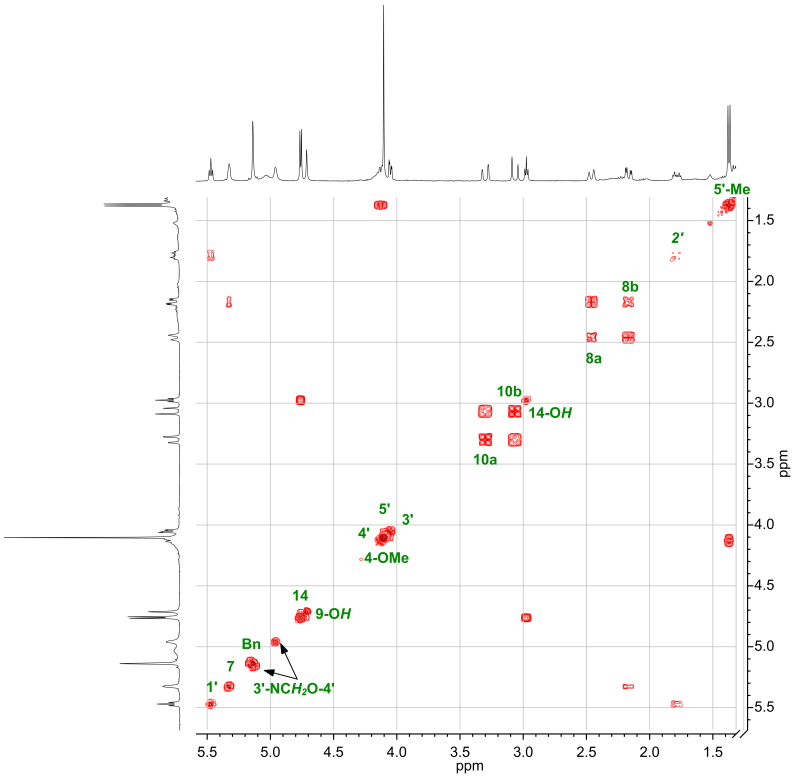

Figure 6.4 gCOSY NMR spectrum (0−5.5 ppm) of **1** in $CDCl_3$ at 40 °C and 400 MHz.

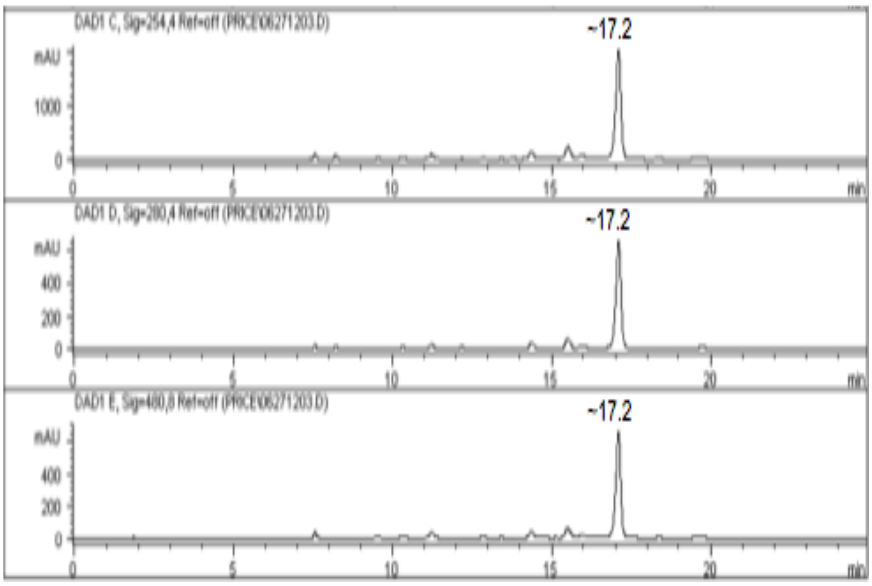

Figure 6.5 RP-HPLC chromatogram of **1** showing absorbance at 254, 280 and 480 nm using HPLC method 1; a description of the method is provided in section 6.5 under *General Methods*.

The dox analogue **2** was prepared in similar fashion using material diverted from the synthesis of doxaz.[7] However, in this case, the increased nucleophilicity of the 1° amine of dox relative to that of the oxazolidine **3** permitted reaction of dox free-base with 1 equiv of carbonate **6** to reach completion after only 2 h of stirring at ambient temperature in THF, and recrystallization of the crude product from MeCN afforded **2** in 94% overall yield from the clinical starting material. The ^{1}H and gCOSY NMR spectra acquired at 500 MHz in $CDCl_3$, as well as, an analytical RP-HPLC chromatogram of **2** are shown in Figures 6.6−6.8, respectively, as an indication of purity.

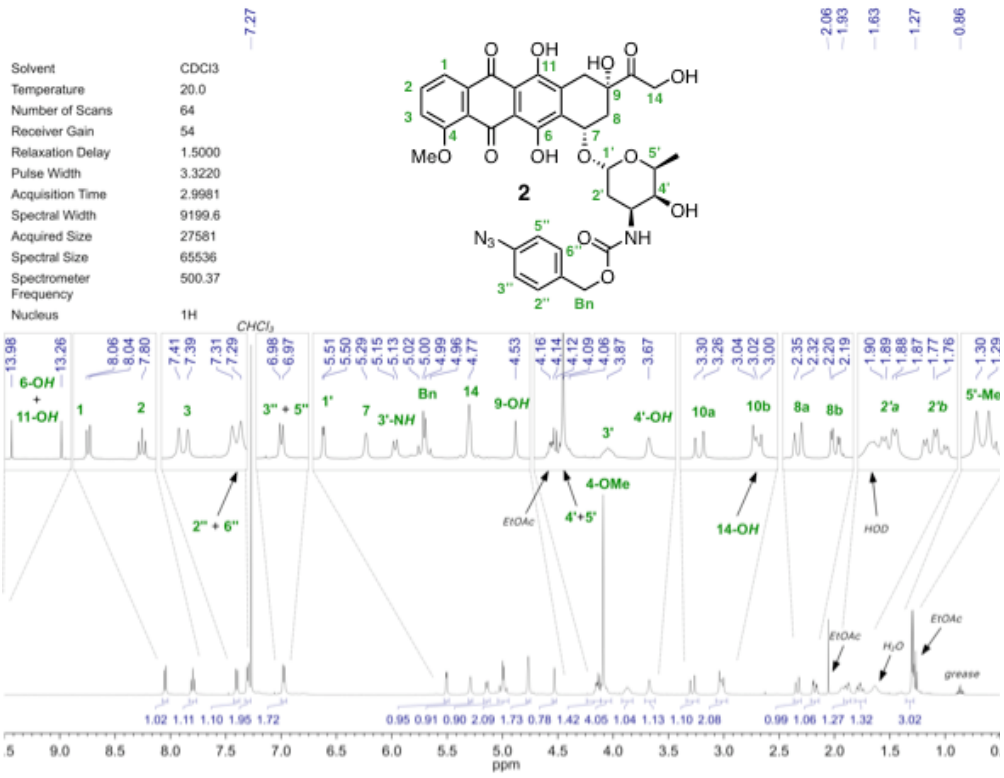

Figure 6.6 ^{1}H NMR spectrum of **2** in $CDCl_3$ at 500 MHz.

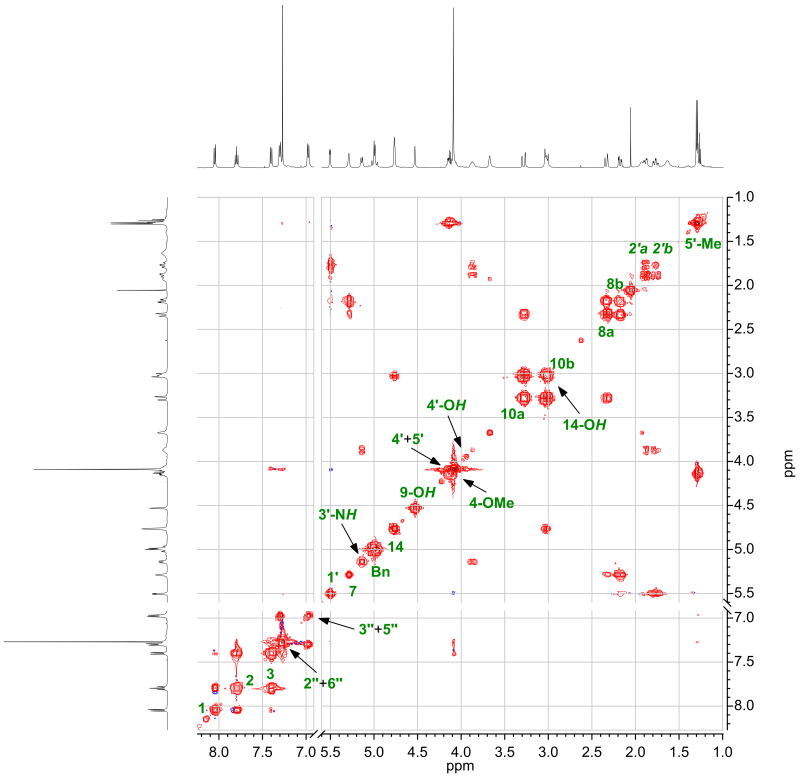

Figure 6.7 gCOSY NMR spectrum of **2** in $CDCl_3$ at 500 MHz.

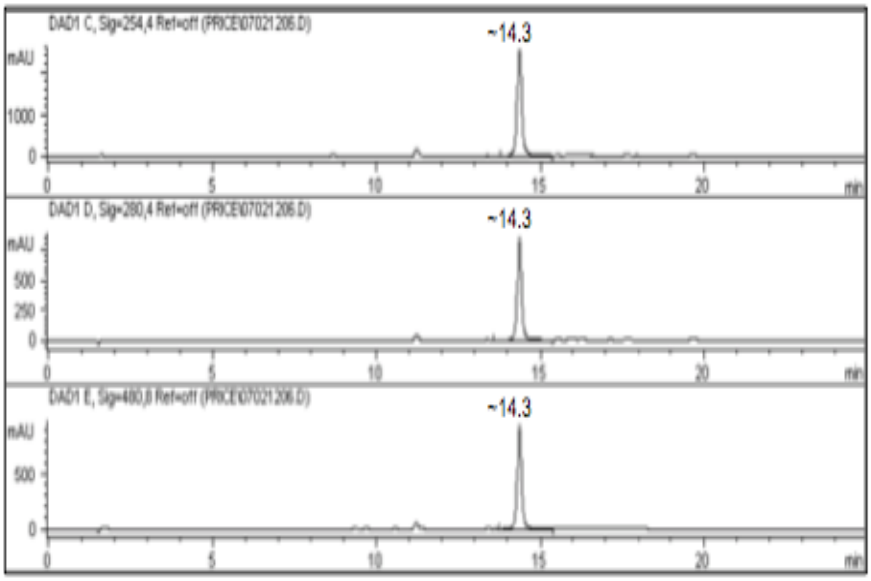

Figure 6.8 RP-HPLC chromatogram of **2** (R_T ~14.3 min) showing absorbance at 254, 280 and 480 nm using HPLC method 1; a description of the method is provided in section 6.5 under *General Methods*.

6.3 Prodrug Synthesis via the Traceless Staudinger Ligation

Originally, we had proposed the use of phosphinyl phenyl ester **7** in the TSL for the final step of synthesis to prepare the peptidase-activated tripartite prodrug of doxazolidine **8**, with **7** being derived from phoshinyl phenyl ester **9a** after deprotection of the Cbz-protected ε-amino group of lysine by catalytic transfer hydrogenolysis (Scheme 6.3). However, in work done by a colleague in the lab, prodrug **8** was found to undergo an intramolecular condensation reaction when the ε-amino group of the lysine residue was unprotonated, as evident from LC-MS analysis. Following isolation of **8** as the acetate salt and drying under reduced pressure, an intermediate was observed to form when the material was reconstituted in *d6*-DMSO for structural characterization. The intermediate was fully resolved from **8** by RP-HPLC and had an identical m/z ratio by LC-MS analysis. However, the intermediate then appeared to lose water as

Scheme 6.3 Initially proposed synthesis of the peptidase-activated tripartite prodrug of doxazolidine **8** starting from the N^{ε}-Cbz protected phosphinyl phenyl ester **9a**.

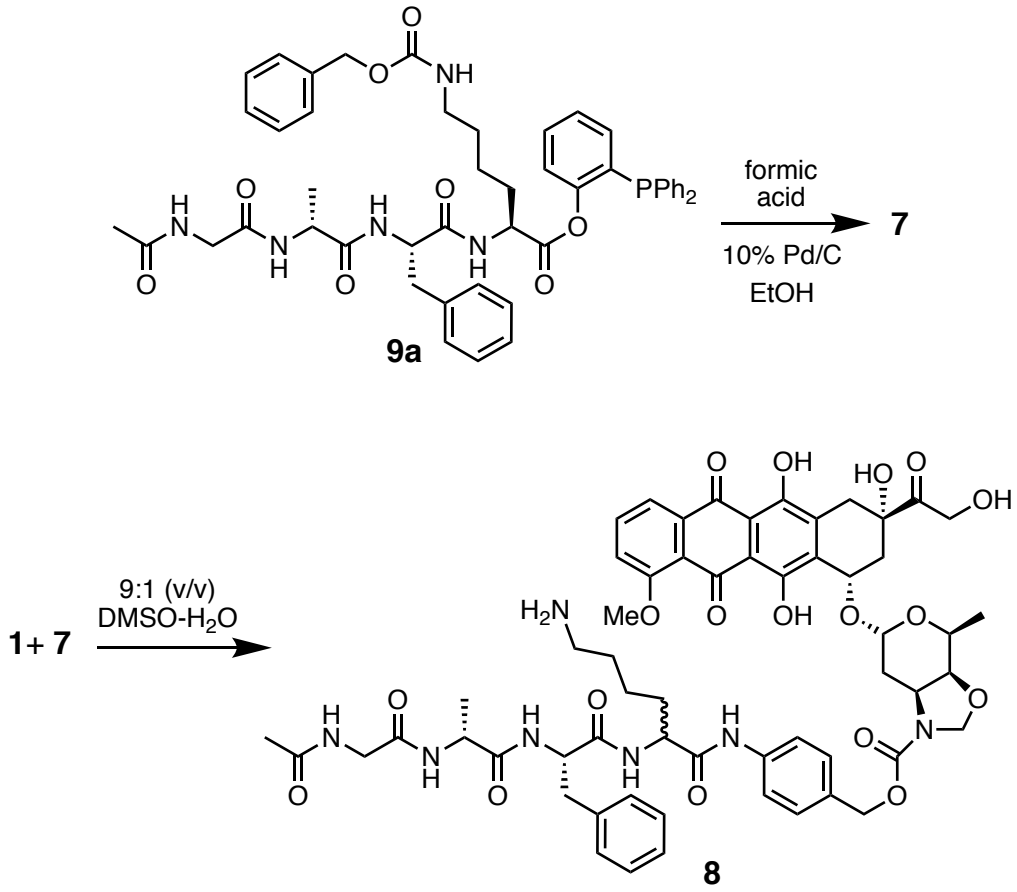

evident in the Δm/z of -18 amu. Presumably, attack on a carbonyl in the tetracyclic core of **8** by the ε-amino group of lysine had occured to first give the hemi-aminal intermediate **11** that then gave imine **12** after dehydration (Scheme 6.4). As the TSL requires neutral or basic conditions in order to avoid protonation of the intermediate phosphazides, which would prevent further reaction in route to the anilide, and given the unanticipated formation of **12** via intramolecular condensation of **8** under these conditions, our proposed use of the deprotected peptidyl ester **7** in the final step of the synthesis was not pursued.

Scheme 6.4 Proposed formation of intermediate **11** and the dehydrated product **12** observed by LC-MS following dissolution of **8** as the free-base.

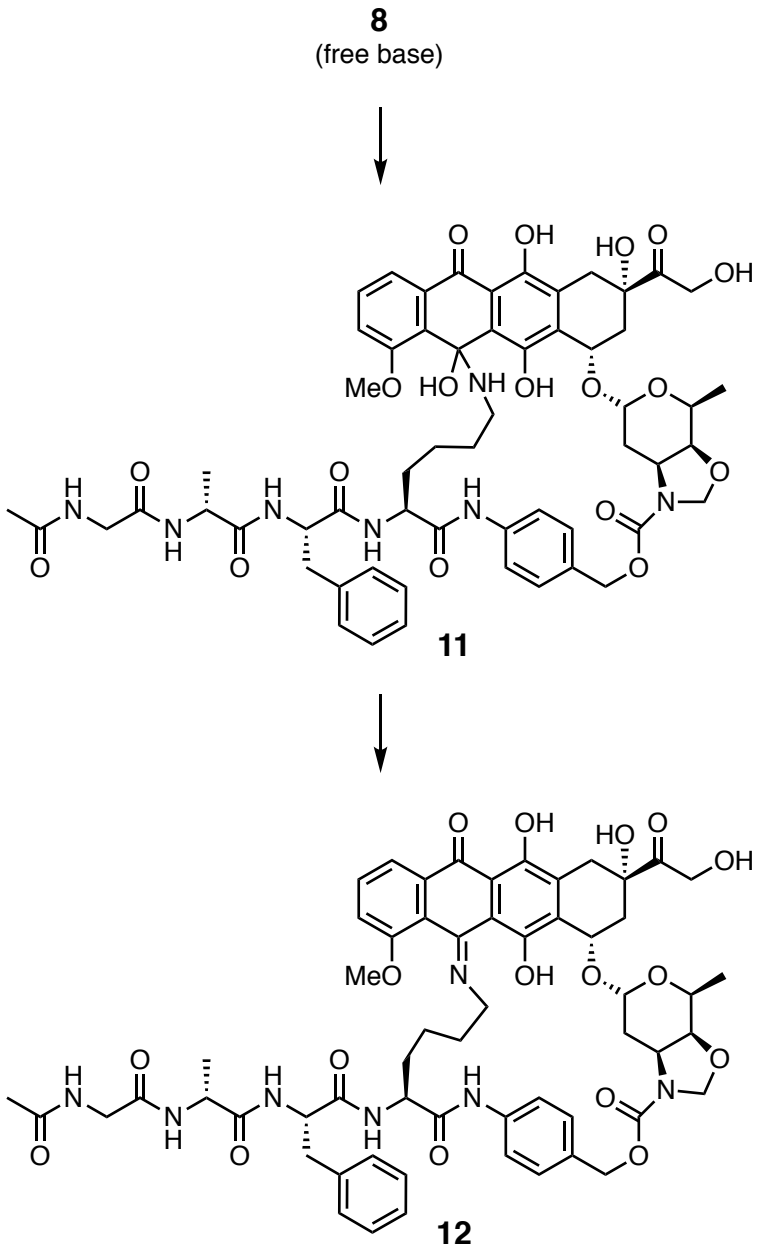

Instead, the alternative strategy of using protected peptidyl phosphinyl phenyl esters in the penultimate step of synthesis was pursued. Gratifyingly, the TSL proceeded smoothly with the ε-

amino group of lysine protected as the allyloxycarbonyl derivative **9b** (Scheme 6.5). At 20 mM concentration, the combination of azide **1** (or **2**) and phosphine **9b** in 9:1 DMSO−H2O (v/v) at ambient temperature gave near quantitative conversion of the starting materials over 6 h and delivered the alloc-protected peptidyl prodrug of doxaz **13b** (or dox **14b**) as a mixture of diatereomers. Analytical RP-HPLC chromatograms showing the conversion of azides **1** and **2** to anilides **13b** and **14b** are shown in Figures 6.9 and 6.10, respectively.

Scheme 6.5 TSL of phosphine **9b**, the alloc-protected GaFK peptidyl ester, and azides **1** (or **2**) afforded the protected peptidyl prodrugs of doxaz **13b** and dox **14b**, respectively.

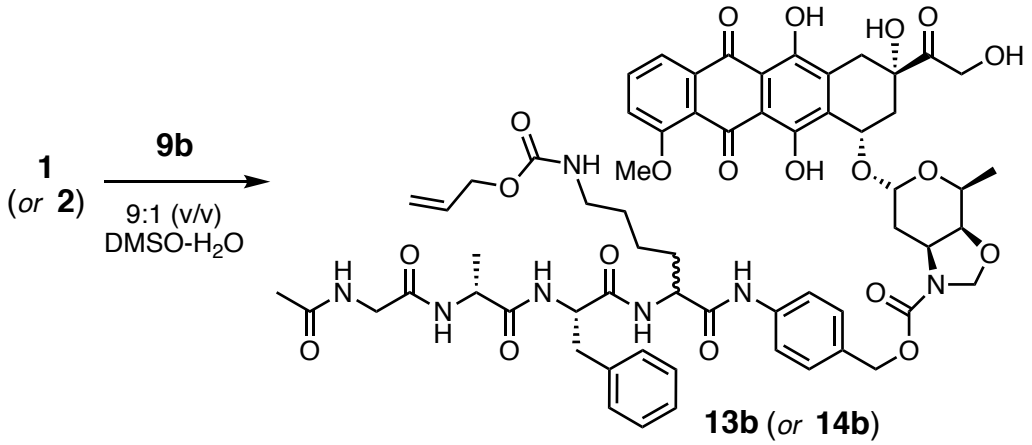

While optically pure *N*-Ac-GaFK(alloc)-PABC-Doxaz has been deprotected using a Tsuji-Trost reaction[8,9] with *tetrakis*(triphenylphosphine)Pd^0, *N*-methylmorpholine and acetic acid to afford **8**, the diasteromeric mixtures **13b** and **14b** were not taken forward. Similar results were nevertheless obtained from the TSL of azide **1** (and **2**) with **9a** (Figure 6.11), which afforded the Cbz-protected peptidyl prodrug of doxaz **13a** (and dox **14a**) also as a mixture of diastereomers. However, no viable deprotection strategy for removal of the Cbz-group at this stage is known to us and neither compound **13a** nor **14a** were not taken forward.

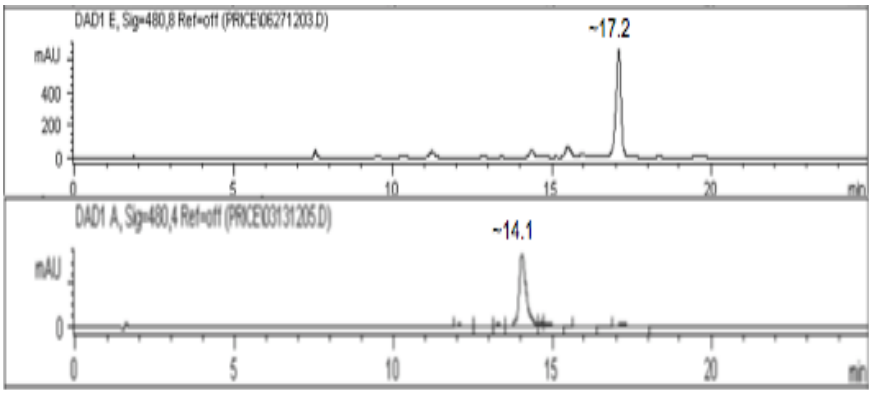

Figure 6.9 Analytical RP-HPLC chromatograms (480 nm) monitoring the conversion of azide **1** (RT ~17.2 min) to anilde **13b** (RT ~14.1 min) using method 1; a description of HPLC methods is provided in section 6.5 under *General Methods*.

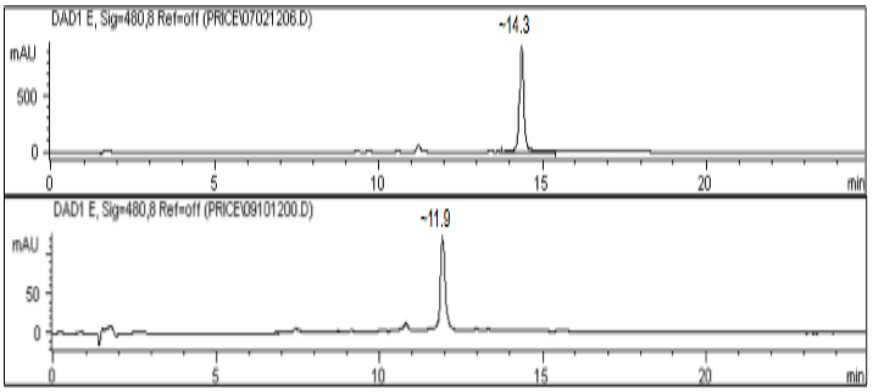

Figure 6.10 Analytical RP-HPLC chromatograms (480 nm) monitoring the conversion of azide **2** (RT ~14.3 min) to anilide **14b** (RT ~11.9 min) using method 1; a description of HPLC methods is provided in section 6.5 under *General Methods*.

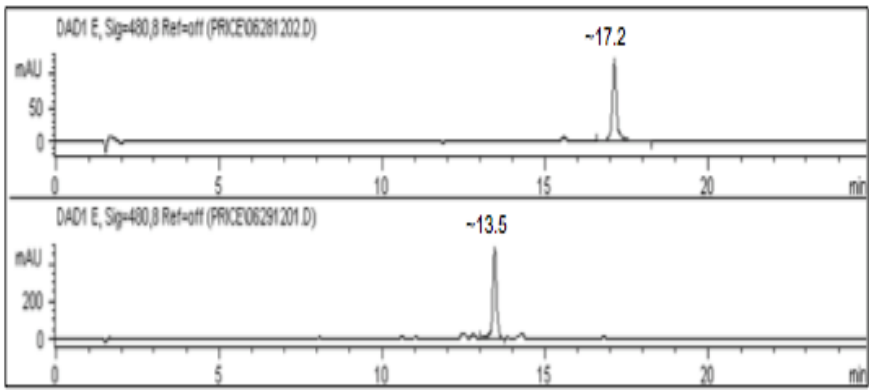

Figure 6.11 Analytical RP-HPLC chromatogram (480 nm) showing the conversion of azide **1** (RT ~17.2 min) to anilide **13a** (RT ~13.5 min) using method 1; a description of HPLC methods is provided in section 6.5 under *General Methods*.

The ^{1}H NMR spectra of compounds **13a**, **13b**, **14a** and **14b** are shown in Figures 6.12−6.15, respectively. As is evident from ^{1}H NMR spectra these compounds, the products obtained following FCC were impure and all were contaminated with the phenolic phosphine oxide co-product of the TSL, which proved exceedingly difficult to remove from the desired materials in its entirty. Radial chromatography failed to completely separate the phosphine oxide from the anthracycline products, and attempts to recrystallize the crude compounds were similarly unsuccesful. Finally, the hydrophobicity of compounds **13** and **14** rendered them highly water-insoluble, which hindered semi-preparative RP-HPLC purification efforts.

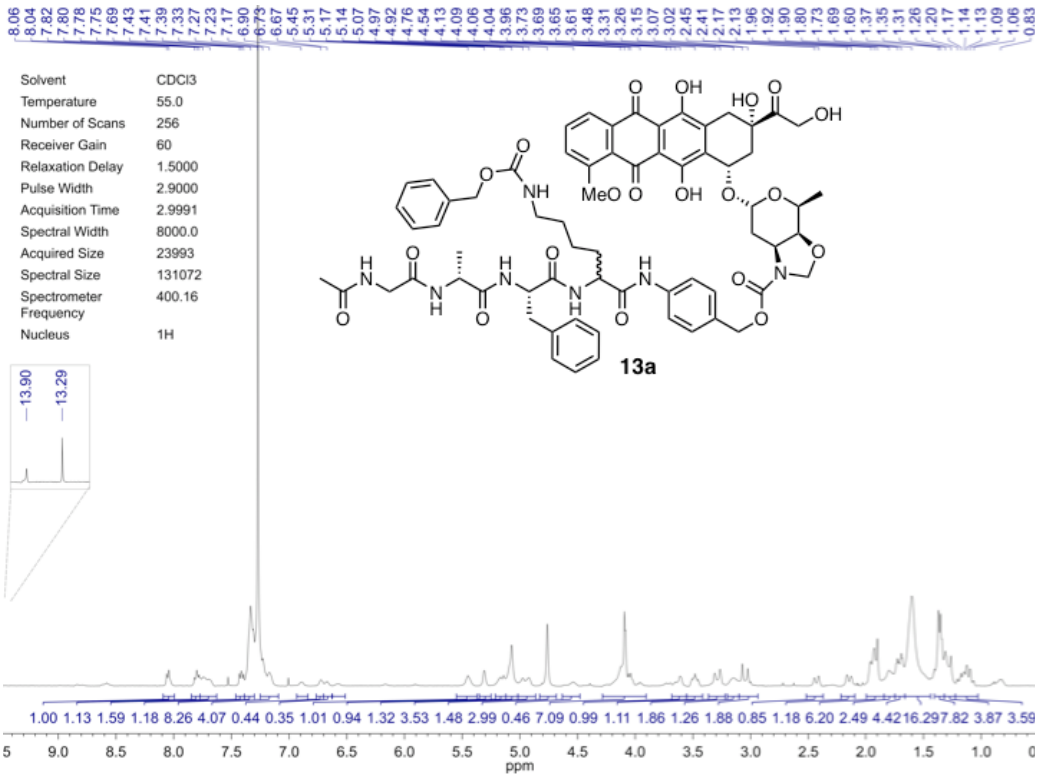

Figure 6.12 ^{1}H NMR spectrum of **13a** in $CDCl_3$ at 55 °C and 400 MHz.

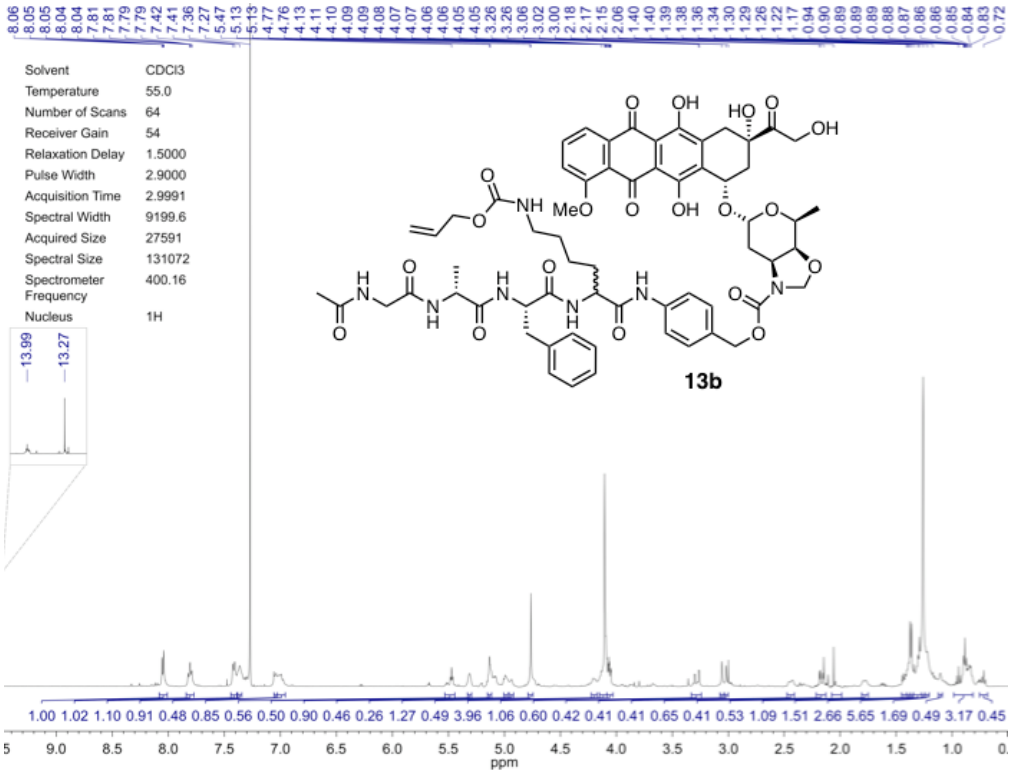

Figure 6.13 ^{1}H NMR spectrum of **13b** in $CDCl_3$ at 55 °C and 400 MHz.

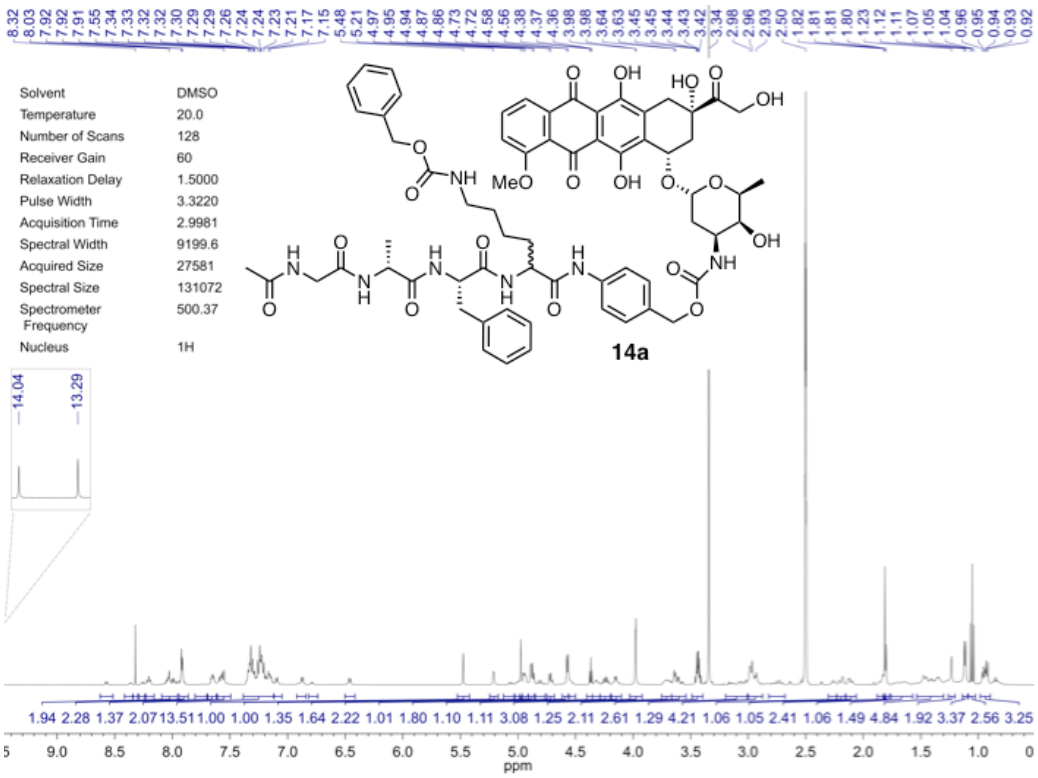

Figure 6.14 ^{1}H NMR spectrum of **14a** in *d6*-DMSO at 500 MHz.

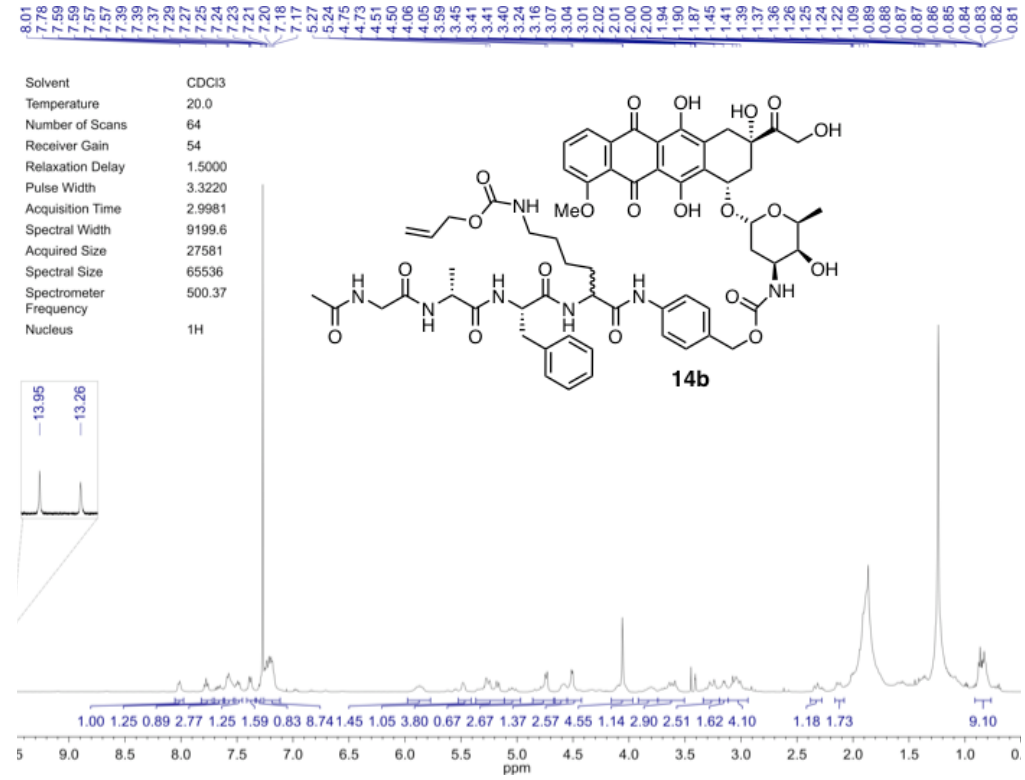

Figure 6.15 ^{1}H NMR spectrum of **14b** in $CDCl_3$ at 500 MHz.

The TSL was also used to prepare *N*-Ac-Gly-DL-Ala-PABC-Doxaz **17** (Scheme 6.6). Combination of azide **1** and phosphine **16** afforded the dipeptidyl prodrug **17** as a mixture of diastereomers, thus confirming the racemic nature of the starting phosphine **16**. An analytical RP-HPLC chromatogram of **17** is shown in Figure 6.16, (the two diastereomers are unresolved), and the ^{1}H NMR spectrum in *d6*-DMSO at 50 °C and 400 MHz is shown in Figure 6.17. As is evident from these figures, purification of compound **17** too was incomplete.

Scheme 6.6 Synthesis of the dipeptidyl prodrug **17** as a mixture of diastereomers via the TSL of azide **1** and racemic peptidyl phosphinyl phenyl ester **16**.

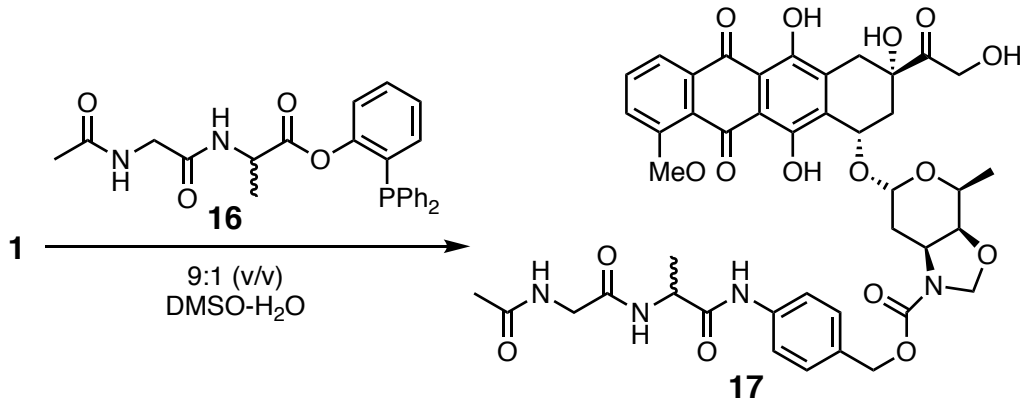

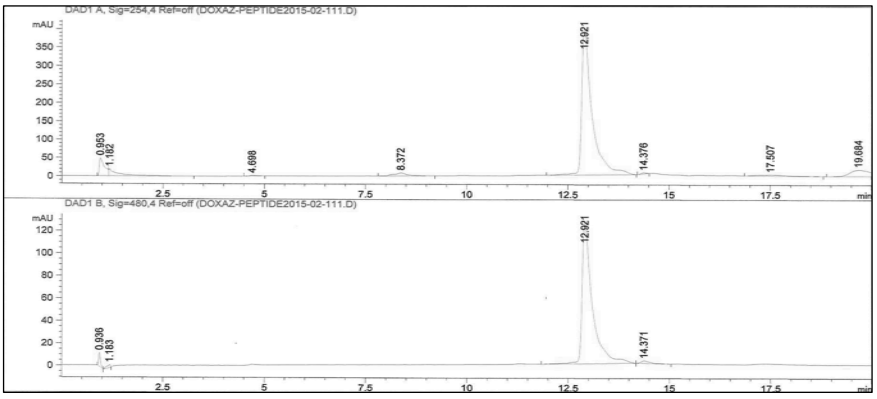

Figure 6.16 Analytical RP-HPLC chromatogram (254 nm and 480 nm) of **17** (R_T ~12.9 min) using method 1; a description of HPLC methods is provided in section 6.5 under *General Methods*.

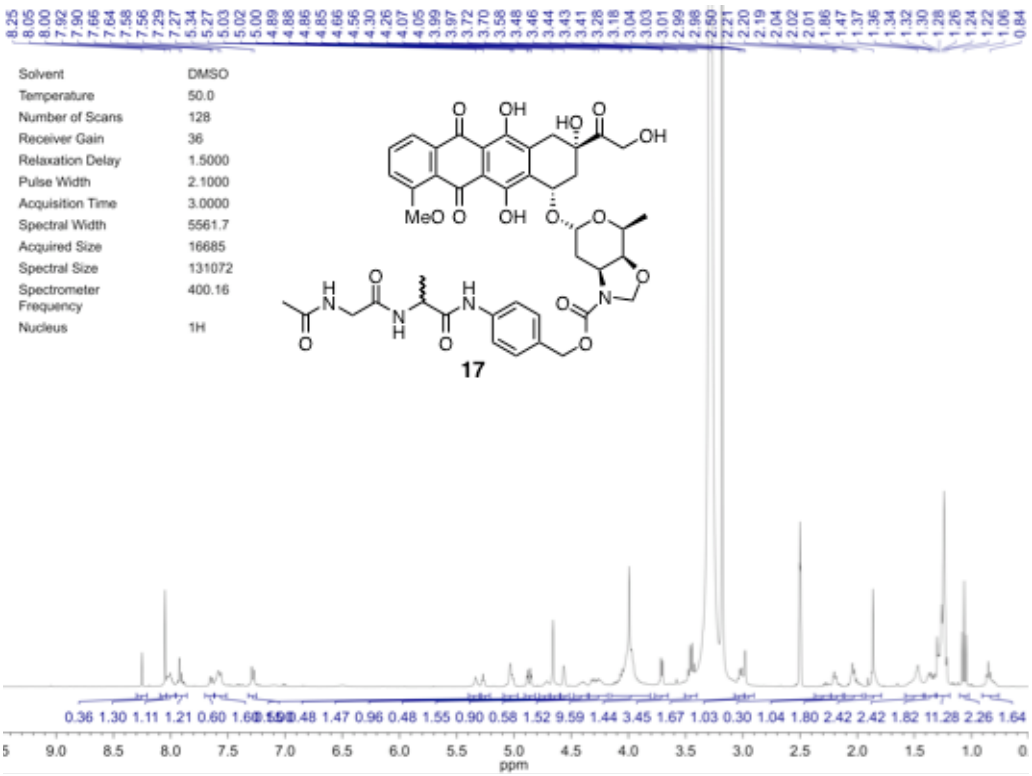

Figure 6.17 ^{1}H NMR spectrum of **17** in *d6*-DMSO at 50 °C and 400 MHz.

Finally, the TSL of azide **1** and phosphine **18** was used to prepare the dipeptidyl prodrug *N*-Cbz-L-Val-Gly-PABC-Doxaz **19** (Scheme 6.7). The RP-HPLC chromatogram shown in Figure 6.18 and UV-vis spectrum of the peak eluting at 9.4 min shown in Figure 6.19 indicate the reaction cleanly afforded the desired anilide **19**. However, the ^{1}H NMR spectrum of the isolated material acquired in $CDCl_3$ at 400 MHz is shown in Figure 6.17 and indicates the **19** obtained was also impure. Once again, the phosphine oxide was present as a major contaminant in the isolated product and attempts to further purify the desired prodrug by preparative TLC were unsuccessful in its removal. The difficulty in removing the phosphine oxide co-product of the TLS remains a substantial limitation to the application of this method for the synthesis of molecules of modest complexity, such as peptidyl prodrugs of the anthracyclines.

Scheme 6.7 Synthesis of the dipeptidyl prodrug **19** via the TSL of azide **1** and peptidyl phosphinyl phenyl ester **18**.

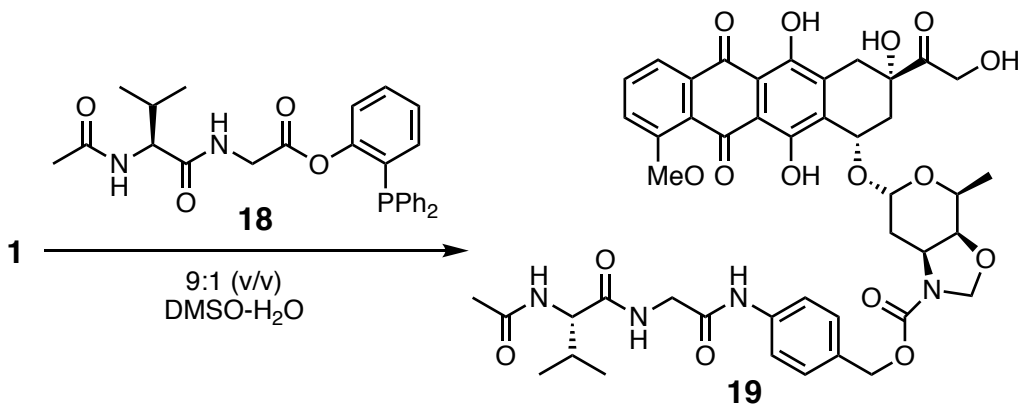

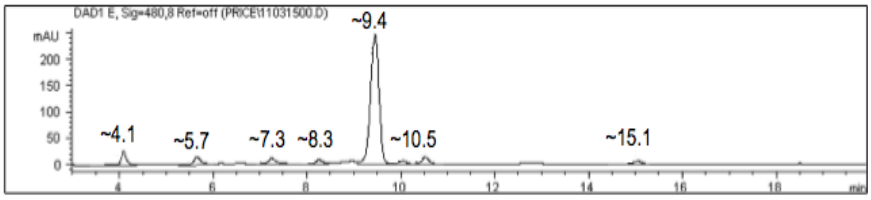

Figure 6.18 Analytical RP-HPLC chromatogram (480 nm) of **19** (R_T ~9.4 min) using method 2; a description of HPLC methods is provided in section 6.5 under *General Methods*.

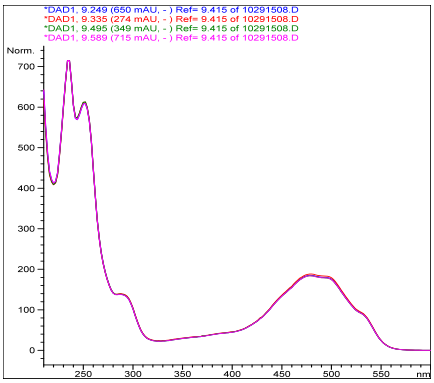

Figure 6.19 UV-vis spectra of **19** (R_T ~9.4 min) acquired at several closely spaced intervals during the above RP-HPLC analysis indicating the peak eluting at 9.4 min is a single compound.

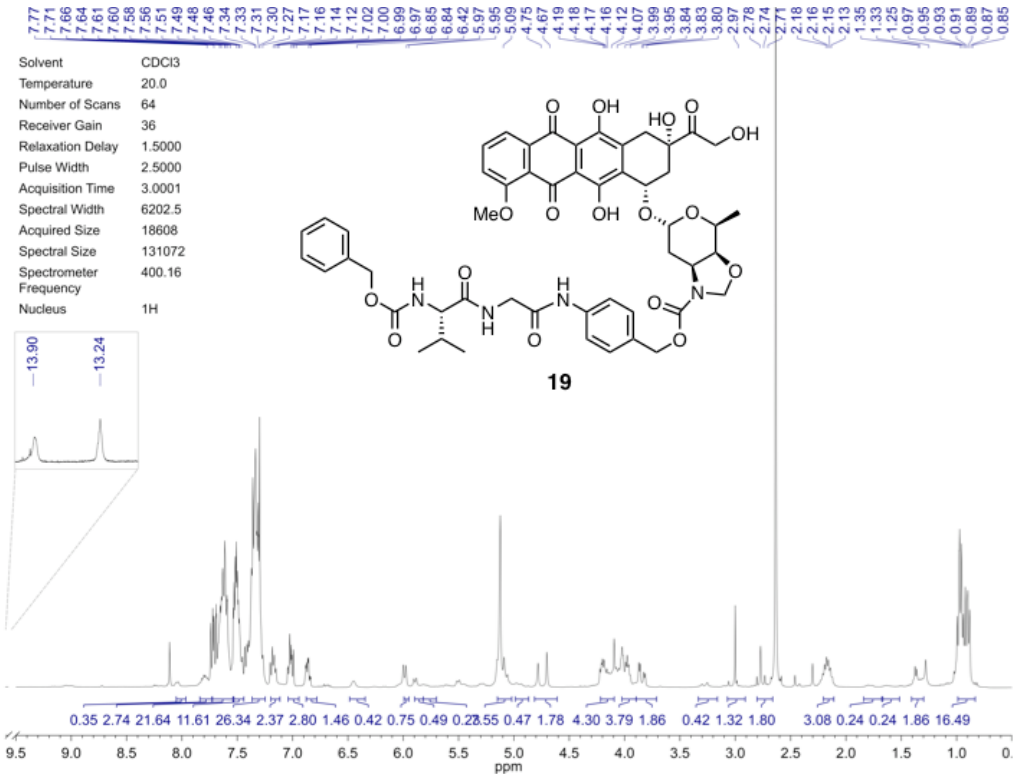

Figure 6.20 ^{1}H NMR spectrum of **19** in $CDCl_3$ at 400 MHz.

6.4 Conclusion

The key "spacer-drug" intermediates **1** and **2** were prepared in excellent purity and good to excellent yield. The TSL of *p*-azidobenzyl anthracycline carbamates **1** and **2** afforded the desired peptidyl prodrugs in all cases, as well. However, difficulties were encountered with the purification of the products, particularly with removal of the phosphine oxide co-product of the TSL, and this prevented isolation of pure materials. Mixtures of diastereomers were obtained in most cases due to the starting phosphines used and this limited our ability to characterize the products both structurally and biochemically.

In retrospect, given the successful application of the TSL methodology in preparation of a PABC-PABC double-spacer model prodrug during the exploratory studies detailed in Chapter 4 of this thesis, more fruitful efforts may have been realized if the cooresponding double-spacer

prodrugs of the anthracyclines would have been prepared. Elongated PABC-PABC double spacer-containing prodrugs are of interest because they have been shown to exhibit improved enzymatic activation kinetics (k_{act} = 2- to 10-fold higher) compared to the analogous single-PABC spacer-containing prodrugs,[10] which conveyed enhanced tumor-growth inhibition and decreased systemic toxicity *in vivo* for a double-PABC spacer-containing prodrug of dox relative to the single-spacer containing analogue.[11] The TSL methodology developed by the author would permit relatively rapid preparation of a small library of optically pure, chiral C-terminal peptidyl prodrugs of doxaz and dox containing the elongated, PABC-PABC double-spacer motif, which would be interesting molecules to examine biochemically.

6.5 Experimental

General Methods. All reactions were performed under an inert atmosphere of dry nitrogen or argon. Clinical samples of doxorubicin hydrochloride formulated with lactose and mannose-excipient were received as a gift from FeRx, Inc. (Aurora, CO). Deuterated NMR solvents were purchased from Cambridge Isotope Laboratories, Inc. (Andover, MA). Reagents were purchased from Sigma Aldrich (St. Louis, MO) and used without further purification unless otherwise noted. EMD glass thin layer chromatography plates (silica gel 60 F_{254}) were used to monitor reactions. Flash column chromatography (FCC)[12] was performed using 60 Å silica gel (37−75 μm, 230−400 mesh) with a $CHCl_3$−MeOH solvent system as eluent. NMR spectra were recorded with either a Varian Inova 500 or 400 MHz spectrometer (Palo Alto, CA) or a Bruker Avance-III 300 MHz spectrometer (Billerica, MA). Chemical shifts are reported in δ values of ppm with internal referencing to the residual solvent peak in ^{1}H and ^{13}C NMR spectra, whose frequencies are given by Gottlieb *et al.*[13] and $^{31}P\{^{1}H\}$ spectra were x-referenced in accordance

with the IUPAC recommendation.[14] Coupling constants are reported as *J*-values in Hertz (Hz) with resonance multiplicities abbreviated as follows: s = singlet, d = doublet, t = triplet, q = quartet, p = pentet, sext = sextet, sept = septet, h = heptet, m = multiplet, br = broadened. NMR data processing and plotting was performed using MestReNova NMR software v12.0.1 (Mestrelab Research, Santiago de Compostela, Spain). Electrospray mass spectra were obtained with a Perkin-Elmer Sciex API III (Norwalk, CT), equipped with a positive ion-spray source, at atmospheric pressure. IR spectra were obtained as thin-films on NaCl using a Nicolet Avatar 320 spectrophotometer, DTGS detector and EZ OMNIC software. UV-vis spectra were recorded with a Hewlett-Packard Agilent 8452A diode array spectrophotometer interfaced to an Agilent data system. Analytical RP-HPLC was performed on Agilent 1050/1100 hybrid instruments equipped with a 1050 series pump and autoinjector and a 1100 series UV-vis diode array detector (Santa Clara, CA). Sample solutions (5 μL) were injected at ambient temperature onto (method 1) an Agilent Zorbax octadecylsilyl (C18) reverse phase column (4.6 mm i.d. x 150 mm, 5 μm) eluted at 1 mL/min with an MeCN−20 mM sodium phosphate buffer (pH 4.6), containing 0.02% sodium azide, solvent system; or, (method 2) an Agilent Poroshell 300SB-C18 reverse phase column (2.1 mm i.d. x 75 mm, 5 μm) eluted at 0.75 mL/min with an MeCN−0.1% aq. TFA solvent system. The gradient elution methods were programmed in terms of %-aq. buffer as follows: (method 1) 0 min (75%), 2.5 min (50%), 5 min (40%), 25 min (20%), 30 min (75%); and, (method 2) 0-2 min (75%), 4 min (50%), 8 min (50%), 10 min (75%). RP-HPLC analyses monitored absorbance at 254, 280 and 480 nm. Retention times (R_T) are reported in min along with other compound characterization data below. Yields of all anthracycline products were determined by optical density at 480 nm using a molar extinction coefficient of 11,500 M^{-1} cm^{-1} in 3:1 DMSO−H_2O (v/v).

Doxorubicin Free Base. Lyophilized pellets of expired clinical samples of doxorubicin hydrochloride (20−50 mg) containing 100−250 mg of lactose monohydrate (Bedford Laboratories, Bedford, OH) were dissolved in MeOH to a final concentration of 2 mg/mL and combined in a separatory funnel. The MeOH solution was diluted with 100 mM sodium phosphate buffer (pH 8.5) for a final concentration of 0.4 mg/mL dox as a mixture of precipitated and solubilized material. The free base of dox was extracted from the solution by two washes with equal volumes of DCM, leaving almost no red color in the aqueous fraction. The organic phase was dried over anh. Na_2SO_4, decanted into a dry flask and concentrated under reduced pressure. The residual solid was dried thoroughly under high vacuum (10^{-2} Torr) for at least 3 h to yield pure dox free base (98%) as a red solid.

Doxazolidine (4). Dox free base was dissolved to a final concentration of 5−10 mg/mL in $CDCl_3$ and 1.1−2.0 equiv of prilled paraformaldehyde was added. The heterogeneous mixture was stirred in the dark at ambient temperature and the reaction was monitored by ^{1}H NMR. Complete consumption of dox occurred after 2−3 days as evidenced by the disappearance of the aromatic triplet pattern for the proton at the 2-position (δ 7.81 ppm). Formation of doxaz (and doxf) was evident by the appearance of a new aromatic triplet at δ 7.78 ppm (and δ 7.70 ppm). Additionally, the doxaz−methylene AX pattern appeared at δ 4.31 and 4.68 ppm and that of doxf appeared at δ 4.21 and 4.73 ppm. As doxaz will react with an additional equiv of CH_2O to form doxf, the reaction time and amount of paraformaldehyde added determines the doxaz/doxf ratio. Once complete, the reaction mixture was filtered through a fine glass frit and the filtrate concentrated under reduced pressure. The doxaz/doxf mixture was used without further purification, since doxf readily hydrolyzes to produces 2 equiv of doxaz.

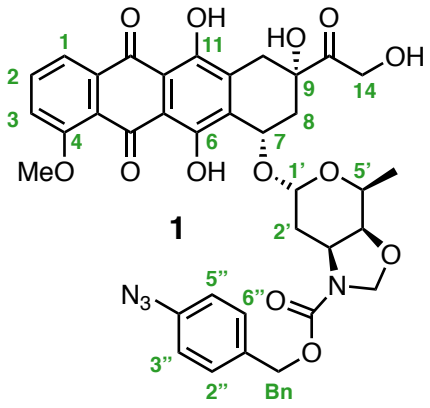

1

***p*-Azidobenzyl doxazolidyl carbamate (1).** To a 0.40 M NMP-solution of the mixed *p*-nitrophenyl carbonate **18** (141 mg, 450 μmol, 5.0 equiv) was added a 0.18 M NMP-solution of doxazolidine (100 mg, 180 μmol, 1.0 equiv) via syringe. The reaction was heated in the dark to 40 °C using a water-bath and monitored by TLC and RP-HPLC. After complete consumption of **18** was observed (24-36 h), the reaction mixture was concentrated to dryness by high-vacuum centrifugation. The resulting red solid was dissolved in DCM containing a small volume of methanol and washed with cold 20 mM sodium phosphate-buffer (pH 4.8) until the aqueous layer no longer appeared red, then cold sat. $NaHCO_3$ until the aqueous layer no longer appeared yellow and then once with brine. The organic phase was dried over anh. Na_2SO_4 and concentrated under reduced pressure at ambient temperature to afford the crude product. The crude material was dissolved in DCM and passed over a short plug of silica gel eluting with 9:1:0.1 $CHCl_3$−MeOH−AcOH (v/v/v). The collected material was concentrated under reduced pressure and dissolved in a minimal volume of warm MeCN, which was stored at 4 °C until a red precipitate formed (~48 h), which was dissolved in a minimal volume of warm MeCN and stored at 4 °C until a red precipitate formed (~48 h). Isolation of the precipitate by centrifugation afforded the desired azide **1** (44.6 mg, 68%) as a red solid: R_f = 0.28 (98:2:0.5 $CHCl_3$−MeOH−AcOH); RT (method 1) = 17.2 min IR (cm^{-1}): 3479, 2926, 2116.5, 1766 and

1708. ^{1}H NMR at 40 °C (400 MHz, $CDCl_3$) δ 13.97 (s, 1H, **6-O*H*** or **11-O*H***), 13.26 (s, 1H, **6-O*H*** or **11-O*H***), 8.06 (d, 1H, *J* = 7.7 Hz, **1**), 7.80 (t, 1H, *J* = 8.1 Hz, **2**), 7.41 (d, 1H, *J* = 8.6 Hz, **3**), 7.37 (d, 2H, *J* = 8.4 Hz, **PABC-2'',6''**), 7.03 (d, 2H, *J* = 7.7 Hz, **PABC-3'',5''**), 5.47 (t, 1H, *J* = 5.4 Hz, **1'**), 5.32 (br. s, 1H, 7), 5.14 (s, 2H, Bn), 5.03 (br. s, 1H, 3'-NCH_2O-4'), 4.96 (br. s, 1H, 3'-NCH_2O-4'), 4.76 (d, 2H, *J* = 5.0 Hz, **14**), 4.71 (s, 1H, **9-O*H***), 4.22 – 4.07 (m, 2H, **5'** and **4'**), 4.10 (s, 3H, **4-OMe**), 4.05 (dd, 1H, *J* = 6.7, 2.0 Hz, **3'**), 3.30 (dd, 1H, *J* = 18.9, 1.6 Hz, **10a**), 3.07 (d, 1H, *J* = 18.9 Hz, **10b**) 2.98 (t, 1H, *J* = 5.0 Hz, **14-O*H***), 2.46 (d, 1H, *J* = 14.7 Hz, **8a**), 2.17 (dd, 1H, *J* = 14.7, 3.9 Hz, **8b**), 1.78 (dt, 2H, *J* = 14.8, 4.9 Hz, **2'**), 1.37 ppm (d, 3H, *J* = 6.5 Hz, **5'-Me**); assignments made using homonuclear gCOSY spectrum. ^{13}C NMR at 40 °C (75 MHz, $CDCl_3$) δ 214.4 (**13**), 187.0 (**12**), 186.7 (**5**), 161.1 (**4**), 156.2 (**11**),155.5 (**6**), 153.2 (**Bn-CO**), 140.7 (**PABC-1''**), 135.52 (**2**), 135.5 (**12a**), 133.57 (**10a**), 133.55 (**6a**), 133.1 (**PABC-4''**), 129.8 (**PABC-2'',6''**), 120.5 (**4a**), 119.7 (**3**), 119.0 (**PABC-3'',5''**), 118.4 (**1**), 111.39 (**11a**), 111.38 (**5a**), 99.9 (**1'**), 79.0 (**3'-N*C*H$_2$O-4'**), 77.6 (**4'**), 73.3 (**9**), 69.2 (**7**), 66.6 (**Bn**), 65.6 (**14**), 65.3 (**5'**), 56.6 (**4-OMe**), 50.3 (**3'**), 35.9 (**8**), 34.0 (**10**), 29.5 (**2'**), 16.2 ppm (**5'-Me**); assignments made using gHSQC and gHMBC spectra. HRMS (ESI-TOF) *m/z*: $[M+Na]^+$ calcd for $C_{36}H_{34}N_4NaO_{13}$ 753.2020; found 753.2053.

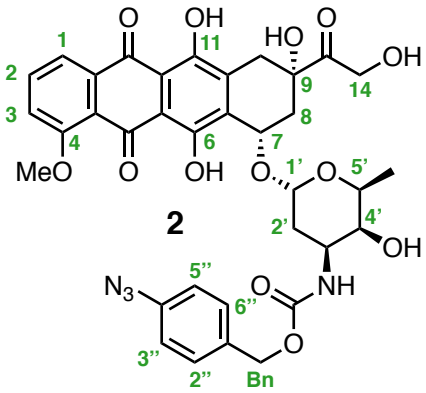

2

p*-Azidobenzyl doxorubicyl carbamate (2).** To a 0.35 M THF-solution of the mixed *p*-nitrophenyl carbonate **18** (108.4 mg, 345 μmol, 1.0 equiv) was added a 0.18 M THF-solution of doxorubicin free-base (191.7 mg, 345 μmol, 1.0 equiv) via syringe. The reaction was stirred at ambient temperature in the dark and monitored by TLC and RP-HPLC. After complete consumption of **18** was observed (~2 h), the reaction mixture was concentrated to dryness and dissolved in DCM. The organic phase was washed with cold 20 mM sodium phosphate-buffer (pH 4.8) until the aqueous layer no longer appeared red, then cold sat. $NaHCO_3$ until the aqueous layer no longer appeared yellow, then once with brine, dried over anh. Na_2SO_4 and concentrated under reduced pressure at ambient temperature to afford the crude product. The crude material was dissolved in a minimal volume of warm MeCN, which was stored at 4 °C until a red precipitate formed (~48 h). Isolation of the precipitate by centrifugation afforded the desired azide **2** (248 mg, 94%) as a red solid: R_f = 0.23 (98:2:0.5 $CHCl_3$–MeOH–AcOH); RT (method 1) = 14.3 min; ^{1}H NMR (500 MHz, $CDCl_3$) δ 13.98 (s, 1H, **6-O*H or **11-O*H***), 13.26 (s, 1H, **6-O*H*** or **11-O*H***), 8.05 (d, 1H, *J* = 7.5 Hz, **1**), 7.80 (t, 1H, *J* = 8.1 Hz, **2**), 7.40 (d, 1H, *J* = 8.4 Hz, **3**), 7.30 (d, 2H, *J* = 8.1 Hz, **PABC-2'',6''**), 6.98 (d, 2H, *J* = 8.2 Hz, **PABC-3'',5''**), 5.51 (d, 1H, *J* = 3.8 Hz, **1'**), 5.29 (br. s, 1H, **7**), 5.14 (d, 1H, **3'-N*H***), 5.01 and 4.98 (AB-pattern, 2H, *J* = 12.4 Hz, **Bn**), 4.77 (br. s, 2H, **14**), 4.53 (s, 1H, **9-O*H***), 4.17 – 4.11 (m, 2H, **5'** and **4'**), 4.09 (s, 3H, **4-OMe**), 3.87 (br. s, 1H, **3'**), 3.67 (br. s, 1H, **14-O*H***), 3.28 (dd, 1H, *J* = 18.8, 1.5 Hz, **10a**), 3.02

(m, 2H, **10b** and **14-O*H***), 2.34 (d, 1H, *J* = 14.7 Hz, **8a**), 2.18 (dd, 1H, *J* = 14.7, 3.9 Hz, **8b**), 1.89 (dd, 1H, *J* = 13.6, 4.9 Hz, **2'a**), 1.77 (td, 1H, *J* = 13.3, 4.1 Hz, **2'b**), 1.30 ppm (d, 3H, *J* = 6.6 Hz, **5'-Me**); assignments made using homonuclear gCOSY spectrum. ^{13}C NMR at 40 °C (75 MHz, $CDCl_3$) δ 214.4 (**13**), 187.0 (**12**), 186.7 (**5**), 161.1 (**4**), 156.2 (**11**),155.5 (**6**), 153.2 (**Bn-CO**), 140.7 (**PABC-1''**), 135.52 (**2**), 135.5 (**12a**), 133.57 (**10a**), 133.55 (**6a**), 133.1 (**PABC-4''**), 129.8 (**PABC-2'',6''**), 120.5 (**4a**), 119.7 (**3**), 119.0 (**PABC-3'',5''**), 118.4 (**1**), 111.39 (**11a**), 111.38 (**5a**), 99.9 (**1'**), 79.0 (**3'-N*C*H$_2$O-4'**), 77.6 (**4'**), 73.3 (**9**), 69.2 (**7**), 66.6 (**Bn**), 65.6 (**14**), 65.3 (**5'**), 56.6 (**4-OMe**), 50.3 (**3'**), 35.9 (**8**), 34.0 (**10**), 29.5 (**2'**), 16.2 ppm (**5'-Me**). HRMS (ESI-TOF) *m/z*: $[M+Na]^+$ calcd for $C_{35}H_{34}N_4NaO_{13}$ 741.2020; found 741.2049.

General Procedure for the Traceless Staudinger Ligation of Anthracycline Azides 1 and 2. Preparation of Compounds 13a, 13b, 14a, 14b, 17 and 19. To a stirred 40 mM solution of phosphine (1.1 equiv) was added an equal volume of azide **(**1.0 equiv) in 9:1 DMSO−H_2O (v/v). The reaction was stirred at ambient temperature and monitored by TLC and RP-HPLC. After complete consumption of the azide starting material was observed, the reaction mixture was concentrated to dryness by high-vacuum centrifugation. The resulting red solid was dissolved in methanolic $CHCl_3$ and passed over a short plug of silica gel eluting with a gradient of $CHCl_3$−MeOH (1:0 to 9:1 v/v) to afford the desired anilide as a thin red film in 50-80% yield.

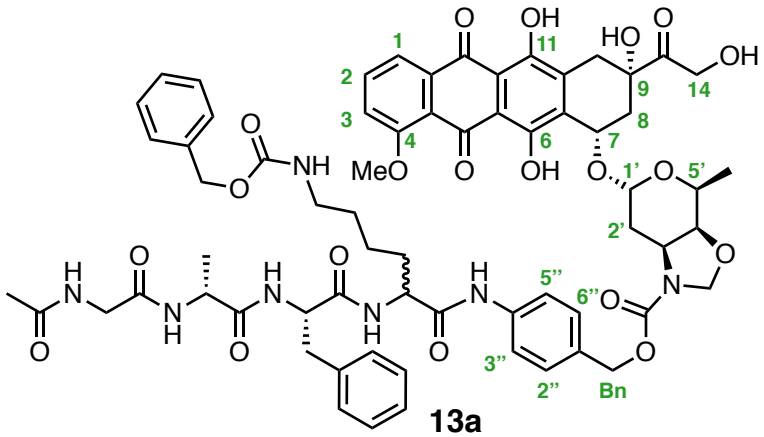

13a

N*-Acetyl-Gly-D-Ala-L-Phe-DL-Lys(Cbz)-PABC-Doxaz (13a).** 40.6 mg (52%) as a red solid: R_f = 0.16 (95:5:0.5 $CHCl_3$−MeOH−AcOH v/v/v); RT = 13.5 min (method 1); ^{1}H NMR at 55 °C (400 MHz, $CDCl_3$) δ 13.90 (s, 1H, **6-O*H or **11-O*H***), 13.29 (s, 1H, **6-O*H*** or **11-O*H***), 8.05 (br. d, 1H, *J* = 8 Hz, **1**), 7.80 (br. t, 1H, *J* = 8 Hz, **2**), 7.77 − 7.63 (m, 2H, **PABC-3,5**), 7.45 − 7.36 (m, 1H **3**), 7.35 – 7.06 (m, 12H, **Cbz-Ar**, **Phe-Ar**, **PABA-2,6**),5.45 (br. s, 1H, **1′**), 5.31 (s, 1H, **7**), 5.22 − 5.11 (m, 2H, **3′-NC*H*$_2$O-4′**), 512 − 5.02 (m, 4H, **PABC-Bn** and **Cbz-Bn**), 5.01 − 4.86 (m, 1H, **Phe-α**), 4.83 − 4.69 (m, 3H, **14** and **ala-α**), 4.54 (br. s, 1H, **9-OH**), 4.29 − 3.90 (m, 6H, **3′**, **4′**, **5′** and **4-OMe**), 3.73 − 3.61 (m, 1H, **Lys-α**), 3.55 − 3.40 (m, 2H, **Gly-α**), 3.29 (d, 1H, *J* = 18.5 Hz, **10a**), 3.15 (br. s, 2H, **Lys-ε**), 3.05 (d, 1H, *J* = 18.5 Hz, **10b**), 2.43 (d, 1H, *J* = 14.5 Hz, **8a**), 2.15 (d, 1H, *J* = 14.5 Hz, **8b**), 1.96 − 1.91 (m, 2H, **Lys-β**), 1.90 (s, 3H, ***N*-Ac**), 1.96 − 1.85 (m, 2H, **Lys-δ**), 1.75 − 1.66 (m, 2H, **2′**), 1.60 − 1.45 (m, 2H, **Lys-γ**), 1.41 − 1.23 (m, 3H, **5′-Me**), 1.22 − 1.02 ppm (m, 3H, **ala-Me**); assignments made using homonuclear (^{1}H, ^{1}H) gCOSY spectrum. HRMS (ESI-TOF) *m/z*: $[M+Na]^+$ calcd for $C_{66}H_{73}N_7NaO_{20}$ 1306.4808; found 1306.4813.

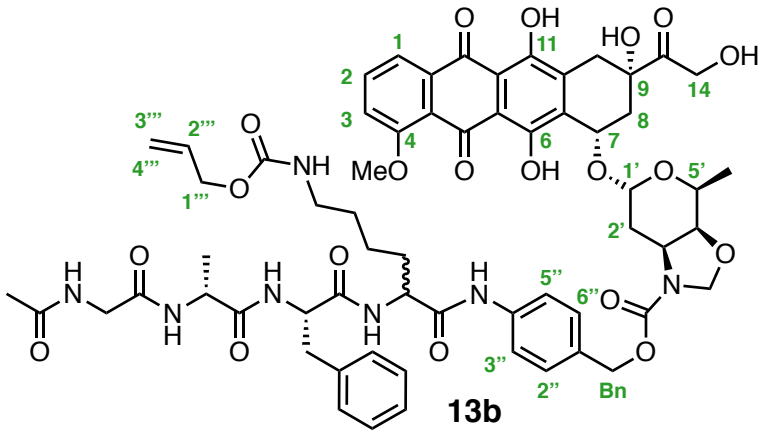

13b

N*-Acetyl-Gly-D-Ala-L-Phe-DL-Lys(alloc)-PABC-Doxaz (13b).** 44.5 mg (60%) as a red solid: R_f = 0.14 (95:5:0.5 $CHCl_3$−MeOH−AcOH v/v/v); RT = 14.1 min (method 1); ^{1}H NMR at 55 °C (400 MHz, $CDCl_3$) δ 13.99 (s, 1H, **6-O*H or **11-O*H***), 13.27 (s, 1H, **6-O*H*** or **11-O*H***), 7.99 ppm (d, 1H, *J* = 8 Hz, **1**), 7.74 (t, 1H, *J* = 8 Hz, **2**), 7.56 (d, 2H, *J* = 8 Hz, **3″**), 7.37 (d, 1H, *J* = 8 Hz, **3**), 7.26 (d, 2H, *J* = 8 Hz, **2″**), 7.25 − 7.20 (m, 2H, **Phe-*m*-Ph**), 7.18 − 7.16 (m, 2H, **Phe-*o*-Ph**), 7.15 − 7.10 (m, 1H, **Phe-*p*-Ph**), 5.85 (ddt, 1H *J* = 16, 10, 5 Hz, **2‴**), 5.39 (t, 1H, *J* = 5 Hz, **1′**), 5.26 (br. s, 1H, **7**), 5.23 (d, 1H, *J* = 18 Hz, **4‴**), 5.14 (d, 1H, *J* = 10 Hz, **3‴**), 5.06 and 5.8 (br. AB pattern, 2H, *J* = 11 Hz, **Bn**), 4.90 and 4.96 (br. AX pattern, 2H, *J* = 4 Hz, **3′-NC*H*$_2$O-4′**), 4.70 (s, 2H, **14**), 4.55 (dd, 1H, *J* = 9, 6 Hz, **Phe- α**), 4.49 (br. s, 2H, **1‴**), 4.45 − 4.35 (m, 1H, **Lys-α**), 4.08 − 4.12 (m, 2H, **4′** and **5′**), 4.10 − 4.05 (m, 1H, **ala-α**), 4.03 (s, 3H, **4-OMe**), 3.98 − 3.88 (m, 1H, **3′**), 3.23 (d, 1H, *J* = 18 Hz, **10a**), 3.23 − 3.15 (m, 1H, **Phe-β**), 3.09 − 3.00 (m, 2H, **Lys-ε**), 3.01 (d, 1H, *J* = 18 Hz, **10b**), 2.98 − 2. 90 (m, 1H, *J* = 9, 5 Hz, **Phe-β**), 2.41 (d, 1H, *J* = 14 Hz, **8b**), 2.25 − 2.15 (m, 1H, **2′**), 2.1 (d, 1H, *J* = 14 Hz, **8a**), 1.88 (s, 3H, **Ac**), 1.87 − 1.80 (m, 1H, **Lys-β**), 1.79 − 1.74 (m, 1H, **2′**), 1.73 − 1.70 (m, 1H, **Lys-β**), 1.50 − 1.40 (m, 2H, **Lys-δ**), 1.38 − 1.32 (m, 2H, **Lys-γ**), 1.31 −1.28 (m, 3H, **5′-Me**), 1.20 − 1.15 ppm (d, 3H, **ala-Me**); assignments made using homonuclear (^{1}H, ^{1}H) gCOSY spectrum. HRMS (ESI-TOF) *m/z*: $[M+Na]^+$ calcd for $C_{62}H_{71}N_7NaO_{20}$ 1256.4652; found 1256.4659.

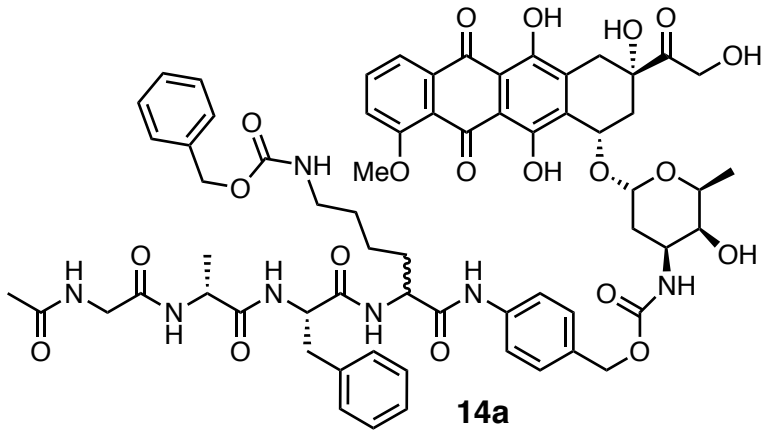

14a

***N*-Acetyl-Gly-D-Ala-L-Phe-DL-Lys(Cbz)-PABC-Dox (14a).** 40.2 mg (64%) as a red solid: R_f = 0.21 (92:8:0.5 $CHCl_3$−MeOH−AcOH v/v/v); RT = 12.8 min (method 1); HRMS (ESI-TOF) *m/z*: $[M+Na]^+$ calcd for $C_{65}H_{73}N_7NaO_{20}$ 1294.4803; found 1294.4817.

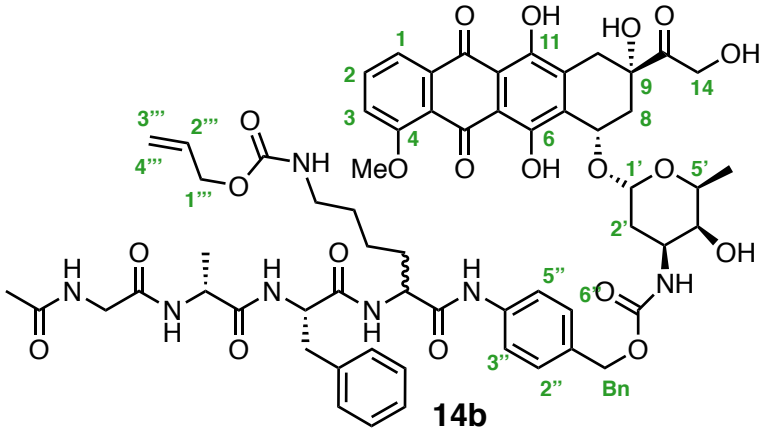

14b

N*-Acetyl-Gly-D-Ala-L-Phe-DL-Lys(alloc)-PABC-Dox (14b).** 41.6 mg (68%) as a red solid: R_f = 0.18 (92:8:0.5 $CHCl_3$−MeOH−AcOH v/v/v); RT = 11.9 min (method 1); ^{1}H NMR (500 MHz, $CDCl_3$) δ 13.95 (s, 1H, **6-O*H or **11-O*H***), 13.26 (s, 1H, **6-O*H*** or **11-O*H***), 8.02 (br. d, 1H, *J* = 8 Hz, **1**), 7.78 (br. t, 1H, *J* = 8 Hz, **2**), 7.70 − 7.62 (m, 1H, **Phe-N*H***), 7.58 (br. d, 2H, *J* = 8.5 Hz, **PABC**), 7.56 − 7.52 (m, 1H, **Lys-N$^{\alpha}$*H***), 7.51 − 7.45 (m, 1H, **ala-N*H***), 7.38 (br. d, 2H, *J* = 8 Hz, **3**), 7.33 − 7.28 (m, 1H, **Gly-N*H***), 7.26 − 7.12 (m, 8H, **Phe-Ar, PABC, Lys-N$^{\varepsilon}$*H***), 5.98 −

5.76 (br. m, 1H, **3‴**), 5.48 (br. S, 1H, **1′**), 5.39 − 5.28 (m, 1H, **7**), 5.28 − 5.12 (m, 2H, **2‴**), 5.08 − 4.95 (m, 2H, **Bn**), 4.86 − 4.76 (m, 2H,**14**), 4.74 − 4.69 (m, 2H, **1‴**), 4.63 − 4.54 (m, 1H, **Phe−α**), 4.51 − 4.10 (m, 1H, **Lys-α** and **ala-α**), 4.16 − 4.07 (m, 2H, **5′** and **4′**), 4.06 (s, 3H, **4-OMe**), 3.91 − 3.74 (m, 1H, **3′**), 3.73 − 3.50 (m, 2H, **Gly-α**), 3.46 − 3.39 (m, 1H, **3′-N*H***), 3.26 (br. d, 1H, *J* = 20 Hz, **10a**), 3.19 − 3.11 (m, 2H, **Lys-ε**), 3.10 − 2.96 (m, 4H, **10b, 4′-O*H*** and **Phe-β**), 2.36 − 2.28 (m, 1H, **8a**), 2.16 − 2.06 (m, 1H, **8b**), 1.87 (s, 3H, **Ac**), 1.65 − 1.46 (m, 4H, **Lys-β,δ**), 1.44 − 1.32 (m, 4H, **Lys-γ** and **2′**), 1.27 − 1.25 (br. m, 3H, **5′-Me**), 1.23 − 1.21 ppm (br. m, 3H, **ala-Me**); assignments made using homonuclear (^{1}H, ^{1}H) gCOSY spectrum. HRMS (ESI-TOF) *m/z*: $[M+Na]^+$ calcd for $C_{61}H_{71}N_7NaO_{20}$ 1244.4652; found 1244.4648.

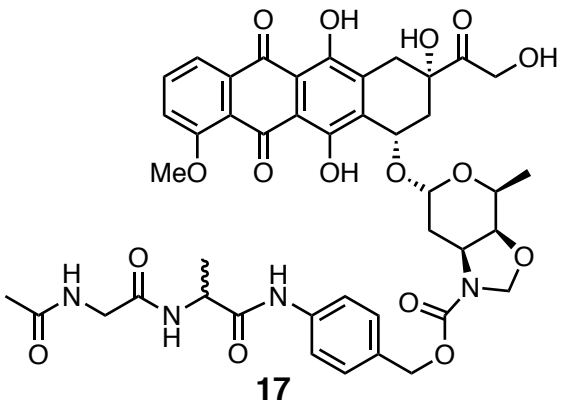

17

***N*-Ac-Gly-DL-Ala-PABC-Doxaz (17).** 28.7 mg (70%) as a red solid: R_f = 0.11 (98:2:0.5 $CHCl_3$−MeOH−AcOH); RT = 12.9 min (method 1); LCMS (ESI) *m/z*: $[M+H]^+$ calcd for $C_{43}H_{47}N_4O_{16}$ 875.30; found 875.30.

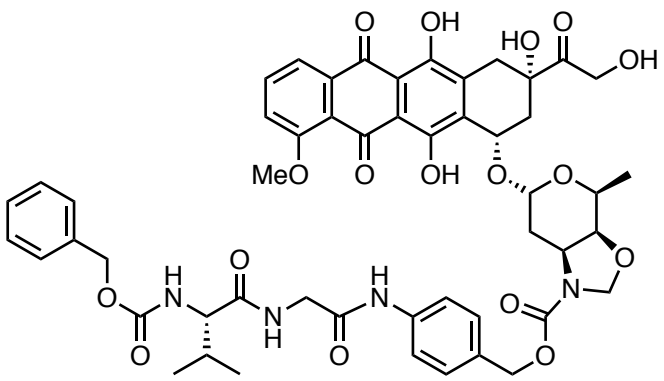

19

***N*-Cbz-L-Val-Gly-PABC-Doxaz (19).** 31.2 mg (81%) as a red solid: R_f = 0.12 (98:2:0.5 $CHCl_3$−MeOH−AcOH); RT = 9.4 min (method 2); LCMS (ESI) *m/z*: $[M+H]^+$ calcd for $C_{51}H_{55}N_4O_{17}$ 995.36; found 995.36.

6.6 References

1. Saxon, E.; Armstrong, J. I.; Bertozzi, C. R. " A Traceless Staudinger Ligation for the Chemoselective Synthesis of Amide Bonds" *Org. Lett.* **2000**, *2*, 2141−2143.

2. Post, G. C.; Barthel, B. L.; Burkhart, D. J.; Hagadorn, J. R.; Koch, T. H. "Doxazolidine, a proposed active metabolite of doxorubicin that cross-links DNA" *J. Med. Chem*. **2005**, *48*, 7648−7657.

3. Fenick, D. J.; Taatjes, D. J.; Koch, T. H. "Doxoform and Daunoform: Anthracycline-Formaldehyde Conjugates Toxic to Resistant Tumor Cells" *J. Med. Chem.* **1997**, *40*, 2452–2461.

4. Barthel, B. L.; Rudnicki, D. L.; Kirby, T. P.; Colvin, S. M.; Burkhart, D. J.; Koch, T. H. "Synthesis and Biological Characterization of Protease-Activated Prodrugs of Doxazolidine" *J. Med. Chem*. **2012**, *55*, 6595–6607.

5. The synthesis of *p*-azidobenzyl 4'-nitrophenyl carbonate **6** is described in Chapter 4 of this thesis and followed a scaled procedure of Griffin *et al.* (ref 7)

6. Griffin, R. J.; Evers, E.; Davison, R.; Gibson, A. E.; Layton, D.; Irwin, W. J. "The 4-Azidobenzyloxycarbonyl Function; Application as a Novel Protecting Group and Potential Prodrug Modification for Amines" *J. Chem. Soc., Perkin Trans. 1*. **1996**, 1205−1211.

7. van Brakel, R.; Vulders, R. C. M.; Bokdam, R. J.; Grüll, H.; Robillard, M. S. "A Doxorubicin Prodrug Activated By the Staudinger Reaction" *Bioconjugate Chem.* **2008**, *19*, 714−718.

8. Trost, B. M.; Verhoeven, T. R., in *Comprehensive Organometallic Chemistry*, Wilkenson, G.; Stone, F. G. A.; Abel, E. W., Eds.; Pergamon: Ocford, (1982); Vol. 8, p. 799.

9. Godleski, S. A., in *Comprehensive Organic Synthesis*, Trost, B. M.; Flemming, I., Eds.; Pergamon: Oxford, (1991); Vol. 4, p. 585.

10. de Groot, F. H.; Loos, W. J.; Koekkoek, R.; van Berkom, L. W. A.; Busscher, G. F.; Seelen, A. E.; Albrecht, C.; de Bruijn, P.; Scheeren, H. W. "Elongated Multiple Electronic Cascade and Cyclization Spacer Systems in Activatible Anticancer Prodrugs for Enhanced Drug Release" *J. Org. Chem.* **2001**, *66*, 8815−8830.

11. Devy, L.; de Groot, F. H. M.; Blacher, S.; Hajitou, A.; Beusker, P.; Scheeren, W.; Foldart, J.-M.; Noel, A. "Plasmin-activated Doxorubicin Prodrugs Containing a Spacer Reduce Tumor Growth and Angiogenesis Without Systemic Toxicity" *FASEB J*. **2004**, *18*, 565−567.

12. Still, C. W.; Kahn, M.; Mitra, A. "Rapid Chromatographic Technique for Preparative Separations with Moderate Resolution" *J. Org. Chem.* **1978**, *43*, 2923−2925.

13. Gottlieb, H. E.; Kotlyar, V. Nudelman, A. "NMR Chemical Shifts of Common Laboratory Solvents as Trace Impurities" *J. Org. Chem.* **1997**, *62*, 7512.

14. Harris, R. K.; Becker, E. D.; Cabral de Menezes, S. M.; Granger, P.; Hoffman, R. E.; Zilm, K. W. "Further Conventions for NMR Shielding and Chemical Shifts (IUPAC Recommendations 2008)" *Pure Appl. Chem.* **2008**, *80*, 59.

Chapter 7

Biochemical Characterization of PAD

7.1 Introduction

The peptidyl prodrug *N*-Ac-GaFK-PABC-Doxaz (PAD) **1** (Figure 7.1) was designed for activation by the tumor-associated protease plasmin.[1,2] Verification of the enzymatic activation of **1** was, therefore, a critically important step in the characterization of the prodrug. Additionally, the stability of **1** in human serum was considered an important indication of the therapeutic potential of the prodrug. This chapter details the biological characterization of **1** through experiments performed by the author while under the immediate supervision of Dr. Ben Barthel, the senior biochemist in the Koch group.

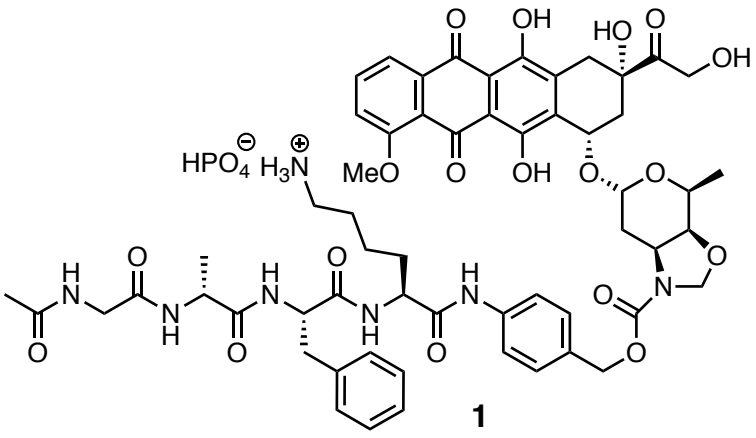

Figure 7.1 Structure of *N*-Ac-GaFK-PABC-Doxaz (PAD) **1**.[1,2]

7.2 Enzyme-Activation Assays

Activation of **1** was measured by RP-HPLC, monitoring formation of dox produced from hydrolysis of the doxaz liberated following enzyme-mediated cleavage of the anilide bond. In a

time course of activation, 50 μM **1** was incubated at 37 °C with 1.2 μg/mL human plasmin in PBS. Analogous to the results obtained during our characterization of the related aFK-PABC-doxaz prodrug, combination of **1** and plasmin resulted in rapid prodrug activation and release of doxaz, as evidenced by the formation of dox, with near quantitative consumption of **1** observed after 2 h (Figure 7.2). In separate reactions containing no enzyme, there was no observable increase in dox over the course of 24 h, showing that **1** is stable in the absence of enzyme.

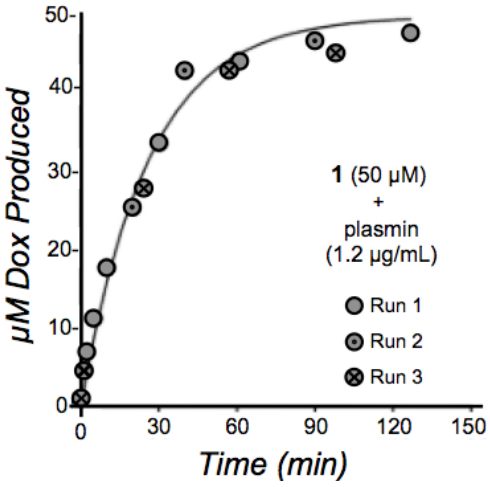

Figure 7.2 RP-HPLC analysis of an enzymatic reaction between 50 μM **1** and 1.2 μg/mL human plasmin. The reaction was performed in PBS, pH 7.4, at 37 °C. Repeated measurements with slightly different reaction times are shown as either circles (run 1), circles with a center dot (run 2) or crosses (run 3).

7.3 Human Plasma Stability

The activity of proteases in the bloodstream is hindered by the presence of α2-macroglobulin and α2-antiplasmins; therefore, **1** should show little to no products of hydrolysis when incubated with human plasma. To demonstrate this, 50 μM **1** was incubated for 24 h at 37 °C in plasma from healthy adult human donors. Periodically, samples were removed and

analyzed for the appearance of dox and disappearance of **1** by RP-HPLC and absorbance at 480 nm. To prevent damage to the analytical reverse phase column, the proteins were first removed by precipitation with ethanol. The results shown in Figure 7.3 indicate that levels of **1** in the supernatant do decrease with time, but a similar increase in dox is not observed, with dox accounting for only approximately 9% of the total absorbance at 480 nm after 48 h. Additionally, the loss of 480 nm absorbance from the prodrug was not distributed to other, unidentified red products either but instead was lost from the total absorbance of the sample. This suggests that **1** was incorporated into the pellet upon ethanol precipitation, likely through nonspecific binding to serum albumin, which is well-known as a drug carrier.[3,4] The lack of dox production indicates that, in human plasma, **1** is very stable over 24 h and is unlikely to be prematurely activated.

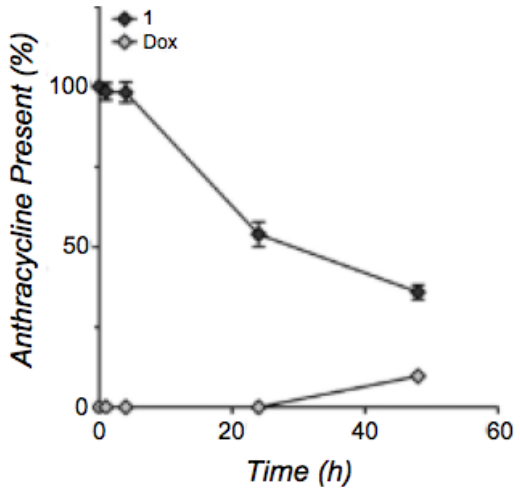

Figure 7.3 HPLC analysis of the stability of **1** in human plasma over 48 h. **1** (50 μM) was incubated with undiluted human plasma from healthy individuals, and the time points were analyzed for the presence of all 480 nm absorbing species after precipitation of the protein fraction with absolute ethanol. Only **1** (dark diamonds) and dox (light diamonds) were observed. The points represent the mean ± the standard deviation of three measurements, and percentages are relative to the **1** peak area present at the start of the experiment.

7.4 Growth Inhibition Assays.

Initial growth inhibition tests with **1** were performed on the MCF-7 human cancer cell line. The cells responded well to prodrug alone, with log IC_{50} values in the range of -6.6 to -6.7 (data not shown). When co-treated with 0.2 U plasmin, the potency of the treatments increased by approximately 10-fold, confirming that plasmin can mediate the release of doxaz from **1** (Figure 7.4). Co-treatment with bovine trypsin (0.2 U) reduced growth to a similar extent as

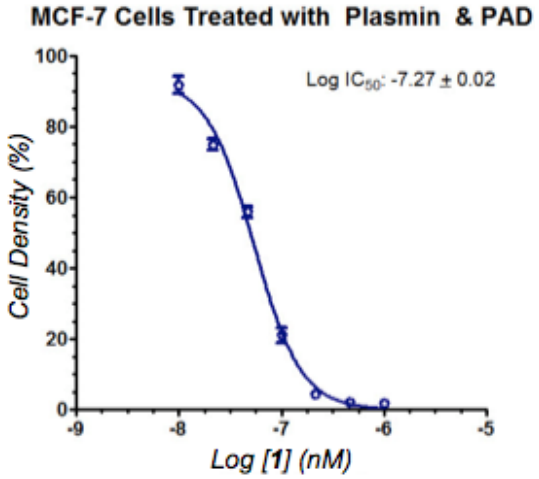

Figure 7.4 Plot of %-cell density *vs.* log [PAD] (nM) values for MCF−7 cells co-treated with **1** and plasmin.

plasmin, demonstrating that other serine proteases can easily activate **1**. This has potential to be very beneficial, as many cancers have been found to have high levels of trypsin or trypsin-like serine protease activity.[5−8] When proteolytic activity is inhibited with either 5 μM aprotinin to inhibit serine proteases or Roche's Complete protease inhibitor cocktail (made to 1x according to the manufacturer's instructions), the reduction in cellular response to **1** is apparent but not significant (Figure 7.5). This may be due to constant secretion of active proteases by the cell,

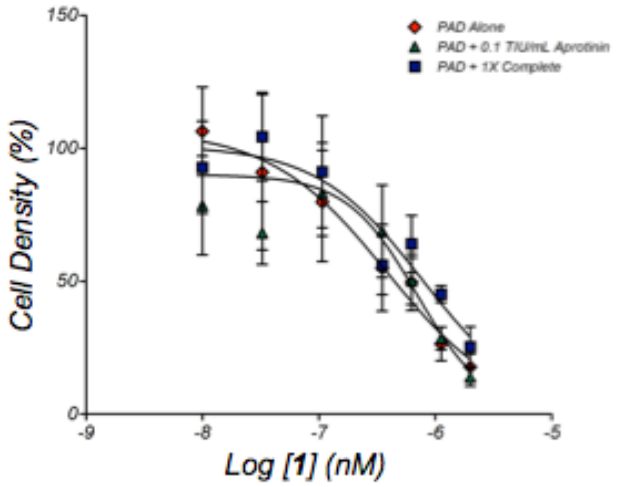

Figure 7.5 Plot of %-Cell Density *vs.* log [PAD] (nM) values for MCF-7 cells treated with either **1** (red diamonds), **1** and aprotinin (green triangles) or **1** and Roche's Complete protease inhibitor cocktail (blue squares).

which effectively overwhelms the limited amount of added inhibitor, since the potency of the inhibitors was verified by their ability to prevent the increase in potency of a **1**−plasmin co-treatment over **1** treatment alone (data not shown). However, the inability of high concentrations of protease inhibitors to protect cells could also could indicate that there are alternative mechanisms of activation beyond those probed in this study.

7.5 Experimental

Enzyme-Activation Assays. Assays to determine the activities of various enzymes toward protease-cleavable doxaz prodrugs were performed as a hydrolysis time course to assess the activity of each enzyme stock. Time course experiments were conducted at 37 °C by incubating 50 μM prodrug with varying concentrations of either plasmin (EMD Biosciences, La Jolla, CA) or trypsin (Research Products International, Mt. Prospect, IL) in PBS. At various times, 50 μL of the reaction mixture was added to an equal volume of absolute ethanol to quench

the reaction. The collected samples were stored at −20 °C for at least 2 h and then centrifuged at 15000g for 5 min to precipitate the protein. The supernatant was analyzed by RP-HPLC (method 1), monitoring the loss of the starting material (elution at 8−9 min) and accumulation of dox (elution at 4−5 min).

Human Plasma Stability. To assay for the stability of the prodrug in blood plasma, **1** was diluted with human plasma collected from healthy individuals (a gift from Somalogic, Inc., Boulder, CO) to a final drug concentration of 50 μM. The reaction was incubated at 37 °C for 24 h. Aliquots were taken at 0.25, 1, 3, 8, 12, and 24 h, quenched with an equal volume of EtOH, and incubated at −20 °C overnight to precipitate the proteins. Precipitated protein was removed by centrifugation in a desktop centrifuge for 5 min at 15000g. The supernatant was analyzed by RP-HPLC (plasma method: acetonitrile from 20% to 40% over 5 min, to 70% at 10 min, to 80% at 13 min, isocratic for 2 min, then back to 20% by 17 min). The percent compositions of **1** (eluting at 8−9 min) and dox (eluting at 6.5−7.0 min) were determined from their relative absorbances at 480 nm, taking into account all other unknown products that appeared during the reaction and absorbed at 480 nm. The experiment was repeated in triplicate.

IC_{50} Experiments. Initial characterization of **1** was performed in the MCF-7 human breast cancer cell line. The cells were seeded into 96-well plates at a density of 1000 cells/well and allowed to adhere overnight. The medium was replaced with 90 μL of serum-free medium containing one or more of plasmin (0.2 U/well), trypsin (0.2 U/well), aprotinin (5 μM, Research Products International, Mt. Prospect, IL), or Complete Mini protease inhibitors (1× according to package instructions, Roche Applied Science, Indianapolis, IN). A DMSO-solution of **1** (10 μL) was added to the wells for a final concentrations between 2000 and 1 nM, and controls received only vehicle (either DMSO or saline with 10% PEG). The cells were treated with **1** and

activator/inhibitor for 24 h, at which point the treatment medium was replaced with Complete medium and the cells were allowed to grow for 5 days or until the control wells reached 80% confluency, whichever was shorter. The cells were then fixed with 5% formalin in PBS for 10 min and stained with crystal violet (0.01% w/v in water) for 20−30 min. The plates were rinsed and air-dried, and the stain was redissolved either in a 6:3:1 mixture of EtOH−water−MeOH (v/v/v) or in a 1:1 mixture of 2-propanol−water (v/v) with 2% sodium dodecylsulfate (SDS). Cell density was measured by absorbance at 582 nm. Percent optical density, relative to control wells, was fit to a variable slope sigmoidal dose−response curve by nonlinear regression analysis in GraphPad Prism 5.0. All experiments were performed in triplicate.

7.6 References

1. Barthel, B. L.; Rudnicki, D. L.; Kirby, T. P.; Colvin, S. M.; Burkhart, D. J.; Koch, T. H. "Synthesis and Biological Characterization of Protease-Activated Prodrugs of Doxazolidine" *J. Med. Chem*. **2012**, *55*, 6595–6607.

2. de Groot, F. M. H.; de Bart, A. C. W.; Verheijen, J. H.; Scheeren, H. W. "Synthesis and Biological Evaluation of Novel Prodrugs of Anthracyclines for Selective Activation by the Tumor-associated Protease Plasmin" *J. Med. Chem.* **1999**, *42*, 5277−5283.

3. Fehske, K. J.; Muller, W. E.; Wollert, U. "The Location of Drug Binding Sites in Human Serum Albumin" *Biochem. Pharmacol.* **1981**, *30*, 687−692.

4. Kratochwil, N. A.; Huber, W.; Muller, F.; Kansy, M.; Gerber, P. R. "Predicting Plasma Protein Binding of Drugs: A New Approach" *Biochem. Pharmacol*. **2002**, *64*, 1355−1374.

5. Koivunen, E.; Ristimaki, A.; Itkonen, O.; Osman, S.; Vuento, M.; Stenman, U. H. "Tumor-associated Trypsin Participates in Cancer Cell-mediated Degradation of Extracellular Matrix" *Cancer Res.* **1991**, *51*, 2107−2112.

6. Miszczuk-Jamska, B.; Merten, M.; Guy-Crotte, O.; Amouric, M.; Clemente, F.; Schoumacher, R. A.; Figarella, C. "Characterization of Trypsinogens 1 and 2 in Two Human Pancreatic Adenocarcinoma Cell Lines; CFPAC-1 and CAPAN-1" *FEBS Lett*. **1991**, *294*, 175−178.

7. Yamamoto, H.; Iku, S.; Itoh, F.; Tang, X.; Hosokawa, M.; Imai, K. "Association of Trypsin Expression with Recurrence and Poor Prognosis in Human Esophageal Squamous Cell Carcinoma" *Cancer* **2001**, *91*, 1324− 1331.

8. Santin, A. D.; Cane, S.; Bellone, S.; Bignotti, E.; Palmieri, M.; De Las Casas, L. E.; Anfossi, S.; Roman, J. J.; O'Brien, T.; Pecorelli, S. "The Novel Serine Protease Tumor-associated Differentially Expressed Gene-15 (matriptase/MT-SP1) is Highly Overexpressed in Cervical Carcinoma" *Cancer* **2003**, *98*, 1898−1904.

Chapter 8

Evidence for a Revised Mechanism Governing the Traceless Staudinger Ligation of an Aryl Azide

8.1 Putative Mechanism for the Staudinger Ligation

Both the Bertozzi and Raines groups have published detailed studies on their variants of the Staudinger ligation and both proposed mechanisms which proceed through an iminophosphorane intermediate **2** in route to the amide **3** (Figure 8.1).[1,2] However, these studies dealt almost exclusively with reactions involving alkyl azides. Soellner *et al.* did not report the use of any aryl azides in their mechanistic investigation[2] and, although Lin *et al.* did report products and kinetic data for three aryl azides in their mechanistic examination, product characterization in these cases was limited to ^{31}P NMR spectroscopy.[1]

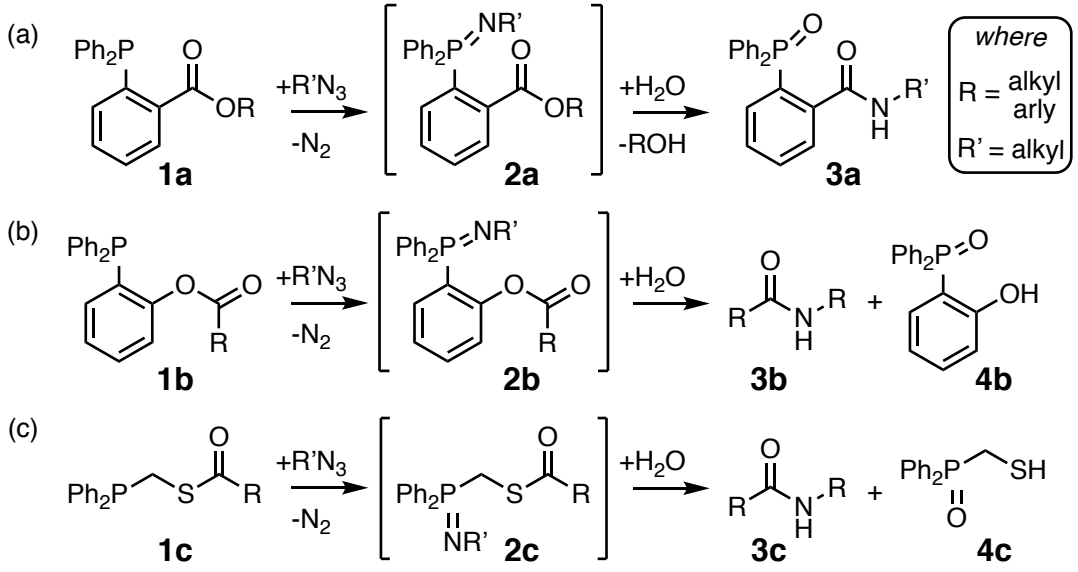

Figure 8.1 Illustrations of (a) Bertozzi's Staudinger ligation[5] (b) Bertozzi's traceless Staudinger ligation[6] & (c) Raines' traceless Staudinger ligation[7] of phosphines **1a-c** and an alkyl azide. Iminophosphoranes **2a-c** were proposed to be intermediates in each case.[1,2]

While several applications of aryl azides in the TSL have appeared in the literature since the outset of our work, curiously, the results described in these cases vary considerably from one account to another.[3–5] Lin *et al.* indicated that aryl azides react with phosphines analogously to alkyl azides, albeit perhaps more slowly, to afford the expected anilide as the major product.[1] Similarly, Tsao *et al.* reported the conversion of aryl azides into anilides for the modification of proteins.[3] However, in both of these cases, product characterization was quite limited. In contrast, Restituyo *et al.* reported that the Staudinger ligation of an aryl azide does not afford the anilide at all, but rather affords an *O*-alkyl imidate **6** as the major product of the reaction (Figure 8.2).[5] Strengthening the credibility of the latter report, a series of such imidates were fully characterized after isolation by silica gel chromatography. Additional independent reports of both aryl− and allyl−azides giving rise to *O*-alkyl imidates via the Staudinger ligation were also found to corroborated this claim.[6,7] Still, no detailed mechanistic study on the TSL of an aryl azide has thus far appeared in the literature to aid in the explanation of these discrepancies.

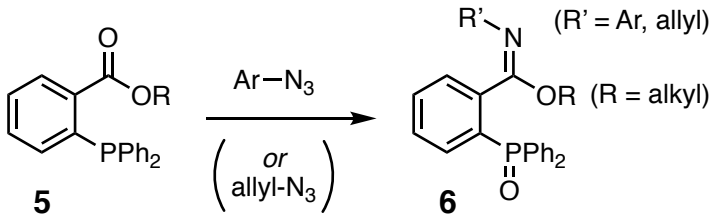

Figure 8.2 *O*-Alkyl imidate **6** formation from the Staudinger ligation of an aryl (or allyl) azide.[5–7]

In this chapter, we report the results from an investigation into the mechanism of the TSL of an aryl azide and phosphinophenyl ester using a combination of HPLC & NMR reaction monitoring experiments. The combination of these findings are presented as evidence for a

revised mechanism governing the reaction. Finally, a comparison of the various kinetic models consistent with the data is made and the most probable mechanism based on this analysis is identified.

8.2 *Occasionem Cognosce*: A Chance Observation

During our studies of the anthracycline anticancer drug candidate doxazolidine,[8] aryl azide **7** was combined with phosphine **8** in DMSO from a freshly opened bottle, in an attempt to synthesize anilide **9** (Scheme 8.1). It was assumed that the DMSO would contain a sufficient amount of water to permit the reaction to proceed as intended and, thus, no additional water was added to the reaction medium. The course of the reaction was followed by RP-HPLC, monitoring the characteristic absorption of anthracyclines at 480 nm, and produced the chromatograms shown below (Figure 8.3). At the earliest time point ($t = 5$ min; Fig. 8.3a), the starting azide **7** (R_T ~ 14 min), as well as, three additional anthracycline-containing compounds were detected and are labeled **P1,** (R_T ~ 13 min); **I**, (R_T ~ 13.3 min); and **P2**, (R_T ~ 16 min). By the 3 h time point (Fig. 8.3b), only the two compounds eluting at ~13 min and ~16 min, respectively, were observed and the reaction was deemed complete. Semi-preparative RP-HPLC permitted small quantities of the two products to be isolated and subsequent mass spectral analysis indicated that **P1** (R_T ~ 13 min; Fig. 8.3c) was the desired anilide **9** [HRMS (ESI-TOF) *m/z*: $[M+Na]^+$ calcd for $C_{66}H_{73}N_7NaO_{200}$ 1306.4808; found 1306.4813]; and **P2** (R_T ~ 16 min; Fig. 8.3d) was the iminophosphorane **10** [HRMS (ESI-TOF) *m/z*: $[M+Na]^+$ calcd for $C_{84}H_{86}N_7NaO_{21}P$ 1582.5512; found 1582.5521].

Scheme 8.1 TSL of aryl azide **7** and phosphine **8** in DMSO from a freshly opened bottle with no additional H_2O added prior to combining the reactants in solution afforded anilide **9** and iminophosphorane **10**.

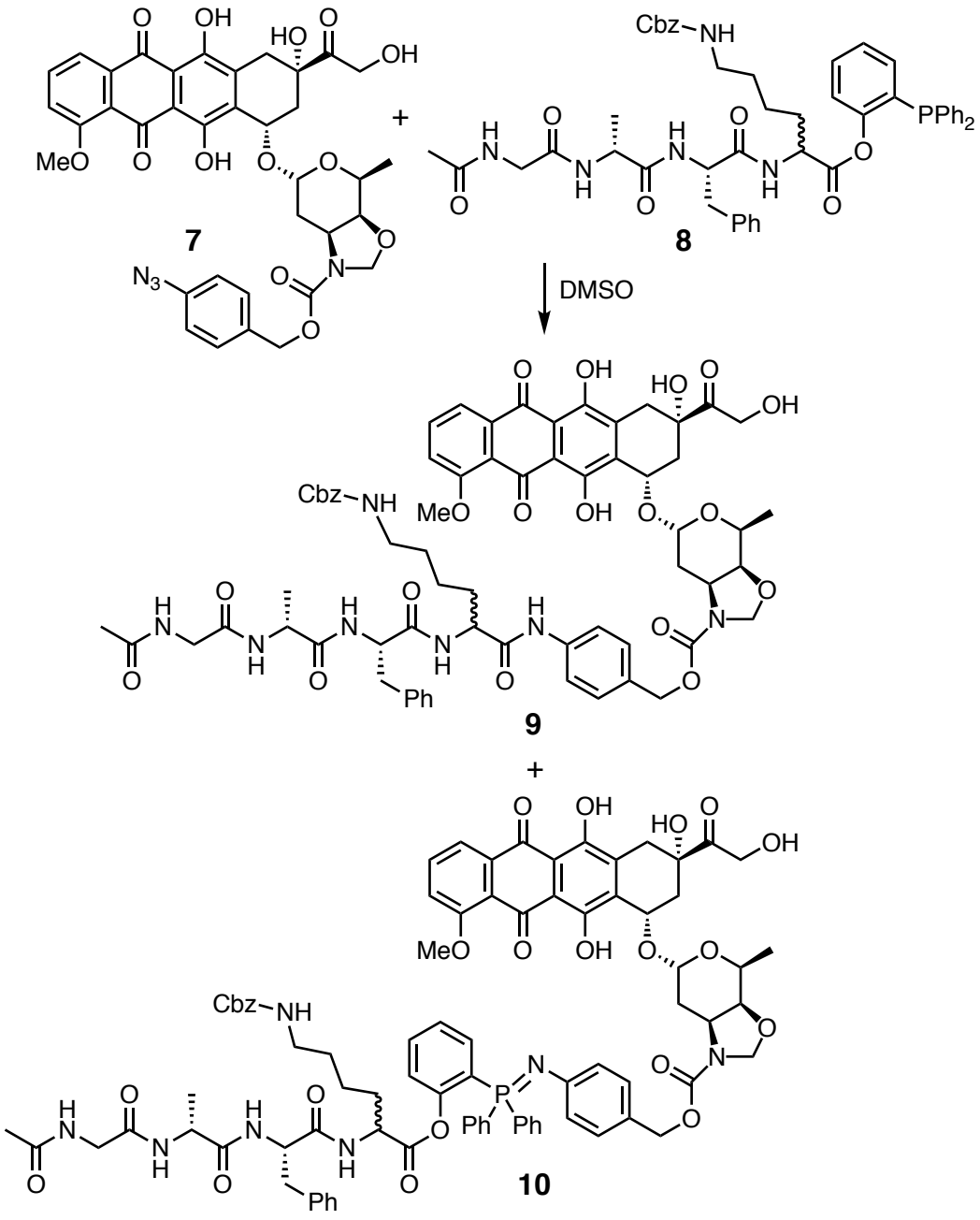

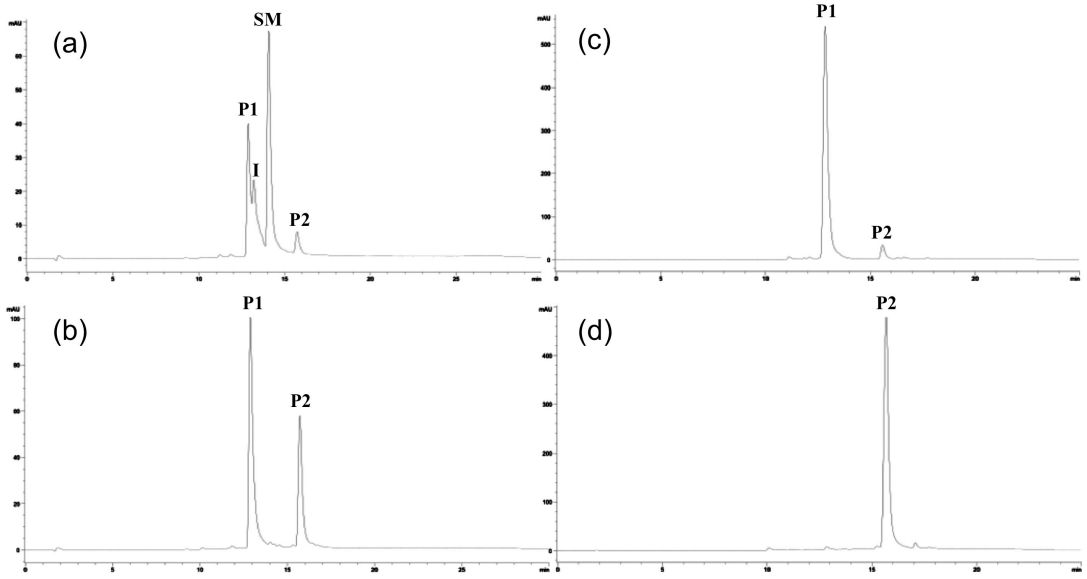

Figure 8.3 Analytical HPLC chromatograms (480 nm, method 1) monitoring the TSL of azide **7** and phosphine **8** in "dry" DMSO after (a) 5 min; (b) 3 h; (c) isolation of **P1** = **9**; and (d) isolation of **P2** = **10**; a description of HPLC methods is provided in section 8.5 under *General Methods.*

Isolation of **10** was not surprising given that the HPLC aqueous phase used in its collection was acidic (pH 4.5). Iminophosphoranes are basic compounds (pKa ~ 8.4 for Ph-HN^{+}=PPh_3 in H_2O at 25 ^{o}C)[9] and numerous examples of stable iminophosphoranes appear in the literature.[10] However, our inability to convert **10** to **9** did come as a surprise. When the collected material **10** was dissolved in wet DMSO and stirred for several hours, no reaction was observed. Triethylamine (TEA) was added (1 equiv) and stirring continued; again, no reaction was observed. Over the course of several days of stirring, however, the reaction produced doxorubicin (dox), the product from hydrolysis of the oxazolidine ring and loss of formaldehyde from doxazolidine (doxaz).[11] This observation suggested that dox was being produced via 1,6-elimination of the iminoquinone methide and decarboxylation of the resulting carbamic acid in a mechanism resembling that of prodrug activation (Figure 8.4).[12] Thus, slow hydrolysis of the P=N bond of iminophosphorane **10** resulted in the formation of dox, while the acyl-transfer

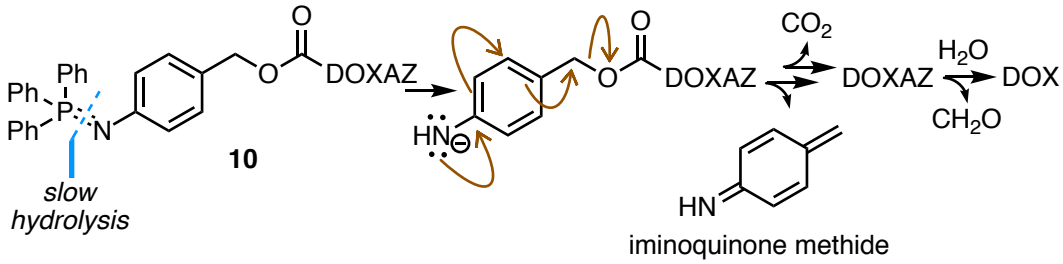

Figure 8.4 Putative 1,6-elimination mechanism by which doxorubicin (DOX) is produced following the slow hydrolysis of the P=N bond of iminophosphorane **10**.[12]

necessary to convert **10** to **9** was not observed. Interestingly, however, when the TSL was repeated using superstoichiometric quantity of water (9:1 DMSO−H_2O), azide **7** and phosphine **8** combined to give anilide **9** cleanly as the sole anthracycline-containing product (Figure 8.5). Based on these observations, a more in-depth investigation into the mechanism governing the TSL of an aryl azide and phosphinyl phenyl ester was undertaken.

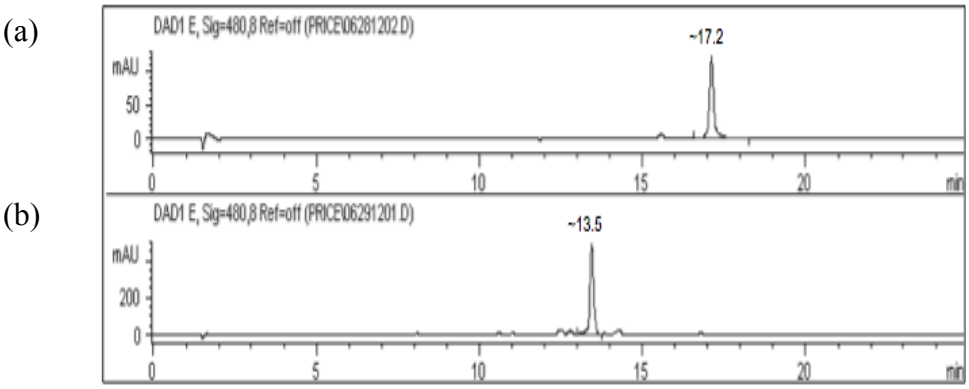

Figure 8.5 Analytical RP-HPLC chromatograms (480 nm) monitoring the conversion of azide **1** (RT ~17.2 min) to anilde **9** (RT ~13.5 min) using method 2; a description of HPLC methods is provided in section 6.5 under *General Methods*.

8.3 The Effects of "Wet" *vs.* "Dry" Initial Reaction Conditions

Esterification of chiral C-terminal peptides with 2-(diphenylphosphino)phenol, in our hands, led inextricably to racimization of the terminal residue and afforded phosphinyl phenyl esters, such as **8,** as a mixture of diastereomers.[13] Accordingly, so too were obtained any products derived from **8**, such as anilide **9** and iminophosphorane **10**, as mixtures of diastereomers. Thus, to avoid unnecessary complications with the characterization of the intermediates and products of the reaction during our mechanistic studies, the achiral model system prepared in Chapter 4 was used for subsequent studies on the mechanism of the TSL.

The reaction between azide **11** and phosphine **12** was examined first by varying the amount of water added to the reaction solvent (Table 8.1). When a large excess of water (350 equiv) was used, the reaction afforded anilide **13** with no detectable formation of the iminophosphorane **14**. With decreasing concentrations of water, a mixture of **13** and **14** resulted. When 4Å mol. sieves were added to dry the reaction *in situ*, only the iminophosphorane **14** was obtained. ^{1}H NMR of the crude reaction mixture indicated that the ester of **14** was intact following the reaction. However, attempts to isolate this material by flash column chromatography over silica gel resulted in hydrolysis of the ester, allowing only the phenolic iminophosphorane **15** to be obtained (Figure 8.6).

Table 8.1 Results of the TSL between azide **11** and phosphine **12** with varying amounts of water present in solution.

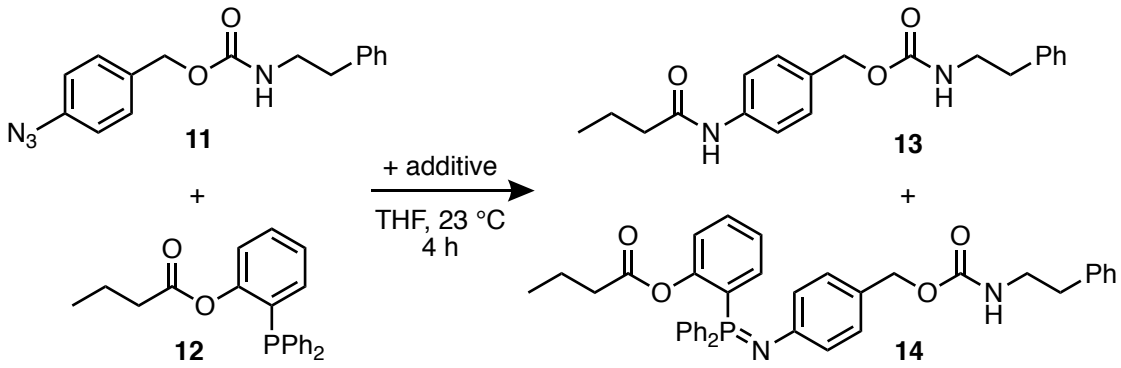

Additive	Product Ratio[a] (13:14)
H_2O (350 equiv)	1:0
H_2O (50 equiv)	3:2
4Å mol. sieves	0:1

[a] Determined by ^{31}P NMR.

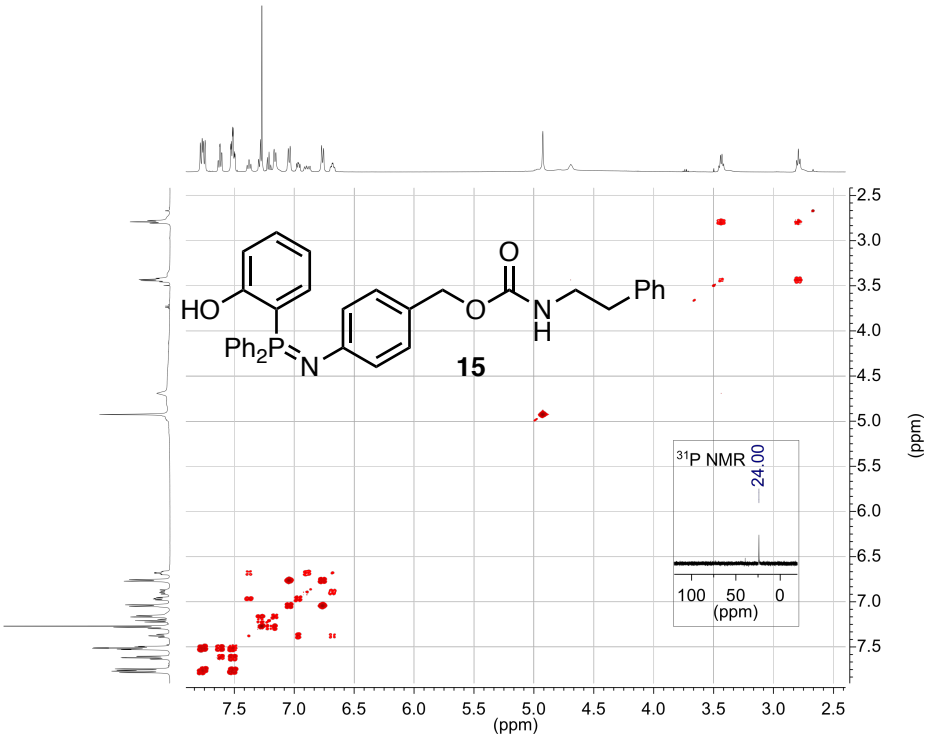

Figure 8.6 gCOSY and ^{31}P NMR spectra in $CDCl_3$ of the isolated iminophosphorane **15**.

8.4 $^{31}P\{^{1}H\}$ VT-NMR Reaction Monitoring Experiments.

A series of proton-decoupled variable temperature (VT) ^{31}P NMR experiments were next conducted. Stock 0.05 M solutions of azide **11** and phosphine **12** were prepared in "dry" CD_3CN (containing ~0.5 equiv of residual water) and placed in a bath (-20 °C) for several minutes prior to use. An aliquot of each solution (300 μL) was then transferred via microsyringe to an NMR tube and placed into a Varian INOVA spectrometer at -20 °C. ^{31}P NMR spectra were acquired over the course of 24 h to monitor the reaction and the results are shown in Figure 8.7.

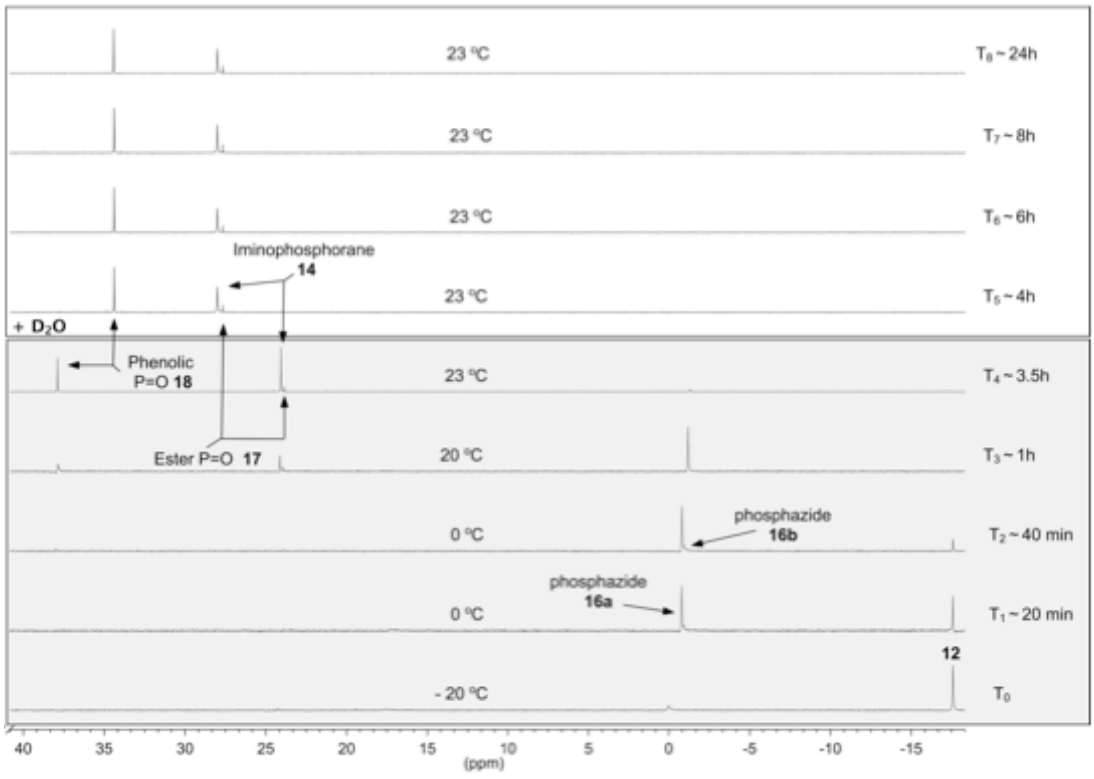

Figure 8.7 $^{31}P\{^{1}H\}$ VT-NMR spectra monitoring the reaction of azide **11** and phosphine **12** at 122 MHz in "dry" CD_3CN (grey) and after the addition of excess D_2O (white) showing that iminophosphorane **14** does not hydrolyze to the phosphine oxide **18**.

The spectrum acquired at -20 °C showed only the starting phosphine **12** (δ -17.6 ppm) present in solution. The reaction was then warmed to 0 °C inside of the spectrometer and two additional spectra were acquired at 20 min intervals. In the first such spectrum acquired at 0 °C, two signals appeared downfield from the starting material: a sharpe peak (δ -0.8 ppm) and a very low-intensity, broad signal just upfield of the first (δ -0.9 ppm). These signals were tentatively assigned as the *cis*- & *trans*-phosphazides **16a** and **16b**, respectively, (Scheme 8.2) as phosphazides are the first intermediates formed following combination of an azide and phosphine.[14,15] While such compounds are generally unstable at ambient temperature and rapidly decompose by extrusion of dinitrogen gas to form an iminophosphorane, phosphazides are sufficiently stable to be detected when formed in a cold solution[16] and the observation of intermediate **I** in the RP-HPLC reaction monitoring experiment (Fig. 8.3a) suggested that a phosphazide intermediate might also be observed by NMR. After 40 min at 0 °C, nearly all of the starting phosphine **12** had been converted into **16a** and **16b** and no other signals appeared elsewhere in the spectrum. Continued warming of the reaction mixture to 20 °C led to the presumed pair of phosphazides **16a** and **16b** being consumed and the appearance of three additional signals further downfield in the spectrum. These signals were readily assigned based on their chemical shifts to be (a) the phosphine oxide still bearing an intact ester **17** (δ 23.9 ppm), derived from oxidation of **12** and which was likely present at t_0 of the reaction as a trace impurity in the phosphine starting material but is too insoluble in *d3*-acetonitrile at colder temperatures to have been observed in the earlier spectra; (b) the iminophosphorane also bearing an intact ester **14 (**δ 24.1 ppm), derived from a reaction between **11** and **12** that proceeded to a stable P^V-intermediate without acyl-transfer having occured; and (c) (2-hydroxyphenyl)diphenylphosphine oxide **18** (δ 37.9 ppm), normally obtained as a stoichiometric by-product from the TSL of a

phosphinyl phenyl ester and produced in this experiment due to the ~0.5 equiv of water present in the *d3*-acetonitrile used as the NMR solvent.

In order to show that the addition of water would not convert the iminophosphorane **14** (δ 24.1 ppm) to the anilide **13** along with additional phosphine oxide **18** (δ 37.9 ppm), a superstoichiometric quantity of D_2O (100 μL) was added after 3.5 h to the reaction still inside of the NMR tube and several additional spectra were acquired at 23 °C. Although substantial changes in the chemical shifts for both **14** (δ 28.0 ppm; Δδ +3.9 ppm) and **18** (δ 34.4 ppm; Δδ -3.5) were observed following the addition of D_2O, this was attributed to changes in the medium and not a chemical reaction involving either component of the mixture. Further, while there appeared to be a decrease in the ratio of **14**/**18** over time, this proved to be an optical illusion attributable to pronounced peak broadening observed with the signal from **14**, which occurred following D_2O-addition. Integration of the AUC, using **17** as an internal reference, confirmed that no change in the ratio of **14**/**18** occurred after addition of D_2O. Thus, despite the addition of excess D_2O, no hydrolysis of the P=N bond was detected during the course of this experiment and iminophosphorane **14** remained intact until the experiment was terminated (t_f ~24 h) and these observations led us to tentatively propose the reaction sequence shown in Scheme 8.2

Scheme 8.2 Proposed reaction sequence of the TSL of azide **11** and phosphine **12**.

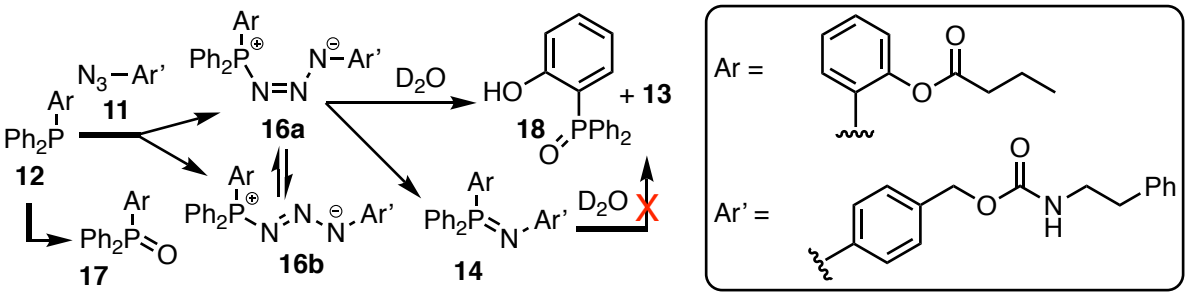

8.5 ^{1}H NMR Reaction Monitoring Experiments

^{1}H NMR was also used to follow the reaction of azide **11** and phosphine **12** at ambient temperature. Equal volumes of a 0.40 M solution of **11** and 0.025 M solution of **12** in 2:1 CD_3CN−D_2O (v/v) were combined under pseudo-first-order conditions and the arrayed ^{1}H NMR spectra acquired are shown in Figure 8.8 (note: only signals from alkyl protons on the acid side of the acyl-moiety are shown here for clarity).

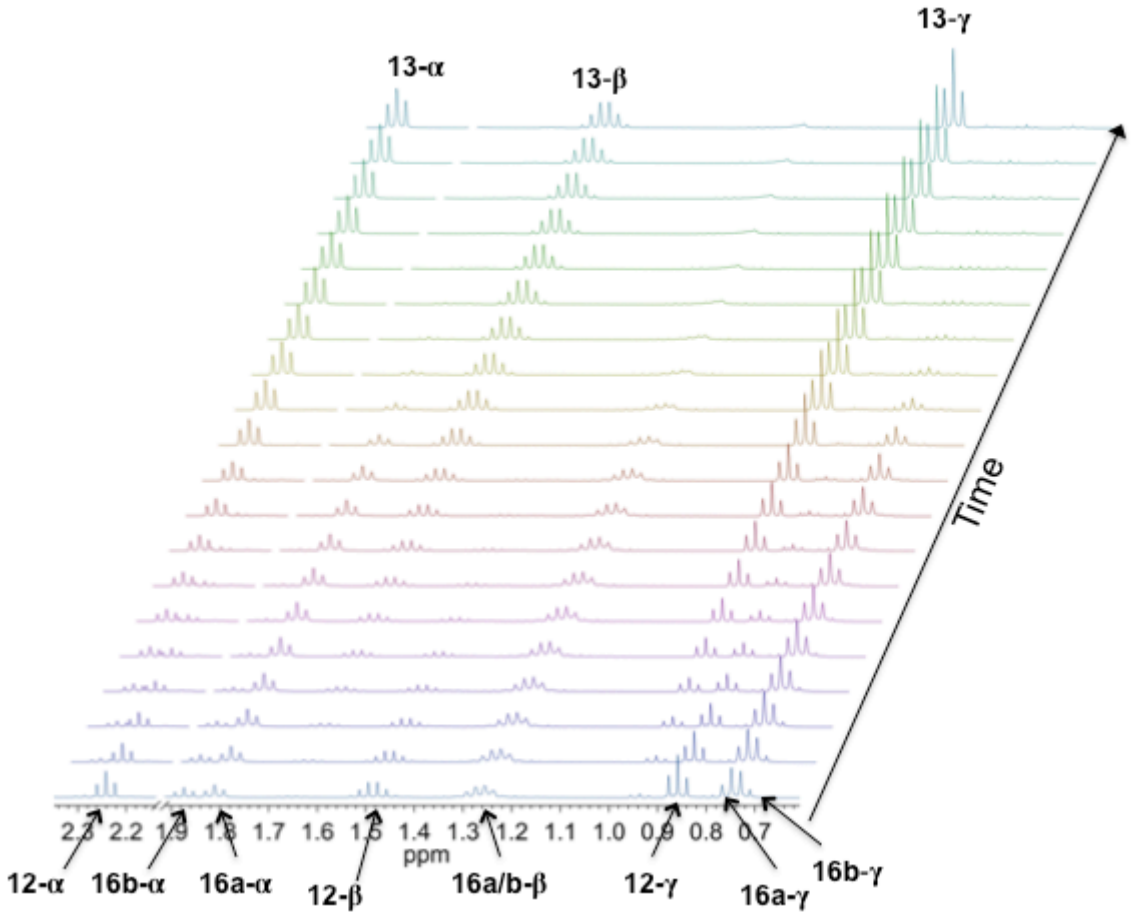

Figure 8.8 Arrayed ^{1}H NMR spectra monitoring the reaction of azide **11** (0.20 M) and phosphine **12** (0.012 M) in 2:1 CD_3N−D_2O (v/v) at ambient temperature. Peak assignments are given in bold around the stack plot.

We observed initial formation of two intermediates with similar chemical shifts for each of the three sets of chemically non-equivalent protons on the acyl-chain (α-CH_2, β-CH_2, and γ-CH_3), followed by the rapid consumption of one intermediate, assigned as the *trans*-phosphazide **16b**, and the slower consumption of the second intermediate, *cis*-phosphazide **16a**. Concomitant with the disappearance of these signals was the appearance of signals for the product anilide **13**. No other intermediate (i.e. iminophosphorane **14**) was observed under these conditions. Thus, under "wet" initial conditions, the combination of azide **11** and phosphine **12** afforded anilide **13** cleanly without formation of iminophosphorane **14**. These results stand in contrast to the putative mechanisms proposed by Bertozzi[1] and Raines[2] for the TSL of alkyl azides.

8.6 Kinetic Models Based on ^{1}H NMR Reaction Monitoring Experiments

Integration of the baseline-resolved signals observed in the ^{1}H NMR spectra from the propyl chain of the acyl-moiety for the starting phosphine **12**, anilide **13** and the two intermediates **16a** and **16b** allowed for several kinetic models of the reaction mechanism to be generated[17] and the results are displayed in Figures 8.9−8.13. As Figure 8.9 shows, the mechanism we had initially proposed in which **12** reacts to give both **16a** and **16b**, which themselves are in equilibrium, does not provide an adequate fit for the consumption of the *trans*-phosphazide **16b**. A revised model shown in Figure 8.10 assumed that **12** reacts irreversibly to give **16a** and reversibly to give **16b**, **16b** then reacts irreversibly to give **16a**, which gives **13**. Of course, if formation of **16b** is reversible, then the reaction of **12** to give **16a** may also be reversible, and the results of this assumption are shown in Figure 8.11. Both of these models provide an improved fit for the consumption of **16b** relative to the first model, but also show a disconcerting maximum for the appearance of the *trans*-phosphazide **16b** (shown in red). A model in which **12** reacts irreversibly

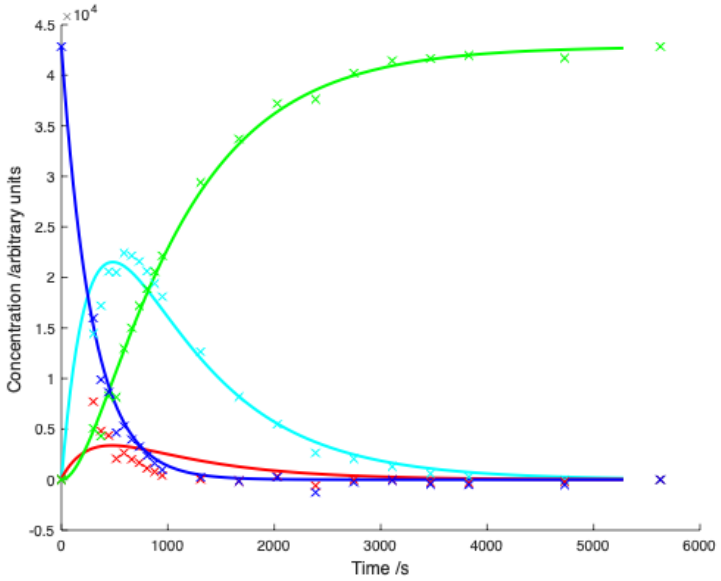

Figure 8.9 Plot of the concentrations of the phosphine **12** (blue), *cis*-phosphazide **16a** (light blue), *trans*-phosphazide **16b** (red) and anilide **13** (green) determined from integration of the AUC of the diagnostic alkyl peaks observed in the ^{1}H NMR spectra recorded under pseudo-first-order conditions (y-axis) *vs* time (x-axis). This model assumes that **12** reacts to give both **16a** and **16b**, which themselves are in equilibrium, and **16a** reacts to give **13**.[17]

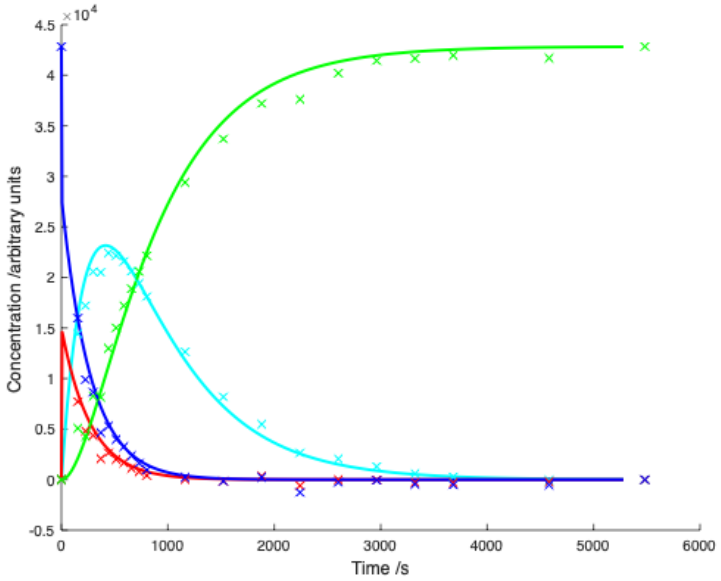

Figure 8.10 Plot of the concentrations of the phosphine **12** (blue), *cis*-phosphazide **16a** (light blue), *trans*-phosphazide **16b** (red) and anilide **13** (green) determined from integration of the AUC of the diagnostic alkyl peaks observed in the ^{1}H NMR spectra recorded under pseudo-first-order conditions (y-axis) *vs* time (x-axis). This model assumes that **12** reacts reversibly to give **16b**, **16b** reacts to give **16a** and **16a** reacts to give **13**.[17]

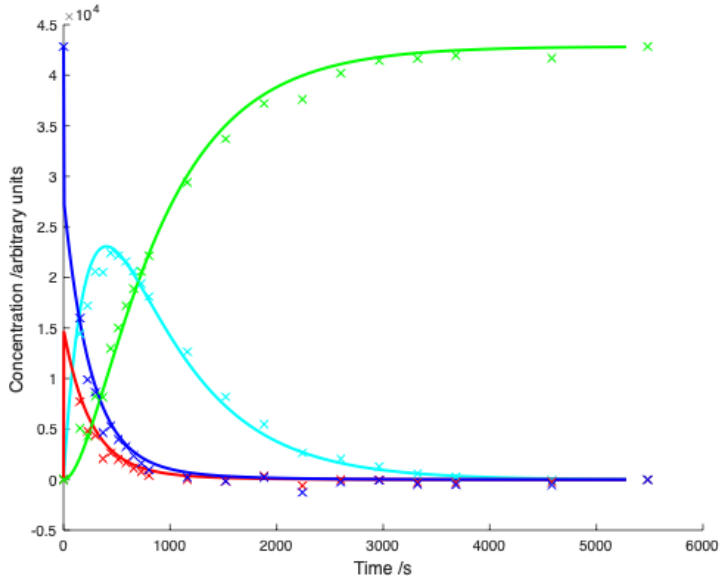

Figure 8.11 Plot of the concentrations of the phosphine **12** (blue), *cis*-phosphazide **16a** (light blue), *trans*-phosphazide **16b** (red) and anilide **13** (green) determined from integration of the AUC of the diagnostic alkyl peaks observed in the ^{1}H NMR spectra recorded under pseudo-first-order conditions (y-axis) *vs* time (x-axis). This model assumes that **12** reacts reversibly to give both **16a** and **16b** and that **16a** reacts to give **13**.[17]

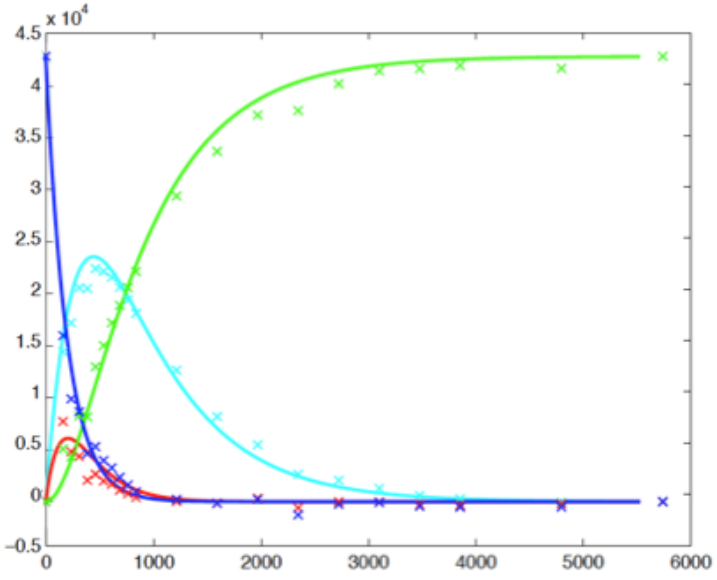

Figure 8.12 Plot of the concentrations of the phosphine **12** (blue), *cis*-phosphazide **16a** (light blue), *trans*-phosphazide **16b** (red) and anilide **13** (green) determined from integration of the AUC of the diagnostic alkyl peaks observed in the ^{1}H NMR spectra recorded under pseudo-first-order conditions (y-axis) *vs.* time (x-axis). This model assumes that **12** reacts irreversibly to give both **16a** and **16b**, **16b** reacts irreversibly to give **16a**, which gives **13**.[17]

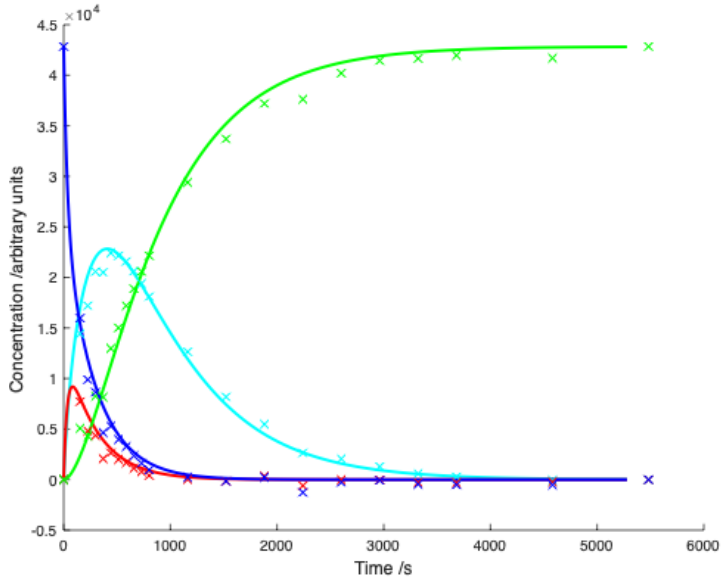

Figure 8.13 Plot of the concentrations of the phosphine **12** (blue), *cis*-phosphazide **16a** (light blue), *trans*-phosphazide **16b** (red) and anilide **13** (green) determined from integration of the AUC of the diagnostic alkyl peaks observed in the ^{1}H NMR spectra recorded under pseudo-first-order conditions (y-axis) *vs.* time (x-axis). This model assumes that **12** reacts to give **16a** and reversibly to give **16b** and **16a** reacts to give **13**.[17]

to give both **16a** and **16b**, with **16b** also reacting irreversibly to give **16a**, which gives **13** is shown in Figure 8.12. This model gives a reasonable fit of the data, generally, but fails to accurately predict the maximum concentration of **16b** observed experimentally. The final kinetic model we considered assumed that **12** reacts irreversibly to give **16a** and reversibly to give **16b**, and **16a** reacts to give **13**. This model is shown in Figure 8.13 and gives the best overall fit to the empirical data. Based on this analysis, we propose the revised mechanism for the TSL of an aryl azide **11** and phosphinyl phenyl ester **12** shown in Scheme 8.3. The indicated pseudo-first-order rate constants, k_n, and equilibrium constant, K_{eq}, were determined by a collaborator, Professor David Brook of San Jose State University, San Jose, CA, from numerical integration of differential rate equations using MATLAB[17] and represent our best approximation of the true

values. However, limitations to the analytical method employed, namely the delay in time between the mixing of the reagents and the acquisition of the first data point, prevent a more precise calculation of these values. The rate of formation of the *trans*-phosphazide, k_2, is particularly dubious, as the error term readily indicates. Nevertheless, a more accurate method for measuring the kinetics of this reaction that is capable of distinguishing between *cis*- and *trans*-phosphazides is not known to us.

Scheme 8.3 Revised mechanism for the TSL of an aryl azide **11** and phosphinyl phenyl ester **12** in 2:1 *d3*-acetonitrile–D_2O (v/v). The pseudo-first-order rate constants, k_n, and equilibrium constant, K_{eq}, were determined from numerical integration of the differential rate equations using MATLAB.[17]

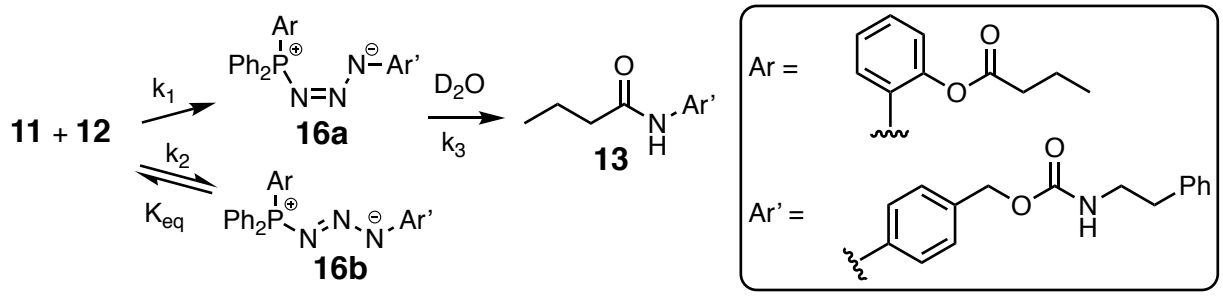

$k_1 = 5.3 \pm 0.2 \times 10^{-3}\ s^{-1}$
$k_2 = 8 \pm 6 \times 10^{-3}\ s^{-1}$ $K_{eq} = 0.44 \pm 0.05$
$k_3 = 1.49 \pm 0.03 \times 10^{-3}\ s^{-1}$

8.7 Discussion

Interpretation of our data with guidance from the existing literature suggests that initial combination of azide and phosphine commences with attack from the phosphorus lone pair on the terminal nitrogen of the azide and formation of a mixture of resonance stabilized s-*cis*- and s-*trans*-phosphazides. Under aqueous conditions, we propose that water attacks the phosphorus

of the s-*cis*-phosphazide, thereby converting the tetrahedral phosphazide **19** into a trigonal bipyrimidal (tbp) intermediate **20** with the oxygen− and nitrogen−substituents occupying the two apical positions and the three phenyl rings equitorial to the phosphorus (Scheme 8.4). The tbp geometry positions the carbonyl of the phenyl ester in closer proximity with the nucleophilic γ-nitrogen atom than in the tetrahedral arrangement and this conformational change may greatly facilitate acyl-transfer. However, additional electronic effects may also facilitate the reaction. Addition of water to the phosphazide creates a new P−O σ-bond, which weakens the existing P−N bond and shifts electron density onto the nitrogen. The flow of electron density back into the conjugated nitrogen triad may facilitate the acyl-transfer reaction by increasing the nucleophilicity of the γ-nitrogen, but it is also noteworthy to recognize that subsequent lone-pair donation from the oxygen would result in the final P−N bond breaking towards the more electronegative nitrogen atom. Water may also attack the initially formed *trans*-phosphazide

Scheme 8.4 Mechanism for the conversion of the tetrahedral s-*cis*-phosphazide intermediate **19** into the trigonal bipyrimidal (tbp) intermediate **20** upon reaction with water.

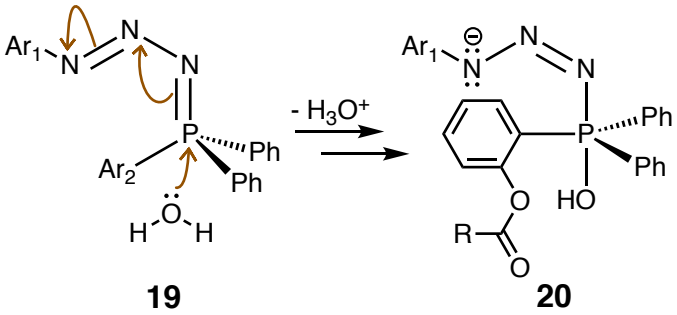

19 **20**

16b intermediate, but it may not if that reaction is slow and the reverse reaction back to starting materials occurs more readily. In either case, absent an isomerization pathway, **16b** must ultimately revert back into the two starting materials so that they may then recombine to give **16a** along the productive pathway in order to account for the observed conversion of all of the starting material into product.

Given the absence of any other signals in the NMR spectra recorded during the reaction monitoring experiements, we further conclude that the rate determining step for formation of **13** is the reaction of **16a** with water (or D_2O). An approximate second-order rate constant for formation of the amide **13** was calculated by dividing k_3 by the concentration of D_2O and was found to be 8.1×10^{-5} M^{-1} s^{-1}. This suggests the reaction of **16a** with water is quite sluggish and that good yields of anilide **13** should require a high concentration water to be present in solution. Gratifyingly, this assertion is consistent with our previous observation that when only ~50 equiv of water were added, the reaction performed in DMSO gave a mixture of anilide and iminophosphorane (Section 8.3; Table 8.1).

In the absence of water, however, we propose the *cis*-phosphazide **16a** retains its tetrahedral geometry and combined with the absense of additional electronic effects that may also promote acyl-transfer, this reaction does not occur. Competative extrusion of N_2 occurs instead via a four-membered transition state and formation of iminophosphorane **14** results. What differentiates this system from reactions with alkyl azides, however, is that the aryl azide-derived iminophosphorane **14** is a stable compound and does not undergo acyl-transfer to complete the TSL. Even if water is subsequently added to the reaction mixture, iminophosphorane **14** is not converted to anilide **13**. This result stands in stark contrast to the reported case for the intermediate isolated following combination of an alkyl azide and a

phosphine under anhydrous conditions, which rapidly hydrolyzed to afford the amide and phosphine oxide upon addition of water.[1]

8.8 Concluding Remarks

A combination of empirical findings were presented as evidence for a revised mechanism governing the traceless Staudinger ligation (TSL) of an aryl azide and phosphinophenyl ester. Both the anilide and iminophosphorane were afforded as isolable products from the TSL and the ratio of these products was dependent upon the initial reaction conditions. Unsurprisingly, wet solvent systems favored anilide formation, while dry reaction conditions favored formation of the iminophosphorane. Surprisingly, however, the aryl azide-derived iminophosphoranes were not hydrolyzed to the corresponding anilides through a subsequent reaction with water. Instead, addition of water to a solution of the iminophosphorane led only to the slow hydrolysis of the P=N bond without concomitant acyl-transfer from the adjacent ester ever being observed. The inability to hydrolyze the iminophosphorane to the anilide conflicts with the putative mechanism of the TSL found in the literature and prompted our investigation into the conditions under which the two products were being formed as a function of the concentration of water added in solution prior to combing the reactants. Formation of the anilide was concluded to proceed via a mechanism that does not have an iminophosphorane intermediate along its pathway. A ^{1}H NMR kinetic study under consecutive pseudo-first order conditions was used to construct several mechanistic models and a comparison of those models allowed for the selection of the most probable mechanism.

8.9 Experimental

General Methods. Unless otherwise specified, all reactions were performed under an inert atmosphere of nitrogen or argon. Molecular sieves (3Å & 4Å) were activated in a vacuum drying oven at 180 °C and 10^{-2} Torr for 72 h and stored in a drying oven at 160 °C prior to use. Wet solvent systems were prepared using either D_2O or purified water obtained from a Milli-Q Direct water purification system from EMD Millipore (Burlington, MA). Analytical RP-HPLC was performed on Agilent 1050/1100 hybrid instruments equipped with a 1050 series pump and autoinjector and a 1100 series UV/visible diode array detector (Santa Clara, CA). Sample solutions (5 μL) were injected onto an Agilent Zorbax octadecylsilyl (C18) reverse phase column (4.6 mm i.d. × 150 mm, 5 μm) at ambient temperature and eluted with an 15 mM PO_4 (pH 4-5)−MeCN solvent system (1 mL/min). The gradient elution method was programmed as follows in terms of %-aq. buffer: 0-2 min (80%), 5 min (70%), 15 min (25%), 15-22 min (25%), 25 min (5%) and 25-30 min (5%). All RP-HPLC analyses monitored absorbance at 220, 254 and 280 nm. The presence of anthracycline-containing molecules was additionally monitored by absorbance at 480 nm. Retention times (R_T) are reported in the text. ^{1}H NMR spectra were recorded at 400 or 500 MHz on Varian Unity INOVA spectrometers (Palo Alto, CA) or at 300 MHz on a Bruker-Avance III spectrometer (Billerica, MA). $^{31}P\{^1H\}$ NMR spectra were acquired at 164 MHz on a Varian Unity INOVA spectrometer. Chemical shifts are reported in δ values of ppm with internal referencing to the residual solvent peak, whose frequencies are given by Gottlieb *et al*.[18] Coupling constants are reported as *J*-values in Hertz (Hz) with resonance multiplicities abbreviated as follows: s = singlet, d = doublet, t = triplet, q = quartet, p = pentet, sept = septet, m = multiplet, br = broad. NMR data processing and plotting, including x-referencing of $^{31}P\{^1H\}$, was performed using MestReNova NMR software v12.0.1 (Mestrelab

Research, Santiago de Compostela, Spain). The synthesis of all compounds depicted in this chapter has been described previously in this thesis.

$^{31}P\{^{1}H\}$ VT-NMR Study. Stock 0.05 M solutions of phosphine **12** (10.45 mg, 30 μmol dissolved 600 μL of *d3*-acetonitrile) and azide **11** (24.6 mg, 83 μmol dissolved in 1.66 mL of *d3*-acetonitrile) were cooled in an *iso*-propyl alcohol/CO_2 bath for 10 min before being combined. Aliquots (300 μL) of each stock solution were transferred to a vented NMR tube, quickly vortexed and placed in the spectrometer pre-cooled to -20 °C. $^{31}P\{^{1}H\}$ NMR spectra were acquired at various temperatures (-20 °C, 0 °C, 20 °C and 23 °C) over the course of a 24 h period. After 3.5 h, D_2O (100 μL) was added, the sample vortexed and returned to the spectrometer at 23 °C. Spectral acquisition was resumed by the 4 h mark and additional spectra were acquired at the 6, 8 and 24 h time points, after which the experiment was terminated.

^{1}H NMR Kinetic Study. A 300 μL volume of a 0.025 M stock solution of phosphine **12** (8.69 mg, 24.9 μmol dissolved in 1000 μL of 2:1 *d3*-acetonitrile−D_2O (v/v)) was combined with 300 μL of a 0.40 M stock solution of azide **11** (89.3 mg, 301 μmol dissolved in 750 μL of 2:1 *d3*-acetonitrile−D_2O (v/v)) in a vented NMR tube. The reaction was quickly vortexed and then placed in the spectrometer. ^{1}H NMR spectra were acquired over 15 h and the AUC of the baseline resolved alkyl peaks were plotted.

Kinetic Modeling. Kinetic data were modeled using MATLAB.[17] Differential rate equations were integrated numerically using the built-in MATLAB function 'ode45' and the resulting solutions were optimized to fit the experimental data using the MATLAB optimization toolbox.

8.10 References

1. Lin, F. L.; Hoyt, H. M.; Halbeek, H. Van; Bergman, R. G.; Bertozzi, C. R.; Berkeley, L. "Mechanistic Investigation of the Staudinger Ligation" *J. Am. Chem. Soc.* **2005**, *127*, 2686−2695.

2. Soellner, M. B.; Nilsson, B. L.; Raines, R. T. "Reaction Mechanism and Kinetics of the Traceless Staudinger Ligation" *J. Am. Chem. Soc.* **2006**, *128*, 8820−8828.

3. Tsao, M.; Tian, F.; Schultz, P. G. "Selective Staudinger Modification of Proteins Containing *p*-Azidophenylalanine" *ChemBioChem*, **2005**, *6*, 2147−2149.

4. Baruah, H.; Puthenveetil, S.; Choi, Y-A.; Shah, S.; Ting, A. Y. "An Engineered Aryl Azide Ligase for Site-Specific Mapping of Protein–Protein Interactions through Photo-Cross-Linking" *Angew. Chem., Int. Ed*. **2008**, *47,* 7018−7021.

5. Restituyo, J. A.; Comstock, L. R.; Petersen, S. G.; Stringfellow, T.; Rajski, S. R. "Conversion of Aryl Azides to *O*-Alkyl Imidates via Modified Staudinger Ligation" *Org. Lett.* **2003**, *5*, 4357−4360.

6. Xu, J.; DeGraw, A. J.; Duckworth, B. P.; Lenevich, S.; Tann, C.-M.; Jenson, E. C.; Gruber, S. J.; Barany, G. Distefano, M. D. "Synthesis and Reactivity of 6, 7-Dihydrogeranylazides: Reagents for Primary Azide Incorporation into Peptides and Subsequent Staudinger Ligation" *Chem. Biol. Drug Des.* **2006**, *68*, 85−96.

7. Shalimov, A. A.; Malenko, D. M.; Repina, L. A.; Sinitsa, A. D. "*N*-Substituted *N*-Phosphinotrifluoroactetamides in the Staudinger Reaction" *Russ. J. Gen. Chem.* **2005**, *75*, 1376−1378.

8. Barthel, B. L.; Rudnicki, D. L.; Kirby, T. P.; Colvin, S. M.; Burkhart, D. J.; Koch, T. H. "Synthesis and Biological Characterization of Protease-Activated Prodrugs of Doxazolidine" *J. Med. Chem.* **2012**, *55*, 6595−6607.

9. Laynez, J.; Menendez, M.; Velasco, J. L. S.; Llamas-Saiz, A. L.; Foces, C. F.; Elguero, J.; Molina, P.; Alajarin, M.; Vidal, A. "Iminophosphorane-substituted proton sponges. Part 4. Comparison of X-ray molecular structures with solution properties (pKa, ^{1}H and ^{13}C NMR spectroscopy)" *J. Chem. Soc. Perkin. Trans. 2*, **1993**, *2*, 709−713.

10. Molina, P.; Vilaplana, M. J. "Iminophosphoranes: Useful Building Blocks for the Preparation of Nitrogen-Containing Heterocycles" *Synthesis* **1994**, 1197−1218.

11. Post, G. C.; Barthel, B. L.; Burkhart, D. J.; Hagadorn, J. R.; Koch, T. H. "Doxazolidine, a Proposed Active Metabolite of Doxorubicin That Cross-Links DNA." *J. Med. Chem.* **2005**, *48*, 7648−7657.

12. Carl, P. L.; Chakravarty, P. K.; Katzenellenbogen, J. A. "A Novel Connector Linkage Applicable in Prodrug Design" *J. Med. Chem.* **1981**, *24*, 479−480.

13. Goodman, M.; Stueben, K. C. "Amino Acid Active Esters. III. Base-Catalyzed Racemization of Peptide Active Esters" *J. Org. Chem.* **1962**, *27*, 3409−3416.

14. Staudinger, H.; Meyer, J. "Über neue organische Phosphorverbindungen III. Phosphinmethylenderivate und Phosphinimine" Helv. Chim. Acta 1919, 2, 635−646

15. Leffler, J. E.; Temple, R. D. "The Staudinger Reaction between Triarylphosphines and Azides. A Study of the Mechanism." *J. Am. Chem. Soc.* **1967**, *89*, 5235−5246.

16. Velasco, M.; D.; Molina, P.; Fresneda, P. M.; Sanz, M. A. "Isolation, Reactivity and Intramolecular Trapping of Phosphazide Intermediates in the Staudinger Reaction of Tertiary Phosphines with Azides" *Tetrahedron* **2000**, *56*, 4079−4084.

17. *MATLAB and Optimization Toolbox Release 2019a*, The Mathworks Inc.: Natick, Massachusetts, United States., 2019.

18. Gottlieb, H. E.; Kotlyar, V.; Nudelman, A "NMR Chemical Shifts of Common Laboratory Solvents as Trace Impurities" *J. Org. Chem.* **1997**, *62*, 7512−7515.

Bibliography

Agarwal, N.; Rich, D. H. "An Improved Cathepsin-D Substrate and Assay Procedure" *Anal. Biochem*. **1983**, *130*, 158−165.

Akiyama, K.; Nakamura, T.; Iwanaga, S.; Hara, M. "The Chymotrypsin-like Activity of Human Prostate-Specific Antigen, γ-Seminoprotein" *FEBS Lett*. **1987**, *225*, 168−172.

Alberichio, F.; Bofill, J. M.; El-Faham, A.; Kates, S. A. "Use of Onium Salt-Based Coupling Reagents in Peptide Synthesis" *J. Org. Chem.* **1998**, *63*, 9678−9683.

Albert, A. "Chemical Aspects of Selective Toxicity" *Nature* **1958**, *182*, 421−423.

Albert, A. "Selective Toxicity" John Wiley and Sons Inc., New York, 1964; pp 57−63.

Albright, C. F.; Graciani, N.; Han, W.; Yue, E.; Stein, R.; Lai, Z.; Diamond, M.; Dowling, R.; Grimminger, L.; Zhang, S. Y.; Behrens, D.; Musselman, A.; Bruckner, R.; Zhang, M.; Jiang, X.; Hu, D.; Higley, A.; Dimeo, S.; Rafalski, M.; Mandlekar, S.; Car, B.; Yeleswaram, S.; Stern, A.; Copeland, R. A.; Combs, A.; Seitz, S. P.; Trainor, G. L.; Taub, R.; Huang, P.; Oliff, A. "Matrix Metalloproteinase-activated Doxorubicin Prodrugs Inhibit HT1080 Xenograft Growth Better than Doxorubicin with Less Toxicity" *Mol*. *Cancer Ther.* **2005**, *4*, 751−760.

Andreasen, P. A.; Egelund, R.; Petersen, H. H. "The Plasminogen Activation System in Tumor Growth, Invasion, and Metastasis" *Cell. Mol. Life Sci*. **2000**, *57*, 25−40.

Arcamone, F. *Doxorubicin Anticancer Antibiotics*. Academic Press: New York, 1981.

Arcamone, F.; Bernardi, L.; Giardino, P.; Patelli, B.; Di Marco, A.; Casazza, A. M.; Pratesi, G.; Reggiani, P. "Synthesis and Antitumor Activity of 4-Demethoxydaunorubicin, 4-Demethoxy-7,9-diepidaunorubicin, and Their β-Anomers" *Cancer Treat. Rep*. **1976**, *60*, 829–834.

Arcamone, F.; Cassinelli, G.; Fantini, G.; Grein, A.; Orezzi, P.; Pol, C.; and Spalla, C. "Adriamycin, 14-Hydroxydaunomycin, a New Antitumor Antibiotic from *S. peucetius* var. *caesius*" *Biotechnol. Bioeng*. **1969**, *11*, 1101−1110.

Atherton, E.; Sheppard, R. C. in *Solid Phase Synthesis: A Practical Approach*; IRL Press: Oxford, U.K., 1989.

Atherton, E.; Logan, C. J.; Sheppard, R. C. "Peptide Synthesis. Part 2. Procedures for Solid-Phase Synthesis Using N^{α}-Fluorenylmethoxycarbonylamino Acids on Polyamide Supports. Synthesis of Substance P and of Acyl Carrier Protein 65–74 Decapeptide" *J. Chem. Soc. Perkin Trans. I* **1981**, 538−546.

Avan, I.; Tala, S. R.; Steel, P. J.; Katritsky, A. R. "Benzotriazole-Mediated Syntheses of Depsipeptides and Oligoesters" *J. Org. Chem.* **2011**, *76*, 4884−4893.

Backes, B. J.; Harris, J. L.; Leonetti, F.; Craik, C. S.; Ellman, J. A. "Synthesis of Positional-Scanning Libraries of Fluorogenic Peptide Substrates to Define the Extended Substrate Specificity of Plasmin and Thrombin" *Nature Biotechnology* **2000**, *18*, 187−193.

Bagchi, D.; Bagchi, M.; Hassoun, E. A.; Kelly, J.; Stohs, S. J. "Adriamycin-Induced Hepatic and Myocardial Lipid Peroxidation and DNA Damage, and Enhanced Excretion of Urinary Lipid Metabolites in Rats" *Toxicology* **1995**, *95*, 1−9.

Bakina, E.; Wu, Z.; Rosenblum, M.; Farquhar, D. "Intensely Cytotoxic Anthracycline Prodrugs: Glucuronides" *J. Med. Chem*. **1997**, *40*, 4013−4018.

Balant, L. P.; Doelker, E.; Burl, P. "Prodrugs for the Improvement of Drug Absorption via Different Routes of Administration" *Euro. J. Drug Metab. Pharmacokinet.* **1990**, *15*, 143−153.

Barlos, K.; Chatzi, O.; Gatos, D.; Stavropoulos, G. "2-Chlorotrityl Chloride Resin. Studies on Anchoring of Fmoc-Amino Acids and Peptide Cleavage" *Int. J. Pept. Protein Res.* **1991**, *37*, 513−520.

Barthel, B. L.; Rudnicki, D. L.; Kirby, T. P.; Colvin, S. M.; Burkhart, D. J.; Koch, T. H. "Synthesis and Biological Characterization of Protease-Activated Prodrugs of Doxazolidine" *J. Med. Chem*. **2012**, *55*, 6595–6607.

Barthel, B. L.; Torres, R. C.; Hyatt, J. L.; Edwards, C. C.; Hatfield, J. M.; Potter, P. M.; Koch, T. H. "Identification of Human Intestinal Carboxylesterase as the Primary Enzyme for Activation of a Doxazolidine Carbamate Prodrug" *J. Med. Chem.* **2008**, *51*, 298–304.

Barthel, B. L.; Zhang, Z.; Rudnicki, D. L.; Coldren, C. D.; Polinkovsky, M.; Sun, H.; Koch, G. G.; Chan, D. C. F. F.; Koch, T. H. "Preclinical Efficacy of a Carboxylesterase 2-Activated Prodrug of Doxazolidine" *J. Med. Chem.* **2009**, *52*, 7678–7688.

Bartoszek, A.; Wolf, C. R. "Enhancement of Doxorubicin Toxicity Following Activation by NADPH Cytochrome P450 Reductase" *Biochem. Pharmacol.* **1992**, *43*, 1449−1457.

Baruah, H.; Puthenveetil, S.; Choi, Y-A.; Shah, S.; Ting, A. Y. "An Engineered Aryl Azide Ligase for Site-Specific Mapping of Protein–Protein Interactions through Photo- Cross-Linking" *Angew. Chem., Int. Ed. Engl.* **2008**, *47*, 7018−7021.

Baumgrass, R.; Williamson, M. K.; Price, P. A. "Identification of Peptide Fragments Generated by Digestion of Bovine and Human Osteocalcin with the Lysosomal Proteinases Cathepsin B, D, L, H, and S" *J. Bone Miner. Res.* **1997**, *12*, 447–455.

Beck, H.; Schwarz, G.; Schroter, C. J.; Deeg, M.; Baier, D.; Stevanovic, S.; Weber, E.; Driessen, C.; Kalbacher, H. "Cathepsin S and an Asparagine-specific Endoprotease Dominate the Proteolytic Processing of Human Myelin Basic Protein In Vitro" *Eur. J. Immunol*. **2001**, *31*, 3726–3736.

Bellarosa, D.; Ciucci, A.; Bullo, A.; Nardelli, F.; Manzini, S.; Maggi, C. A." Apoptotic Events in a Human Ovarian Cancer Cell Line Exposed to Anthracyclines" *J. Pharmacol. Exp. Ther*. **2001**, *296*, 276−283.

Belleau, B.; Malek, G. "A New Convenient Reagent for Peptide Syntheses" *J. Am. Chem. Soc.* **1968**, *90*, 1651−1652.

Bemis, L. T.; Schedin, P. "Reproductive State of Rat Mammary Gland Stroma Modulates Human Breast Cancer Cell Migration and Invasion" *Cancer Res.* **2000**, *60*, 3414−3418.

Bergel, F.; Stock, J. A. "Cyto-active Amino Acids and Peptides. Part VIII. N^{α}-Acyl, Amide, Ester and Peptide Derivatives of Melphalan" *J. Chem. Soc.* **1960**, 3658−3669.

Biniossek, M. L.; Nagler, D. K.; Becker-Pauly, C.; Schilling, O. "Proteomic Identification of Protease Cleavage Sites Characterizes Prime and Non-Prime Specificity of Cysteine Cathepsins B, L, and S" *J. Proteome Res.* **2011**, *10*, 5363–5373.

Boissonnas, R. A.; Preitner, G. "Comparisons of Cleavage of Various α-Amino Function-Blocking Groups of α-Amino Acids" *Helv. Chim. Acta* **1953**, *36*, 875−886.

Bolihaggen, R.; Schmiedberger, M.; Barlos, K.; Grell, E. "A New Reagent for the Cleavage of Fully Protected Peptides Synthesized on 2-Chlorotrityl Chloride Resin" *J. Chem. Soc., Chem Commun.* **1994**, 2559−2560.

Bolt, M.; Guadiano, G.; Koch, T. H. "Substituent Effects on the Redox Chemistry of Anthracycline Antitumor Drugs" *J. Org. Chem.* **1987**, *52*, 2146−2153.

Bonadonna, G.; Monfardini, S.; de Lena, M.; Fossati-Bellani, F.; Beretta, G. "Phase I and Preliminary Phase II Evaluation of Adriamycin (NSC 123127)" *Cancer Res*. **1970**, *30*, 2572−2582.

Bosslet, K.; Czech, J.; Hoffmann, D. "Tumor-selective Prodrug Activation by Fusion Protein-mediated Catalysis" *Cancer Res*. **1994**, *54*, 2151−2159.

Brase, S.; Gil, C.; Knepper, K.; Zimmermann, V. "Organic Azides: An Exploding Diversity of a Unique Class of Compounds" *Angew. Chem., Int. Ed. Engl.* **2005**, 44, 5188−5240.

Brighton, D.; Wood, M. *The Royal Marsden Hospital Handbook of Cancer Chemotherapy: A Guide for the Multidisciplinary Team*; Elsevier Churchill Livingstone: Edinburgh, NY, 2005.

Bromme, D.; Kirschke, H. "*N*-Peptidyl-*O*-carbamoyl Amino Acid Hydroxamates: Irreversible Inhibitors for the Study of the S2' Specificity of Cysteine Proteinases" *FEBS Lett.* **1993**, *322*, 211–214.

Burkhart, D. J.; Barthel, B. L.; Post, G. C.; Kalet, B. T.; Nafie, J. W.; Shoemaker, R. K.; Koch, T. H. "Design, Synthesis, and Preliminary Evaluation of Doxazolidine Carbamates as Prodrugs Activated by Carboxylesterases" *J. Med. Chem.* **2006**, *49*, 7002−7012.

Cantero, D.; Friess, H.; Deflorin, J.; Zimmermann, A.; Brundler, M. A.; Riesle, E.; Korc, M.; Buchler, M. W. "Enhanced Expression of Urokinase Plasminogen Activator and its Receptor in Pancreatic Carcinoma" *Br. J. Cancer* **1997**, *75*, 388−395.

Carl, P. L.; Chakravarty, P. K.; Katzenellenbogen, J. A. "A Novel Connector Linkage Applicable in Prodrug Design" *J. Med. Chem.* **1981**, *24*, 479−480.

Carl, P. L.; Chakravarty, P. K.; Katzenellenbogen, J. A.; Weber, M. J. "Protease Activated Prodrugs for Cancer Chemotherapy" *Proc. Natl. Acad. Sci. U.S.A.* **1980**, *77*, 2224−2228.

Carpino, L. A. "1-Hydroxy-7-azabenzotriazole. An Efficient Peptide Coupling Additive" *J. Am. Chem. Soc*. **1993**, *115*, 4397−4398.

Carpino, L. A.; Han, G. Y. "9-Fluorenylmethoxycarbonyl Amino-Protecting Group" *J. Org. Chem.* **1972**, *37*, 3404−3409.

Carpino, L. A; Imazumi, H.; Foxman, B. M.; Vela, M. J; Henklein, P.; El-Faham, A.; Klose, J.; Bienert, M. "Comparison of the Effects of 5- and 6-HOAt on Model Peptide Coupling Reactions Relative to the Cases for the 4- and 7-Isomers" *Org. Lett.* **2000**, *2*, 2253−2256.

Casazza, A. M.; Di Marco, A.; Bonadonna, G.; Bonfante, V.; Bertazzoli, C.; Bellini, O.; Pratesi, G.; Sala, L.; Ballerini, L. Effects of Modifications in Position 4 of the Chromophore or in Position 4′ of the Aminosugar, on the Antitumor Activity and Toxicity of Daunorubicin and Doxorubicin. In *Anthracyclines: Current Status and New Developments*; Crooke, S. T., Reich, S. D., Eds.; Academic Press: New York, 1980; pp 403–430.

Casazza, A. M.; Pratesi, G.; Giuliani, F.; Di Marco, A. "Antileukemic Activity of 4-Demethoxydaunorubicin in Mice" *Tumori* **1980**, *66*, 549–564.

Cassinelli, G.; Orezzi, P. "La Daunomicina: Un Nuovo Antibiotico ad Attivita Citostatica, Isolamento e Propriety" *G. Microbiol.* **1963**, *11*, 167−174.

Chan, W. C., White, P. D., Eds.; *Fmoc Solid Phase Peptide Synthesis: A Practical Approach*; Oxford University Press: New York, 2000.

Chen, X.; Wu, B.; Wang, G. W. "Glucuronides in Anti-Cancer Therapy" *Curr. Med. Chem. Anticancer Agents* **2003**, *3*, 139−150.

Choe, Y.; Leonetti, F.; Greenbaum, D. C.; Lecaille, F.; Bogyo, M.; Bromme, D.; Ellman, J. A.; Craik, C. S. "Substrate Profiling of Cysteine Proteases Using a Combinatorial Peptide Library Identifies Functionally Unique Specificities" *J. Biol. Chem.* **2006**, *281*, 12824–12832.

Choong, P. F. M.; Nadesapillai, A. P. W. "Urokinase Plasminogen Activator System: A Multifunctional Role in Tumor Progression and Metastasis" *Clin. Orthop. Relat. Res.* **2003**, *415*, S46−S58.

Chung, D. E.; Kratz, F. "Development of a Novel Albumin-Binding Prodrug that is Cleaved by Urokinase-type-Plasminogen Activator (uPA)" *Bioorg. Med. Chem. Lett*. **2006**, *16*, 5157−5163.

Cobos, E.; Jumper, C.; Lox, C. "Pretreatment Determination of the Serum Urokinase Plasminogen Activator and its Soluble Receptor in Advanced Small-Cell Lung Cancer or Non-Small-Cell Lung Cancer" *Clin. Appl. Thromb. Hemostasis* **2003**, *9*, 241−246.

Cohen, A. S.; Dubikovskaya, E. A.; Rush, J. S.; Bertozzi, C. R. "Real-Time Bio-luminescent Imaging of Glycans on Live Cells and in Living Animals" *J. Am. Chem. Soc.* **2010**, *132*, 8563−8565.

Coldwell, K. E.; Cutts, S. M.; Ognibene, T. J.; Henderson, P. T.; Phillips, D. R." Detection of Adriamycin–DNA Adducts by Accelerator Mass Spectrometry at Clinically Relevant Adriamycin Concentrations" *Nucleic Acids Res*. **2008**, *36*, e100.

Coley, H. M.; Amos, W. B.; Twentyman, P. R.; Workman, P. "Examination by Laser Scanning Confocal Fluorescence Imaging Microscopy of the Subcellular Localization of Anthracyclines in Parent and Multidrug Resistant Cell Lines" *Br. J. Cancer* **1993**, *67*, 1316−1323.

Corey, E. J.; Samuelsson, B.; Luzzio, F. A. "A New Method for the Synthesis of Nitro Compounds" *J. Am. Chem. Soc.* **1984**, *106*, 3682−3683.

Cremin, D. J.; Hergarty, A. F.; Begley, M. J. "Mechanism of Reaction of 2-Ethoxy-1-ethoxycarbonyl-1,2-dihydroquinoline (EEDQ) with Nucleophiles and its Crystal Structure" *J. Chem. Soc. Perkin II* **1980**, 412−420.

Cullinane, C.; Cutts, S. M.; Panousis, C.; Phillips, D. R. "Interstrand Cross-Linking by Adriamycin in Nuclear and Mitochondrial DNA of MCF-7 Cells" *Nucleic Acids Res.* **2000**, *28*, 1019−1025.

Cullinane, C.; Phillips, D. R. "Induction of Stable Transcriptional Blockage Sites By Adriamycin: GpC Specificity of Apparent Adriamycin-DNA Adducts and Dependence on Iron (III) Ions" *Biochemistry* **1990**, *29*, 5638−5646.

Cutts, S. M.; Phillips, D. R. "Use of Oligonucletides to Define the Site of Interstrand Crosslinks Induced by Adriamycin" *Nucleic Acids Res*. **1995**, *23*, 2450−2456.

Damen, E. W.; Nevalainen, T. J.; van den Bergh, T. J. M.; de Groot, F. M.; Scheeren, H. W. "Synthesis of Novel Paclitaxel Prodrugs Designed for Bio-reductive Activation in Hypoxic Tumour Tissue" *Bioorg. Med. Chem*. **2002**, *10,* 71−77.

D'Amico, T. A.; Brooks, K. R.; Joshi, M. B.; Conlon, D.; Herndon, J.; Petersen, R. P.; Harpole, D. H. "Serum Protein Expression Predicts Recurrence in Patients with Early-stage Lung Cancer After Resection" *Ann. Thorac. Surg*. **2006**, *81*, 1982−1987.

Dawson, P. E.; Kent, S. B. H. "Synthesis of Native Proteins by Chemical Ligation" *Ann. Rev. Biochem.* **2000**, *69*, 923−960.

DeFeo-Jones, D.; Garsky, V. M.; Wong, B. K.; Feng, D. M.; Bolyar, T.; Haskell, K.; Kiefer, D. M.; Leander, K.; McAvoy, E.; Lumma, P.; Wai, J.; Senderak, E. T.; Motzel, S. L.; Keenan, K.; van Zwieten, M.; Lin, J. H.; Freidinger, R.; Huff, J.; Oliff, A.; Jones, R. E. "A Peptide-Doxorubicin 'Prodrug' Activated by Prostate-Specific Antigen Selectively Kills Prostate Tumor Cells Positive for Prostate-Specific Antigen In Vivo" *Nat. Med*. **2000**, *6*, 1248−1252.

Deffie, A. M.; Batra, J. K.; Goldenberg, G. J. "Direct Correlation Between DNA Topoisomerase II Activity and Cytotoxicity in Adriamycin-Sensitive and –Resistant P388 Leukemia Cell Lines" *Cancer Res*. **1989**, *49*, 58−62.

de Graaf, M.; Boven, E.; Scheeren, H. W.; Haisma, H. J.; Pinedo, H. M. "β-Glucuronidase-mediated Drug Release" *Curr. Pharm. Des.* **2002**, *8*, 1391−1403.

de Groot, F. M. H.; de Bart, A. C. W.; Verheijen, J. H.; Scheeren, H. W. "Synthesis and Biological Evaluation of Novel Prodrugs of Anthracyclines for Selective Activation by the Tumor-associated Protease Plasmin" *J. Med. Chem.* **1999**, *42*, 5277−5283.

de Groot, F . M.; Loos, W. J.; Koekkoek, R.; van Berkom, L. W.; Busscher, G. F.; Seelen, A. E.; Albrecht, C.; de Bruijn, P.; Scheeren, H. W. "Elongated Multiple Electronic Cascade and Cyclization Spacer Systems in Activatable Anticancer Prodrugs for Enhanced Drug Release" *J. Org. Chem.* **2001**, *66*, 8815−8830.

de Groot, M.; van Berkom, L. W.; Scheeren, H. W. "Synthesis and Biological Evaluation of 2'-Carbamate-Linked and 2'-Carbonate-Linked Prodrugs of Paclitaxel: Selective Activation by the Tumor-Associated Protease Plasmin" *J. Med. Chem*. **2000**, *43*, 3093−3102.

Del Nery, E.; Alves, L. C.; Melo, R. L.; Cesari, M. H.; Juliano, L.; Juliano, M. A. "Specificity of Cathepsin B to Fluorescent Substrates Containing Benzyl Side-chain-substituted Amino Acids at P1 Subsite" *J. Protein Chem.* **2000**, *19*, 33–38.

Demchik, L. L.; Sameni, M.; Nelson, K.; Mikkelsen, T.; Sloane, B. F. "Cathepsin B and Glioma Invasion" *Int. J. Dev. Neurosci.* **1999**, *17*, 483−494.

Denmeade, S. R.; Isaacs, J. T. "A History of Prostate Cancer Treatment" *Nat. Rev. Cancer* **2002**, *2*, 389−396.

Denmeade, S. R.; Nagy, A.; Gao, J.; Lilja, H.; Schally, A. V.; Isaacs, J. T. "Enzymatic Activation of a Doxorubicin-Peptide Prodrug by Prostate-Specific Antigen" *Cancer Res.* **1998**, *58*, 2537−2540.

Denmeade, S. R.; Sokoll, L. J.; Chan, D. W.; Khan, S. R.; Isaacs, J. T. "Concentration of Enzymatically Active Prostate-Specific Antigen in the Extracellular Fluid of Primary Human Prostate Cancers and Human Prostate Cancer Xenograft Models" *Prostate* **2001**, *48*, 1−6.

Dennemarker, J.; Lohmuller, T.; Müller, S.; Aguilar, S. V.; Tobin, D. J.; Peters, C.; Reinheckel, T. "Impaired Turnover of Autophagolysosomes in Cathepsin L Deficiency" *Biol. Chem.* **2010**, *391*, 913–922.

de Petro, G.; Tavian, D.; Copeta, A.; Portolani, N.; Giulini, S. M.; Barlati, S. "Expression of Urokinase-type Plasminogen Activator (u-PA), u-PA Receptor, and Tissue-type PA Messenger RNAs in Human Hepatocellular Carcinoma" *Cancer Res.* **1998**, *58*, 2234−2239.

DeVita, V. T.; Hellman, S.; Rosenberg, S. A. In *Cancer: Principles and Practice of Oncology*, 7th ed.; Lippincott-Raven: Philadelphia, PA, 2005.

Devy, L.; de Groot, F. H. M.; Blacher, S.; Hajitou, A.; Beusker, P.; Scheeren, W.; Foldart, J.-M.; Noel, A. "Plasmin-activated Doxorubicin Prodrugs Containing a Spacer Reduce Tumor Growth and Angiogenesis Without Systemic Toxicity" *FASEB J.* **2004**, *18*, 565−567.

Di Marco, A.; Gaetani, M.; Orezzi, P.; Scarpinato, B. M.; Silvestrini, R.; Soldati, M.; Dasdia, T.; Valentini, L. "Daunomycin: A New Antibiotic of the Rhodomycin Group" *Nature* **1964**, *201*, 706−707.

Di Marco, A.; Gaetani, M; Scarpinato, B. "Adriamycin (NSC-123,127): A New Antibiotic with Antitumor Activity" *Cancer Chemother. Rep. (Part 1)* **1969**, *53*, 33−37.

Doroshow, J. H. Role of Reactive Oxygen Metabolism in Cardio Toxicity of Anthracycline Antibiotics. In *Anthracycline Antibiotics: New Analogues, Methods of Delivery and Mechanisms of Action* (Priebe, W., ed.); American Chemical Society: Washington, DC, 1995; pp 259−267.

Dubowchik, G. M.; Firestone, R. A; Padilla, L.; Willner, D.; Hofstead, S. J.; Mosure, K.; Knipe, J. O.; Lasch, S. J.; Trail, P. A. "Cathepsin B-Labile Dipeptide Linkers for Lysosomal Release of Doxorubicin from Internalizing Immunoconjugates: Model Studies of Enzymatic Drug Release and Antigen-Specific in Vitro Anticancer Activity" *Bioconjugate Chem.* **2002**, *13*, 855–869.

Duffy, M. J.; O'Grady, P.; Devaney, D.; O'Siorain, L.; Fennelly, J. J.; Lijnen, H. R. "Tissue-type Plasminogen Activator, A New Prognostic Marker in Breast Cancer" *Cancer Res.* **1988**, *48*, 1348−1349.

Duncan, R.; Cable, H. C.; Lloyd, J. B.; Rejmanov, P.; Kopecek, V. J. "Polymers Containing Enzymatically Degradable Bonds, 7. Design of Oligopeptide Side-Chains in Poly-[*N*-(2-Hydroxypropyl)methacrylamide] Copolymers to Promote Efficient Degradation by Lysosomal Enzymes" *Makromol. Chem.* **1983**, *184*, 1997−2008.

Dunn, A. D.; Crutchfield, H. E.; Dunn, J. T. "Thyroglobulin Processing by Thyroidal Proteases. Major Sites of Cleavage by Cathepsins B, D, and L" *J. Biol. Chem.* **1991**, *266*, 20198–20204.

Fenick, D. J.; Taatjes, D. J.; Koch, T. H. "Doxoform and Daunoform: Anthracycline-Formaldehyde Conjugates Toxic to Resistant Tumor Cells" *J. Med. Chem.* **1997**, *40*, 2452–2461.

Fehske, K. J.; Muller, W. E.; Wollert, U. "The Location of Drug Binding Sites in Human Serum Albumin" *Biochem. Pharmacol.* **1981**, *30*, 687−692.

Fernandez, J. M. G.; Mellet, C. O.; Diaz, V. M.; Fuentes, P. J.; Kovacs, J.; Pinter, I. "Aza-Wittig Reaction of Sugar Isothiocyanates and Sugar Iminophosphoranes: An Easy Entry to Unsymmetrical Sugar Carbodiimides" *Tetrahedron Lett.* **1997**, *38*, 4161−4164.

Ferreira, A. L.; Matsubara, L. S.; Matsubara, B. B. "Anthracycline-induced Cardiotoxicity" *Cardiovasc. Hematol. Agents Med. Chem*. **2008**, *6*, 278−281.

Fey, N.; Howell, J. A.; Lovatt, J. D.; Yates, P. C.; Cunningham, D.; McArdle, P.; Gottlieb, H. E. Coles, S. J. "A Molecular Mechanics Approach to Mapping the Conformational Space of Diaryl and Triarylphosphines" *Dalton Trans.* **2006**, 5464−5475.

Fields, G. B.; Tian, Z.; Barany, G. In *Synthetic Peptides: A User's Guide*; Grant, G. A. Ed.; W. H. Freeman: New York, 1992; pp 77−183.

Fosang, A. J.; Neame, P. J.; Last, K.; Hardingham, T. E.; Murphy, G.; Hamilton, J. A. "The Interglobular Domain of Cartilage Aggrecan is Cleaved by PUMP, Gelatinases, and Cathepsin B" *J. Biol. Chem.* **1992**, *267*, 19470–19474.

Friedrichs, B.; Tepel, C.; Reinheckel, T.; Deussing, J.; von Figura, K.; Herzog, V.; Peters, C.; Saftig, P.; Brix, K. "Thyroid Functions of Mouse Cathepsins B, K, and L" *J. Clin. Invest*. **2003**, *111*, 1733–1745.

Fuchs, J. R.; Funk, R. L. "Total Synthesis of (±) Perophoramidine" *J. Am. Chem. Soc.* **2004**, *126*, 5068−5069.

Fulmer, G. R.; Miller, A. J. M.; Sherden, N. H.; Gottlieb, H. E.; Nudelman, A.; Stoltz, B. M.; Bercaw, J. E.; Goldberg, K. I. "Chemical Shifts of Trace Impurities: Common Laboratories Solvents, Organics, and Gases in Deuterated Solvents Relevant to the Organometallic Chemist" *Organometallics* **2010**, *29*, 2176−2179.

Gao, Y. G.; Liaw, Y. C.; Li, Y. K.; Van der Marel, G. A.; Van Boom, J. H.; Wang, A. H. J. "Facile Formation of a Crosslinked Adduct Between DNA and the Daunorubicin Derivative MAR70 Mediated by Formaldehyde: Molecular Structure of the MAR70-d(CGTnACG) Covalent Adduct" *Proc. Nat. Acad. Sci. U.S.A.* **1991**, *88*, 4845−4849.

Garsky, M.; Lumma, P. K.; Feng, D. M.; Wai, J.; Ramjit, H. G.; Sardana, M. K.; Oliff, A.; Jones, R. E.; DeFeo-Jones, D.; Freidinger, R. M. "The Synthesis of a Prodrug of Doxorubicin Designed to Provide Reduced Systemic Toxicity and Greater Target Efficacy" *J. Med. Chem*. **2001**, *44*, 4216−4224.

Gaudiano, G.; Koch, T. H. “Redox Chemistry of Anthracycline Antitumor Drugs and Use of Captodative Radicals as Tools for its Elucidation and Control” *Chem. Res. Toxicol*. **1991**, *4*, 2−16.

Gewirtz, D. A. “A Critical Evaluation of the Mechanisms of Action Proposed for the Antitumor Effects of the Anthracycline Antibiotics Adriamycin and Daunorubicin” *Biochem. Pharmacol.* **1999**, *57*, 727−741.
Giannelli, G.; Falk-Marzillier, J.; Schiraldi, O.; Stetler-Stevenson, W. G.; Quaranta, V. “Induction of Cell Migration by Matrix Metalloprotease-2 Cleavage of Laminin-5” *Science* **1997**, *277*, 225−228.

Gigli, M.; Doglia, S. M.; Millot, J. M.; Valentini, L.; Manfait, M. “Quantitative Study of Doxorubicin in Living Cell Nuclei by Microspectrofluorometry” *Biochim. Biophys. Acta* **1988**, *950*, 13−20.

Gocheva, V.; Zeng, W.; Ke, D.; Klimstra, D.; Reinheckel, T.; Peters, C.; Hanahan, D.; Joyce, J. A. “Distinct Roles for Cysteine Cathepsin Genes in Multistage Tumorigenesis” *Genes Dev.* **2006**, *20*, 543−556.

Godleski, S. A., In *Comprehensive Organic Synthesis*, Trost, B. M.; Flemming, I., Eds.; Pergamon: Oxford, 1991; Vol. 4, pp 585.

Goodman, M., Felix, A., Moroder, L., Toniolo, C., Eds.; Synthesis of Peptides and Peptidomimetics. In *Methods of Organic Synthesis*; Thieme Stuttgart: New York, 2004; Vol. E22a, pp 716.

Goodman, M.; Levine, L. “Peptide Synthesis via Active Esters. IV. Racemization and Ring-Opening Reactions of Optically Active Oxazolones” *J. Am. Chem. Soc.* **1964**, *86*, 2918−2922.

Goodman, M.; McGahren, W. J. “Optically Active Peptide Oxazolones. Preliminary Racemization Studies Under Peptide Coupling Conditions” *J. Am. Chem. Soc.* **1965**, *87*, 3028−3029.

Goodman, M.; Stueben, K. C. “Amino Acid Active Esters. III. Base-Catalyzed Racemization of Peptide Active Esters” *J. Org. Chem.* **1962**, *27*, 3409−3416.

Gosalia, D. N.; Salisbury, C. M.; Maly, D. J.; Ellman, J. A.; Diamond, S. L. “Profiling Serine Protease Substrate Specificity with Solution Phase Fluorogenic Peptide Microarrays” *Proteomics* **2005**, *5*, 1292−1298.

Gottlieb, H. E.; Kotlyar, V.; Nudelman, A “NMR Chemical Shifts of Common Laboratory Solvents as Trace Impurities” *J. Org. Chem.* **1997**, *62*, 7512−7515.

Greenbaum, D. C.; Arnold, W. D.; Lu, F.; Hayrapetian, L.; Baruch, A.; Krumrine, J.; Toba, S.; Chehade, K.; Br€omme, D.; Kuntz, I. D.; Bogyo, M. “Small Molecule Affinity Fingerprinting. A Tool for Enzyme Family Subclassification, Target Identification, and Inhibitor Design” *Chem. Biol.* **2002**, *9*, 1085–1094.

Greene, T. W.; Wuts, P. G. M. In *Protective Groups in Organic Synthesis*, 2nd ed.; John Wiley, New York, 1991.

Greenwald, R. B. "PEG Drugs: An Overview" *J. Control Release* **2001**, *74*, 159−171.

Greenwald, R. B.; Choe, Y. H.; Conover, C.; Shum, K.; Wu, D.; Royzen, M. "Drug Delivery Systems Based on Trimethyl Lock Lactonization: Poly(ethylene glycol) Prodrugs of Amino-Containing Compounds" *J. Med. Chem.* **2000**, *43*, 475−487.

Greenwald, R. B.; Conover, C. D.; Choe, Y. H. "Poly(ethylene glycol) Conjugated Drugs and Prodrugs: A Comprehensive Review" *Crit. Rev. Ther. Drug Carrier Syst.* **2000**, *17*, 101−161.

Greenwald, R. B.; Pendri, A.; Conover, C. D.; Zhao, H.; Choe, Y. H.; Martinez, A.; Shum, K.; Guan, S. "Drug Delivery Systems Employing 1,4- or 1,6-Elimination: Poly(ethylene glycol) Prodrugs of Amine-Containing Compounds" *J. Med. Chem.* **1999**, *42*, 3657−3667.

Griffin, R. J.; Evers, E.; Davison, R.; Gibson, A. E.; Layton, D.; Irwin, W. J. "The 4-Azidobenzyloxycarbonyl Function: Application as a Novel Protecting Group and Potential Prodrug Modification for Amines" *J. Chem. Soc., Perkin Trans. 1* **1996**, 1205−1211.

Groskopf, W. R.; Summaria, L.; Robbins, K. C. "Studies on the Active Center of Human Plasmin. Partial Amino Acid Sequence of a Peptide Containing the Active Center Serine Residue" *J. Biol. Chem*. **1969**, *244*, 3590−3597.

Gude, M.; Ryf, J.; White, P. D. "An Accurate Method for the Quantitation of Fmoc-derivatized Solid Phase Supports" *Lett. Pept. Sci.* **2002**, *9*, 203−206.

Guibé, F. "Allylic Protecting Groups and Their Use in a Complex Environment Part II: Allylic Protecting Groups and Their Removal Through Catalytic Palladium π-Allyl Methodology" *Tetrahedron* **1998**, *54*, 2967−3042.

Hang, H. C.; Bertozzi, C. R. "From Mechanism to Mouse: A Tale of Two Bioorthogonal Reactions" *Acc. Chem. Res.* **2001**, *34*, 727−736.

Hang, H. C.; Yu, C.; Kato, D. L.; Bertozzi, C. R. "A Metabolic Labeling Approach Toward Proteomic Analysis of Mucin-type *O*-linked Glycosylation" *Proc. Natl. Acad. Sci. U.S.A.* **2003**, *100*, 14846−14851.

Harland, R. M.; Weintraub, H.; McKnight, S. L. "Transcription of DNA Injected Into *Xenopus* Oocytes is Influenced by Template Topology" *Nature* **1983**, *302*, 38−43.

Harris, J. L.; Backes, B. J.; Leonetti, F.; Mahrus, S.; Ellman, J. A.; Craik, C. S. "Rapid and General Profiling of Protease Specificity by Using Combinatorial Fluorogenic Substrate Libraries" *Proc. Natl. Acad. Sci. U.S.A.* **2000**, *97*, 7754−7759.

Harris, R. K.; Becker, E. D.; Cabral de Menezes, S. M.; Granger, P.; Hoffman, R. E.; Zilm, K. W. "Further Conventions for NMR Shielding and Chemical Shifts (IUPAC Recommendations 2008)" *Pure Appl. Chem.* **2008**, *80*, 59.

Harris, J. L.; Niles, A.; Burdick, K.; Maffitt, M.; Backes, B. J.; Ellman, J. A.; Kunts, I.; Haak-Frendscho, M.; Craik, C. S. "Definition of the Extended Substrate Specificity Determinants of β-Tryptases I and II" *J. Biol. Chem.* **2001**, *276*, 34941−34947.

Hashimoto, Y.; Kakegawa, H.; Narita, Y.; Hachiya, Y.; Hayakawa, T.; Kos, J.; Turk, V.; Katunuma, N. "Significance of Cathepsin B Accumulation in Synovial Fluid of Rheumatoid Arthritis" *Biochem. Biophys. Res. Commun*. **2001**, *283*, 334−339.

Hatfield, J. M.; Wierdl, M.; Wadknis, R. M.; Potter, P. M. "Modification of Human Carboxylesterase for Improved Prodrug Activation" *Expert Opin. Drug Metab. Toxical.* **2008**, *4*, 1153−1165.

Heck, M. M. S.; Earnshaw, W. C. "Topoisomerase II: A Specific Marker for Cell Proliferation" *J. Cell Biol.* **1986**, *103*, 2569−2581.

Hewitt, R.; Dano, K. "Stromal Cell Expression of Components of Matrix-Degrading Protease Systems in Human Cancer" *Enzyme Protein* **1996**, *49*, 163−173.

Hiebel, J.; Baumgartner, H.; Bernwieser, I.; Blanka, M.; Bodenteich, M.; Leitner K.; Rio , A.; Rovenszky, F.; Alberts, D. P.; Bhatnagar, P. K.; Banyard , A. F.; Baresch , K.; Esch, P. M.; Kollmann , H.; Mayrhofer, G.; Weihtrager, H.; Welz, W.; Winkler, K.; Chen, T.; Patel, R.; Lantos, I.; Stevenson, D.; Tubman, K. D.; Undheim, K. "Large-scale Synthesis of Hemato-regulatory Nonapeptide SK&F 107647 by Fragment Condensation" *J. Pept. Res.* **1999**, *54*, 54−65.

Hofmann, U. B.; Westphal, J. R.; Waas, E. T.; Zendman, A. J.; Cornelissen, I. M.; Ruiter, D. J.; van Muijen, G. N. "Matrix Metalloproteinases in Human Melanoma Cell Lines and Xenografts: Increased Expression of Activated Matrix Metalloproteinase-2 (MMP-2) Correlates with Melanoma Progression" *Br. J. Cancer* **1999**, *81*, 774−782.

Holm, C.; Goto, T.; Wang, J. C.; Botstein, D. "DNA Topoisomerase II is Required at the Time of Mitosis in Yeast" *Cell* **1985**, *41*, 553−563.

Imlay, J. A.; Chin, S. M.; Linn, S. "Toxic DNA Damage by Hydrogen Peroxide Through the Fenton Reaction *In Vivo* and *In Vitro*" *Science* **1988**, 2*40*, 640−642.

Jane, D. T.; Morvay, L.; Dasilva, L.; Cavallo-Medved, D.; Sloane, B. F.; Dufresne, M. J. "Cathepsin B Localizes to Plasma Membrane Caveolae of Differentiating Myoblasts and is Secreted in an Active Form at Physiological pH" *Biol. Chem.* **2006**, *387*, 223–234.

Johnson, A. W. In *Ylides and Imines of Phosphorus*, Wiley: New York, 1993.

Johnson, A. W.; Wong, S. C. K. “The Chemistry of Ylides: Mechanism of the Reaction of Iminophosphoranes with Carbonyl Compounds” *Can. J. Chem.* **1966**, *44*, 2793−2803.

Kaguni, J. M.; Kornberg, A. “Replication Initiated at the Origin (oriC) of E. coli Chromosome Reconstituted with Purified Enzymes” *Cell* **1984**, *38*, 183−190.

Kalet, B. T.; McBryde, M. B.; Espinosa, J. M.; Koch, T. H. “Doxazolidine Induction of Apoptosis by a Topoisomerase II Independent Mechanism” *J. Med. Chem.* **2007**, *50*, 4493−4500.

Kato, S.; Burke, P. J.; Fenick, D. J.; Taatjes, D. J.; Bierbaum, V. M.; Koch, T. H. “Mass Spectrometric Measurement of Formaldehyde Generated in Breast Cancer Cells Upon Treatment with Anthracycline Antitumor Drugs” *Chem. Res. Toxicol*. **2000**, *13*, 509−516.

Khan, S. R.; Denmeade, S. R. “In Vivo Activity of a PSA-activated Doxorubicin Prodrug Against PSA-producing Human Prostate Cancer Xenografts” *Prostate* **2000**, *45*, 80−83.

Kiick, K. L.; Saxon, E.; Tirrell, D. A.; Bertozzi, C. R. “Incorporation of Azides into Recombinant Proteins for Chemoselective Modification by the Staudinger Ligation” *Proc. Natl. Acad. Sci. U.S.A.* **2002**, *99*, 19−24.

Kleyer, D. L.; Koch, T. H. “Electrophilic Trapping of the Tautomer of 7-Deoxy-daunomycinone. A Possible Mechanism for Covalent Binding of Daunomycin to DNA” *J. Am. Chem. Soc.* **1983**, *105*, 5154−5155.

Kleyer, D. L.; Koch, T. H. “Mechanistic Investigation of Reduction of Daunomycin and 7-Deoxydaunomycinone with Bi(3,5,5-trimethyl-2-oxomorpholin-3-yl)” *J. Am. Chem. Soc.* **1984**, *106*, 2380−2387.

Kline, T .; Torgov, M. Y.; Mendelsohn, , B. A.; Cerveny, C. G.; Senter, P. D. “Novel Antitumor Prodrugs Designed for Activation by Matrix Metalloproteinases-2 and -9” *Mol. Pharm*. **2004**, *1*, 9−22.

Knorr, R.; Trzeciak, A.; Bannwarth, W.; Gillessen, D. “New Coupling Reagents in Peptide Chemistry” *Tetrahedron Lett.* **1989**, *30*, 1927−1930.

Köhn, M.; Breinbauer, R. "The Staudinger Ligation - A Gift to Chemical Biology" *Angew. Chem. Int. Ed. Engl.* **2004**, *43*, 3106−3116.

Köhn, M.; Wacker, R.; Peters, C.; Schroder, H.; Soulere, L.; Breinbauer, R.; Niemeyer, C. M.; Waldmann, H. “Staudinger Ligation: A New Immobilization Strategy for the Preparation of Small-Molecule Arrays” *Angew. Chem., Int. Ed. Engl.* **2003**, *42*, 5830−5834.

Koivunen, E.; Ristimaki, A.; Itkonen, O.; Osman, S.; Vuento, M.; Stenman, U. H. “Tumor-associated Trypsin Participates in Cancer Cell-mediated Degradation of Extracellular Matrix” *Cancer Res.* **1991**, *51*, 2107−2112.

Kölmel, C.; Ochsenfeld, C. Ahlrichs, R. "An *Ab Initio* Investigation of Structure and Inversion Barrier of Triisopropylamine and Related Amines and Phosphines" *Theor. Chim. Acta* **1991**, *82*, 271−284.

Kosal, A. D.; Wilson, E. E.; Ashfeld, B. L. "Phosphine-based Redox Catalysis in the Direct Traceless Staudinger Ligation of Carboxylic Acids and Azides" *Angew. Chem., Int. Ed. Engl.* **2012**, *51*, 12036−12040.

Kovacs, J.; Kisfaludy, L.; Ceprini, M. Q. "On the Optical Purity of Peptide Active Esters Prepared by *N,N′*-Dicydohexylcarbodiimide and Complexes of *N,N′*-Dicyclohexylcarbodiimide-Pentachlorophenol and *N,N′*-Dicyclohexylcarbodiimide Pentafluorophenol" *J. Am. Chem. Soc.* **1967**, *89*, 183−184.

Kovar, M.; Strohalm, J.; Etrych, T.; Ulbrich, K.; Rihova, B. "Star Structure of Antibody-Targeted HPMA Copolymer-Bound Doxorubicin: A Novel Type of Polymeric Conjugate for Targeted Drug Delivery with Potent Antitumor Effect" *Bioconjugate Chem*. **2002**, *13*, 206−215.

Kratochwil, N. A.; Huber, W.; Muller, F.; Kansy, M.; Gerber, P. R. "Predicting Plasma Protein Binding of Drugs: A New Approach" *Biochem. Pharmacol*. **2002**, *64*, 1355−1374.

Kratz, F.; Drevs, J.; Bing, G.; Stockmar, C.; Scheuermann, K.; Lazar, P.; Unger, C. "Development and In Vitro Efficacy of Novel MMP2 and MMP9 Specific Doxorubicin Albumin Conjugates" *Bioorg. Med. Chem. Lett.* **2001**, *11*, 2001−2006.

Kratz, F.; Muller, I. A.; Ryppa, C.; Warnecke, A. "Prodrug Strategies in Anticancer Chemotherapy" *ChemMedChem* **2008**, *3*, 20−53.

Laynez, J.; Menendez, M.; Velasco, J. L. S.; Llamas-Saiz, A. L.; Foces, C. F.; Elguero, J.; Molina, P.; Alajarin, M.; Vidal, A. "Iminophosphorane-substituted Proton Sponges. Part 4. Comparison of X-ray Molecular Structures with Solution Properties (pKa, ^{1}H and ^{13}C NMR Spectroscopy)" *J. Chem. Soc. Perkin. Trans. 2* **1993**, *2*, 709−713.

Le, J. Drug Excretion. In *Merck Manual for Professionals*; Kenilworth, NJ, 2017.

Leffler, J. E.; Temple, R. D. "The Staudinger Reaction Between Triarylphosphines and Azides. A Study of the Mechanism" *J. Am. Chem. Soc.* **1967**, *89*, 5235−5246.

Leffler, J. E.; Tsuno, Y. "Some Decomposition Reactions of Acid Azides" *J. Org. Chem.* **1963**, *28*, 902−906.

Legters, J.; Thijs, L.; Zwanenburg, B. "A Convenient Synthesis of Optically Active 1H-Aziridine-2-Carboxylic Acids (Esters)" *Tetrahedron Lett*. **1989**, *30*, 4881−4884.

Lieber, E.; Rao, C. N. R.; Chao, T. S.; Hoffman, C. W. W. "Infrared Spectra of Organic Azides" *Anal. Chem.* **1957**, *29*, 916−918.

Lijnen, H. R. “Plasmin and Matrix Metalloproteinases in Vascular Remodeling” *Thromb. Haemostasis* **2001**, *86*, 324−333.

Lilja, H. “A Kallikrein-like Serine Protease in Prostatic Fluid Cleaves the Predominant Seminal Vesicle Protein” *J. Clin. Invest*. **1985**, *76*, 1899−1903.

Lilja, H.; Abrahamsson, P. A.; Lundwall, A. “Semenogelin, the Predominant Protein in Human Semen. Primary Structure and Identification of Closely Related Proteins in the Male Accessory Sex Glands and on the Spermatozoa” *J. Biol. Chem*. **1989**, *264*, 1894−1900.

Lin, F. L.; Hoyt, H. M.; Halbeek, H. Van; Bergman, R. G.; Bertozzi, C. R.; Berkeley, L. “Mechanistic Investigation of the Staudinger Ligation” *J. Am. Chem. Soc.* **2005**, *127*, 2686−2695.

Liu, L. F.; Liu, C. C.; Alberts, B. M. “Type II DNA Topoisomerases: Enzymes that can Unknot a Topologically Knotted DNA Molecule via a Reversible Double-Strand Break” *Cell* **1980**, *19*, 697−707.

Liu, L. F.; Rowe, T. C.; Yang, L.; Tewey, K. M.; Chen, G. L. ”Cleavage of DNA by Mammalian DNA Topoisomerase II” *J. Biol. Chem*. **1983**, *258*, 15365−15370.

Liu, M.; Sun, Y.; Zhao, S.; Li, Y.; Piao, R.; Yang, Y.; Gu, J. “A Novel Prodrug Strategy to Improve the Oral Absorption of *O*-Desmethylvenlafaxine” *Exp. Ther. Med.* **2016**, *12*, 1611−1617.

Lorenzo, A.; Aller, E.; Molina, P. “Iminophosphorane-based Synthesis of Multinuclear Ferrocenyl Urea, Thiourea and Guanidine Derivatives and Exploration of Their Anion Sensing Properties” *Tetrahedron* **2009**, *65*, 1397−1401.

Lown, W. J.; Chen, J. A.; Plambeck, J. A.; Acton, E. M. “Further Studies on the Generation of Reactive Oxygen Species from Activated Anthracyclines and the Relationship to Cytotoxic Action and Cardiotoxic Effects” *Biochem. Pharmacol.* **1982**, *31*, 575−581.

Luchansky, S. J.; Argade, S.; Hayes, B. K.; Bertozzi, C. R. “Metabolic Functionalization of Recombinant Glycoproteins” *Biochem*istry **2004***, 43,* 12358−12366.

Maag, H. “Overcoming Poor Permeability: The Role of Prodrugs for Oral Drug Delivery” *Drug Discov. Today* **2012**, *9*, 121−130.

Madison, E. L.; Coombs, G. S.; Corey, D. R. “Substrate Specificity of Tissue Type Plasminogen Activator. Characterization of the Fibrin Independent Specificity of t-PA for Plasminogen” *J. Biol. Chem*. **1995**, *270*, 7558−7562.

Mai, J.; Waisman, D. M.; Sloane, B. F. “Cell Surface Complex of Cathepsin B/Annexin II Tetramer in Malignant Progression” *Biochim. Biophys. Acta* **2000**, *1477*, 215−230.

Manfait, M.; Alix, A. J.; Jeannesson, P.; Jardillier, J. C.; Theophanides, T. “Interaction of

Adriamycin with DNA as Studied by Resonance Raman Spectroscopy" *Nucleic Acids Res*. **1982**, *10*, 3803−3816.

Mansour, A. M.; Drevs, J.; Esser, N.; Hamada, F. M.; Badary, O. A.; Unger, C.; Fichtner, I.; Kratz, F. "A New Approach for the Treatment of Malignant Melanoma: Enhanced Antitumor Efficacy of an Albumin-binding Doxorubicin Prodrug that is Cleaved by Matrix Metalloproteinase 2" *Cancer Res.* **2003**, *63*, 4062−4066.

Masquelier, M.; Baurain, R.; Trouet, A. "Amino Acid and Dipeptide Derivatives of Daunorubicin. 1. Synthesis, Physicochemical Properties, and Lysosomal Digestion" *J. Med. Chem*. **1980***, 23*, 1166−1170.

MATLAB and Optimization Toolbox Release 2019a, The Mathworks Inc.: Natick, MA, 2019.

McGrath, N. A.; Raines, R. T. "Chemoselectivity in Chemical Biology: Acyl Transfer Reactions with Sulfur and Selenium" *Acc. Chem. Res.* **2011**, *44*, 752−761.

Merkx, R.; Rijkers, D. T. S.; Kemmink, J. Liskamp, R. M. J. "Chemoselective Coupling of Peptide Fragments Using the Staudinger Ligation" *Tetrahedron Lett.* **2003**, *44*, 4515−4518.

Minotti, G., Menna, P., Salvatorelli, E., Cairo, G., and Gianni, L. "Anthracyclines: Molecular Advances and Pharmacologic Developments in Antitumor Activity and Cardiotoxicity" *Pharmacol. Rev*. **2004**, *56*, 185−229.

Miszczuk-Jamska, B.; Merten, M.; Guy-Crotte, O.; Amouric, M.; Clemente, F.; Schoumacher, R. A.; Figarella, C. "Characterization of Trypsinogens 1 and 2 in Two Human Pancreatic Adenocarcinoma Cell Lines; CFPAC-1 and CAPAN-1" *FEBS Lett*. **1991**, *294*, 175−178.

Miwa, M.; Ura, M.; Nishida, M.; Sawada, N.; Ishikawa, T.; Mori, K.; Shimma, N.; Umeda, I.; Ishitsuka, H. "Design of a Novel Oral Fluoropyrimidine Carbamate, Capecitabine, which Generates 5-Fluorouracil Selectively in Tumours by Enzymes Concentrated in Human Liver and Cancer Tissue" *Eur. J. Cancer* **1998**, *34*, 1274−1281.

Molina, P.; Vilaplana, M. J. "Iminophosphoranes: Useful Building Blocks for the Preparation of Nitrogen-Containing Heterocycles" *Synthesis* **1994**, 1197−1218.

Moore, H. W. "Bioactivation as a Model for Drug Design Bioreductive Alkylation" *Science* **1977**, *197*, 527−532.

Moore, H. W.; Czerniak, R. "Naturally Occurring Quinones as Potential Bioreductive Alkylating Agents" *Med. Res. Rev.* **1981**, *1*, 249−280.

Moskowitz, C. H.; Nademanee, A.; Masszi, T.; Agura, E.; Holowiecki, J.; Abidi, M. H.; Chen, A. I.; Stiff, P.; Gianni, A. M.; Carella, A.; Osmanov, D.; Bachanova, V.; Sweetenham, J.; Sureda, A.; Huebner, D.; Sievers, E. L.; Chi, A.; Larsen, E. K.; Hunder, N. N.; Walewsji, J. "Brentuximab vedotin as Consolidation Therapy After Autologous Stem-Cell Transplantation in

Patients with Hodgkin's Lymphoma at Risk of Relapse or Progression (AETHERA): A Randomised, Double-Blind, Placebo-Controlled, Phase 3 Trial" *Lancet* **2015**, *385*, 1853−1862.

Moufarij, M. A.; Cutts, S. M.; Neumann, G. M.; Kimura, K.; Phillips, D. R. "Barminomycin Functions as a Potent Pre-Activated Analogue of Adriamycin" *Chem. Biol. Interact*. **2001**, *138*, 137−153.

Muller, C. E. "Prodrug Approaches for Enhancing the Bioavailability of Drugs with Low Solubility" *Chem. Biodivers.* **2017**, *6*, 2071−2083.

Murdter, T . E.; Sperker, B.; Kivisto, K. T.; McClellan, M.; Fritz, P.; Friedel, G.; Linder, A.; Bosslet, K.; Toomes, H.; Dierkesmann, R.; Kroemer, H. K. "Enhanced Uptake of Doxo-rubicin into Bronchial Carcinoma: β-Glucuronidase Mediates Release of Doxorubicin from a Glucuronide Prodrug (HMR 1826) at the Tumor Site" *Cancer Res.* **1997**, *57*, 2440−2445.

Myers, C. E.; Gianni, L.; Simone, C. B.; Klecker, R.; Greene, R. "Oxidative Destruction of Erythrocyte Ghost Membranes Catalyzed by the Doxorubicin-Iron Complex" *Biochemistry* **1982**, *21*, 1707−1712.

Najib, J. "The Efficacy and Safety Profile of Lisdexamfetamine Dimesylate, a Prodrug of d-Amphetamine, for the Treatment of Attention-Deficit/Hyperactivity Disorder in Children" *Clin. Ther.* **2009**, *31*, 142−176.

Neises, B.; Steglich, W. "A Simple Method for the Esterification of Carboxylic Acids" *Angew. Chem., Int. Ed. Engl.* **1978**, *17*, 522−524.

Nilsson, B. L.; Kiessling, L. L.; Raines, R. T. "Staudinger Ligation: A Peptide from a Thioester and Azide" *Org. Lett.* **2000**, *2*, 1939−1941.

Nilsson, B. L.; Hondal, R. J.; Soellner, M. B.; Raines, R. T. "Protein Assembly by Orthogonal Chemical Ligation Methods" *J. Am. Chem. Soc.* **2003**, *125*, 5268−5269.

Painter, R. B. "A Replication Model for Sister Chromatid Exchange" *Mutat. Res.* **1980**, *70*, 337−341.

Park, C-M.; Niu, W.; Liu, C.; Biggs, T. D.; Guo, J.; Xian, M. "A Proline-based Phosphine Template for Staudinger Ligation" *Org. Lett.* **2012**, *14*, 4694−4697.

Pluger, E. B. E.; Boes, M.; Alfonso, C.; Schr€oter, C. J.; Kalbacher, H.; Ploegh, H. L.;Driessen, C. "Specific Role for Cathepsin S in the Generation of Antigenic Peptides In Vivo" *Eur. J. Immunol*. **2002**, *32*, 467–476.

Pöchlauer, P.; Müller, E. P.; Peringer, P. "On the Mechanism of Aziridine Synthesis from 2-Azido-Alcohols and Triphenylphosphine" *Helv. Chim. Acta* **1984**, *67*, 1238−1247.

Portaro, F. C. V.; Santos, A. B. F.; Cezari, M. H. S.; Juliano, M. A.; Juliano, L.; Carmona, E. "Probing the Specificity of Cysteine Proteinases at Subsites Remote from the Active Site: Analysis of P4, P3, P2' and P3' Variations in Extended Substrates" *Biochem. J.* **2000**, *347*, 123–129.

Post, G. C.; Barthel, B. L.; Burkhart, D. J.; Hagadorn, J. R.; Koch, T. H. "Doxazolidine, A Proposed Active Metabolite of Doxorubicin That Cross-Links DNA" *J. Med. Chem.* **2005**, *48*, 7648−7657.

Quax, P. H.; de Bart, A. C.; Schalken, J. A.; Verheijen, J. H. "Plasminogen Activator and Matrix Metalloproteinase Production and Extracellular Matrix Degradation by Rat Prostate Cancer Cells In Vitro: Correlation with Metastatic Behavior In Vivo" *Prostate* **1997**, *32*, 196−204.

Rautio, J.; Kumpulainen, H.; Heimbach, T.; Oliyai, R.; Oh, D.; Jaervinen, T.; Savolainen, J. "Prodrugs: Design and Clinical Applications" *Nature Rev. Drug Discovery* **2008**, *7*, 255−270.

Restituyo, J. A.; Comstock, L. R.; Petersen, S. G.; Stringfellow, T.; Rajski, S. R. "Conversion of Aryl Azides to *O*-Alkyl Imidates via Modified Staudinger Ligation" *Org. Lett.* **2003**, *5*, 4357−4360.

Rivault, F.; Tranoy-Opalinski, I.; Gesson, J. P. "A New Linker for Glucuronylated Anticancer Prodrugs" *Bioorg. Med. Chem.* **2004**, *12*, 675−682.

Roshy, S.; Sloane, B. F.; Moin, K. "Pericellular Cathepsin B and Malignant Progression" *Cancer Metastasis Rev*. **2003**, *22*, 271−286.

Ryppa, C.; Mann-Steinberg, H.; Biniossek, M. L.; Satchi-Fainaro, R.; Kratz, F. "*In Vitro* and *In Vivo* Evaluation of a Paclitaxel Conjugate with the Divalent Peptide E-[c(RGDfK)$_2$] that Targets Integrin $\alpha_v\beta_3$" *Int. J. Pharm.* **2008**, *368*, 89−97.

"Salicin" *Merck Index*, 11th ed., Whitehouse Station, NJ, M9730.

Sanghani, S. P.; Quinney, S. K.; Fredenburg, T. B.; Sun, Z.; Davis, W. I.; Murry, D. J.; Cummings, O. W.; Seitz, D. E.; Bosron, W. F. "Carboxylesterases Expressed in Human Colon Tumor Tissue and their Role in CPT-11 Hydrolysis" *Clin. Cancer Res*. **2003**, *9*, 4983−4991.

Santin, A. D.; Cane, S.; Bellone, S.; Bignotti, E.; Palmieri, M.; De Las Casas, L. E.; Anfossi, S.; Roman, J. J.; O'Brien, T.; Pecorelli, S. "The Novel Serine Protease Tumor-associated Differentially Expressed Gene-15 (matriptase/MT-SP1) is Highly Overexpressed in Cervical Carcinoma" *Cancer* **2003**, *98*, 1898−1904.

Saxon, E.; Armstrong, J. I.; Bertozzi, C. R. "A Traceless Staudinger Ligation for the Chemoselective Synthesis of Amide Bonds" *Org. Lett.* **2000**, *2*, 2141−2143.

Saxon, E.; Bertozzi, C. R. "Cell Surface Engineering by a Modified Staudinger Reaction" *Science* **2000**, *287*, 2007−2010.

Saxon, E.; Luchansky, S. J.; Hang, H. C.; Yu, C.; Lee, S. C.; Bertozzi, C. R. "Investigating Cellular Metabolism of Synthetic Azidosugars with the Staudinger Ligation" *J. Am. Chem. Soc.* **2002**, *124*, 14893−14902.

Schlechter, I.; Berger, A. "On the Size of the Active Site in Proteases. I. Papain" *Biochem. Biophys. Res. Commun.* **1967**, *27*, 157−162.

Senter, P. D.; Sievers, E. L. "The Discovery and Development of Brentuximab Vedotin for Use in Relapsed Hodgkin Lymphoma and Systemic Anaplastic Large Cell Lymphoma" *Nature Biotechnol.* **2012**, *30*, 631−637.

Sevenich, L.; Schurigt, U.; Sachse, K.; Gajda, M.; Werner, F.; Muller, S.; Vasiljeva, O.; Schwinde, A.; Klemm, N.; Deussing, J.; Peters, C.; Reinheckel, T. "Synergistic Antitumor Effects of Combined Cathepsin B and Cathepsin Z Deficiencies on Breast Cancer Progression and Metastasis in Mice" *Proc. Natl. Acad. Sci. U.S.A.* **2010**, *107*, 2497–2502.

Shah, L.; Laughlin, S. T.; Carrico, I. S. "Light-Activated Staudinger-Bertozzi Ligation within Living Animals" *J. Am. Chem. Soc.* **2016**, *138*, 5186−5189.

Shalimov, A. A.; Malenko, D. M.; Repina, L. A.; Sinitsa, A. D. "*N*-Substituted *N*-Phosphinotrifluoroactetamides in the Staudinger Reaction" *Russ. J. Gen. Chem.* **2005**, *75*, 1376−1378.

Shen, L.; Sigal, L. J.; Boes, M.; Rock, K. L. "Important Role of Cathepsin S in Generating Peptides for TAP-independent MHC Class I Crosspresentation In Vivo" *Immunity* **2004**, *21*, 155–165.

Shimma, N.; Umeda, I.; Arasaki, M.; Murasaki, C.; Masubuchi, K.; Kohchi, Y.; Miwa, M.; Ura, M.; Sawada, N.; Tahara, H.; Kuruma, I.; Horii, I.; Ishitsuka, H. "The Design and Synthesis of a New Tumor-Selective Fluoropyrimidine Carbamate, Capecitabine" *Bioorg. Med. Chem.* **2000**, *8*, 1697−1706.

Shin, S. J.; Kim, K. O.; Kim, M. K.; Lee, K. H.; Hyun, M. S.; Kim, K. J.; Choi, J. H.; Song, H. S. "Expression of E-cadherin and uPA and Their Association with the Prognosis of Pancreatic Cancer" *Jpn. J. Clin. Oncol.* **2005**, *35*, 342−348.

Simunek, T.; Sterba, M.; Popelova, O.; Adamcova, M.; Hrdina, R.; Gersl, V. "Anthracycline-induced Cardiotoxicity: Overview of Studies Examining the Roles of Oxidative Stress and Free Cellular Iron" *Pharmacol. Rep.* **2009**, *61*, 154−171.

Sinha, B. K. "Binding Specificity of Chemically and Enzymatically Activated Anthracycline Anticancer Agents to Nucleic Acids" *Chem. Biol. Interact*. **1980**, *30*, 67−77.
Sinha, B. K.; Gregory, J. L. "Role of One-Electron and Two-Electron Reduction Products of Adriamycin and Daunomycin in Deoxyribonucleic Acid Binding" *Biochem. Pharmacol*. **1981**, *30*, 2626−2629.

Sinha, A. A.; Jamuar, M. P.; Wilson, M. J.; Rozhin, J.; Sloane, B. F. "Plasma Membrane Association of Cathepsin B in Human Prostate Cancer: Biochemical and Immunogold Electron Microscopic Analysis*" Prostate* **2001**, *49*, 172−184.

Sinha, B. K.; Trush, M. A.; Kennedy, K. A.; Mimnaugh, E. G. "Enzymatic Activation and Binding of Adriamycin to Nuclear DNA" *Cancer Res*. **1984**, *44*, 2892−2896.

Sneader, W. "The Discovery of Aspirin: A Reappraisal" *BMJ Clin. Res.* **2000**, *321*, 1591−1594.

Soellner, M. B.; Dickson, K. A.; Nilsson, B. L.; Raines, R. T. "Site-Specific Protein Immobilization by Staudinger Ligation" *J. Am. Chem. Soc.* **2003**, *125*, 5268−5269.

Soellner, M. B.; Nilsson, B. L.; Raines, R. T. "Reaction Mechanism and Kinetics of the Traceless Staudinger Ligation" *J. Am. Chem. Soc.* **2006**, *128*, 8820−8828.

Sperker, B.; Backman, J. T.; Kroemer, H. K. "The Role of β-Glucuronidase in Drug Disposition and Drug Targeting in Humans" *Clin. Pharmacokinet*. **1997**, *33*, 18−31.

Sperker, B.; Werner, U.; Murdter, T. E.; Tekkaya, C.; Fritz, P.; Wacke, R.; Adam, U.; Gerken, M.; Drewelow, B.; Kroemer, H. K. "Expression and Function of β-Glucuronidase in Pancreatic Cancer: Potential Role in Drug Targeting" *Naunyn-Schmiedeberg's Arch. Pharmacol*. **2000**, *362*, 110−115.

Spira, D.; Stypmann, J.; Tobin, D. J.; Petermann, I.; Mayer, C.; Hagemann, S.; Vasiljeva, O.; Gunther, T.; Schule, R.; Peters, C.; Reinheckel, T. "Cell Type-specific Functions of the Lysosomal Protease Cathepsin L in the Heart" *J. Biol. Chem.* **2007**, *282*, 37045−37052.

Staudinger, H.; Meyer, J. "Über Neue Organische Phosphorverbindungen III. Phosphinmethylenderivate und Phosphinimine" *Helv. Chim. Acta* **1919**, *2*, 635−646.

Steinherz, L.; Steinherz, P. "Delayed Cardiac Toxicity from Anthracycline Therapy" *Pediatrician* **1991**, *18*, 49−52.

Stella, V. *Pro-drugs: An Overview and Definition*; ACS Symposium Series; American Chemical Society: Washington, DC, 1975.

Stella, V. J.; Burchardt, R. T.; Hageman, M. J.; Oliyai, R.; Maah, H.; Tilley, J. W. In *Prodrugs: Challenges and Rewards. Part 1*; Springer: New York, 2007.

Still, C. W.; Kahn, M.; Mitra, A. "Rapid Chromatographic Technique for Preparative Separations with Moderate Resolution" *J. Org. Chem.* **1978**, *43*, 2923−2925.

Studer, M.; Kroger, L. A.; DeNardo, S. J.; Kukis, D. L.; Meares, C. F. "Influence of a Peptide Linker on Biodistribution and Metabolism of Antibody-Conjugated Benzyl-EDTA. Comparison of Enzymatic Digestion In Vitro and In Vivo" *Bioconjugate Chem*. **1992**, *3*, 424−429.

Stypmann, J.; Glaser, K.; Roth, W.; Tobin, D. J.; Petermann, I.; Matthias, R.; Monnig, G.; Haverkamp, W.; Breithardt, G.; Schmahl, W.; Peters, C.; Reinheckel, T. "Dilated Cardiomyopathy in Mice Deficient for the Lysosomal Cysteine Peptidase Cathepsin L" *Proc. Natl. Acad. Sci. U.S.A.* **2002**, *99*, 6234–6239.

Sun, J.; Dahan, A.; Amidon, G. L. "Enhancing the Intestinal Absorption of Molecules Containing the Polar Guanidine Functionality: A Double-Targeted Prodrug Approach" *J. Med. Chem.* **2010**, *53*, 624−632.

Sweatman, T. W.; Isreal, M. Anthracyclines. In *Cancer Therapeutics, Experimental and Clinical Agents.* Teicher B. A., Ed.; Humana Press: Totowa, NJ, 1997; pp 113−135.

Swift, L. P.; Rephaeli, A.; Nudelman, A.; Phillips, D. R.; Cutts, S. M. "Doxorubicin-DNA Adducts Induce a Non-Topoisomerase II–Mediated Form of Cell Death" *Cancer Res.* **2006**, *66*, 4863−4871.

Taatjes, D. J.; Gaudiano, G.; Koch, T. H. "Production of Formaldehyde and DNA−Adriamycin or DNA−Daunomycin Adducts, Initiated through Redox Chemistry of Dithiothreitol/Iron, Xanthine Oxidase/NADH/Iron, or Glutathione/Iron" *Chem. Res. Toxicol*. **1997**, *10*, 953−961.

Taatjes, D. J.; Gaudiano, G.; Resing, K.; Koch, T. H. "Alkylation of DNA By the Anthracycline, Antitumor Drugs Adriamycin and Daunomycin" *J. Med. Chem*. **1996**, *39*, 4135−4138.

Taatjes, D. J.; Gaudiano, G.; Resing, K.; Koch, T. H. "Redox Pathway Leading to the Alkylation of DNA By the Anthracycline, Antitumor Drugs Adriamycin and Daunomycin" *J. Med. Chem.* **1997**, *40*, 1276−1286.

Taatjes, D. J.; Koch, T. H. "Growth Inhibition, Nuclear Uptake, and Retention of Anthracycline-Formaldehyde Conjugates in Prostate Cancer Cells Relative to Clinical Anthracyclines" *Anticancer Res*. **1999**, *19*, 1201−1208.

Tabata, T.; Katoh, M.; Tokudome, S.; Nakajima, M.; Yokoi, T. "Identification of the Cytosolic Carboxylesterase Catalyzing the 5'-Deoxy-5-Fluorocytidine Formation from Capecitabine in Human Liver" *Drug. Metab. Dispos.* **2004**, *32*, 1103−1110.

Takeuchi, T.; Harris, J. L.; Huang, W.; Yan, K. W.; Coughlin, S. R.; Craik, C. S. "Cellular Localization of Membrane-type Serine Protease 1 and Identification of Protease-activated Receptor-2 and Single-chain Urokinase-type Plasminogen Activator as Substrates" *J. Biol. Chem*. **2000**, *275*, 26333–26342.

Takeuchi, Y.; Nakao, A.; Harada, A.; Nonami, T.; Fukatsu, T.; Takagi, H. "Expression of Plasminogen Activators and Their Inhibitors in Human Pancreatic Carcinoma: Immunohisto-chemical Study" *Am. J. Gastroenterol*. **1993**, *88*, 1928−1933.

Tan, C.; Etcubanas, E.; Wollner, N.; Rosen, G.; Gilladoga, A.; Showel, J. "Adriamycin−An

Antitumor Antibiotic in the Treatment of Neoplastic Diseases" *Cancer* **1973**, *32*, 9−17.

Tan, C.; Tasaka, H.; Yu, K. P.; Murphy, M. L.; Karnofsky, D. A. "Daunomycin, an Antitumor Antibiotic, In the Treatment of Neoplastic Disease: Clinical Evaluation with Special Reference to Childhood Leukemia" *Cancer* **1967**, *20*, 333−353.

Taralp, A.; Kaplan, H.; Sytwu, I. I.; Vlattas, I.; Bohacek, R.; Knap, A. K.; Hirama, T.; Huber, C. P.; Hasnain, S. "Characterization of the S3 Subsite Specificity of Cathepsin B" *J. Biol. Chem.* **1995**, *270*, 18036−18043.

Tewey, K. M.; Rowe, T. C.; Yang, L.; Halligan, B. D.; Liu, L. F. "Adriamycin-Induced DNA Damge Mediated by Mammalian DNA Topoisomerase II" *Science* **1984**, *226*, 466−468.

Thanou, M.; Duncan, R. "Polymer-Protein and Polymer-Drug Conjugates in Cancer Therapy" *Curr. Opin. Invest. Drugs* **2003**, *4*, 701−709.

Thomssen, C.; Schmitt, M.; Goretzki, L.; Oppelt, P.; Pache, L.; Dettmar, P.; Janicke, F.; Graeff, H. "Prognostic Value of the Cysteine Proteases Cathepsins B and Cathepsin L in Human Breast Cancer" *Clin. Cancer Res*. **1995**, *1*, 741−746.

Trost, B. M.; Verhoeven, T. R. In *Comprehensive Organometallic Chemistry*; Wilkenson, G., Stone, F. G. A., Abel, E. W., Eds.; Pergamon Press: Oxford, 1982; Vol. 8, pp 799−854.

Tsao, M.; Tian, F.; Schultz, P. G. "Selective Staudinger Modification of Proteins Containing *p*-Azidophenylalanine" *ChemBioChem* **2005**, *6*, 2147−2149.

Tsuge, O.; Kanemasa, S.; Matsuda, K. "One-pot Synthesis of *N*-[(Trimethylsilyl) Methyl] Imines and (Trimethylsilyl) Methyl-substituted Heterocumulenes from (Trimethylsilyl) Methyl Azide" *J. Org. Chem.* **1984**, *49*, 2688−2691.

Ulisse, S.; Baldini, E.; Sorrenti, S.; D'Armiento, M. "The Urokinase Plasminogen Activator System: A Target for Anti-Cancer Therapy" *Curr. Cancer Drug Targets* **2009**, *9*, 32−71.

van Brakel, R.; Vulders, R. C. M.; Bokdam, R. J.; Grüll, H.; Robillard, M. S. "A Doxorubicin Prodrug Activated By the Staudinger Reaction" *Bioconjugate Chem.* **2008**, *19*, 714−718.

van Cauwenberge, H. "Aspirin, An Always Current Drug" *Rev. Med. Liege* **1996**, *51*, 7−18.

van Rosmalen, A.; Cullinane, C.; Cutts, S. M.; Phillips, D. R. "Stability of Adriamycin-induced DNA Adducts and Interstrand Crosslinks" *Nucleic Acids Res.* **1995**, *23*, 42−50.

Vasiljeva, O.; Korovin, M.; Gajda, M.; Brodoefel, H.; Bojic, L.; Kruger, A.; Schurigt, U.; Sevenich, L.; Turk, B.; Peters, C.; Reinheckel, T. "Reduced Tumour Cell Proliferation and Delayed Development of High Grade Mammary Carcinomas in Cathepsin B-deficient Mice" *Oncogene* **2008**, *27*, 4191–4199.

Vassalli, J. D.; Pepper, M. S. "Tumour Biology. Membrane Proteases In Focus" *Nature* **1994**, *370*, 14−15.

Velasco, M.; D.; Molina, P.; Fresneda, P. M.; Sanz, M. A. "Isolation, Reactivity and Intramolecular Trapping of Phosphazide Intermediates in the Staudinger Reaction of Tertiary Phosphines with Azides" *Tetrahedron* **2000**, *56*, 4079−4084.

Versluis, A. J.; Rump, E. T.; Rensen, P. C.; van Berkel, T. J.; Bijsterbosch, M. K. "Synthesis of a Lipophilic Daunorubicin Derivative and Its Incorporation into Lipidic Carriers Developed for LDL Receptor-Mediated Tumor Therapy" *Pharm. Res.* **1998**, *15*, 531−537.

Vocadlo, D. J.; Hang, H. C.; Kim, E. J.; Hanover, J. A.; Bertozzi, C. R. "A Chemical Approach for Identifying *O*-Glc*N*Ac-modified Proteins in Cells" *Proc. Natl. Acad. Sci. U.S.A.* **2003**, *100*, 9116−9121.

Von Hoff, D. D.; Layard, M. W.; Basa, P.; Davis, H. L., Jr.; Von Hoff, A. L.; Rozencweig, M.; Muggia, F. M. "Risk Factors for Doxorubicin-lnduced Congestive Heart Failure" *Ann. Intern. Med*. **1979**, *91*, 710−717.

Wakselman, M. "The 1,4 and 1,6 Eliminations from Hydroxy- and Amino-substituted Benzyl Systems: Chemical and Biochemical Applications" *Nouv. J. Chim.* **1983**, *7,* 439−447.

Wang, J. C. "DNA Topoisomerases" *Annu. Rev. Biochem.* **1985**, *54*, 665−697.

Wang, A. H. J.; Gao, Y. G.; Liaw, Y. C.; Li, Y. K. "Formaldehyde Crosslinks Daunorubicin and DNA Efficiently: HPLC and X-ray Diffraction Studies" *Biochemistry* **1991**, *30*, 3812−3815.

Wang, B.; Zhang, H.; Wang, W. "Chemical Feasibility Studies of a Potential Coumarin-Based Prodrug System" *Bioorg. Med. Chem. Lett.* **1996**, *6*, 945−950.

Wang, B.; Zhang, H.; Zheng, A.; Wang, W. "Coumarin-based Prodrugs. Part 3: Structural Effects on the Release Kinetics of Esterase-Sensitive Prodrugs of Amines" *Bioorg. Med. Chem*. **1998**, *6*, 417−426.

Webb, C. D.; Latham, M. D.; Lock, R. B.; Sullivan, D. M. "Attenuated Topoisomerase II Content Directly Correlates with a Low Level of Drug Resistance in a Chinese Hamster Ovary Cell Line" *Cancer Res*. **1991**, *51*, 6543−6549.

Weiss, R. B. "The Anthracyclines: Will We Ever Find a Better Doxorubicin?" *Semin. Oncol*. **1992**, *19*, 670−686.

Weiss, G.; Loyevsky, M.; Gordeuk, V. R. "Dexrazoxane (ICRF-187)" *Gen. Pharmacol. The Vascular Sys.* **1999**, *32*, 155−158.

Werle, B.; Kotzsch, M.; Lah, T. T.; Kos, J.; Gabrijelcic-Geiger, D.; Spiess, E.; Schirren, J.; Ebert, W.; Fiehn, W.; Luther, T.; Magdolen, V.; Schmitt, M.; Harbeck, N. "Cathepsin B,

Plasminogen Activator-Inhibitor (PAI-1) and Plasminogen Activator-Receptor (uPAR) are Prognostic Factors for Patients with Non-Small Cell Lung Cancer" *Anticancer Res.* **2004**, *24*, 4147−4161.

Williams, R. M.; Liu, J. "Asymmetric Synthesis of Differentially Protected 2,7-Diaminosuberic Acid, a Ring-Closure Metathesis Approach" *J. Org. Chem.* **1998**, *63*, 2130−2132.

Williams, M. W.; Young, G. T. "Amino-acids and Peptides. Part XIXJ The Mechanism of Racemization During Peptide Synthesis. The Chloride Effect" *J. Chem. Soc.* **1964**, 3701−3708.

Woessner, R.; An, Z.; Li, X.; Hoffman, R. M.; Dix, R.; Bitonti, A. "Comparison of Three Approaches to Doxorubicin Therapy: Free Doxorubicin, Liposomal Doxorubicin, and β-Glucuronidase-activated Prodrug (HMR 1826)" *Anticancer Res*. **2000**, *20*, 2289−2296.

Xu, J.; DeGraw, A. J.; Duckworth, B. P.; Lenevich, S.; Tann, C.-M.; Jenson, E. C.; Gruber, S. J.; Barany, G.; Distefano, M. D. "Synthesis and Reactivity of 6,7-Dihydrogeranylazides: Reagents for Primary Azide Incorporation into Peptides and Subsequent Staudinger Ligation" *Chem. Biol. Drug Des.* **2006**, *68*, 85−96.

Xu, G.; Zhang, W.; Ma, M. K.; McLeod, H. L. "Human Carboxylesterase 2 is Commonly Expressed in Tumor Tissue and is Correlated with Activation of Irinotecan" *Clin. Cancer Res*. **2002**, *8*, 2605−2611.

Yamamoto, H.; Iku, S.; Itoh, F.; Tang, X.; Hosokawa, M.; Imai, K. "Association of Trypsin Expression with Recurrence and Poor Prognosis in Human Esophageal Squamous Cell Carcinoma" *Cancer* **2001**, *91*, 1324−1331.

Yasothornsrikul, S.; Greenbaum, D.; Medzihradszky, K. F.; Toneff, T.; Bundey, R.; Miller, R.; Schilling, B.; Petermann, I.; Dehnert, J.; Logvinova, A.; Goldsmith, P.; Neveu, J. M.; Lane, W. S.; Gibson, B.; Reinheckel, T.; Peters, C.; Bogyo, M.; Hook, V. "Cathepsin L in Secretory Vesicles Functions as a Prohormone-processing Enzyme for Production of the Enkephalin Peptide Neurotransmitter" *Proc. Natl. Acad. Sci. U.S.A.* **2003**, *100*, 9590–9595.

Young, R. C.; Ozols, R. F.; Myers, C. E. "Medical Progress: The Anthracycline Antineoplastic Drugs" *New Engl. J. Med.* **1981**, *305*, 139−153.

Zawilska, J. B.; Wojciesza, J.; Olejniczak, A. B. "Prodrugs: A Challenge for the Drug Development" *Pharmacological Reports* **2013**, *65*, 1−14.

Zeman, S. M.; Phillips, D. R.; Crothers, D. M. "Characterization of Covalent Adriamycin-DNA Adducts" *Proc Natl. Acad. Sci. U.S.A.* **1998**, *95*, 11561−11565.

Zheng, Q.; Tang, Z. Y.; Xue, Q.; Shi, D. R.; Song, H. Y.; Tang, H. B. "Invasion and Metastasis of Hepatocellular Carcinoma in Relation to Urokinase-type Plasminogen Activator, its Receptor and Inhibitor" *J. Cancer Res. Clin. Oncol.* **2000**, *126*, 641−646.